

**FORMULATION AND CHARACTERIZATION OF POLYMERIC
NANOPARTICLES FOR IMPROVING BIOAVAILABILITY OF
SOME ANTICANCER AND ANTI-HIV DRUGS**

A Thesis submitted to

The Maharaja Sayajirao University of Baroda

For the Degree of

**DOCTOR OF PHILOSOPHY
IN
PHARMACY**

By
Garima Joshi

Supervised by

Prof. Krutika K. Sawant

Professor in Pharmacy



Pharmacy Department

Faculty of Technology and Engineering, Kalabhavan,

The M. S. University of Baroda, Vadodara-390001

August 2013



Pharmacy Department
Faculty of Technology & Engineering
The Maharaja Sayajirao University of Baroda
Post Box No. 51, Kalabhavan, Vadodara – 390 001, India.
Ph. : (+91-265) 2434187 Fax : (0265) 2423898/2418927
E-mail : head-pharm@msubaroda.ac.in

August 8, 2013

CERTIFICATE

This is to certify that the thesis entitled “Formulation and Characterization of Polymeric Nanoparticles for Improving Bioavailability of Some Anticancer and Anti HIV Drugs”, submitted for Ph.D. degree in Pharmacy by Garima Joshi comprises the original research work carried out by her under my guidance and supervision.

Guide

Prof. Krutika Sawant

Pharmacy Department



Head

Pharmacy Department

Head,
Pharmacy Department
Faculty of Tech. & Engg.,
M. S. Univ. of Baroda,
Kalabhavan, BARODA-1.

Dean

Faculty of Technology and Engineering

Dean
Faculty of Tech. & Engg.
M. S. University of Baroda,
Baroda.

DECLARATION

I hereby declare that the thesis on the topic entitled "**Formulation and Characterization of Polymeric Nanoparticles for Improving Bioavailability of Some Anticancer and Anti HIV Drugs**" which is submitted herewith to "The Maharaja Sayajirao University of Baroda, Vadodara" for the award of Ph.D. in Pharmacy is the result of work done by me in the Pharmacy Department, Faculty of Technology & Engineering, The Maharaja Sayajirao University of Baroda, under the able guidance of Prof. Krutika Sawant, Professor in Pharmacy, Pharmacy Department, Faculty of Technology & Engineering, The Maharaja Sayajirao University of Baroda. I further declare that the result of this work has not been previously submitted for any degree.



(Garima Joshi)

Certified by and forwarded through the research guide,



Prof Krutika Sawant,
Professor in Pharmacy,
Pharmacy Department,
Faculty of Technology & Engineering
The Maharaja Sayajirao University of Baroda,
Vadodara-390001

Acknowledgement

On the verge of accomplishing a cherished dream, I offer my gratitude to the almighty that has been a source of strength throughout.

*I am indebted to my guide, mentor **Prof Krutika Sawant** for being very generous in sharing her precious time and knowledge with me and giving me this golden opportunity. I owe her a debt of gratitude; she went over each section of this text with a fine toothed comb. Under her able guidance and due to her constant motivation and constructive criticism my dream has become a reality. No words will ever be able to justify my gratitude for her.*

It is my privilege to acknowledge Prof M. R. Yadav, Head, Pharmacy Department to allow me to use the departmental facilities. I am grateful to Prof A. N. Misra, Dean, Faculty of Technology and Engineering for valuable suggestions and help whenever sought for. I am thankful to all the teaching and non-teaching staff for the support extended.

I am thankful to Ranbaxy ltd, Gurgaon, Aurobindo Pharma ltd, Hyderabad and Purac Biomaterials, The Netherlands for the generous gift samples. I am thankful to Director, SICARTI, Vallabh Vidhyanagar for carrying out TEM studies.

I take this opportunity to sincerely thank All India Council for Technical Education (AICTE), New Delhi for the financial support in term of National Doctoral Fellowship during this course.

I wholeheartedly thank my friend Hardik Gandhi for his tireless efforts in all in vivo studies, without any constraint. I wish to express my heartiest thanks to my close friends Manisha Lalan, Abhinesh Kumar and Sandip Chavhan for motivation and support provided by them.

I am extremely grateful to my father Mr Uttam Chand Ojha and mother ShailBala ojha who have been a perennial source of inspiration and providing me encouragement.

I want to express my deep appreciation to my husband, my parents and siblings who have unfailingly lent a helping hand whenever needed. I owe for their patience until completion of my Dissertation. My son, Garv needs a special mention for his never ending love and support.

I am grateful to all those who have made this project a success. Finally, I dedicate this work to my late grandmother Rampyari Dadhich and my Family.

Garima Joshi

Table of Contents

Contents	I-IV
List of Tables	V-VII
List of Figures	VIII-XI
List of Abbreviations	XII
CHAPTER 1 Introduction	1-10
1.1 Introduction	1
1.2 Aims and Objectives	5
1.3 Plan of Work	6
1.4 References	8
CHAPTER 2 Literature Review	11-65
2 Oral Drug Delivery	11
2.1 Physiological Considerations of Gastro-intestinal Tract for Oral Delivery of Nanoparticles	14
2.2 Transport of Nanoparticles across the Intestinal Mucosa	16
2.2.1 Paracellular Transport	17
2.2.2 Transcellular Transport	18
2.2.3 Carrier Mediated Transport	19
2.2.4 Receptor Mediated Transport	19
2.3 Nanoparticles for Anticancer Drug Delivery	21
2.4 Nanoparticles for Antiretroviral Drug Delivery	24
2.5 Method for Preparation of Nanoparticles	29
2.5.1 Nanoparticles Prepared by Polymerization Process of Monomers	29
2.5.2 Nanoparticles Prepared from Dispersion of Preformed Polymers	30
2.6 Characterization of Nanoparticles	35
2.7 Biodegradable Polymers	41
2.8 Stabilizers	47
2.9 Drug Profiles	49
2.9.1 Drug Profile of Gemcitabine HCl	49
2.9.2 Drug Profile of Lopinavir	54
2.10 References	57
CHAPTER 3 Analytical Methods	66-88
3.1 Materials	66
3.2 Estimation of Gemcitabine HCl by UV Spectroscopy	66
3.2.1 Calibration Plot in Distilled Water	66

3.2.2 Analytical Method Validation	67
3.2.3 Results and Discussion	68
3.3 Estimation of Gemcitabine HCl by HPLC	70
3.3.1 Calibration Plot of Gemcitabine HCl in Buffer: Methanol	71
3.3.2 Results and Discussion	71
3.4 Estimation of Gemcitabine HCl in Plasma by HPLC	73
3.4.1 Calibration Plot of Gemcitabine HCL in Plasma	74
3.4.2 Results and Discussion	75
3.5 Estimation of Lopinavir by Derivative Ultraviolet Spectroscopy	78
3.5.1 Calibration Plot in Acetonitrile	78
3.5.2 Results and Discussion	77
3.6 HPLC Method for Estimation of Lopinavir	80
3.6.1 Calibration Plot of Lopinavir in Acetonitrile: Buffer	81
3.6.2 Results and Discussion	81
3.7 Calibration Plot of Lopinavir in Plasma by HPLC	84
3.7.1 Validation	84
3.7.2 Results and Discussion	85
3.7.3 Absolute Recovery	87
3.8 References	88
CHAPTER 4 Experimental Gemcitabine HCl Loaded Nanoparticles	89-120
4.1 Introduction	89
4.2 Materials	92
4.3 Equipments	92
4.4 Formulation of Gemcitabine HCl Loaded Nanoparticles by Multiple Emulsification	
Solvent Evaporation Method	92
4.5 Preliminary Optimization of Parameters	93
4.6 Optimization by Factorial Design	93
4.7 Lyophilization of Gemcitabine HCl loaded Nanoparticles and Optimization of Cryoprotectant	98
4.8 Characterization of Optimized Gemcitabine HCl loaded Nanoparticles	98
4.9 Results and Discussion	
4.9.1 Preliminary Optimization	100
4.9.2 Optimization by Factorial Design	102
4.9.3 Optimization of Cryoprotectant for Lyophilization of Nanoparticles	112
4.9.4 Characterization of Gemcitabine HCl Loaded Nanoparticles	113
4.10 References	118

CHAPTER 5 Experimental Lopinavir Loaded Nanoparticles	121-146
5.1 Introduction	121
5.2 Materials	122
5.3 Equipments	122
5.4 Formulation of Lopinavir Loaded Nanoparticles	122
5.5 Preliminary Optimization of Parameters	123
5.6 Optimization by Factorial Design	123
5.7 Optimization Data Analysis	125
5.8 Lyophilization of Lopinavir Loaded Nanoparticles and Optimization of Cryoprotectant	127
5.9 Characterization of Optimized Lopinavir Loaded Nanoparticles	128
5.10 Results and Discussion	129
5.10.1 Preliminary Optimization	129
5.10.2 Optimization by Factorial Design	130
5.10.3 Optimization of Cryoprotectant for Lyophilization of Nanoparticles	131
5.10.4 Characterization of Lopinavir Loaded Nanoparticles	141
5.11 References	146
CHAPTER 6 <i>In Vitro</i> and <i>Ex Vivo</i> Release Studies	147-160
6.1 <i>In Vitro</i> Release Studies	147
6.2 <i>Ex Vivo</i> Diffusion Studies	147
6.3 Kinetics of Drug Release	147
6.4 Gemcitabine HCl Loaded Nanoparticles	150
6.4.1 <i>In Vitro</i> Release Studies through Dialysis Membrane	150
6.4.2 <i>Ex Vivo</i> Release Studies through Rat stomach and Intestinal Segment	150
6.5 Lopinavir Loaded Nanoparticles	151
6.5.1 <i>In Vitro</i> Release Studies through Dialysis Membrane	151
6.5.2 <i>Ex Vivo</i> Release Studies through Rat stomach and Intestinal Segment	152
6.6 Results and Discussion	153
6.6.1 <i>In Vitro</i> Drug Release Studies of Gemcitabine HCl loaded Nanoparticles	153
6.6.2 <i>Ex Vivo</i> Drug Release Studies of Gemcitabine HCl Loaded Nanoparticles	154
6.6.3 <i>In Vitro</i> Drug Release Studies of Lopinavir loaded Nanoparticles	155
6.6.4 <i>Ex vivo</i> Drug Release Studies of Lopinavir Loaded Nanoparticles	156
6.7 References	159

CHAPTER 7 Cell Line Studies.....	161-186
7.1 Cell Line Studies.....	161
7.2 Intestinal Transport and Uptake Studies Using Cell Lines	161
7.3 Materials.....	162
7.4 Methods	162
7.4.1 Cell Culture.....	162
7.4.2 Method of Preparation for Rhodamine B and 6-Coumarin Loaded Nanoparticles	163
7.4.3 Qualitative Uptake of Nanoparticles in Caco-2 Cells by Confocal Microscopy	163
7.4.4 Quantitative uptake of 6-Coumarin loaded Nanoparticles in Caco-2 cells	164
7.4.5 Cytotoxicity studies (MTT assay)	164
7.4.6 Transport/permeability of Nanoparticles across Caco-2 Cells	165
7.5 Results and Discussion	165
7.5.1 Qualitative cell uptake studies by confocal microscopy	166
7.5.2 Quantitative cell uptake studies of 6-Coumarin loaded Nanoparticles	166
7.5.3 Cytotoxicity studies	177
7.5.4 Transport / permeability studies in Caco-2 cells	182
7.6 References	185
CHAPTER 8 <i>In Vivo</i> Studies	187-199
8.1 Introduction	187
8.2 Animals	187
8.3 <i>In Vivo</i> Nanoparticle uptake into Rat Intestinal Tissue after Oral Delivery by Confocal Laser Scanning Microscopy	188
8.3.1 Methods	188
8.3.2 Results and Discussion	188
8.4 <i>In Vivo</i> Pharmacokinetic Studies for Gemcitabine HCl Loaded Nanoparticles	191
8.4.1 Methods	191
8.4.2 Results and Discussion	192
8.5 <i>In Vivo</i> Pharmacokinetic Studies for Lopinavir Loaded Nanoparticles	195
8.5.1 Methods	195
8.5.2 Results and Discussion	195
8.6 References	199
CHAPTER 9 Summary and Conclusions	200-208

List of Tables

Table No	Title	Page
Table 2.1	Inherent viscosity and molecular weight for PLGA 50:50	44
Table 3.1	Calibration data for Gemcitabine HCl in distilled water by UV Spectroscopy	68
Table 3.2	Parameters for estimation of Gemcitabine HCl in distilled water by UV spectroscopy	68
Table 3.3	Precision and accuracy for estimation Gemcitabine HCl in distilled water by UV spectroscopy.	70
Table 3.4	Calibration data for estimation of Gemcitabine HCl in buffer: methanol by HPLC	71
Table 3.5	Parameters for estimation of Gemcitabine HCl in buffer: methanol by HPLC	73
Table 3.6	Precision and accuracy for Gemcitabine HCl in buffer: methanol by HPLC	74
Table 3.7	Calibration data of Gemcitabine HCl in plasma by HPLC	75
Table 3.8	Parameters for estimation of Gemcitabine HCl in plasma by HPLC	77
Table 3.9	Precision and accuracy for estimation of Gemcitabine HCl in plasma by HPLC	77
Table 3.10	Calibration data for Lopinavir in acetonitrile by UV spectroscopy	79
Table 3.11	Parameters for estimation of Lopinavir in acetonitrile by UV spectroscopy	80
Table 3.12	Precision and accuracy for estimation of Lopinavir in acetonitrile by UV spectroscopy	80
Table 3.13	Calibration data of Lopinavir in acetonitrile: buffer (60:40) by HPLC	82
Table 3.14	Parameters for estimation of Lopinavir in acetonitrile: buffer by HPLC	83
Table 3.15	Precision and accuracy for estimation of Lopinavir in acetonitrile: buffer by HPLC	83
Table 3.16	Calibration data for estimation of Lopinavir in plasma by HPLC	85
Table 3.17	Parameters for estimation of Lopinavir in plasma by HPLC	86
Table 3.18	Precision and accuracy for estimation of Lopinavir in plasma by HPLC	86
Table 3.19	Extraction efficiency of Lopinavir at various concentrations in plasma	87
Table 4.1	Factorial design parameters and experimental conditions	94
Table 4.2	Formulation of Gemcitabine HCl loaded nanoparticles by coded values	94
Table 4.3	Effect of type of solvent on particle size, PDI and EE of Gemcitabine HCl loaded NPs	100
Table 4.4	Effect of type of surfactant on particle size, PDI and EE of Gemcitabine HCl loaded NPs	101
Table 4.5	Effect of volume of internal aqueous phase on particle size, PDI and EE of Gemcitabine HCl loaded NPs	101
Table 4.6	Effect of pH of internal aqueous phase on particle size, PDI and EE of Gemcitabine HCl loaded NPs	102

Table 4.7	Full factorial design layout of Gemcitabine HCl loaded NPs showing effect of independent variables X_1 (Polymer concentration), X_2 (Surfactant concentration) and X_3 (sonication time) on responses PS and EE	104
Table 4.8	Model coefficients estimated by multiple regression analysis for PS and EE of Gemcitabine HCl loaded NPs	106
Table 4.9	Analysis of Variance (ANOVA) of full and reduced models for PS of Gemcitabine HCl loaded NPs	107
Table 4.10	Analysis of Variance (ANOVA) of full and reduced models for EE of Gemcitabine HCl loaded NPs	108
Table 4.11	Check point analysis, t test analysis and normalized error determination for Gemcitabine HCl loaded NPs	112
Table 4.12	Optimization of cryoprotectant concentration for Gemcitabine HCl loaded NPs	113
Table 4.13	Stability of Gemcitabine HCl loaded NPs at RT and (2-8°C)	117
Table 5.1	Constant parameters for optimization of Lopinavir loaded NPs	122
Table 5.2	Factorial design parameters and experimental conditions	124
Table 5.3	Formulation of Lopinavir loaded NPs utilizing coded values	124
Table 5.4	Effect of type of solvent on particle size, PDI and EE of Lopinavir loaded NPs	130
Table 5.5	Effect of type of surfactant on particle size, PDI and EE of Lopinavir loaded NPs	130
Table 5.6	Full factorial design layout of Lopinavir loaded NPs showing the effect of independent variables X_1 (Polymer concentration), X_2 (Surfactant concentration) and X_3 (sonication time) on PS and EE	131
Table 5.7	Model coefficients estimated by multiple regression analysis for PS of Lopinavir loaded NPs	133
Table 5.8	Model coefficients estimated by multiple regression analysis for EE of Lopinavir loaded NPs	133
Table 5.9	Analysis of Variance (ANOVA) of full and reduced models for PS of Lopinavir loaded NPs	135
Table 5.10	Analysis of Variance (ANOVA) of full and reduced models for EE of Lopinavir loaded NPs	135
Table 5.11	Check point analysis, t test analysis and normalized error determination for Lopinavir loaded NPs	137
Table 5.12	Optimization of cryoprotectant for Lopinavir loaded NPs	138
Table 5.13	Stability of Lopinavir loaded NPs at RT and (2-8°C)	145
Table 6.1	<i>In vitro</i> drug release data for plain drug solution and Gemcitabine HCl loaded NPs by using dialysis technique	153
Table 6.2	<i>Ex vivo</i> drug release data for plain drug solution and Gemcitabine HCl loaded NPs in rat stomach and intestine segment	154
Table 6.3	Release kinetics of Gemcitabine HCl loaded NPs	155

Table 6.4	<i>In vitro</i> drug release profile of Lopinavir loaded NPs and plain drug suspension in PBS 7.4 by dialysis technique	156
Table 6.5	<i>Ex vivo</i> drug release studies of Lopinavir loaded NPs in rat stomach (0.1N HCl for 2 h) and intestinal segment (PBS 6.8 for 6h)	157
Table 6.6	Release Kinetics of Lopinavir loaded PLGA NPs	158
Table 7.1	<i>In vitro</i> cytotoxicity studies of Gemcitabine HCl loaded NPs in Caco2 cells	
Table 7.2	<i>In vitro</i> cytotoxicity of Gemcitabine HCl loaded NPs in K562 cells	
Table 7.3	IC50 values of plain drug solution and Gemcitabine HCl loaded NPs in Caco -2 cells and K562 cells	178
Table 7.4	<i>In vitro</i> cytotoxicity of Lopinavir loaded NPs and plain drug suspension on Caco 2 cells	181
Table 7.5	Drug transfer across the Caco 2 cell lines for Gemcitabine loaded NPs and plain drug solution	183
Table 7.6	Drug transfer across the Caco 2 cell lines for Gemcitabine loaded NPs and plain drug solution	184
Table 8.1	Plasma concentration time profile of Gemcitabine HCl loaded NPs and plain drug solution in male Wistar rats (n=5)	193
Table 8.2	Pharmacokinetic parameters after oral administration of Gemcitabine HCl loaded NPs and Plain drug solution to male Wistar rats (n=5) for single dose oral bioavailability study	194
Table 8.3	Plasma concentration time profile of plain drug solution and Lopinavir loaded NPs in male Wistar rats (n=5)	197
Table 8.4	Pharmacokinetic parameters after oral administration of Lopinavir loaded NPs and Plain drug suspension to male Wistar rats (n=5) for single dose oral bioavailability study	198

List of Figures

Figure No	Title	Page
Fig. 2.1	GIT targets, formulation principles, opportunities and applications	15
Fig. 2.2	Schematic transverse sections of a Peyer's patch lymphoid follicle and overlying follicle-associated epithelium (FAE), depicting M cell transport of particulate delivery vehicles	16
Fig. 2.3	Mechanism of uptake of orally administered NPs: (I) M cells of the PP, (II) enterocytes, and (III) GALT	17
Fig. 2.4	The pathways that a drug can take to cross the intestinal mucosal barrier	20
Fig. 2.5	Schematic diagram of o/w emulsion method for preparation of nanoparticles	31
Fig. 2.6	Schematic diagram of w/o/w in-liquid drying process for nanoparticle preparation	32
Fig. 2.7	Schematic illustration of the nanoprecipitation process	34
Fig. 2.8	Structure of Poly glycolic acid (PGA), Poly lactic acid (PLA) and Poly (lactic-co-glycolic) acid (PLGA) 43	43
Fig. 2.9	Schematic illustration of the changes of polymer matrix during (a) surface erosion and (b) bulk erosion	45
Fig. 3.1	Standard plot of Gemcitabine HCl in distilled water by UV spectroscopy	69
Fig. 3.2	UV spectrum of Gemcitabine HCl in distilled water	69
Fig. 3.3	Standard plot of Gemcitabine HCl in buffer: methanol (97:3) by HPLC	72
Fig. 3.4	Overlay graph of calibration curve of Gemcitabine HCl in buffer: methanol by HPLC	72
Fig. 3.5	HPLC chromatogram of Gemcitabine HCl in buffer: methanol	73
Fig. 3.6	Standard plot of Gemcitabine HCl in Plasma by HPLC	76
Fig. 3.7	HPLC chromatogram of Gemcitabine HCl in plasma	76
Fig. 3.8	Second derivative UV spectra of Lopinavir at concentration 5-30 $\mu\text{g/ml}$	80
Fig. 3.9	Standard curve of Lopinavir in acetonitrile by UV spectroscopy	80
Fig. 3.10	Chromatogram of Lopinavir 25 mcg/ml in acetonitrile: buffer	83
Fig. 3.11	Standard plot of Lopinavir in acetonitrile: buffer by HPLC	83
Fig. 3.12	HPLC chromatogram of Lopinavir in plasma	85
Fig. 3.13	Standard plot of Lopinavir in plasma by HPLC	86
Fig. 4.1	Contour plots showing effect of (a) X_1 versus X_2 (b) X_2 versus X_3 (c) X_1 versus X_3 on PS of Gemcitabine HCl loaded NPs	110
Fig. 4.2	Response surface plots showing effect of (a) X_1 versus X_2 (b) X_2 versus X_3 (c) X_1 versus X_3 on PS of	110

	Gemcitabine HCl loaded NPs	
Fig. 4.3	Contour plots showing effect of (a) X_1 versus X_2 (b) X_2 versus X_3 (c) X_1 versus X_3 on EE of Gemcitabine HCl loaded NPs	111
Fig. 4.4	Response surface plots showing effect of (a) X_1 versus X_2 (b) X_2 versus X_3 (c) X_1 versus X_3 on EE of Gemcitabine HCl loaded NPs	111
Fig. 4.5	TEM image of Gemcitabine HCl loaded NPs	114
Fig. 4.6	Particle size distribution of optimized Gemcitabine HCl loaded NPs by Malvern Zetasizer	114
Fig. 4.7	DSC thermogram of Gemcitabine HCl (A), PLGA (B), Physical mixture (C) and Gemcitabine HCl loaded NPs (D)	115
Fig. 4.8	FTIR spectra of Gemcitabine HCl (A), PLGA (B), Physical mixture (C), Gemcitabine HCl loaded NPs (D)	116
Fig. 5.1	Contour plots showing effect of (a) X_1 versus X_2 (b) X_2 versus X_3 (c) X_1 versus X_3 on PS of Lopinavir loaded NPs	139
Fig. 5.2	Response surface plots showing effect of (a) X_1 versus X_2 (b) X_2 versus X_3 (c) X_1 versus X_3 on PS of Lopinavir loaded NPs	139
Fig. 5.3	Contour plots showing effect of (a) X_1 versus X_2 (b) X_2 versus X_3 (c) X_1 versus X_3 on EE of Lopinavir loaded NPs	140
Fig. 5.4	Response surface plots showing effect of (a) X_1 versus X_2 (b) X_2 versus X_3 (c) X_1 versus X_3 on PS of Lopinavir loaded NPs	140
Fig. 5.5	TEM image of Lopinavir loaded NPs	141
Fig. 5.6	Particle size distribution of Lopinavir loaded NPs by Malvern Zetasizer	142
Fig. 5.7	DSC thermograms of Lopinavir (A), PLGA (B), Physical mixture (C) and Lopinavir loaded PLGA NPs	143
Fig. 5.8	FTIR spectra of Lopinavir (A), PLGA (B), Physical mixture (C) and Lopinavir loaded PLGA NPs	144
Fig. 6.1	<i>In vitro</i> release profile of Gemcitabine HCl loaded NPs and plain drug solution in PBS 7.4 through dialysis membrane	154
Fig. 6.2	<i>Ex vivo</i> drug release studies of Gemcitabine HCl loaded NPs and plain drug solution in rat stomach (at 0.1 N HCl for 2h) and intestine (PBS 6.8 for 4h)	155
Fig. 6.3	<i>In vitro</i> drug release profile of Lopinavir loaded NPs and plain drug solution in PBS 7.4 by dialysis technique	156
Fig. 6.4	<i>Ex vivo</i> drug release studies of Lopinavir loaded NPs in rat stomach (0.1N HCl for 2 h) and intestinal segment (PBS 6.8 for 6h)	158
Fig. 7.1	Rhodamine loaded NPs at 30 min in Caco-2 cells; (A) NPs (B) DAPI stained Nuclei (C) Overlapped image showing internalization of NPs in cells	168
Fig. 7.2	Rhodamine solution at 30 min in Caco-2 cells (A) Dye solution	168

	(B) DAPI Stained nucleus (C) Overlapped image showing clearly no internalization	
Fig. 7.3	Rhodamine loaded NPs at 60 min in Caco-2 cells; (A) NPs (B) DAPI stained Nuclei (C) Overlapped image showing internalization of NPs in cells	169
Fig. 7.4	Rhodamine solution at 60 min in Caco-2 cells (A) Dye solution (B) DAPI Stained nucleus (C) Overlapped image showing clearly no internalization	169
Fig. 7.5	Rhodamine loaded NPs at 90 min in Caco-2 cells (A) NPs (B) DAPI stained Nuclei (C) Overlapped image showing internalization of NPs in cells	170
Fig. 7.6	Rhodamine solution at 90 min in Caco-2 cells (A) Dye solution (B) DAPI stained Nuclei (C) Overlapped image showing no internalization of NPs in cells	170
Fig. 7.7	6-Coumarin loaded NPs at 30 min in Caco-2 cells; (A) NPs (B) DAPI stained Nuclei (C) Overlapped image showing internalization of NPs in cells	171
Fig. 7.8	6-Coumarin solution at 30 min in Caco-2 cells (A) Dye solution (B) DAPI stained Nuclei (C) Overlapped image showing less fluorescence in cells	171
Fig. 7.9	6-Coumarin loaded NPs at 60 min in Caco-2 cells; (A) NPs (B) DAPI stained Nuclei (C) Overlapped image showing internalization of NPs in cells	172
Fig. 7.10	6-Coumarin solution at 60 min in Caco-2 cells; (A) Dye solution (B) DAPI stained Nuclei (C) Overlapped image showing less fluorescence in cells	172
Fig. 7.11	6-Coumarin loaded NPs at 90 min in Caco-2 cells; (A) NPs (B) DAPI stained Nuclei (C) Overlapped image showing internalization of NPs in cells	173
Fig. 7.12	6-Coumarin solution at 90 min in Caco-2 cells; (A) Dye solution (B) DAPI stained Nuclei (C) Overlapped image showing internalization of NPs in cells	173
Fig. 7.13	Quantitative cellular uptake of 6-Coumarin solution and 6-Coumarin loaded NPs at (a) 1h (b) 2h (c) 4h	174
Fig. 7.14	Overlay graph of mean fluorescent intensity of 6-Coumarin loaded NPs showing a shift in intensity in comparison to plain dye solution at 1h (A), 2h (B) and 4h(C)	175
Fig. 7.15	Mean fluorescent intensity graphs showing the 6-Coumarin and 6-Coumarin loaded NPs uptake in Caco 2 cells at 1h (A, B), 2h (C,D) and 4h (E,F)	176
Fig. 7.16	<i>In vitro</i> Cytotoxicity of Gemcitabine HCl loaded NPs and plain drug solution on Caco 2 cells at 6h	179
Fig. 7.17	<i>In vitro</i> Cytotoxicity of Gemcitabine HCl loaded NPs and plain	179

	drug solution on Caco 2 cells at 24h	
Fig. 7.18	<i>In vitro</i> Cytotoxicity of Gemcitabine HCl loaded NPs and plain drug solution on K562 cells at 6h	180
Fig. 7.19	<i>In vitro</i> Cytotoxicity of Gemcitabine HCl loaded NPs and plain drug solution on K562 cells at 24h	180
Fig. 7.20	<i>In vitro</i> Cytotoxicity of Gemcitabine HCl loaded NPs and plain drug solution on K562 cells at 48h	180
Fig. 7.21	<i>In vitro</i> Cytotoxicity of Lopinavir loaded NPs and plain drug suspension on Caco 2 cells at 6h	182
Fig. 7.22	<i>In vitro</i> Cytotoxicity of Lopinavir loaded NPs and plain drug suspension on Caco 2 cells at 24h	182
Fig. 8.1(a)	Transverse section of intestine of rat after oral delivery of Rhodamine loaded Nanoparticles (at 10x)	189
Fig. 8.1(b)	Transverse section of intestine of rat after oral delivery of Rhodamine loaded Nanoparticles (at 63x)	189
Fig. 8.1(c)	Negative control, transverse section of intestinal tissue without administration of fluorescent Nanoparticles (at 10x)	190
Fig. 8.1(d)	Transverse section of intestine of rat after oral delivery of 6-Coumarin loaded Nanoparticles (at 10 x)	190
Fig. 8.1(e)	Transverse section of intestine of rat after oral delivery of 6-Coumarin loaded Nanoparticles (at 63x)	191
Fig. 8.2	Plasma concentration time profile of Gemcitabine HCl loaded NPs and plain drug solution in male Wistar rats (n=5) showing the bioavailability enhancement of Nanoparticles	194
Fig. 8.3	Plasma concentration time profile of Lopinavir loaded NPs and plain drug suspension in male Wistar rats (n=5) showing the bioavailability enhancement of nanoparticles	197

List of Abbreviations

DMEM Dulbecco's Minimum Essential Medium

DSC Differential Scanning Calorimetry

EE Entrapment Efficiency

HBSS Hank's Balanced Salt Solution

FBS Fetal Bovine Serum

FTIR Fourier Transform Infra Red spectroscopy

MFI Mean Fluorescence Intensity

MTT Mitochondrial Toxicity

NPs Nanoparticles

PDS Plain Drug Solution

PS Particle Size

RSM Response surface Methodology

TEM Transmission Electron Microscopy

CHAPTER 1

INTRODUCTION

1.1 Introduction

Despite the extensive research and success stories with other routes for drug delivery, the oral route is still the most preferred route because of its basic functionality and the advantages that ensue. Oral delivery is by far the easiest and most convenient way for drug delivery, especially when repeated or routine administration is necessary (Florence and Jani; 1993). But, the challenges associated with oral route include exposure to extreme pH variations, intestinal motility, mucus barrier, P-glycoprotein efflux pump and impermeability of the epithelium (Vincent and Johnny; 2001). Moreover, the gastrointestinal tract provides a variety of barriers to the delivery of drugs, including proteolytic enzymes in gut lumen and on the brush border membrane, mucus layer, gut flora and epithelial cell lining.

One of the most attractive areas of research in drug delivery today is the design of nanosystems that are able to deliver drugs to right place, at appropriate times and at the right dosage. Nanoparticles are solid polymeric colloidal drug carriers ranging from 1 to 1000 nm. Nanoparticulate delivery systems have the potential power to improve drug stability, increase the duration of the therapeutic effect and permits administration through enteral or parenteral administration, which may prevent or minimise the drug degradation and metabolism as well as cellular p-glycoprotein efflux (Ping et al; 2008, Sarmiento et al; 2007).

Nanoparticles have been extensively studied for peroral drug delivery, for systemic effect following uptake from enteron, or to act locally in the gastrointestinal tract. Nanoparticles are expected to address the specific issues for drug delivery like low mucosal permeability, absorption windows, low solubility of the drugs, gut metabolism and first pass effect. The potential advantages of nanoparticles as oral drug carriers are enhancement of bioavailability, delivery of vaccine antigens to the gut associated lymphoid tissues (GALT), controlled release, and reduction of the gastrointestinal irritation caused by drugs (Hariharan et al; 2005). The nanocarriers can improve the oral bioavailability of poorly bioavailable drugs due to their specialised uptake mechanism by preventing first pass metabolism of encapsulated drugs (Bhardwaj et al; 2005).

The nanoparticles by virtue their size and colloidal properties can be targeted to GALT (Gut associated lymphoid tissue) to deliver high loads of drug to lymphatic tissue and then to systemic circulation. The nanoparticles are taken up intact by M cells of peyer's patches in the intestine associated Lymphoid tissue. M cells lack fully developed microvilli in comparison to the neighbouring absorptive cells and deliver the particles taken up to the lymphatics from where they, in a size-dependent manner, are then released into the bloodstream (Ravikumar and Bhardwaj; 2006).

This mechanism provides a chance to target cancers of lymphatics as well as targeting antiretroviral drugs to the viral reservoirs. Furthermore, nanoparticles are capable of sustaining drug release in plasma for longer time period, thus reduces frequency of administration (Sonaje et al; 2007).

Nucleoside analogues, together with nucleobases and nucleotide analogues are commonly used in the treatment of viral infections and cancer. In both cases, they act as antimetabolite agents and interfere with the synthesis of cellular or viral nucleic acids. However the need of high doses due to rapid elimination of these compounds, to their poor activation and /or to their non specific distribution, often leads to side effects, toxicities and resistances.

For anticancer agents, higher toxic levels in blood by infusions and lower levels reaching at lymphatic tumour sites lead to resistances and ineffective therapy. Moreover, many of the most potent anticancer therapies can be administered only by injection, which means that cancer patients must travel to receive their medication. Hence, they prefer oral medicaments and home therapy. Oral chemotherapy is convenient, preferred by the patients and can greatly improve the quality of life of old age patients with advanced or metastatic cancer. Oral chemotherapy can eventually promote a new concept of chemotherapy: "chemotherapy at home" (Yun et al; 2012, Feng et al; 2003).

Unfortunately, orally administered anticancer drugs have little chance to get into the blood system and reach the tumor site due to their pure solubility, stability and permeability. As orally administered anticancer drugs would be eliminated by the first metabolic process with cytochrome P450 and by the efflux pump of P-glycoproteins (P-gp). P450/P-gp suppressors such as cyclosporine A can make oral chemotherapy feasible but they fail the immune system of the patients and thus may cause complex medication problems to the patients (Win and Feng; 2005).

Thus, providing oral delivery of anticancer drugs is a challenge and should provide a long-time, continuous exposure of the cancer cells to the anticancer drugs of a relatively lower thus safer concentration and thus give little chance for the tumour blood vessels to grow, resulting in much better efficacy and fewer side effects.

Researchers have been extensively working for oral delivery of anticancer formulations through nanoparticulate systems. The potential of PLGA nanoparticles of small enough size and appropriate surface coating for oral delivery of anticancer drugs showing enhanced uptake of nanoparticles in Caco-2 cells was proved and studied (Win and Feng; 2005). PLGA/ montmorillonite nanoparticles promoting the oral delivery of paclitaxel were synthesized and evaluated (Dong and Feng; 2005). Bhardwaj et al formulated PLGA nanoparticles for oral delivery of paclitaxel to treat breast cancer (Bhardwaj et al; 2009). Kalaria et al designed PLGA nanoparticles for oral delivery of doxorubicin to improve the bioavailability and found that PLGA nanoparticles have the potential for oral delivery of anticancer drugs (Kalaria et al; 2009). Feng et al formulated docetaxel loaded biodegradable polymeric NPs for oral delivery and improved bioavailability (Feng et al; 2009). Zhang et al formulated nanocarriers to improve oral delivery of anticancer drug and achieved higher drug concentration in tumour (Zhang et al; 2013).

Similarly, for anti-retroviral agents, the reduced bioavailability and short residence time at viral reservoir sites lead to resistance on discontinuation of therapy and inefficient eradication. HIV is able to re-seed the systemic circulation and continue to propagate the infection (Vyas et al; 2008). The combination therapy (HAART) can suppress the HIV replication below the limit of detection in peripheral blood. But it has issues like toxicity, insufficient efficacy, and drug resistance. Moreover, most of antiretroviral drugs suffer from poor solubility, permeability and stability. The major problem with antiviral treatment is to maintain adequate drug levels in the lymphoid tissue which is a major site for storage and replication of virus (Briesen et al; 2000). Main anatomical reservoir sites of HIV include the lymphoid organs (particularly the spleen, lymph nodes, and GALT) and the central nervous system (CNS) [Certain types of lymphoid cells, such as memory CD4+ T lymphocytes are seen in GALT where HIV persists and replicate even after HAART] (Macal et al; 2008, Tincati et al; 2009).

Various nanotechnology based systems are studied extensively by scientists to address the specific issues associated with antiretroviral therapy. Dussere et al (1995) developed a liposomal formulation of foscarnet and found higher drug concentrations with liposomes in lungs and lymph nodes, both the organs are viral reservoir sites. But the main obstacle with liposomal formulations is the physical stability as the systems are digested by physiological enzymes, which would result in immediate release of entrapped drug in the GI tract (Kreuter; 1991).

Alex et al (2011) developed solid lipid nanoparticles of Lopinavir for lymphatic targeting and results showed that the percentage bioavailability was enhanced but the poor drug loading may nevertheless be pointed out as a major drawback in SLN formulations. Polymeric nanoparticles containing antiretroviral drugs can overcome the drawback of physiological stability as well as drug loading. PLGA nanoparticles containing combination of Lopinavir and ritonavir were developed and studied for cytotoxicity (Destache et al; 2009). It has been found that the size of the nanoparticles plays a key role in their adhesion to and interaction with the biological cells. The possible mechanisms for the particles to pass through the gastrointestinal (and other physiological) barriers could be (1) paracellular passage; particles “kneading” between intestinal epithelial cells due to their extremely small size (50 nm); (2) endocytotic uptake—particles absorbed by intestinal enterocytes through endocytosis (particles size 500 nm) (3) lymphatic uptake—particles adsorbed by M cells of the Peyer’s patches (particle size 5 μm) (Florence et al; 1995).

Nanoparticles consisting of synthetic biodegradable polymers, natural biopolymers and polysaccharides have been developed and tested over past decades. Biodegradable polymers may be synthetic or natural in origin. Natural biodegradable polymers include human serum albumin, low-density lipoproteins (LDLs), bovine serum albumin, gelatin, collagen, hemoglobin, polysaccharides like chitosan etc. Today, many synthetic biodegradable polymers are being employed successfully for drug delivery applications. Some synthetic biodegradable polymers are widely used in drug delivery technology are polyesters, polylactic acids, polylactones, poly (amino acids), and polyphosphazenes, Alkylcyanoacrylate, PLGA etc.

Gemcitabine HCl, an anticancer agent, is currently in clinical use for the treatment of several types of cancer. Gemcitabine is a difluoro analog of deoxycytidine.

Unfortunately, the drug is rapidly metabolised with a short plasma half-life and its cytostatic action is strongly exposure-time dependent. It is rapidly and extensively deaminated by cytidine deaminase in blood, liver, kidney and other tissues (Derakhshandeh and Fathi; 2012). In order to achieve the required concentration over sufficient periods of time, repeated application of relatively high doses is required (Vandana and Sahoo; 2010). This, in turn, leads to dose-limiting systemic toxicity. The plasma half life after intravenous infusion is 8- 17 min in human plasma. Therefore, it is required in high doses. Furthermore, Gemcitabine is highly hydrophilic molecule with log P value 1.4 (Trickler et al; 2010). Till now, there is no oral formulation of Gemcitabine HCl in the market. It is available in the market in the freeze-dried form of an aqueous solution of the HCl salt known as Gemzar. After reconstitution Gemzar is used for intravenous administration as an infusion only (EliLilly; 1997).

Lopinavir is a potent protease inhibitor used as a leading component in combined chemotherapy commonly referred as Highly Active Anti-Retroviral Therapy (HAART). Lopinavir has poor oral bioavailability due to poor drug solubility characteristics as well as extensive first pass metabolism, primarily mediated by cytochrome P450 and P-glycoprotein efflux which limits intestinal uptake (Chattopadhyay et al; 2008, Griffin and O Driscoll; 2008 and Jain et al; 2009). In marketed preparations, Lopinavir is always co-administered with ritonavir, as ritonavir inhibits the cytochrome P450 enzyme, responsible for extensive first pass metabolism (Prot et al; 2006).

1.2 Aims and Objectives

The present investigation was aimed at development and characterization of PLGA nanoparticles of Gemcitabine HCl and Lopinavir for oral delivery with the following objectives:

- To formulate and optimize orally delivered nanoparticles of Gemcitabine HCl and Lopinavir, capable of absorption through M cell of Peyer's patches in intestine, therefore, bypassing presystemic hepatic metabolism and enhancing the bioavailability of drugs.
- To prove the utility of PLGA nanoparticles in improving oral bioavailability of anticancer drug and antiretroviral drug.

- To enhance the absorption of drugs by entrapping in nanocarrier, so that Gemcitabine HCl could be administered orally and Lopinavir could be administered alone without need of Ritonavir.
- To compare the prepared nanoparticulate systems with respect to ease of formulation, characterization, *in vitro* and *ex vivo* drug release, *in vitro* cell uptake and transport studies in Caco 2 cells, cytotoxicity studies, stability and *in vivo* performance viz. pharmacokinetic studies.

Hypothesis: Nanoparticles of biodegradable polymers may provide an alternative solution for **oral delivery of anticancer drugs and targeting anti-retroviral drugs** to the intestinal lymphatic tissue with tumour sites and high viral load respectively across the gastrointestinal barrier due to their extremely small size and their appropriate surface coating to escape from the recognition by P450/P-gp. Further, nanoparticles have the ability to circumvent the p-glycoprotein efflux which is present on the membranes of HIV reservoir cells as well as intestinal epithelial cells. This in turn, increases the absorption as well as target the antiretroviral drug to HIV reservoir sites and anticancer drugs to lymphatic tumours as well as systemic circulation.

It was hypothesized that PLGA nanoparticles would be absorbed through the M-cells of the Peyer's patches and then undergo lymphatic uptake, thereby bypassing liver metabolism and increasing bioavailability of the drug. Moreover, reach the lymphatic sites directly before reaching the systemic circulation.

1.3 Plan of Work

1. Literature survey, procurement of APIs and excipients.
2. Preformulation studies – Screening of excipients and characterization of API.
3. Analytical methods.
4. Formulation of Nanoparticles by multiple emulsification and nanoprecipitation method.
5. Optimization of process and formulation variables by factorial design.
6. Characterization (Particle size, Zeta potential, TEM, DSC and FTIR) and *in vitro* and *ex vivo* drug release studies of formulation in comparison with plain drug solutions.

7. *In vitro* cell line studies: quantitative uptake studies by FACS and qualitative uptake studies by confocal laser microscope, transport/ permeability studies in Caco 2 cells and cytotoxicity studies by MTT assay in K562 cell lines.
8. Stability studies – Short term stability studies as per ICH guidelines.
9. *In vivo* absorption and pharmacokinetic studies of Gemcitabine HCl loaded PLGA nanoparticles.
10. *In vivo* absorption and pharmacokinetic studies of Lopinavir loaded PLGA nanoparticles.

1.4 References

- ❖ Alex A, Chacko AJ, Jose S, Souto EB. Lopinavir loaded solid lipid nanoparticles (SLN) for intestinal lymphatic targeting. *Eur J Pharm Sci*, 42, 2011, 11–18.
- ❖ Bhardwaj V, Hariharan S, Bala I, Lamprecht A, Kumar R. Pharmaceutical aspects of polymeric nanoparticles for oral delivery. *J Biomed Nanotech*, 1, 2005, 235-258.
- ❖ Bhardwaj V, Ankola DD, Gupta SC, Schneider M, Lehr CM, Kumar, MNV. PLGA nanoparticles stabilized with cationic surfactant: safety studies and application in oral delivery of paclitaxel to treat chemical-induced breast cancer in rat. *Pharm Res*, 26(11), 2009, 2495-2503.
- ❖ Chattopadhyay N, Zastre J, Wong HL, Wu XY, Bendayan R. Solid lipid nanoparticles enhance the delivery of the HIV protease inhibitor, atazanavir, by a human brain endothelial cell line. *Pharm Res*, 25, 2008, 2262–2271.
- ❖ Derakhshandeh K and Fathi S. Role of chitosan nanoparticles in the oral absorption of Gemcitabine. *International Journal of Pharmaceutics*, 437(1–2), 2012, 172-177.
- ❖ Destache CJ, Todd B, Christensen K, Shibata A, Sharma A, Dash A. Combination antiretroviral drugs in PLGA nanoparticle for HIV-1. *BMC Infectious Diseases*, 9, 2009, 198.
- ❖ Dusserre N, Lessard C, Paquette N, Perron S, Poulin L, Tremblay M, Beauchamp D, Désormeaux A, Bergeron MG. Encapsulation of foscarnet in liposomes modifies drug intracellular accumulation, *in vitro* anti-HIV-1 activity, tissue distribution and pharmacokinetics. *AIDS*, 9(8), 1995, 833-841.
- ❖ Dong Y and Feng SS. Poly(d,l-lactide-co-glycolide)/montmorillonite nanoparticles for oral delivery of anticancer drugs. *Biomaterials*, 26(30), 2005, 6068-6076.
- ❖ Eli Lilly. Summary of Product Characteristics: Gemcitabine, UK Prescribing Information. Eli Lilly Co. 1997.
- ❖ Feng SS, Chein S. Chemotherapeutic engineering: application and further development of chemical engineering principles for chemotherapy of cancer and other diseases. *Chem Eng Sci*, 58, 2003, 4087–114.
- ❖ Feng SS, L. Mei, Anitha P, Gan CW, Zhou W. Poly(lactide)-vitamin E derivative/montmorillonite nanoparticle formulations for the oral delivery of Docetaxel. *Biomaterials*, 30(19), 2009, 3297-3306.

- ❖ Florence AT. Nanoparticles uptake by the oral route; fulfilling its potential. *Drug Disc Today Tech*, 2, 2005, 75-81.
- ❖ Florence AT, Hillery AM, Hussain N, Jani PU. Nanoparticles as carriers for oral peptide absorption: studies on particle uptake and fate. *J Control Release*, 36, 1995, 39-46.
- ❖ Florence AT, Jani PU. Particulate delivery: the challenge of the oral route. In A. Rolland (Ed.), *Pharmaceutical Particulate Carriers: Therapeutic Applications*, Marcel Dekker: New York, 1993, 65-107.
- ❖ Griffin BT, O Driscoll CM. An examination of the effect of intestinal first pass extraction on intestinal lymphatic transport of saquinavir in the rat. *Pharm Res*, 25, 2008, 1125-1133.
- ❖ Hariharan S, Bharadwaj V, Bala I, Sitterberg J, Bakowsky U, Kumar R. Design of estradiol loaded PLGA nanoparticulate formulations: a potential oral delivery system for hormone therapy. *Pharm Res*, 23, 2005, 184-195.
- ❖ Jain V, Prasad V, Jadhav P, Mishra PR. Preparation and performance evaluation of saquinavir laden cationic submicron emulsions. *Drug Deliv*, 16, 2009, 37-44.
- ❖ Kalaria D, Sharma RG, Beniwal V, Ravi Kumar MNV. Design of biodegradable nanoparticles for oral delivery of doxorubicin: *in vivo* pharmacokinetics and toxicity studies in rats. *Pharm Res*, 26(3), 2009, 492-501.
- ❖ Kreuter. Peroral administration of nanoparticles. *Adv Drug Deliv Rev*, 7, 1991, 71-86.
- ❖ Macal M., et al. Effective CD4+ T-cell restoration in gut-associated lymphoid tissue of HIV-infected patients is associated with enhanced Th17 cells and polyfunctional HIV-specific T-cell responses. *Mucosal Immunol*, 1, 2008, 475-488.
- ❖ Ping Li, Dai YN, Zhang, JP, Wang AQ. Chitosan-alginate nanoparticles as a novel drug delivery system for nifedipine. *Int J Biomed Sci*, 2008, 221-228.
- ❖ Prot M, Heripret L, Cardot-Leccia N, Perrin C, Aouadi M, Lavrut T, Garraffo R, Dellamonica P, Durant J, Marchand-Brustel LY, Binetruy B. Long-term treatment with lopinavir-ritonavir induces a reduction in peripheral adipose depots in mice. *Antimicrob Agents Chemother*, 50, 2006, 3998-4004.
- ❖ Ravi Kumar MNV, Bhardwaj V. Polymeric Nanoparticles for Oral Delivery. In *Nanoparticle Technology for Drug Delivery*, Taylor and Francis, 159, 2006, 230-240.

- ❖ Sarmiento B, Riberio AJ, Veiga F, Ferrera DC. Insulin loaded nanoparticles are prepared by alginate ionotropic gelation followed by chitosan polyelectrolyte complexation. *J Nanosci Nanotech*, 7, 2007, 2833-2841.
- ❖ Sonaje K, Italia JL, Sharma G, Bhardwaj V, Kumar R. Development of biodegradable nanoparticles for oral delivery of ellagic acid and evaluation of their antioxidant efficacy against cyclosporine induced nephrotoxicity in rats. *Pharm Res*, 24(5), 2007, 899-910.
- ❖ Tincati C, Biasin M, Bandera A, Violin M, Marchetti G, Piancintini L, Vago L, Balotta C, Maroni M, Franzetti F. Early initiation of highly active antiretroviral therapy fails to reverse immunovirological abnormalities in gut-associated lymphoid tissue induced by acute HIV infection. *Antivir Ther*, 14(3), 2009, 321-30.
- ❖ Trickler WJ, Khurana J, Nagvekar AA, Dash AK. Chitosan and glyceryl monooleate nanostructures containing gemcitabine: potential delivery system for pancreatic cancer treatment. *AAPS PharmSciTech* 11(1), 2010, 392-401.
- ❖ Vandana, M. and S. K. Sahoo. Long circulation and cytotoxicity of PEGylated gemcitabine and its potential for the treatment of pancreatic cancer. *Biomaterials* 31(35), 2010, 9340-9356
- ❖ Vincent L, Johnny Y. Oral Drug Delivery. In Hillery AM, Loyd AW, Swarbrick J (Ed) *Drug Delivery and Targeting for Pharmacists and Pharmaceutical Scientists*, Taylor and Francis, 2001, 132-167.
- ❖ Vyas TK, Amiji M, Shahiwala A. Improved oral bioavailability and brain transport of saquinavir upon administration in novel nanoemulsion formulations. *Int J Pharm*, 347, 2008, 93-101.
- ❖ Von Brissen H, Ramge P, Kreuter J. Controlled release of antiretroviral drugs. *AIDS review*, 2, 2000, 231-38.
- ❖ Win KY, Feng SS. Effects of particle size and surface coating on cellular uptake of polymeric nanoparticles for oral delivery of anticancer drugs. *Biomaterials*, 26(15), 2005, 2713-2722.
- ❖ Yun Y, Cho Y W, Park K. Nanoparticles for oral delivery: Targeted nanoparticles with peptidic ligands for oral delivery, *Adv Drug Deliv Reviews*, 2012.
- ❖ Zhang, Z., Ma Li, Jiang S, Zeying L, Jian H. Chen L, Yu H, Yaping L. A self-assembled nanocarrier loading teniposide improves the oral delivery and drug concentration in tumor. *J Control Release*, 166(1), 2013, 30-37.

CHAPTER 2

LITERATURE REVIEW

2. Oral Drug Delivery

Oral drug delivery is the choicest and most readily accepted form of drug administration because of its non-invasive nature. It is preferred because of the various advantages over other routes of drug delivery. The oral route presents the advantage of avoiding pain and discomfort associated with injections as well as eliminating contaminations. The other advantages include patient convenience and compliance, which increase the therapeutic efficacy of the drug. Oral formulations are also cheaper to produce because they do not need to be manufactured under sterile conditions (Salama et al; 2006).

Despite these potential advantages, oral formulations face several common problems: (i) poor stability in the gastric environment, (ii) poor bioavailability and (iii) the mucus barrier can prevent drug penetration and subsequent absorption. Many drugs are currently used as parenteral formulations because of their poor oral bioavailability. This is due to several unfavourable physicochemical properties, such as large molecular size, susceptibility to enzymatic degradation, poor stability in the gastric low pH environment, poor penetration of the intestinal membrane, short plasma half-life, immunogenicity, and the tendency to undergo aggregation, adsorption, and denaturation, enzymatic degradation prior to absorption and poor penetration of the intestinal membrane (Yun et al; 2012).

For many years, many studies have been focused on the improvement of oral delivery and bioavailability of drugs. One of the approaches to overcome various limitations associated with oral delivery is nanoparticle formulation that encapsulates and protects drugs and releases them in a temporally or spatially controlled manner. The nanoparticle surface can also be modified to enhance or reduce bioadhesion to target specific cells. Polymeric nanoparticles are of especial interest from the pharmaceutical point of view. First, they are more stable in the gastrointestinal tract than other colloidal carriers, such as liposomes, and can protect encapsulated drugs from gastrointestinal environment. Second, the use of various polymeric materials enable the modulation of physicochemical characteristics (e.g. hydrophobicity, zeta potential), drug release properties (e.g. delayed, prolonged, triggered), and biological behaviour (e.g. targeting, bioadhesion, improved cellular uptake) of nanoparticles (Florence; 1997). Third, their submicron size and their large specific surface area favour their absorption compared

to larger carriers. Also, the particle surface can be modified by adsorption or chemical grafting of certain molecules such as poly (ethylene glycol) (PEG), poloxamers, and bioactive molecules (lectins, invasins).

Nanoparticles

Nanoparticles as a carrier or a device have become the focus of attention in this field recently. The nanoparticles possess certain advantages such as greater stability during storage, stability *in vivo* after administration and ease of scale-up without an aseptic process for oral administration (Kreuter; 1995).

Nanoparticles are defined as particulate dispersions or solid particles with a size in the range of 10-1000nm. The drug is dissolved, entrapped, encapsulated or attached to a nanoparticle matrix. Depending upon the method of preparation, nanoparticles, nanospheres or nanocapsules can be obtained. The major goals in designing nanoparticles as a delivery system are to control particle size, surface properties and release of pharmacologically active agents in order to achieve the site-specific action of the drug at the therapeutically optimal rate and dose regimen. This system also helps to increase the stability of drugs/proteins and possess useful controlled release properties (Mohanraj and Chen; 2006).

The advantages of using nanoparticles as a drug delivery system includes:

1. Particle size and surface characteristics of nanoparticles can be easily manipulated to achieve both passive and active drug targeting after parenteral administration.
2. They control and sustain release of the drug during the transportation and at the site of localization, altering organ distribution of the drug and subsequent clearance of the drug so as to achieve increase in drug therapeutic efficacy and reduction in side effects.
3. Controlled release and particle degradation characteristics can be readily modulated by the choice of matrix constituents. Drug loading is relatively high and drugs can be incorporated into the systems without any chemical reaction; this is an important factor for preserving the drug activity.
4. Site-specific targeting can be achieved by attaching targeting ligands to surface of particles or use of magnetic guidance.

5. The system can be used for various routes of administration including oral, nasal, parenteral, intra-ocular etc.

In spite of these advantages, nanoparticles do have limitations. For example, their small size and large surface area can lead to particle- particle aggregation, making physical handling of nanoparticles difficult in liquid and dry forms. In addition, small particles size and large surface area readily result in limited Poor drug loading, which is usually less than 5% (weight % of the transported drug with respect to the carrier material). As a result, either the quantity of the drug administered is not sufficient to reach a pharmacologically active concentration in the body, or the amount of the carrier material required is too great, leading to toxicity or undesirable side-effects , as well as, too rapid release (so called “burst release”) of the encapsulated drug after administration. As a consequence, a significant fraction of the drug will be released before reaching its pharmacological target in the body, leading to lower activity and more side-effects. These practical problems have to be overcome before nanoparticles can be use clinically or made commercially available (Couvreur; 2013).

Nanoparticles have versatile potential for efficient exploitation of different drug delivery formulations and routes because of the properties provided by their small size. These possible benefits include controlled release, protection of the active pharmaceutical ingredient and drug targeting. Nanoparticles are expected to offer new solutions e.g. for gene therapy and delivery of peptide drugs. Generally, nanoparticles are applied as an injectable or oral solution, but their use as dried material in formulations such as tablets or inhalable powders is equally conceivable (Langer et al; 2000, Lee et al; 2005).

Pharmaceutical nanoparticles are submicron-sized, colloidal vehicles that carry drugs to the target or release drugs in a controlled way in the body. Nanoparticles are usually dispersed in liquid. Such a system can be administered to humans for example by injection, by the oral route, or used in ointments and ocular products. Alternatively, nanoparticles can be dried to a powder, which allows pulmonary delivery or further processing to tablets or capsules (Vila et al; 2002).

2.1. Physiological Considerations of Gastro-intestinal Tract for Oral Delivery of Nanoparticles:

The gastrointestinal tract is a continuous tube-like structure beginning with the mouth (oral cavity) and extending further as pharynx, esophagus, stomach, small intestine, large intestine, rectum and finally culminating into the anal canal.

The human intestinal epithelium is highly absorptive and is composed of villi that increase the total absorptive surface area in the gastrointestinal (GI) tract to 300–400 m² (Ensign et al; 2012). Enterocytes (absorptive) and goblet cells (mucus secreting) cover the villi, which are interspersed with Follicle Associated Epithelium (FAE). These lymphoid regions, Peyer's patches, are covered with M cells specialized for antigen sampling. M cells are significant for drug delivery, since they are relatively less protected by mucus and have a high transcytotic capacity (Plapied et al; 2011).

Figure 2.1 provides a quick understanding of the GI targets, principles of formulation development that could be utilized and the application opportunities of the nanoparticles-based drug delivery system throughout the GIT (Amiji et al; 2006). Different types of cells and structures compose the intestinal epithelium. Epithelium of villi is mainly constituted of enterocytes and goblet cells. One of the main functions of enterocytes is to control the passage of macromolecules and pathogens, and, at the same time, to allow the digestive absorption of dietary nutrients. Goblet cells secrete the mucus gel layer, a viscous fluid composed primarily of highly glycosylated proteins (mucins) suspended in a solution of electrolytes. Dispersed through the intestinal mucosa, lymphoid nodules called O-MALT (Organized Associated Lymphoid Mucosa), individually or aggregated into Peyer's patches, have interested scientists, mainly due to the presence in these structures of particular cells, named M cells (Gebert et al; 1996). M cells are mainly located within the epithelium of Peyer's patches, called Follicle Associated Epithelium (FAE) (Fig. 2.2), which is also composed of enterocytes and few goblet cells. M cells deliver samples of foreign material from the lumen to the underlying organized mucosa lymphoid tissues in order to induce immune responses. (Anne et al; 2006)

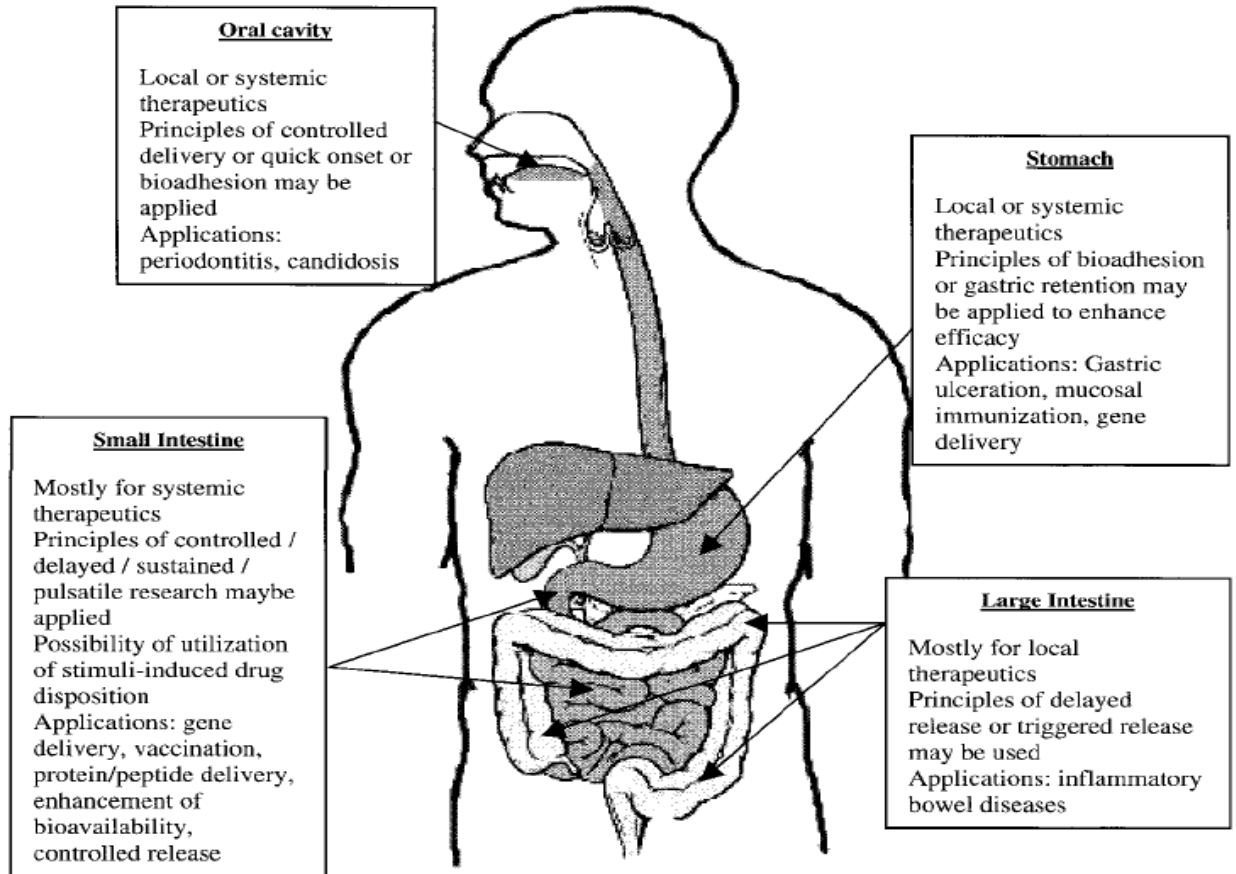


Fig. 2.1 GIT targets, formulation principles, opportunities and applications

M cells are specialized for antigen sampling, but they are also exploited as a route of host invasion by many pathogens. Furthermore, M cells represent a potential portal for oral delivery of peptides and proteins and for mucosal vaccination, since they possess a high transcytotic capacity and are able to transport a broad range of materials, including nanoparticles. Uptake of particles, microorganisms and macromolecules by M cells, have been described to occur through adsorptive endocytosis by way of clathrin coated pits and vesicles, fluid phase endocytosis and phagocytosis. In addition, M cells, compared with normal epithelial cells have reduced levels of membrane hydrolase activity, which can influence the uptake of nanoparticles. The relatively sparse nature of the glycocalyx facilitates the adherence of both microorganisms and inert particles to their surfaces. Villous-M cells located outside the FAE have been also observed, but the transport of antigens and microorganisms across the intestinal mucosa is carried out mainly by the FAE-M cells. Although less numerous than enterocytes, M cells present

enhanced transcytosis abilities which made them very interesting for oral drug delivery applications (Florence; 2005).

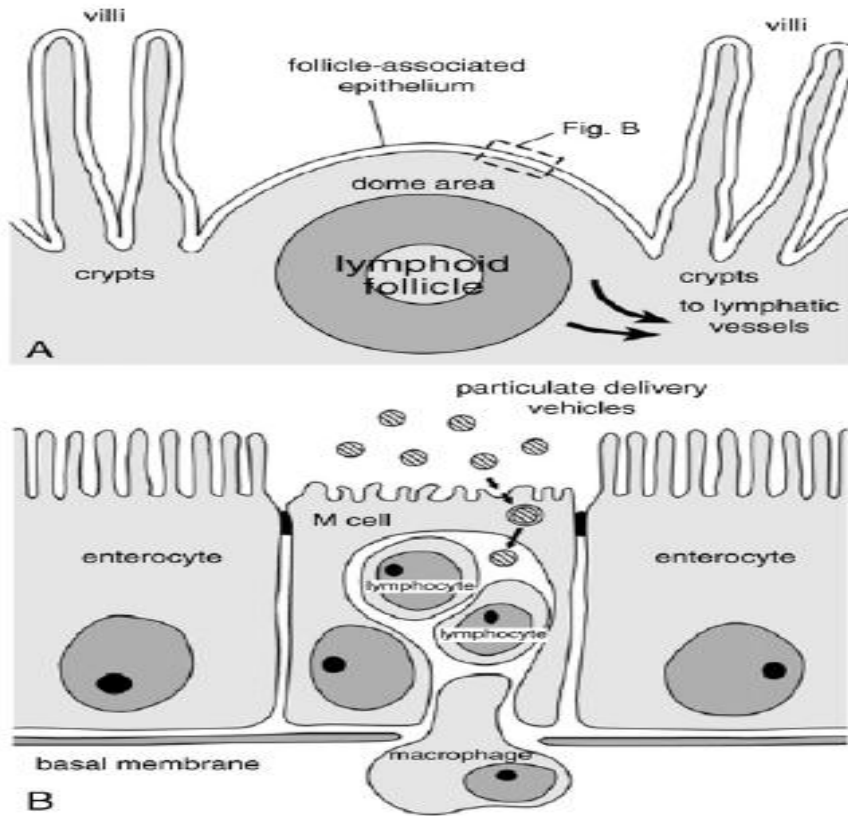


Fig. 2.2 Schematic transverse sections of a Peyer's patch lymphoid follicle and overlying follicle-associated epithelium (FAE), depicting M cell transport of particulate delivery vehicles

The general structure of intestinal organized mucosa-associated lymphoid tissues (O-MALT) is represented by the schematic transverse section of a Peyer's patch lymphoid follicle and associated structures in (A). The FAE is characterized by the presence of specialized antigen sampling M cells (B) (Reprinted from *Adv. Drug. Del. Rev.*, 50, 2001, Clark et al., Exploiting M cells for drug and vaccine delivery, 81–106.)

2.2 Transport of Nanoparticles across the Intestinal Mucosa:

There are four distinct mechanisms for molecules to cross the cell membrane: via paracellular, transcellular, carrier-mediated, and receptor-mediated transport. Absorption through each pathway is dependent on different physical characteristics,

such as molecular weight, hydrophobicity, ionization constants, and pH stability of absorbing molecules as well as biological barriers that restrict protein absorption from the GI tract. To deliver their drug content in the blood, lymph, or target organs, NPs have to cross the gastrointestinal barrier either by passive diffusion via transcellular or paracellular pathways or by active processes mediated by membrane-bound carriers or membrane-derived vesicles.

A schematic diagram of uptake mechanisms of NPs administered orally is shown in Fig. 2.3 (Vivekananda et al; 2007)

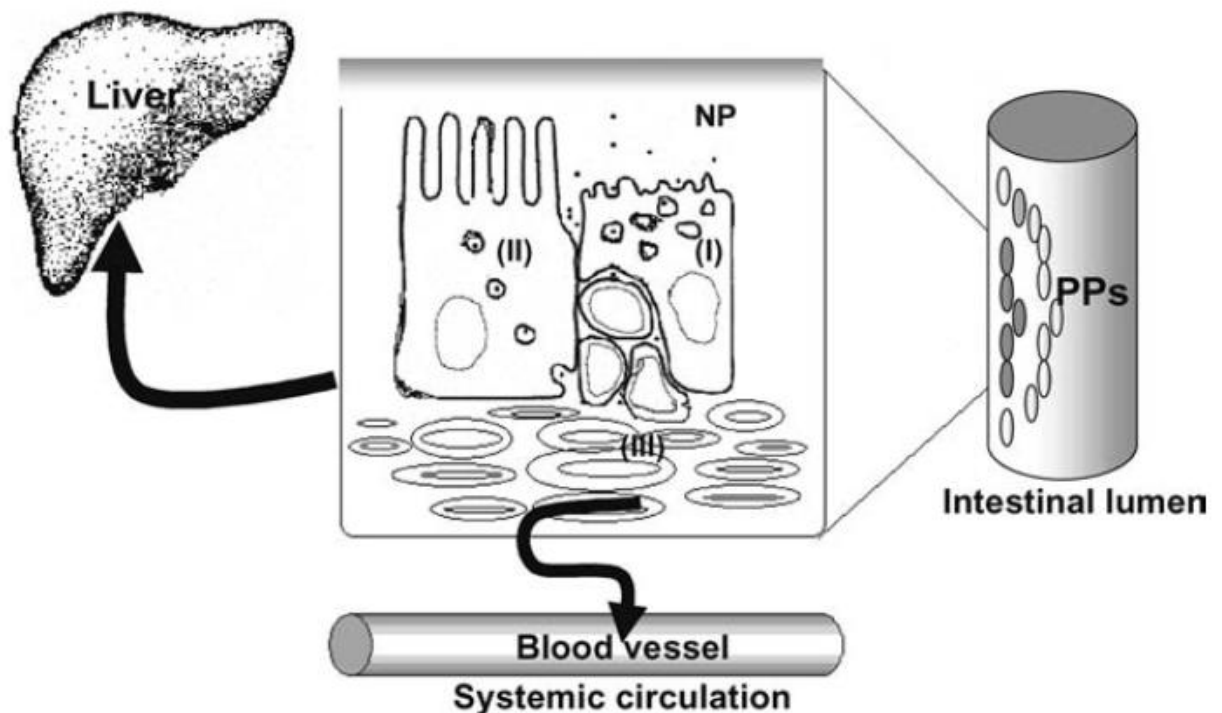


Fig. 2.3 Mechanism of uptake of orally administered NPs: (I) M cells of the PP, (II) enterocytes, and (III) GALT

The direct uptake of NPs through the lymph into the systemic circulation bypassing the liver reduces the first pass metabolism, thus improving bioavailability (Vivekananda et al; 2007).

2.2.1 Paracellular Transport:

Paracellular transport is the pathway of substances across an epithelium by passing through the intercellular spaces in between epithelial cells. Paracellular transport is passive and results from diffusion. This transport is under the control of tight junctions. A tight junction constitutes the major rate limiting barrier towards the paracellular

transport for permeation of ions and larger substances (Madara; 1998). The dimension of the paracellular space is on the order of 10 Å. The average size of aqueous pores created by epithelial tight junctions is approximately 7–9 Å for the jejunum, 3–4 Å for the ileum, and 8–9 Å for the colon in the human intestine. The solutes with a molecular radius exceeding 15 Å (approximately 3.5 kDa) cannot be transported via this route. Furthermore, tight junctions comprise only about 0.01% of the total absorption surface area of the intestine (Rubas et al; 1996). In physiological conditions, the paracellular route is limited, on one hand, by the very small surface area of the intercellular spaces and, on the other hand, by the tightness of the junctions between the epithelial cells (pore diameter between 3 and 10 Å). Paracellular transport can be enhanced by some polymers in solution or in the form of nanoparticles. Chitosan and poly (acrylic acids) in solution can enhance paracellular transport of drugs through interactions between the negatively-charged cell membrane and the positive charges of the polymer, or by complexing Ca^{2+} involved in the structure of tight junctions (Shakweh et al; 2004, Smith et al; 2004).

2.2.2 Transcellular Transport:

Transcellular transport occurs through the intestinal epithelial cells by transcytosis, a particular process by which particles are taken up by cells. A typical example is the movement of glucose from the intestinal lumen to extracellular fluid by epithelial cells. This starts with an endocytic process that takes place at the cell apical membrane. Then, particles are transported through the cells and released at the basolateral pole.

The basolateral membrane is thinner and more permeable than the apical membrane because the protein-to-lipid ratio is very low in the basolateral membrane. Transport of particles by the transcellular transport depends on several factors: (i) various physicochemical properties of particles, such as size, lipophilicity, hydrogen bond potential, charge, surface hydrophobicity or the presence of a ligand at the particle surface; (ii) the physiology of the GI tract; Enterocytes and M cells are the primary intestinal cells for transport (Florence; 2004). Furthermore, M cells represent a potential portal for oral delivery of proteins and peptides due to their high endocytosis ability. M cells possess a high transcytotic capacity and transport a wide variety of materials, including nanoparticles. M cells take up macromolecules, particles and

microorganisms by adsorptive endocytosis via clathrin-coated pits and vesicles, fluid phase endocytosis and phagocytosis. Although there has been some controversy in the literature on the extent of particle absorption, there is evidence that particle translocation can occur across enterocytes in the villi part of the intestine (Jani et al; 1992). However, the number of particles translocated through these routes is mostly very low because of the low endocytic activity of the enterocytes. It has been generally observed that the bulk of particle translocation mainly occurs in FAE (Lavelle et al; 1995, Hagan et al; 1990). As a result, many researchers have studied with great interest the Peyer's patches and M cells which have adapted to absorb a large range of materials. Nevertheless, this route is limited to the transport of relatively low molecular-weight lipophilic drugs. Transcellular transport of nanoparticles occurs by transcytosis, a particular process by which particles are taken up by cells. This begins with an endocytic process that takes place at the cell apical membrane. Then, particles are transported through the cells and released at the basolateral pole (Shakweh et al; 2005) Figure 2.4 shows the different pathways taken up by the drug to cross intestinal barrier.

2.2.3 Carrier Mediated Transport

Drugs are transferred across the cell membrane or entire cell and then released from the basal surface of the enterocyte into circulation. The process is suitable and utilized by small hydrophilic molecules. Active absorption requires energy-dependent uptake of specific molecules by carriers (Russell; 1996). The carriers recognize target molecules through membrane receptors and transport them across the membranes into the GI epithelium, even against the concentration gradient and in trace quantities. For example, small di/tripeptides (including β -lactam antibiotics and angiotensin converting enzyme (ACE) inhibitors), monosaccharides, and amino acids are transported transcellularly by a carrier-mediated transport process. Shah and Shen investigated the carrier-mediated transport of insulin across Caco-2 cell monolayers.

2.2.4 Receptor Mediated Transport

In receptor-mediated transport, protein drugs act either as a receptor specific ligand for surface-attached receptors or as a receptor for surface-attached ligands. Receptor-mediated transport has also been exploited to increase the oral bioavailability of

protein and drugs by modification such as receptor specific ligands with peptide and protein drugs. This transportation entails cell invagination, which leads to formation of a vesicle. This transportation, in general, is known as endocytosis and comprises phagocytosis, pinocytosis, receptor-mediated endocytosis (clathrin-mediated), and potocytosis(nonclathrin-mediated). After protein drugs are transported to the GI tract, they take access to the systemic circulation via two separate and functionally distinct absorption pathways: portal blood and the intestinal lymphatics. The physicochemical and metabolic features of the protein drug and the characteristics of the formulation largely control the relative proportion of protein drug absorbed via these two pathways. Portal blood represents the major pathway for the majority of orally administered protein drugs. During this process, hydrophilic ligands are carried to the liver via the hepatic portal vein, and then by the hepatic artery gain access to the systemic circulation, for subsequent delivery to their sites of action. On the other hand, highly lipophilic ligands ($\log P > 5$) that cross the same epithelial barrier are transported to the intestinal lymphatics, which directly deliver them to the vena cava, thereby bypassing the hepatic first-pass metabolism

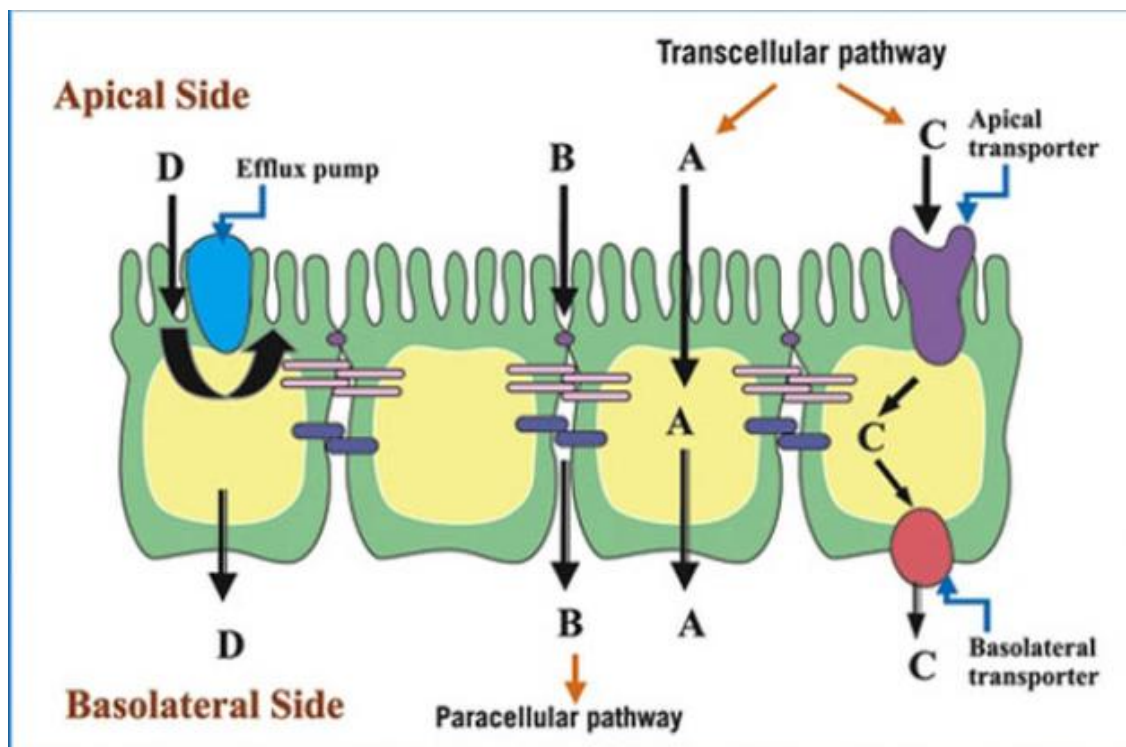


Fig. 2.4 The pathways that a drug can take to cross the intestinal mucosal barrier Pathway, A is the transcellular route in which a drug passively permeates the cell

membranes. Pathway B is the paracellular route; the drug passively diffuses via the intercellular junctions. Pathway C is the route of active transport of the drug by transporters. Pathway D is the route of drug permeation that is modified by efflux pumps (Wang et al; 2005).

2.3 Nanoparticles for Anticancer Drug Delivery

To deliver therapeutic agents to tumor cells *in vivo*, one must overcome the following problems: (i) drug resistance at the tumor level due to physiological barriers (non cellular based mechanisms), (ii) drug resistance at the cellular level (cellular mechanisms), and (iii) distribution, biotransformation and clearance of anticancer drugs in the body.

A strategy could be to associate antitumor drugs with colloidal nanoparticles, with the aim to overcome non-cellular and cellular based mechanisms of resistance and to increase selectivity of drugs towards cancer cells while reducing their toxicity towards normal tissues. If designed appropriately, nanoparticles may act as a drug vehicle able to target tumor tissues or cells, to a certain extent, while protecting the drug from premature inactivation during its transport. Indeed, at the tumor level, the accumulation mechanism of nanoparticles relies on a passive diffusion or convection across the leaky, hyper permeable tumor vasculature. The uptake can also result from a specific recognition in case of ligand decorated nanoparticles ('active targeting'). Moreover, nanoparticles may also act at the cellular level. They can be endocytosed/phagocytosed by cells, with a resulting cell internalization of the encapsulated drug. Nanoparticles were also found to be able to overcome MDR resistance, which is due to the presence of the P-glycoprotein efflux system localized at the cancerous cell membrane (Brigger et al; 2012).

Today, most of the anticancer drugs are administered through i.v. injection or infusion. Such a way causes high peak above the maximum tolerable concentration (MTC) of the drug in the plasma and then fast excretion of the drug from the circulation system, resulting in a limited area-under the- curve (AUC), which is a quantitative measurement of the therapeutic effects, and a large part of AUC would be associated with high drug concentration above MTC, thus causing serious side effects. Instead, **oral**

chemotherapy could maintain a sustained moderate concentration of the drug in the circulation to achieve a prolonged exposure of cancerous cells to the drug as well as to avoid high peak above MTC. This will increase the therapeutic efficacy and decrease the side effects. Oral chemotherapy is a key step towards “Chemotherapy at Home”, a dream of cancer patients, which will radically change the clinical practice of chemotherapy and greatly improve the quality of life of the patients. Moreover, oral chemotherapy can provide an easy way for the patients to take the drug by themselves at home. This will greatly reduce their medical expenses and improve their quality of life. Oral chemotherapy is especially important for cancer patients at the latest stage, who are too weak to withstand harsh medical treatment. Oral chemotherapy can provide at least a palliative treatment to give them hope for survival prolongation (Mei et al; 2013, Feng et al; 2011).

Unfortunately, most anticancer drugs especially those with excellent anticancer effects such as Taxanes (paclitaxel and docetaxel) are not orally bioavailable, i.e., not absorbable/interactive in the gastrointestinal (GI) tract. For example, the oral bioavailability of paclitaxel has been found less than 1%. It is well-known that our body is so perfectly structured that all important organs are protected from external toxins by the so-called physiological drug barriers such as the gastrointestinal barrier (GI barrier) and the blood–brain barrier (BBB). The molecular basis of the various physiological drug barriers has been intensively investigated in the past decades and the various solutions including the various medical solutions and pharmaceutical nanotechnology solutions have thus developed (Farokhzad and Langer;2009).

For oral bioavailability of Taxanes, which are the #1 seller among the various anticancer drugs and had \$3.5 billion annual sale in the world market, an intensive investigation showed that orally administrated anticancer drugs such as paclitaxel would be eliminated from the first-pass extraction by the cytochrome P450-dependent metabolic processes and the over expression of plasma membrane transporter P-glycoprotein (P-gp) in the involved physiological systems especially intestine, liver, kidney (Mei et al; 2013).

Research work using wild-type and P-glycoprotein knock-out mice has shown the role of P-gp in multi-drug resistance and enhancing the bioavailability of paclitaxel and other anticancer drugs. Measurements of paclitaxel concentration in the plasma after oral

administration indicated that the area-under-the-curve (AUC) of the drug concentration in the plasma versus time was 6-fold higher for the P-gp knock-out mice than that for the wild-type mice. After intravenous administration of paclitaxel, the AUC was only 2-fold higher in the P-gp knock-out mice compared to the wild-type. Many anticancer drugs are substrates by P-gp. P-gp transporter impedes the permeability of drugs through physiological barriers producing limited pharmacological response (Malingre et al; 2001)

Thus, the inhibition of this efflux pump is also a common strategy to overcome the low oral bioavailability of many anticancer drugs. Inhibition of P-gp may be tackled by (i) co-administration of drugs known as P-gp substrates in order to act as inhibitors of the transporter, (ii) development of novel drugs that are non P-gp substrates, and (iii) design of novel delivery systems that allow the drug to bypass efflux pump transport.

The most popular and prospective strategies used in pharmaceutical cancer nanotechnology include prodrugs, nanoemulsions, dendrimers, micelles, liposomes, solid lipid nanoparticles and nanoparticles of biodegradable polymers for controlled, sustained and targeted drug delivery across the various physiological drug barriers including the gastrointestinal barrier for oral chemotherapy (Feng et al; 2009).

The use of biodegradable polymeric nanoparticles for oral drug delivery has shown significant therapeutic potential for cancer treatment. Polymeric nanoparticles that combine bioadhesive properties with a certain inhibitory activity of the cytochrome P-450 complex and P-gp efflux system and thus promote drug permeability across the mucosal membrane can be an adequate strategy for oral chemotherapy. Another advantage from these polymeric nanoparticles can be their inherent properties to control the release of the incorporated drug, which may be of interest to obtain sustained release of the drug.

Biodegradable polymers and phospholipids are the two most important materials that have been widely used in development of the nanoparticle-based drug delivery systems for oral chemotherapy.

Biodegradable polymers can be seen as a special kind of excipients for drug formulation, which carry the drug, improve its pharmaceutical properties and enhance its ADME process, thus strongly influencing PK or/and PD of the drug. They are biodegradable and thus can be easily eliminated from the body after fulfilling their task

as a drug carrier. Various FDA approved biodegradable and biocompatible polymers are used most often in the research of polymeric nanoparticle-based drug delivery systems include poly (lactic acid) (PLA), poly (lactic-co-glycolic acid) PLGA), poly(ϵ -caprolactone) (PCL), etc. However, they are highly hydrophobic and thus not friendly to hydrophilic drugs such as peptides and proteins. They are too strong in mechanical strength and their degradation rates are too slow, thus resulting in too slow drug release to meet the therapeutic needs. Moreover, nanoparticles made from those polymers are hard to be directly conjugated to hydrophilic targeting ligands, for which amphiphilic linker molecules are needed, causing complications in targeting technology. Since it usually takes quite a long time to develop a new biomaterial and have it approved for clinical use, two simple and practical strategies have been adopted to solve this problem. One is to coat the nanoparticles by hydrophilic polymer such as PEG, Chitosan and TPGS, and the other is to synthesize copolymers to incorporate hydrophilic elements in the hydrophobic chains of the polymers. It is well known that drug conjugation to polyethylene glycol (PEG) or formulated in PEG copolymer nanocarriers can enhance its solubility, permeability, stability and thus oral bioavailability (Zhang et al; 2012, Arima et al; 2001).

2.4 Nanoparticles for Antiretroviral Drug Delivery

HIV/AIDS is a global pandemic that has become the leading infectious killer of adults worldwide. By 2006, more than 65 million people had been infected with the HIV virus worldwide and 25 million had died of AIDS. At the end of 2007, around 33 million people were living with the virus, with 2.7 million new infections and 2 million deaths each year. This has caused tremendous social and economic damage worldwide, with developing countries, particularly Sub-Saharan Africa, heavily affected (Merson et al; 2006)

After fast development of antiretroviral resistance in individuals treated with single drug regimens, the concept of highly active antiretroviral therapy (HAART) was introduced in the late 1990s, comprising the intense use of combination drug regimens. There are now around 30 individual drugs and fixed-dose combinations available to treat HIV infection. Currently used antiretroviral drug classes include reverse

transcriptase inhibitors (RTIs), protease inhibitors (PIs), entry inhibitors (CCR5 antagonists and fusion inhibitors), and integrase inhibitors (Neves et al; 2010).

Introduction of a combination of three or more different classes of drugs; triple-drug therapy (HAART) revolutionized HIV/AIDS treatment. The use of the HAART regimen, particularly in the developed world, has resulted in tremendous success in improving the expectancy and quality of lives for patients. However, some HAART regimens have serious side effects and, in all cases, HAART has to be taken for a lifetime, with daily dosing of one or more pills. Some patients also develop resistance to certain combinations of drugs, resulting in failure of the treatment. The absence of complete cure under current treatment underscores the great need for continued efforts in seeking innovative approaches for treatment of HIV/AIDS (Walensky et al; 2006, Richman et al; 2001).

But, HAART is not able to provide a cure mainly because of HIV's ability to persist in latency state in cellular and anatomical reservoir sites. Beside this fact, problems of current antiretroviral therapy also include prolonged treatment periods with drugs possessing important adverse effects, poor drug-regimen compliance, drug resistance, drug–drug interactions, poor drug pharmacokinetics, viral levels rebound after therapy cessation, and costs (Marsden and Jack; 2009) .

Even if current antiretroviral therapy is able to reduce the viral load to undetectable levels, HIV is able to persist in the human body, namely in several reservoir sites. Reservoir sites are able to protect the virus from biological elimination pathways, immune response and/or antiretroviral drugs, making it impossible to eradicate the virus and achieve a cure with currently available therapy.

Generally, cellular reservoirs are able to sustain HIV infection by allowing its residence in a physical state capable of surviving for prolonged periods despite otherwise therapeutic levels of antiretroviral drugs. In the case of anatomical reservoir sites, the problem is mainly to achieve and sustain adequate levels of antiretroviral agents within these spaces (Blankson et al; 2002). After initial HIV infection and local amplification at the mucosal site, infected cells migrate to regional lymph nodes, leading to a mild initial viral amplification in naïve T cells. The viral infection is then quickly disseminated by T cells to lymphoid organs, particularly the gut-associated lymphoid tissues (GALT),

spleen, and bone marrow, being accompanied by a burst in the viral load (acute infection) (Shrager et al; 1998).

Main anatomical reservoir sites of HIV include the lymphoid organs (particularly the spleen, lymph nodes, and GALT) and the central nervous system (CNS). Other potential sites have also been reported as possible reservoirs, namely the testicles and the female genital tract. The importance of lymphoid organs is directly related with their role in the circulation and production of lymphocytes and the abundant presence of HIV-susceptible immune cells, namely those able to constitute reservoirs as discussed above. Poor penetration of antiretroviral in the CNS due to insufficient blood-brain barrier (BBB) permeation is a matter of concern, resulting in suboptimal drug levels that allow continuous replication of HIV (Mamo et al; 2010).

Protease inhibitors (PIs), one of the components of HAART are substrate for the efflux cellular membrane transporter P-glycoprotein, which is able to mediate unidirectional transport of these drugs to the cell exterior. The presence of this membrane transporter in macrophages and endothelial cells of the BBB explains the poor concentrations achieved by PIs in these reservoir sites. Conversely, incomplete absorption of some PIs when administered by the oral route can be partially explained, alongside with their poor aqueous solubility, by the presence of this transporter in intestinal epithelial cells. Poor placental penetration of PIs, which may have important clinical implications in mother-to-child transmission, is also justified by the presence of high levels of P-glycoprotein placenta (Neves et al; 2010).

Affordability of antiretroviral drugs is an increasingly huge burden for developed countries and an unattainable goal for developing ones. An interesting approach for reducing overall costs with antiretroviral therapy would be to increase older drugs therapeutic lifespan (i.e. before treatment-compromising adverse effects or drug resistance occurs) by improving their delivery.

Although at an earlier stage, applications of nanotechnology for prevention and treatment of HIV/AIDS have also gained attention in recent years. There are emerging novel approaches in which nanotechnology can enhance current treatment as well as advance new therapeutic strategies, such as gene therapy and immunotherapy.

Nanoscale delivery systems enhance and modulate the distribution of hydrophobic and hydrophilic drugs into and within different tissues due to their small size. This

particular feature of nanoscale delivery systems appears to hold the most promise for their use in clinical treatment and prevention of HIV.

General properties of nanoparticles that favour their use in antiretroviral drug delivery are well known and include versatility (virtually all drugs may be encapsulated), good toxicity profile (depending on used excipients), possibility of drug-release modulation, high drug payloads, relative low cost, easiness to produce and possible scale-up to mass production scale. Their ability to incorporate, protect and/or promote the absorption of non-orally administrable anti-HIV drugs, namely mono- or oligonucleotides, is of importance to improve the bioavailability of several molecules. Once bioavailable, protection of incorporated drugs from metabolism is a favorable feature of nanosystems, allowing prolonged drug residence in the human body, thus reducing needed doses and prolonging time between administrations.

Nanoparticles seem to be able to reduce antiretroviral drugs toxicity, namely at the cellular level, providing that rigorous selection of materials and adequate preparation techniques are assured (Vyas et al; 2006). Even if drug uptake is increased when encapsulated in nanocarriers, cell toxicity seems to be diminished, probably due to the slow-release properties of these systems. This possibility is particularly interesting taking in consideration the well-known toxicity associated with anti-HIV therapy (Mamo et al; 2010).

Specifically, targeted delivery of antiretroviral drugs to CD4+ T cells and macrophages as well as delivery to the brain and other organ systems could ensure that drugs reach latent reservoirs. Moreover, by controlling the release profiles of the delivery systems, drugs could be released over a longer time and at higher effective doses to the specific targets (Nowacek et al; 2009, Amiji et al; 2006).

Passive targeting is based in the inherent properties of different nanosystems, namely size, particle shape, and surface charge, which can modulate its bioavailability, biodistribution and/or targeting.

Active targeting strategies have also been employed for antiretroviral drug delivery. In the case of active targeting, nanotechnology-based systems are conveniently modified, most commonly by surface attachment of specific ligands that are able to recognize target cells or sites, and/or escape bio elimination processes. Once opsonization and endocytosis occur, nanoparticles are incorporated in an endolysosome, being degraded;

however, the ability of various nanoparticles to escape the endolysosomal compartment allows incorporated drugs to be delivered to the cytoplasm and, eventually, to the nucleus. Nanoparticles have the ability to enhance uptake of drug by macrophages, particularly when these cells were infected by HIV (up to 60% more than for uninfected macrophages (Dou et al; 2007)).

The presence of wide amounts of HIV-susceptible immune cells in the lymphoid organs makes its interesting to target antiretroviral drug to these sites in HIV therapy. This strategy comprises targeting nanosystems to immune cell populations, particularly macrophages. The normal uptake of nanoparticles by macrophages present in the RES is indeed an important passive method for targeting this anatomical reservoir site, as early demonstrated *in vivo* by Lobenberg et al (1997).

In one study, [¹⁴C]-zidovudine-loaded PHCA nanoparticles were administered intravenously in a rat model; soon after administration, the drug was detected in the organs of the RES in concentrations above 18-fold of those for the drug aqueous solution. Identical effects were also observed by these investigators after oral intake, providing evidence that cell/organ drug targeting may also be achieved by administering drug-loaded nanoparticles through more patient-friendly routes (Lobenberg et al; 1997).

Dembri and coworkers studied the applicability of oral administration for zidovudine-loaded poly (iso-hexylcyanoacrylate) nanoparticles in rats and observed drug accumulation in the intestinal mucosa after direct gastric administration, being the concentration of zidovudine in Peyer's patches around 4-times higher for nanoparticles than for drug solution; also, tissue concentrations (30–45 μ M) were much higher than those reported for HIV IC₅₀ (0.06–1.36 μ M). This approach showed to be efficient in concentrating zidovudine in the gastrointestinal tract and GALT, which are important sites for HIV replication and perpetuation, as highlighted previously (Dembri et al; 2000).

Kinman and coworkers optimized indinavir loaded liposomes in order to improve lymphoid tissue localization and pharmacokinetic profile. PEGylation of liposomes demonstrated to provide 6-fold higher indinavir levels in lymph nodes and enhance drug exposure in blood and also indicate that the concomitant use of the proposed nanocarrier and conventional oral indinavir regimens could be a valuable strategy in

order to prolong the utility (i.e. drug lifespan before resistance occurs) of antiretroviral drugs (Kinman et al; 2006).

2.5 Methods of Preparation of Nanoparticles

Nanoparticles can be prepared from a variety of materials such as proteins, polysaccharides and synthetic polymers. The selection of matrix materials is dependent on many factors including: (a) size of nanoparticles required; (b) inherent properties of the drug, e.g., aqueous solubility and stability; (c) surface characteristics such as charge and permeability; (d) degree of biodegradability, biocompatibility and toxicity. (Kreuter et al; 1994)

2.5.1 Nanoparticles Prepared by Polymerization Process of Monomers:

In this method, monomers are polymerized to form nanoparticles in an aqueous solution. Drug is incorporated either by being dissolved in the polymerization medium or by adsorption onto the nanoparticles after polymerization completed. The Nanoparticle suspension is then purified to remove various stabilizers and surfactants employed for polymerization by ultracentrifugation and re-suspending the particles in an isotonic surfactant-free medium. Nanocapsules formation and their particle size depend on the concentration of the surfactants and stabilizers used. Two types of polymerization processes have been adopted to prepare polymeric nanoparticles (Jain et al; 2000, Mohanraj and Chen; 2006).

a) Dispersion Polymerization: Dispersion polymerization starts with monomer, an initiator, solvent in which the formed polymer is insoluble, and a polymeric stabilizer. Polymer forms in the continuous phase and precipitates into a new particle phase which is stabilized by the polymeric stabilizer. Small particles are formed by aggregation of growing polymer chains precipitating from the continuous phase as these chains exceed a critical chain length. Coalescence of these precursor particles with themselves and with their aggregates results in the formation of stable colloidal particles, which occurs when sufficient stabilizer covers the particles.

b) Emulsion Polymerization: In this technique the monomer is emulsified in non-solvent containing surfactant, which leads to the formation of monomer swollen micelles and stabilized monomer droplets. The polymerization is performed in the

presence of initiator. Emulsion polymerization may be performed using either organic or aqueous media as continuous phase. Poly (methyl methacrylate), poly (alkyl cyanoacrylate), acrylic copolymer, polystyrene, poly (vinyl pyridine) and polyacrolen nanoparticles are prepared by emulsion polymerization technique.

2.5.2 Nanoparticles Prepared from Dispersion of Preformed Polymers: Several techniques have been suggested to prepare the biodegradable polymeric nanoparticles from preformed polymers such as poly (D,L-lactide) (PLA), poly (D,L-glycolide) (PLG) and poly (D,L-lactide-co-glycolide) (PLGA) (Kompella et al, 2001, Ravikumar et al; 2004). The basic methodologies of the commonly used preparation methods are as follows:

a) Emulsion/evaporation

This is one of the most frequently used methods. The preformed polymer and drug are first dissolved in a water-immiscible organic solvent, which is then emulsified in an aqueous solution containing stabilizer. The emulsification is brought about by subsequent exposure to a high-energy source such as an ultrasonic device, homogenizer, or colloid mill. The organic phase is evaporated under reduced pressure or vacuum, resulting in the formation of the aqueous dispersion of nanoparticles. The nanoparticles are collected by ultracentrifugation and washed with distilled water to remove stabilizer residues or any free drug and lyophilized for storage (Guarrero et al 1998; Song; 1997). Modification of this method, known as high-pressure emulsification solvent evaporation (HPESE), has been reported by (Jaiswal et al; 2004) This method involves preparation of a coarse emulsion, which is then subjected to homogenization under high-pressure followed by overnight stirring to remove organic solvent. This method has the advantage of obtaining small, monodispersed nanoparticles with high encapsulation efficiency and reproducibility. The emulsion evaporation method can be used for preparation of particles with sizes varying from a few nanometers to micrometers by controlling the stirring rates and conditions (Ubrich; 2004). A diagrammatic representation of this method is shown in Fig. 2.5

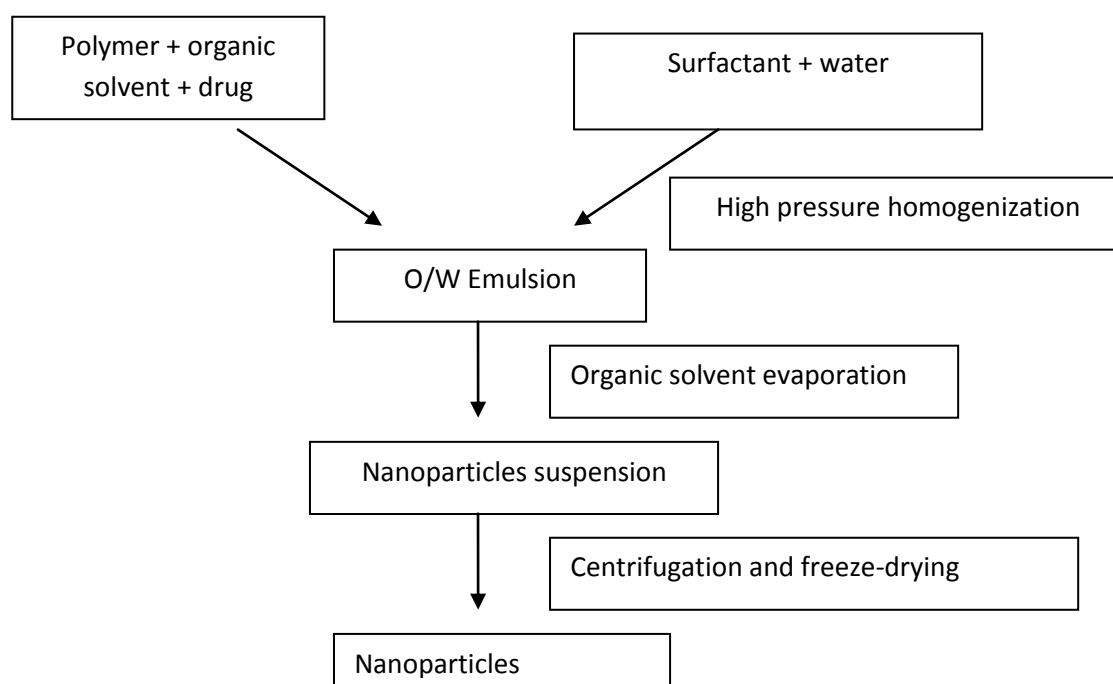


Fig. 2.5 Schematic diagram of o/w emulsion method for preparation of nanoparticles

b) Double emulsion process

The emulsion evaporation method suffers from the limitation of poor entrapment of hydrophilic drugs because of their diffusion and partitioning from the dispersed oil phase into the aqueous continuous phase. Therefore, to encapsulate hydrophilic drugs and proteins, the double-emulsion technique is employed, which involves the addition of aqueous drug solution to organic polymer solution under vigorous stirring to form a w/o emulsion. This w/o emulsion is added into second aqueous phase containing more stabilizers with stirring to form the w/o/w emulsion. The emulsion is then subjected to solvent removal by evaporation (Vandervoort et al; 2002). A number of hydrophilic drugs like the peptide leuprolide acetate, a lutenizing hormone-releasing agonist, vaccines, proteins/peptides and conventional molecules have been successfully encapsulated by this method. After evaporation of organic solvent under reduced pressure, the polymer precipitates and nanoparticles can be isolated by centrifugation at high speed. The formed nanoparticles must be thoroughly washed before lyophilization (Jain; 2000). A diagrammatic representation of this method is shown in Fig. 2.6.

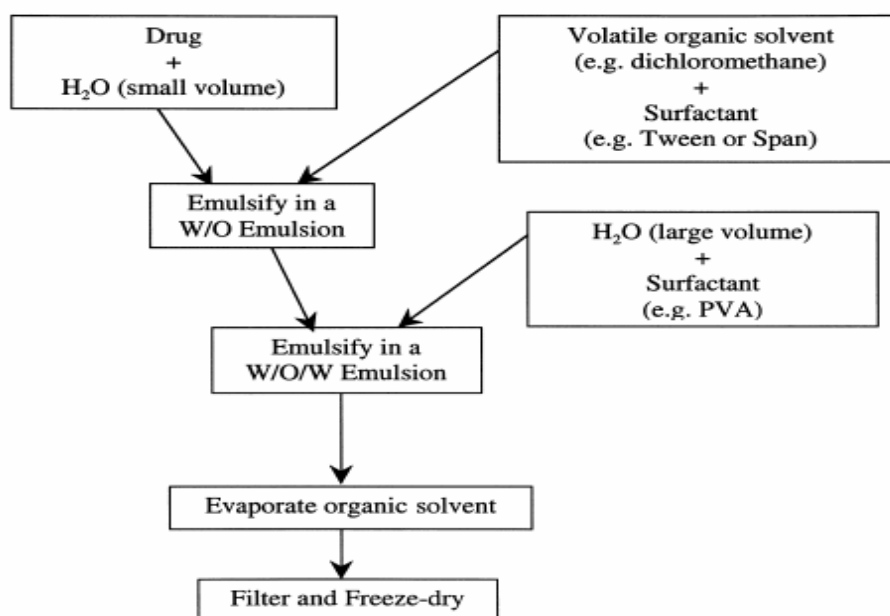


Fig. 2.6 Schematic diagram of w/o/w in-liquid drying process for preparation of Nanoparticles

c) Salting-out

This technique involves the addition of polymer and drug solution in a slightly water miscible solvent such as acetone to an aqueous solution containing the salting out agent and a colloidal stabilizer under vigorous mechanical stirring. When this o/w emulsion is diluted with a sufficient volume of water, it induces the formation of Nanoparticles by enhancing the diffusion of acetone into the aqueous phase. The remaining solvent and salting-out agent are eliminated by cross-flow filtration (Allemann et al; 1998). Several manufacturing parameters can be varied including stirring rate, internal/external phase ratio, concentration of polymer in the organic phase, type of electrolyte, concentration, and type of stabilizer in the aqueous phase. By considering the entrapment efficiency of nanoparticles, this method is most suitable for water insoluble drugs. Salt permeate biological systems and are crucial for life. However salts also affect the stability of proteins. It has been reported since many years that neutral salts perturb various protein structures in ways that go well beyond simple, non-specific charge effects (Doming et al;2002).

d) Emulsification-diffusion

This is another widely used method involving polymer solution in partially water miscible solvent (such as ethyl acetate, benzyl alcohol, propylene carbonate) presaturated with water, added to an aqueous solution containing stabilizer under vigorous stirring. The subsequent addition of water to the system destabilizes the equilibrium between the two phases and causes the solvent to diffuse into the external phase, resulting in reduction of the interfacial tension and in nanoparticle formation, which gradually becomes poorer in solvent.

Although this method is a modification of the salting out procedure, it provides the advantage of avoiding the use of salts and thus eliminates the need for intensive purification steps. While this method also suffers from low entrapment efficiency of hydrophilic drugs in nanoparticles, incorporation of medium chain glyceride into aqueous solution has been found to improve the encapsulation efficiency of water-soluble drugs into nanospheres offering the advantage of simplicity, narrow particle size distribution, and ready dispersibility of the resultant particles (Jain; 2000).

e) Nanoprecipitation

In nanoprecipitation, introduced by Fessi and co-workers (Fessi et al; 1995), the particle formation is based on precipitation and subsequent solidification of the polymer at the interface of a solvent and a non-solvent. Thus, the process is often called solvent displacement or interfacial deposition. This method is usually employed to incorporate lipophilic drugs into the carriers based on the interfacial deposition of a polymer following displacement of a semi-polar solvent miscible with water from a lipophilic solution (Molpeceres et al; 1996, Barichello et al; 1999)

The polymer is dissolved in a water miscible organic solvent (or solvent mixture) and added to an aqueous solution, in which the organic solvent diffuses (Fig. 2.7). Particle formation is spontaneous, because the polymer precipitates in the aqueous environment. According to the current opinion, the Marangoni effect is considered to explain the process: solvent flow, diffusion and surface tensions at the interface of the organic solvent and the aqueous phase cause turbulences, which form small droplets containing the polymer. Subsequently, as the solvent diffuses out from the droplets, the

polymer precipitates. Finally, the organic solvent is typically evaporated with the help of a vacuum.

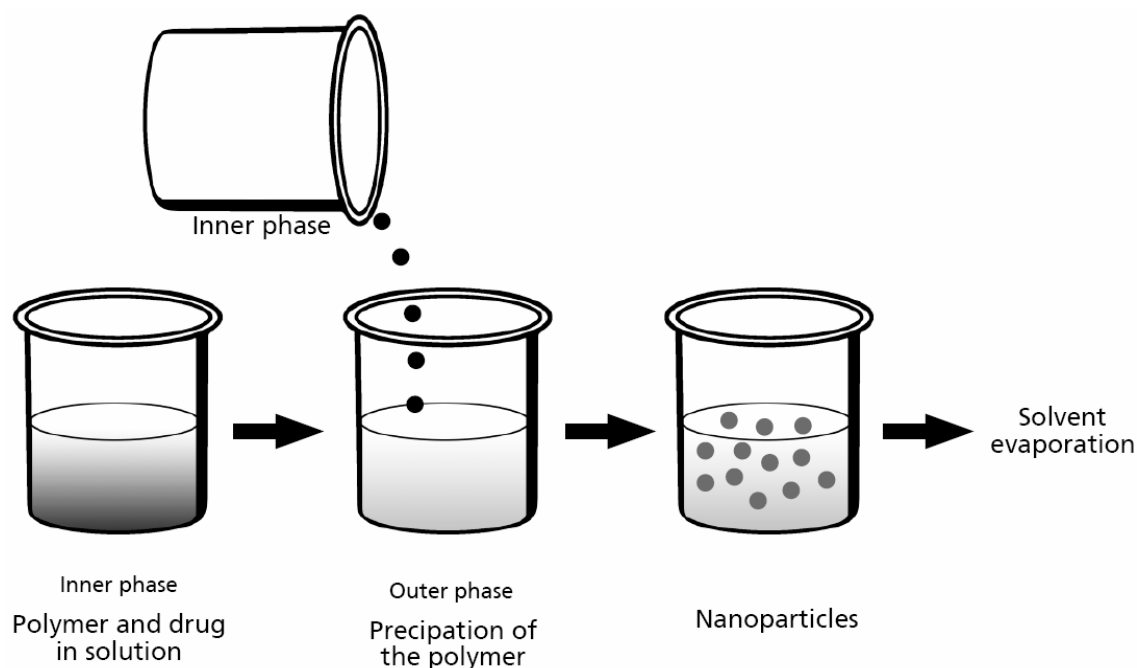


Fig. 2.7 Schematic illustration of the nanoprecipitation process

The injection rate of the organic phase into the aqueous phase affects the particle size. It was observed that a decrease occurs in both particle size and drug entrapment as the rate of mixing of the two phases increase. This method gave relatively narrow particle size distribution for different formulations evaluated.

The drug loading efficiency was found to be lower for the hydrophilic drugs than lipophilic drugs because of their poor interaction with the polymer leading to diffusion of the drug, from the polymer in the organic phase, to the external aqueous environment, although exceptions were found, as seen in case of proteins and peptides Govender et al (1999) showed improved incorporation of the water-soluble drug, procaine hydrochloride, into PLGA nanoparticles by increasing the aqueous phase pH and replacing procaine hydrochloride by procaine dehydrate base. The difficulty faced in this preparation technique is the choice of drug/polymer/solvent/nonsolvent system in which the nanoparticles would be formed and the drug efficiently entrapped.

f) Emulsion-diffusion-evaporation

Employing the emulsion-diffusion-evaporation method, Nanoparticles are prepared by dissolving PLGA in ethyl acetate at room temperature. The organic phase is then added to an aqueous stabilizer mixture containing PVA and chitosan in water under stirring. The emulsion is stirred at room temperature for 3 hours before homogenizing for 10 minutes.

To this emulsion, water is added under stirring, resulting in Nanoprecipitation (Ravikumar et al; 2004). Stirring is continued in a water bath maintained at 40 °C to remove organic solvent. Stirring causes the dispersion of the solvent as irregularly sized globules in equilibrium with the continuous phase, and the stabilizer is then adsorbed on the larger interface created. Homogenization further results in smaller globules. Addition of the water and heating step destabilizes the equilibrium and causes the diffusion of organic solvents to the external surface.

2.6 Characterization of Nanoparticles

The unique qualities and performance of nanoparticulate systems as device for drug delivery arises directly from their physicochemical properties. Hence, determining such characteristics is essential in achieving the mechanistic understanding of their behaviour. A good understanding allows prediction of *in vivo* performance as well as allowing particle designing, formulation development and process troubleshooting to be carried out in a rational fashion. After preparation, nanoparticles are characterized at two levels. The physicochemical characterization consists of the evaluation of the particle size, size distribution, and surface properties (composition, charge, hydrophobicity) of the nanoparticles. The biopharmaceutical characterization includes measurements of drug encapsulation, *in vitro* drug release rates, and *in vivo* studies revealing biodistribution, bioavailability, and efficacy of the drug. Nanoparticles are generally characterized for the following parameters

- Particle size
- Surface charge (Zeta potential)
- Crystalline state
- Surface morphology

- Drug release studies
- Stability

Particle size

The most basic and important property of any nanoparticulate system is its size. The saturation solubility, dissolution velocity, physical stability and even biological performance of these systems depend on their particle size. Saturation solubility and dissolution velocity showed considerable variation with change in particle size of the drug (Muller and Peters; 1998). The most frequently used techniques for particle size measurement of nanosized systems are dynamic light scattering techniques, static light scattering techniques and microscopy. Each method has its own advantages as well as disadvantages. The mean size and width of distribution (polydispersity index) is typically determined by photon correlation spectroscopy (PCS). This technique can be used for rapid and accurate determination of the mean particle diameter of nanoparticles (Muller; 1984). It records the variation in the intensity of scattered light on the microsecond time scale (Pecora; 2000). The measuring range of PCS is limited to approximately 3 nm–3mm. Therefore, Laser Diffraction (LD) is also used to detect any particles in the micrometer range or aggregates of drug nanoparticles. For nanoparticles intended for intravenous use, particle size determination by coulter counter is also essential as few particles with particle size more than 5 μm may cause problem of blockage of blood vessels. Depending on the type of equipment employed, the measuring size range is approximately 0.01–80 μm . The instrument and the material to be analyzed are important parameters which will affect the accurate particle size measurement. The stability of the sample during analysis is the most important requisite for correct and reproducible results (Keck; 2010). Thus, all above things must be considered during selection of appropriate technique for particle size determination for a particular sample.

Surface charge (Zeta potential)

Particle charge is a stability determining parameter in nanoparticles. It is measured by electrophoresis and typically expressed as phoretic mobility $[(\text{mm}/\text{S}) / (\text{V}/\text{cm})]$ or zeta

potential (mV). Zeta potential is used as surrogate for surface charge, and is often measured by observing the oscillations in signal that result from light scattered by particles located in an electric field. There are a number of instrumental configurations with different approaches implemented in different equipments, with mostly used Doppler shift. The zeta potential of a nanosuspension is governed by both the surfactant and the drug itself. For a physically stable nanoparticulate suspension solely stabilized by electrostatic repulsion, a zeta potential of ± 30 mV is required as minimum. In case of a combined electrostatic and steric stabilization, ± 20 mV is sufficient as a rough guideline (Muller and Jacobs; 2002).

Crystalline state

Drug particles in amorphous form are likely to be generated when nanoparticles are prepared. Hence, it is essential to investigate the extent of amorphous drug particles generated during production of nanoparticles. The crystalline status of the nanosuspension can be assessed by differential scanning calorimetry (DSC) (Muller et al; 2001). This is particularly very important when the drug exhibits polymorphic forms. The changes in the physical state of the drug particles as well as extent of amorphous fraction can be determined by X-ray diffraction analysis (Muller and Grau; 1998) and can be supplemented by DSC studies. The assessment of the crystalline state and particle morphology together helps in understanding the polymorphic and morphological changes that a drug undergoes when subjected to nanosizing.

Surface morphology

Nanoparticles can be directly observed by Scanning Electron Microscopy (SEM) and Transmission Electron Microscopy (TEM) with the former method being better for morphological examinations (Molpeceres et al; 2000). TEM has a smaller size limit of detection and provides structural information via electron diffraction, but staining is usually required. Researchers must be cognizant of the statistically small sample size and the effect of applied vacuum on the particles during analysis. Very detailed images can be obtained from freeze fracture approach in which a cast is made of the original sample (Mosqueira et al; 2001). Sample corruption resulting from the extensive sample preparation is always a possibility, though lower vacuum instrumentation reduces this manipulation, albeit at the loss of some resolution (Nizri et al; 2004). Atomic force

microscopy (AFM) microscopy can also be used to confirm the size and shape of nanosized particles. AFM is capable of scanning the surfaces in controlled environmental conditions and is a complementary to SEM imaging.

Drug release studies

In vitro release studies are generally performed to accomplish one or more of the following aims:

1. As an indirect measurement of drug availability, especially in preliminary stages of product development
2. Quality control to support batch release and to comply with specifications of batches proven to be clinically and biologically effective
3. Assess formulation factors and manufacturing methods that are likely to influence bioavailability
4. Substantiation of label claim of the product
5. As a compendial requirement

Currently, research is focused on shortening the time span of *in vitro* release experiments with the aim of providing a quick and reliable method for assessing and predicting drug release. For commercial dosage forms that release drug for 30 to 90 days or even longer, accelerated or short-term release provides the potential for conducting an *in vitro* release test in a matter of days rather than months. Release testing of these dosage forms at 37-C would require the addition of preservatives and impose certain limitations on the *in vitro* method, such as stability and compatibility of the components of the release device, like tubings and membranes. Therefore, a short-term release test might even be more reliable for quality-control purposes. In addition, short term studies can provide a rapid assessment of formulation and processing variables that affect drug release from the delivery system, especially in the developmental stage. These short-term studies can be performed by accelerating one or more conditions employed in a real-time *in vitro* release study. Such accelerating conditions include elevated temperature, altering pH, and use of surfactants. As with the real-time *in vitro* release study, the method should be simple, reproducible under the conditions of study, inexpensive, and applicable to biodegradable nanoparticulate formulations that have varying duration of action *in vivo*.

Generally aqueous media such as simulated gastric fluid without enzymes, simulated intestinal fluid without enzymes, water and buffers have been employed to study release of water soluble drugs. For water insoluble drugs, surfactants, bile acids, bile salts and lecithins have been shown to increase the rate of drug release. The level of interest in the *in vitro* dissolution of poorly water soluble drugs has increased in recent years due to the need of finding a suitable dissolution media for pharmaceutical formulations that may reflect their *in vivo* performance.

In vivo poorly water-soluble drugs are solubilised through complex endogenous surfactants such as bile acids, bile salts and lecithin. However, *in vitro* dissolution models in less complex micelle systems have been used. The use of surfactants in the dissolution system for poorly water-soluble drugs may be physiologically more meaningful due to the presence of natural surfactants in the gastrointestinal tract.

Additionally, the following should be considered prior to studying drug release:

1. Sink conditions: Although sink conditions may not exist at the *in vivo* site of action, it is wise to employ sink conditions during *in vitro* testing. In the event that a small volume of media can be used (based on the method employed and assay sensitivity), total media replacement may be used to ensure drug solubility, maintain sink conditions, and prevent accumulation of polymer degradation products.
2. Burst release: The release method employed should be able to identify a high initial release or burst from the formulation. Additionally, the method should provide information about the onset and duration of burst to assess its influence on the *in vivo* efficacy and safety window of the drug being studied.
3. Robustness of technique: The *in vitro* release method employed should be able to assess the influence of changes in the manufacturing procedure on the formulation. This would be useful from a quality-control standpoint and could also aid in the design and development of drug delivery systems. Ideally, an *in vitro* test method should mimic *in vivo* conditions and release mechanism as much as possible (D'Souza and DeLuca 2006). Methods to study the *in vitro* release are: (i) side-by-side diffusion cells with artificial or biological membranes; (ii) dialysis bag diffusion technique; (iii) reverse dialysis sac technique; (Meneau and Ollivon) ultra centrifugation; (v) Ultra filtration; or (vi) centrifugal ultra filtration technique. Despite the continuous efforts in this direction, there are still some technical difficulties to study *in vitro* drug release from NPs. These

are attributed to the separation of NPs from the release media. In order to separate NPs and to avoid the tedious and time-consuming separation dialysis has been used; here, the suspension of NPs is added to the dialysis bags/ tubes of different molecular mass cut-off. These bags are then incubated in the dissolution medium. Another technique involves the use of a diffusion cell consisting of donor and acceptor compartments; this technique was used to separate through the artificial / biological membranes. In this method kinetic study was not performed under the perfect sink conditions, because the NPs were not diluted in the release media, but were separated from the release media through the membrane. Thus, the amount of drug in the release media did not reflect the amount of drug released. In order to avoid the enclosure of NPs in the dialysis bag, Leavy and Benita used a reverse dialysis technique for o/w emulsion. In this method, NPs were added directly into the dissolution medium. The same technique was adopted by Calvo et al. for the release from the NPs, nanocapsules and nanoemulsions (Soppimath, Aminabhavi et al. 2001).

The release rates of NPs depend upon (i) desorption of the surface-bound /adsorbed drug; (ii) diffusion through the NP matrix; (iii) diffusion (in case of nanocapsules) through the polymer wall; (Meneau and Ollivon) NP matrix erosion; and (v) a combined erosion / and diffusion process. Thus, diffusion and biodegradation govern the process of drug release. Release profiles of the drugs from NPs depend upon the nature of the delivery system. In the case of a matrix device, drug is uniformly distributed / dissolved in the matrix and the release occurs by diffusion or erosion of the matrix. If the diffusion of the drug is faster than matrix degradation, then the mechanism of drug release occurs mainly by diffusion, otherwise it depends upon degradation. Rapid initial release is attributed to the fraction of the drug which is adsorbed or weakly bound to large surface area of the NPs, than to the drug incorporated in NPs.

Stability

Physical stability is crucial in formulation of drug nanosuspension. As nanoparticles have mean particle diameter in nanometer range, they are prone to aggregation of the particles. The aggregation may be due to Ostwald ripening which occurs due to different saturation solubilities in the vicinity of very small and larger particles. Stabilizers like surfactants or polymeric macromolecules are required to stabilize the nanoparticles against inter-particulate forces and prevent them from aggregation. Surfactants are

used to minimize the free energy and stabilize the system. The stabilization provided by the stabilizers is by steric, electrostatic or combination of these two processes. Steric stabilization is achieved by adsorbing surfactants/polymers onto the particle surface while electrostatic stabilization is obtained by adsorbing charged molecules, which can be ionic surfactants or charged polymers, onto the particle surface. Generally, steric stabilization alone is sufficient to provide stability to the nanosized particles but electrostatic stabilization is often combined with it as an additional measure.

Formation of impurities due to process and formulation parameters must be studied. The impurities could be identified by various techniques such as infrared spectroscopy (IR), high performance liquid chromatography (HPLC) and mass spectroscopy (MS).

Beside characterization of above properties, additional characterization of the nanoparticles is required if surface modification is done for particles. The parameters for which surface modified nanoparticles are evaluated include adhesion properties, surface hydrophilicity/hydrophobicity and interaction with body proteins. The adhesiveness of the drug nanoparticles is considered to be a major factor contributing towards increasing the bioavailability and reducing variability of absorption. Surface hydrophobicity determines the interaction with the cells prior to phagocytosis and is relevant parameter for adsorption of plasma proteins. It is considered as important parameter affecting *in vivo* organ distribution after i.v. injection. Separation by Hydrophobic Interaction Chromatography (HIC) depends on the reversible adsorption of biomolecules according to their hydrophobicity. HIC is widely used for the separation and purification of proteins in their native state. HIC technique is used for determination of surface hydrophilicity/hydrophobicity. Hydrophobicity of nanoparticles is characterized by HIC in which hydrophilic particles pass the column faster while elution of hydrophobic particles is retarded.

2.7 Biodegradable Polymers

Biodegradable polymers have been extensively used in controlled drug delivery because they have the advantage of not requiring surgical removal after they serve their intended purpose. It offers various advantages like versatile degradation kinetics, non-

toxicity, and biocompatibility. In recent years, additional polymers designed primarily for medical applications have entered the arena of controlled release.

Many of these materials are designed to degrade within the body, among them are following:

- Polylactides (PLA).
- Polyglycolides (PGA).
- Poly (lactide-co-glycolides) (PLGA).
- Polyanhydrides & Polyorthoesters.

Originally, polylactides and polyglycolides were used as absorbable suture material, and it was a natural step to work with these polymers in controlled drug delivery systems. The greatest advantage of these degradable polymers is that they are broken down into biologically acceptable molecules that are metabolized and removed from the body via normal metabolic pathways. However, biodegradable materials do produce degradation by-products that must be tolerated with little or no adverse reactions within the biological environment.

POLY (D, L-LACTIDE-CO-GLYCOLIDE) PLGA

PLGA or **poly(lactic-co-glycolic acid)** is a copolymer which is used in a host of Food and Drug Administration (FDA) approved therapeutic devices, owing to its biodegradability and biocompatibility. PLGA is synthesized by means of random ring-opening co-polymerization of two different monomers, the cyclic dimers (1,4-dioxane-2,5-diones) of glycolic acid and lactic acid. Common catalysts used in the preparation of this polymer include tin (II) 2-ethylhexanoate, tin (II) alkoxides, or aluminum isopropoxide. During polymerization, successive monomeric units (of glycolic or lactic acid) are linked together in PLGA by ester linkages, thus yielding linear, aliphatic polyester as a product. Fig. 2.8 depicts the structure of PLGA and its monomers.

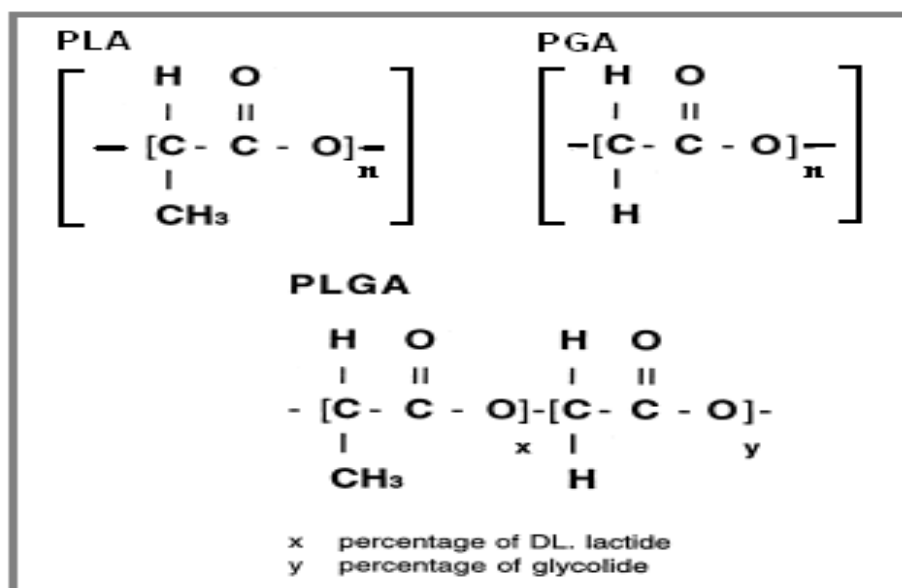


Fig. 2.8 Structure of Poly glycolic acid (PGA), Poly lactic acid (PLA) and Poly (lactic-co-glycolic) acid (PLGA)

The understanding of physical, chemical and biological properties of the polymer is helpful before formulating a controlled drug delivery device. Lactic acid is more hydrophobic than glycolic acid and hence lactide-rich PLGA copolymers are less hydrophilic, absorb less water and subsequently degrade more slowly. The commercially available PLGA polymers are usually characterized in terms of intrinsic viscosity, which is directly related to the molecular weight.

The mechanical strength, swelling behaviour, capacity to undergo hydrolysis, and subsequently the biodegradation rate are directly influenced by the crystallinity of the PLGA polymer. The crystallinity of the PLGA copolymer is directly dependent on the type and molar ratio of the individual monomer components (lactide and glycolide) in the copolymer chain. PLGA polymers containing 50:50 ratios of lactic and glycolic acids are hydrolyzed much faster than those containing higher proportion of either of the two monomers. Gilding and Reed have pointed out that PLGA containing less than 70% glycolide are amorphous in nature. The degree of crystallinity and the melting point of the polymers are directly related to the molecular weight of the polymer.

The T_g (glass transition temperature) of the PLGA copolymers are above the physiological temperature of 37° C and hence they are glassy in nature. Thus they have a fairly rigid chain structure which gives them significant mechanical strength to be formulated as drug delivery devices.

Degradation and metabolic pathway of PLGA

The degradation rate of PLGA in water is a function of the molecular weight and the lactide: glycolide ratio. Higher the glycolide content and lower molecular weight increase the degradation rate. For e.g. the degradation time of PLGA 50:50 is 1-2 months while that of PLGA 70:30 and PLGA 85:15 are higher (approx.12-24 months).

PLGA show a glass transition temperature in the range of 40-60 °C. The inherent viscosity of PLGA is dependent on their molecular weight as shown in Table 2.1. For e.g. for PLGA 50:50 the molecular weight increases with the increase in its inherent viscosity (Purac biomaterials).

Table 2.1: Inherent viscosity and molecular weight for PLGA 50:50 (Purac Biomaterials)

IV [dl/g]	Mw[g/mol]
0.2	17,000
0.3	30,000
0.4	44,000
0.5	59,000
0.6	76,000
0.7	94,000
0.8	113,000
0.9	133,000
1.0	153,000
1.1	174,000
1.2	196,000

Unlike the homopolymers of lactic acid (polylactide) and glycolic acid (polyglycolide) which show poor solubilities, PLGA can be dissolved by a wide range of common solvents, including chlorinated solvents, tetrahydrofuran, acetone or ethyl acetate.

Degradation of PLA or PLGA occurs by autocatalytic cleavage of the ester bonds through spontaneous hydrolysis into oligomers and D, L-lactic and glycolic acid monomers. Lactate converted into pyruvate and glycolate enter the Krebs' cycle to be degraded into CO₂ and H₂O. The polymer erosion in delivery devices is the degradation of polymers to water-soluble fragments, accompanied by a progressive weight loss of the matrix. Generally, the polymer erosion could be classified into two mechanisms, namely surface or bulk erosion (Gopferich; 1996).

In the case of surface erosion, the degradation is faster than the water diffusion. Thus the degradation and erosion take place on the surface of the matrix; in contrast, with bulk erosion, the water penetration is faster and the degradation and erosion affect all the polymer bulk (Fig. 2.9). PLGA are bulk erosion polymers. The weight loss of the polymer devices doesn't take place at the beginning of the degradation of the PLGA. Accompanying with the produced water soluble oligomers, significant weight loss occurs when the molecular weight of the PLGA reaches certain threshold.

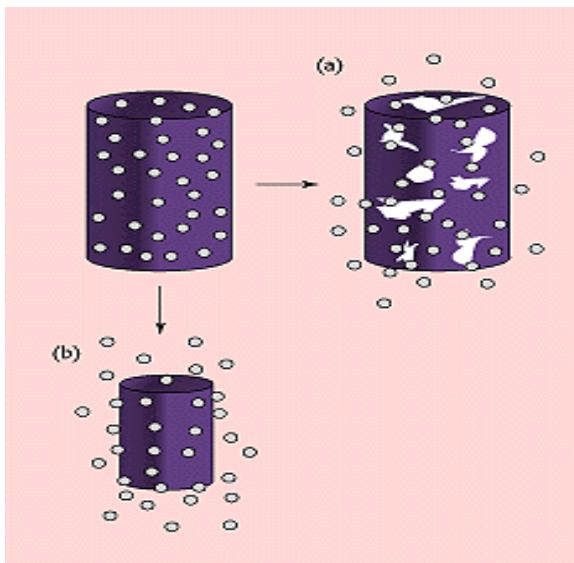


Fig.2.9 Schematic illustration of the changes of polymer matrix during (a) surface erosion and (b) bulk erosion (Burkersrodaa et al; 1997)

Bulk erosion is the main degradation pathway for PLGA copolymer. This occurs by random scission of ester bonds in the polymer backbone proceeding homogeneously throughout the device (Vandervoort et al; 2002). A three-phase mechanism for PLGA biodegradation has been proposed (Jain; 2000). Initially, a significant decrease in

molecular weight of polymer is observed, with no appreciable weight loss and no soluble monomer products formed after random chain scission. This phase is followed by a decrease in molecular weight with rapid loss of mass and formation of soluble mono and oligomeric products. Finally, soluble monomer products are formed from soluble oligomeric fragments, resulting in complete polymer degradation. It has been reported that the drug(s) having amino functional groups such as amines, basic drugs, protein, and peptides have the potential to interact with polymer pendant groups, accelerating the polymer degradation rates and the release of the drugs incorporated in the polyester matrix (Guarrero et al; 1998).

Degradation rate depends on four basic parameters: hydrolysis rate constant (depending on the molecular weight, the lactic/glycolic ratio, and the morphology), amount of water absorbed, diffusion coefficient of the polymer fragments through the polymer matrix, and solubility of the degradation products in the surrounding aqueous medium. All of these parameters are influenced by temperature, additives (including drug molecules), pH, ionic strength, buffering capacity, size and processing history, steric hindrance etc. Polymer properties such as molecular weight, crystallinity and glass transition temperature also control the degradation rate of polymers.

The biodegradation rate of the PLGA copolymers are dependent on the molar ratio of the lactic and glycolic acids in the polymer chain, molecular weight of the polymer, the degree of crystallinity and Tg of the polymer. The role of enzymes in any PLGA biodegradation has not been well established. Most of the literature indicates that the biodegradation of PLGA does not involve any enzymatic activity and is purely through hydrolysis.

Literature data (Huh et al 2003) indicate that *in vivo* degradation times for copolymers of lactides and glycolides vary from a few weeks to more than 1 year. The most widely used PLGA copolymer composition of 50:50 has the fastest degradation rate of the d,l-lactide/glycolide materials, with that polymer degrading in about 50-60 days. The 65:35, 77:25, and 88:15 d,l-lactide/glycolides have progressively longer *in vivo* lifetimes, with the 88:15 lasting about 150 days *in vivo*. Poly (d,l-lactide) requires about 12-16 months to biodegrade completely, and poly (l-lactide), being more crystalline and less hydrophilic, can be found *in vivo* even after 1.5-2 years.

Poly (D, L-lactide-co-glycolide), is a polymer of choice for developing an array of micro and nanoparticulate drug delivery systems as it has excellent biocompatibility and predictable biodegradability. Italia et al (2007) formulated PLGA nanoparticles for oral delivery of cyclosporine and studied their nephrotoxicity and pharmacokinetics. The nanoparticulate formulation showed significantly higher intestinal uptake as compared to suspension. PLGA NPs for oral and lymphatic delivery of insulin and proteins were studied by Patronidou et al (2008). Bhardwaj et al (2009) reported the enhancement in efficacy of paclitaxel by formulating orally delivered NPs using PLGA for the treatment of breast cancer. Kalaria et al (2009) designed biodegradable nanoparticles for oral delivery of doxorubicin. The drug loaded nanoparticles prepared by double emulsion method demonstrated superior performance *in vivo* in terms of enhanced bioavailability and lower toxicity. Jain et al (2011) developed PLGA NPs for oral delivery of temoxifen for breast cancer, with reduced hepatotoxicity.

2.8 Stabilizers

A stabilizer is required to avoid coalescence and formation of agglomerates during and after the emulsification process of nanoparticles. The large interfacial tension of small droplets drives the system to coalescence. Adsorption of stabilizers at the interface prevents this coalescence by lowering the interfacial tension and the energy of the system. The type and concentration of stabilizer used may influence the particle size and particle properties such as ζ potential and mucoadhesion. Both particle size and ζ potential are important physicochemical properties because they determine the physical stability and biopharmaceutical properties of nanoparticles, influencing drug release rate, biodistribution, mucoadhesion, and cellular uptake (Vandervoort et al 2002). Pluronics (Poloxamers) are nonionic block copolymer of poly (oxyethylene) and poly (oxypropylene). Various grades of poloxamers available are Poloxamer 124, Poloxamer 188, Poloxamer 237, Poloxamer 338 and Poloxamer 407 based on ratio of ethylene oxide and propylene oxide units and having molecular weight range from 2090-17400. Poloxamers are widely used as stabilizers for nanoparticles formulated by various polymers like PLGA, Chitosan etc. These are coated on the surface of PLGA and chitosan NPs and can affect the zeta potential, particle size and particle surface properties. Poloxamer coated nanoparticles has long circulating properties and

capabilities of bypassing reticuloendothelial system uptake (Jain D et al; 2013). Polyvinyl alcohol (PVA) used in combination with other polymer resulted in nanoparticle formation, but exclusion of PVA from the formulation increased the size of particles to above 1 μm (Vandervoort et al; 2002). The type of PVA used influences the physical properties such as the particle size and redispersibility of PLGA nanoparticles. The use of less hydrolyzed PVA provided higher percentage yield and uniform sized nanoparticles, whereas the highly hydrolyzed grade resulted in poor productivity and poor redispersibility. It has been shown that a fraction of PVA resides on PLGA nanoparticles surface, even on repeated washing, because PVA forms an interconnected network with the polymer at the interface.

2.9 Drug Profiles

2.9.1 Drug Profile of Gemcitabine HCl

Gemcitabine HCl (USP30 NF27, Drug Bank, Goodman Gilman's the pharmacological basis of therapeutics; 2006, Rx drug List, Martindale; 2009)

Category: Antineoplastic, Antimetabolite (Pyrimidine analogue)

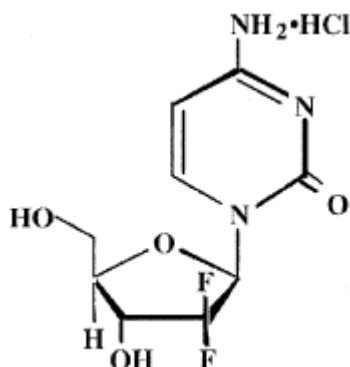
CAS No: 122111-03-9

Proprietary Names: Gemcitera, Gemsar Gemzar, Zefei

Molecular Formula: C₉H₁₁F₂N₃O₄•HCl

Molecular Weight: 299.66

Structural formula and Chemical name:



(2'-deoxy-2',2'-difluorocytidine monohydrochloride (β -isomer)).

Physicochemical properties: Gemcitabine HCl is a white to off-white solid powder.

Solubility: It is soluble in water, slightly soluble in methanol, and practically insoluble in ethanol and polar organic solvents.

pKa: 3.6

Mechanism of Action: Gemcitabine HCl enters cells *via* active nucleoside transporters. Kills malignant cells undergoing DNA synthesis; arrests progression of cells at G1/S border. Intracellularly, deoxycytidine kinase phosphorylates Gemcitabine to produce difluorodeoxycytidine monophosphate (dFdCMP), from which point it is converted to

difluorodeoxycytidine di- and triphosphate (dFdCDP and dFdCTP). Unlike cytarabine, the cytotoxicity of Gemcitabine HCl is not confined to the S phase of the cell cycle, and the drug is equally effective against confluent cells and cells in logarithmic growth phase. The cytotoxic activity may be a result of several actions on DNA synthesis: dFdCTP competes with dCTP as a weak inhibitor of DNA polymerase; dFdCDP is a potent inhibitor of ribonucleotide reductase, resulting in depletion of deoxyribonucleotide pools necessary for DNA synthesis; and dFdCTP is incorporated into DNA and after the incorporation of one more additional nucleotide leads to DNA strand termination. This "extra" nucleotide may be important in hiding the dFdCTP from DNA repair enzymes, as the incorporated dFdCMP appears to be resistant to repair. The ability of cells to incorporate dFdCTP into DNA is critical for Gemcitabine HCl-induced apoptosis.

Pharmacokinetics

Absorption, Fate, and Elimination: Gemcitabine HCl is administered as an intravenous infusion. Patients receiving Gemcitabine HCl 1000 mg/m² once weekly generally demonstrate C_{max} values of 10 to 40 µg/ml and achieve steady state after 15 to 30 minutes, during 30- minute infusion protocol.

The pharmacokinetics of the parent compound are largely determined by deamination, and the predominant urinary elimination product is the inactive metabolite difluorodeoxyuridine (dFdU). Gemcitabine has a short plasma half-life of approximately 15 minutes, with women and elderly subjects having slower clearance. Gemcitabine HCl half-life for short infusions ranged from 42 to 94 minutes, Clearance is dose-independent but can vary widely among individuals. Conversion of Gemcitabine HCl to dFdCMP by deoxycytidine kinase is saturated at infusion rates of approximately 10 mg/m² per minute, which produce plasma drug concentrations in the range of 15 to 20 µM. In an attempt to increase dFdCTP formation, the duration of infusion at this maximum concentration has been extended to 150 minutes. In contrast to fixed infusion duration of 30 minutes, the 150-minute infusion produces a higher level of dFdCTP within peripheral blood mononuclear cells, increases the degree of myelosuppression, but has uncertain effects on antitumor activity.

Therapeutic Uses and administration: The standard dosing schedule for Gemcitabine HCl (GEMZAR) is a 30-minute intravenous infusion of 1 to 1.2 g/m² on days 1, 8, and 15 of each 28-day cycle.

Gemcitabine HCl is a highly hydrophilic drug, first approved by FDA in 1996 for the treatment of breast cancer in combination with paclitaxel. In 2006 it was further approved for ovarian cancer in combination with paclitaxel and has been recently approved as the first line of treatment for pancreatic cancer that is advanced or has metastasized.

Non-small cell lung cancer: First line treatment of locally advanced (Stage IIIA or IIIB), or metastatic (Stage IV) non-small cell lung cancer.

Pancreatic cancer: Treatment of locally advanced (non resectable Stage II or Stage III) or metastatic (Stage IV) adenocarcinoma of the pancreas.

Bladder cancer: Treatment of bladder carcinoma at the invasive stage.

Breast cancer: Indicated in combination with cisplatin for the treatment of relapsed metastatic breast cancer after adjuvant/neoadjuvant chemotherapy. Prior chemotherapy should have included an anthracycline unless clinically contra-indicated.

Ovarian cancer: Indicated alone or in combination with other chemotherapeutic agents in the management of patients with advanced or relapsed epithelial ovarian carcinoma.

Adverse effects and clinical Toxicities: : Paresthesia, nausea, vomiting, diarrhoea, stomatitis, hematuria, proteinuria, hemolytic uremic syndrome, renal failure, anemia, leukopenia, thrombocytopenia, dyspnea, bronchospasm, alopecia, rash, cellulitis, flulike symptoms, fever, edema, injection site reactions, anaphylactoid reactions are common adverse effects. The principal toxicity of Gemcitabine HCl is myelosuppression. In general, the longer-duration infusions lead to greater myelosuppression. Nonhematologic toxicities including a flu-like syndrome, asthenia, and mild elevation in liver transaminases may occur in 40% or more of patients. Rarely, patients on Gemcitabine HCl treatment for many months may develop a slowly progressive hemolytic uremic syndrome, necessitating drug discontinuation.

Contraindications:

The drug is contraindicated in patients with known hypersensitivity to the drug or any component in this formulation. Concomitant administration with radiation therapy is contraindicated due to risk of radio sensitization and of the onset of severe pulmonary and oesophageal fibrosis. Concomitant administration with cisplatin in patients with severe renal failure is contraindicated.

Analytical methods:**UV-spectrophotometric method**

A simple accurate and sensitive UV-spectrophotometric method for estimation of Gemcitabine HCl in distilled water at 269 nm was used by Celano et al; 2004, Arias et al; 2009.

HPLC method

USP method is a gradient HPLC method and uses variable mixture of mobile phase solution A and solution B as mobile phase. [Solution A is filtered and degassed solution of 13.8 gm of monobasic sodium phosphate and 2.5 ml of phosphoric acid in 1000 ml of distilled water] while solution B is filtered and degassed methanol. The liquid chromatography is equipped with a 275 nm detector and a 4.6mm X 25cm column that contain packing 5 μ m. The flow rate is 1.2 ml/min. The retention time for Gemcitabine HCl was 6.2 min.

Formulations available: The clinical formulation is supplied in a sterile form for intravenous use only. Vials of Gemzar (Gemcitabine HCl) contain either 200 mg or 1 g of Gemcitabine HCl (expressed as free base) formulated with mannitol (200 mg or 1 g, respectively) and sodium acetate (12.5 mg or 62.5 mg, respectively) as a sterile lyophilized powder. Hydrochloric acid and/or sodium hydroxide may have been added for pH adjustment. Available as *Powder for injection*: 200 mg in 10-ml vial, 1 g in 50-ml vial.

Research work done on Gemcitabine HCl:

Gang et al (2007) formulated Gemcitabine HCl loaded magnetic polycaprolactone nanoparticles and the anti-tumor effects were examined using nude mice bearing subcutaneous human pancreatic adenocarcinoma cells (HPAC) *in vivo*. The antitumor effect was shown with 15-fold lower dose when compared to free Gemcitabine HCl. Proved therapeutic benefit of magnetic PCL nanoparticles by delivering drugs efficiently to magnetically targeted tumor tissues, thus achieving safe and successful anti-tumor effects with low toxicity.

Reddy et al (2008) developed squalenoyl derivatives of Gemcitabine HCl for oral delivery and absorption enhancement and showed improved pharmacokinetics and tissue distribution over the free Gemcitabine HCl in the treatment of leukaemia by oral route.

Trickler et al (2010) formulated Gemcitabine HCl loaded Chitosan and Glycerol monooleate for treatment of pancreatic cancer and showed a significant decrease in IC₅₀ value for cell survival as compared to Gemcitabine solution (Trickler et al; 2010).

Derakshandeh et al (2012) formulated Chitosan nanoparticles for oral absorption of Gemcitabine HCl and showed that intestinal transport of Gemcitabine increased 3–5 folds by loading in chitosan nanocarrier.

Lim et al (2012) formulated Gemcitabine HCl loaded microspheres using chitosan as mucoadhesive polymer and Eudragit L100-55 as enteric copolymer for improving oral absorption and found 3.8 fold increased uptake in Caco 2 cells.

Vandana and Sahoo (2010) developed pegylated Gemcitabine HCl for intravenous delivery and achieved long circulation time for Pegylated Gemcitabine HCl in comparison to plain drug.

Hosneiyah et al (2013) formulated Gemcitabine HCl loaded chitosan -pluronic nanoparticles for oral delivery were studied for treatment of colon cancer. Cytotoxicity assay in HT 29 cells showed increased cytotoxicity of Gemcitabine loaded nanoparticles.

Senanayake et al (2013) formulated nanogel for oral delivery of Gemcitabine HCl and demonstrated potential of therapeutic nanogel conjugates with activated and stabilized Gemcitabine HCl as a successful oral drug form against Gemcitabine-resistant and other drug-resistant tumours.

Hao et al (2013) developed self micro emulsifying drug delivery system for oral delivery of Gemcitabine HCl and found that the formulation was effective against several cancer types, was metabolized more slowly than Gemcitabine hydrochloride, and exhibited enhanced oral bioavailability.

2.9.2 Drug Profile of Lopinavir

Lopinavir (IP 2007, Rx Drug list, Drug Bank, Goodman Gilman's the pharmacological basis of therapeutics; 2006)

Category: Antiviral, Protease Inhibitor

CAS No: 192725-17-0

Molecular Weight: 628.8

Melting Point: 124 to 127 °C

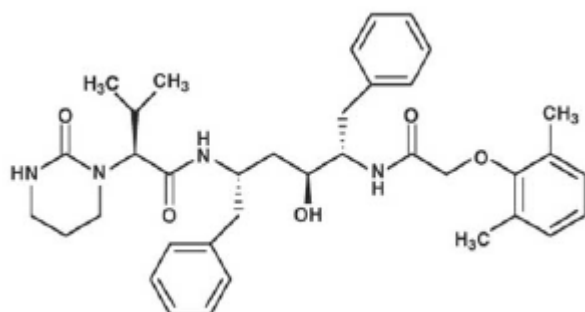
Physicochemical properties: White to light tan powder.

Solubility: Freely soluble in methanol and ethanol; soluble in isopropanol; practically insoluble in water.

Proprietary Names: Kaletra, Aluvia

Molecular Formula: C₃₇-H₄₈-N₄-O₅.C₃₇-H₄₈-N₆-O₅

Structural Formula:



(alphaS)-Tetrahydro- N-[(alphaS)-alpha-[(2S,3S)-2-hydroxy- 4-phenyl-3-[2-(2,6-
xylyloxy)acetamido] butyl]phenethyl]-alpha-isopropyl-2-oxo- 1(2H)-
pyrimidineacetamide

Mechanism of Action: Lopinavir is an inhibitor of the HIV-1 protease, preventing cleavage of the Gag-Pol polyprotein and reducing the probability of viral particles reaching a mature, infectious state. Lopinavir is an antiretroviral agent which inhibits HIV protease, causing the enzyme incapable of processing the polyprotein precursor. This leads to the production of non-infectious and immature HIV particles. Lopinavir is used in combination with ritonavir, which increases the bioavailability to therapeutic levels.

Absorption: It is absorbed from the GI tract. Tablet formulation unaffected by food but liquid capsules and oral liquid have improved bioavailability when taken with food.

Distribution: Approx 98-99% drug is plasma bound.

Metabolism: It is metabolised hepatically by isoenzyme CYP3A.

Excretion: Eliminated via urine (10%) and faeces (83%).

Therapeutic uses and indications: The drug is indicated for treatment of AIDS.

Adverse Drug Reactions: Diarrhoea, abdominal pain, asthenia, headache, dyspepsia, vomiting, myalgia, bronchitis, hypertension, palpitation, thrombophlebitis, vasculitis, agitation, anxiety, ataxia, hypertonic, confusion, depression, dyskinesia, peripheral neuritis; Cushing's syndrome; hypothyroidism, sexual dysfunction, lactic acidosis, arthralgia, abnormal vision, otitis media, tinnitus, acne, alopecia, dry skin, skin discoloration, nail disorders, sweating, Pancreatitis

Contraindications: Hypersensitivity; renal or hepatic failure; lactation; Concomitant use of drugs highly dependent on CYP3A for clearance and associated with serious toxicity.

Analytical methods:

Faux et al, 2001 developed a rapid and simple HPLC method for detection of Lopinavir in plasma samples. In this method, the separation was performed on reverse phase C₈ column (150 X 3.9 mm i.d, 5 µm). The mobile phase consisted of mixture of Acetonitrile and water (41:59, v/v). Flow rate was maintained 1.0 ml/min and compound eluted were recorded by UV detector at 210nm. The method was validated for linearity, accuracy and precision.

Another method was developed by Alex et al, 2011. The method employed a C18 column. The mobile phase consisted of a mixture of 55 volumes of acetonitrile and methanol in the volume ratio 80:20 and 45 volumes of 0.02M potassium dihydrogen phosphate solution with pH adjusted to 3 using orthophosphoric acid. The mobile phase flow rate was adjusted to be 1.5 ml/min. The injection volume was 20microlitre and the maximum wavelength for detection was set as 210 nm.

Dosage forms available:

Film-coated tablets containing Lopinavir 200 mg and ritonavir 50 mg. Oral solution containing Lopinavir 80 mg/ml and ritonavir 20 mg/ml. Soft gelatin capsules containing Lopinavir 133.3 mg and Ritonavir 33.3 mg. Film-coated tablets containing Lopinavir 100 mg and Ritonavir 25 mg.

Research work done on Lopinavir:

PLGA nanoparticles containing combination of Lopinavir and ritonavir were developed by **Destache et al (2009)** and pharmacokinetic studies were performed in rats. They showed the sustained delivery of antiretroviral drugs from the PLGA NPs for 28 days.

Alex et al (2011) developed solid lipid nanoparticles of Lopinavir for lymphatic targeting and results showed that the percentage bioavailability was enhanced but the poor drug loading was nevertheless pointed out as a major drawback in SLN formulations.

Alex et al (2011) proved the enhanced delivery of Lopinavir to CNS by Compritol based solid lipid nanoparticles and demonstrated that SLNs with a poloxamer coating can be effectively absorbed through the lymphatic system, and can effectively target the drug to the CNS due to the combined effect of lipophilicity and surface charge.

Jain et al (2012) formulated surface stabilized nanoparticles of Lopinavir to enhance oral bioavailability without administration of ritonavir and demonstrated 3.11 fold increase in bioavailability in comparison to plain Lopinavir with ritonavir.

Negi et al (2012) developed solid lipid nanoparticles of Lopinavir by hot self nanoemulsifying technique using stearic acid, poloxamer and polyethylene glycol mixture and reported higher oral bioavailability in comparison to plain Lopinavir.

2.10 References

- ❖ Allemann E, Leroux JC, Gurny R. Polymeric nano- and microparticles for the oral delivery of peptides and peptidomimetics. *Adv Drug Deliv Rev*, 34, 1998, 171–189
- ❖ Alex A, Chacko AJ, Jose S, Souto EB. Lopinavir loaded solid lipid nanoparticles (SLN) for intestinal lymphatic targeting. *Eur J Pharm Sci*, 42, 2011, 11–18.
- ❖ Alex A, Paul W, Chacko AJ, Sharma CP. Enhanced delivery of lopinavir to the CNS using Compritol-based solid lipid nanoparticles. *Ther Deliv*, 2(1), 2011, 25-35.
- ❖ Amiji MM, Vyas TK, Shah LK. Role of nanotechnology in HIV/AIDS treatment: Potential to overcome the viral reservoir challenge. *Discov Med*, 6(34), 2006, 157–162.
- ❖ Anne des R, Virginie F, Marie G, Yves-Jacques Schneider B, Veronique P. Nanoparticles as potential oral delivery systems of proteins and vaccines: A mechanistic approach. *Journal of Controlled Release*, 116, 2006, 1–27.
- ❖ Arias JL, Visitaciano G, Adolfini RM. Engineering of Poly (butylcyanoacrylate) Nanoparticles for the enhancement of the antitumor activity of gemcitabine. *Biomacromolecules*, 11, 2010, 308–318.
- ❖ Arima H, Yunomae K, Hirayama F, Uekama K. Contribution of P-glycoprotein to the enhancing effects of dimethyl-beta-cyclodextrin on oral bioavailability of tacrolimus. *J Pharmacol Exp Ther*, 297, 2001, 547–555.
- ❖ Barichello JM et al. Encapsulation of hydrophilic and lipophilic drugs in PLGA nanoparticles by the nanoprecipitation method. *Drug Dev Ind Pharm*, 25 (4), 1999, 471–476.
- ❖ Bhardwaj V, Ankola DD, Gupta SC, Schneider M, Lehr CM and Ravi Kumar MNV. PLGA Nanoparticles Stabilized with Cationic Surfactant: Safety Studies and Application in Oral Delivery of Paclitaxel to Treat Chemical-Induced Breast Cancer in Rat. *Pharmaceutical Research*, 26(11), 2009, 2495-2503.
- ❖ Burkersrodaa FV, Gref R, Gopferich A. Erosion of biodegradable block copolymers made of poly (D,L-lactic acid) and poly(ethylene glycol). *Biomaterials*, 18(24), 1997, 1599-1607.
- ❖ Blankson JN, Persaud D, Siliciano RF. The challenge of viral reservoirs in HIV-1 infection. *Annu Rev Med*, 53, 2002, 557–593.

- ❖ Brigger I, Dubernet C, Couvreur P. Nanoparticles in cancer therapy and diagnosis *Adv Drug Deliv Rev*, 64, 2012, 24–36.
- ❖ Celano M, Calvagno MG, Bulotta S, Paolino D, Arturi F, Rotiroti D, Filetti S, Fresta M & Russo D 2004 Cytotoxic effects of Gemcitabine-loaded liposomes in human anaplastic thyroid carcinoma cells. *BMC Cancer* 4 63,1-5.
- ❖ Chabner BA, Amrein PC, Druker B, Michaelson MD, Mitsiades CS, Goss PE, Ryan DP, et al. Gemcitabine; Chemotherapy of neoplastic diseases. In, Brunton LL, Lazo JS, Parker KL, eds. *Goodman & Gilman's the Pharmacological Basis of Therapeutics*. 11th Ed. New York: McGraw-Hill, 2006, pp. 1346.
- ❖ Clark et al. Exploiting M cells for drug and vaccine delivery. *Adv Drug Deliv Rev*, 50, 2001, 81–106.
- ❖ Couvreur P. Nanoparticles in drug delivery: Past, present and future. *Adv Drug Deliv Rev*, 65, 2013, 21–23.
- ❖ Couvreur P, G. Couarraze, J.-P. Devissaguet, F. Puisieux, Nanoparticles: preparation and characterization, in: S. Benita (Ed.), *Microencapsulation: Methods and Industrial Application*, Marcel Dekker, New York, 1996, pp. 183–211.
- ❖ Dembri A, Montisci MJ, Gantier JC, Chacun H, Ponchel G. Targeting of 3' -azido 3' -deoxythymidine (AZT)-loaded poly(isohexylcyanoacrylate) nanospheres to the gastrointestinal mucosa and associated lymphoid tissues, *Pharm. Res*, 18, 2001, 467–473.
- ❖ Derakhshandeh K, Fathi S. Role of chitosan nanoparticles in the oral absorption of Gemcitabine. *Int J. Pharm*, 437, 2012, 172-177.
- ❖ Destache CJ, Todd B, Goede M, Shibata A, Belshan MA. Antiretroviral release from poly (DL-lactide-co-glycolide) nanoparticles in mice. *J. Antimicrob. Chemotherapy*, 65(10), 2010, 2183-2187.
- ❖ Doming BN, Perl D, Schmid FX, Brooks CL III. The effect of ionic strength on protein stability: The cold shock protein family. *J Mol Biol*, 319, 2002, 541-554.
- ❖ Dou HJ, Morehead CJ, Destache JD, Kingsley L, Shlyakhtenko Y, Zhou M, Chaubal J, Werling JK, Rabinow BE, Gendelman HE. Laboratory investigations for the morphologic, pharmacokinetic, and anti-retroviral properties of indinavir

- nanoparticles in human monocyte-derived macrophages, *Virology*, 358, 2007, 148–158.
- ❖ D'Souza, S. S. and P. P. DeLuca. Methods to assess *in vitro* drug release from injectable polymeric particulate systems. *Pharm Res*, 23(3),2006, 460-474.
 - ❖ Ensign LM, Richard Cone, Hanes J. Oral drug delivery with polymeric nanoparticles: The gastrointestinal mucus barriers. *Adv Drug Deliv Rev*, 64, 2012, 557–570.
 - ❖ Farokhzad OC, Langer R. Impact of nanotechnology on drug delivery. *ACS Nano*, 3(1), 2009, 16–20.
 - ❖ Faux J, Venisse N, Olivier JC, Bouquet Rapid high-performance liquid chromatography determination of lopinavir, a novel HIV-1 protease inhibitor, in human plasma. *Chromatographia*.54, 2001, 469–473.
 - ❖ Feng SS, Zhao LY, Tang JT. Nanomedicine for oral chemotherapy, *Nanomedicine*, 6, 2011, 407–410.
 - ❖ Feng SS, Mei L, Anitha P, Gan CW, Zhou WY. Poly (lactide)–vitamin E derivative/montmorillonite nanoparticle formulations for the oral delivery of docetaxel. *Biomaterials*, 30, 2009, 3297–3306.
 - ❖ Fessi H, Duisieux F, Devissague JP, Ammoury N, Bentia S. Nanocapsule formation by interfacial polymer deposition following solvent displacement. *Int J Pharm*, 113, 1995, 57-63.
 - ❖ Florence AT. The Oral absorption of micro and nanoparticulates: neither exceptional nor unusual. *Pharm Res*, 14(3), 1997, 35-47.
 - ❖ Florence AT. Issues in oral nanoparticle drug carrier uptake and targeting. *Journal of Drug Targeting*, 12 (2), 2004, 65–70.
 - ❖ Florence AT. Nanoparticle uptake by the oral route: fulfilling its potential. *Drug Discov Today Technol*, 2, 2005, 75–81.
 - ❖ Gang J, Park SB, Hyung W, Choi EH, Wen J, Kim HS, Shul YG, Haam S, Song SY. Magnetic poly epsilon-caprolactone nanoparticles containing Fe₃O₄ and gemcitabine enhance anti-tumor effect in pancreatic cancer xenograft mouse model, *J Drug Target*, 15, 2007, 445-453.
 - ❖ Gebert A, Rothkotter HJ, Pabst R. M cells in Peyer's patches of the intestine. *Int Rev Cytol*, 167, 1996, 91–159.

- ❖ Gopferich A. Mechanisms of polymer degradation and erosion. *The Biomaterials*, 17 (2), 1996, 103- 114.
- ❖ Govender T, Stolnik S., Garnett M.C., Illum L, Davis DS. PLGA nanoparticles prepared by nanoprecipitation: drug loading and release studies of a water soluble drug. *J. Controlled Release*, 57, 1999, 171-185.
- ❖ Guerrero Q, Allemann E, Fessi H, Doelker E. Preparation techniques and mechanisms of formation of biodegradable nanoparticles from preformed polymers. *Drug. Dev. Ind. Pharm*, 24, 1998, 1113-1128.
- ❖ Hagan DTO. Intestinal translocation of particulates — implications for drug and antigen delivery, *Adv. Drug Deliv. Rev.* 5, 1990, 265–285.
- ❖ Hao WH, Wang JJ, Hsueh SP, Hsu PJ, Chang LC, Hsu CS, Hsu KY. *In vitro* and *in vivo* studies of pharmacokinetics and antitumor efficacy of D07001-F4, an oral gemcitabine formulation. *Cancer Chemother Pharmacol*, 71, 2013, 379–388.
- ❖ Huh KM et al. PLGA-PEG Copolymers. *Drug Delivery Technol*, 3(8), 2003,.
- ❖ Indian Pharmacopoeia. Indian Pharmacopoeial Commission; Ghaziabad, INDIA, 2, 2007, 697-700.
- ❖ Italia JL, Bhatt DK, Bhardwaj V, RaviKumar MNV. PLGA Nanoparticles for oral delivery of cyclosporine, *J. Control Release*, 119(2), 2007, 197-206.
- ❖ Jain AK, Swarnakar NK, Godugu C, Singh RP, Jain S. The effect of the oral administration of polymeric nanoparticles on the efficacy and toxicity of temoxifen. *Biomaterials*, 32, 2011 503-515.
- ❖ Jain D, Athawale R, Bajaj A, Shrikhande S, Goel P, Gude R. Studies on stabilization mechanism and stealth effect of poloxamer 188 onto PLGA nanoparticles. *Colloids and Surfaces B: Biointerfaces*, 109(1), 2013, 59–67.
- ❖ Jain RA. Transport of molecules in the tumor interstitium: a review. *Cancer Res*, 47, 1987, 3039–3051.
- ❖ Jain RA. The manufacturing techniques of various drug loaded biodegradable Poly (lactide-co-glycolide) (PLGA) devices. *Biomaterials*, 21, 2000, 247-2490.
- ❖ Jain S, Sharma JM, Jain AK, Mahajan RR. Surface-stabilized Lopinavir nanoparticles enhance oral bioavailability without co administration of ritonavir. *Nanomedicine (Lond)*. 2013 Jan 25.

- ❖ Jaiswal J, Gupta SK, Kreuter J. Preparation of biodegradable cyclosporine nanoparticles by high-pressure emulsification-solvent evaporation process. *Journal of Controlled Release*, 96(1), 2004, 169-178.
- ❖ Jani PU, Florence AT, McCarthy DE. Further histological evidence of the gastrointestinal absorption of polystyrene nanospheres in the rat. *Int. J. Pharm.* 84, 1992, 245-252.
- ❖ Kalaria DR, Sharma G, V. Beniwal, M.N. Ravi Kumar, Design of biodegradable nanoparticles for oral delivery of doxorubicin: *in vivo* pharmacokinetics and toxicity studies in rats, *Pharm Res*, 26, 2009, 492-501.
- ❖ Keck CM. Particle size analysis of nanocrystals: Improved analysis method. *Int J Pharm.* 390, 2010, 3-12.
- ❖ Kinman L, Bui T, Larsen K, Tsai C, Anderson D, Morton WR, Hu SL, Ho RJ, Optimization of lipid-indinavir complexes for localization in lymphoid tissues of HIV-infected macaques. *J Acquir Immune Defic Syndr*, 42, 2006, 155-161.
- ❖ Kompella UB, Bandi N, Ayalasonmayajula SP. Poly (lactic acid) nanoparticles for sustained release of budesonide. *Drug Deliv Technol*, 1, 2001, 1-7.
- ❖ Kreuter J. Nanoparticulate systems in drug delivery and targeting. *J Drug Target*, 3, 1995, 171-173.
- ❖ Kreuter J. Nanoparticles. In J. Swarbrick and J.C. Boylan (Eds) *Encyclopedia of Pharmaceutical Technology*. Marcel Dekker Inc.: New York, 10, 1994, 165-190.
- ❖ Langer R. Biomaterials in drug delivery and tissue engineering: one laboratory's experience. *Acc Chem Res*, 33, 2000, 94-101.
- ❖ Lavelle EC, Sharif S, Thomas NW, Holland J, Davis SS. The importance of gastrointestinal uptake of particles in the design of oral delivery systems, *Adv. Drug Deliv Rev*, 18, 1995, 5-22.
- ❖ Lee M, Kim SW. Polyethylene glycol-conjugated copolymers for plasmid DNA delivery. *Pharm Res*, 22, 2005, 1-10.
- ❖ Levy JA, HIV and the pathogenesis of AIDS. American Society of Microbiology Press, Washington, DC, 3rd ed, 2007.
- ❖ Lobenberg L, Araujo J, Kreuter. Body distribution of azidothymidine bound to nanoparticles after oral administration. *Eur J Pharm Biopharm*, 44, 1997, 127-132.

- ❖ Madara JL, Regulation of the movement of solutes across tight junctions, *Annu. Rev. Physiol.* 60, 1998, 143–159.
- ❖ Malingre MM, Richel DJ, Beijnen JH, Rosing H, Koopman FJ, Ten WW, Bokkel H, Schot ME, Schellens JH. Co-administration of cyclosporine strongly enhances the oral bioavailability of docetaxel. *J Clin Oncol*, 19, 2001, 1160–1166.
- ❖ Mamo T, Moseman EA, Kolishetti N, Salvador- Morales C, Shi J, Kuritzkes DR, Langer R, Ulrich VA, Farokhzad OC. Emerging nanotechnology approaches for HIV/AIDS treatment and prevention. *Nanomedicine*, 5(2), 2010, 269–285.
- ❖ Marsden MD, Zack JA. Eradication of HIV: Current challenges and new directions. *J Antimicrob Chemother.* 63(1), 2009, 7–10.
- ❖ Martindale Extra Pharmacopoeia, 36th Ed. Pharmaceutical Press, London, 2009, pp. 804 and 1390-1396.
- ❖ Mei Lin , Zhang Z, Zhao L, Huang L, Yang XL, Tang J, Feng SS. Pharmaceutical nanotechnology for oral delivery of anticancer drugs. *Adv Drug Deliv Rev.* 2013, 1-12.
- ❖ Meneau BPCBF and Ollivon PCM. Interaction of an anticancer drug, gemcitabine, with phospholipid bilayers. *Acta Biomater J Therm Anal Calorim*, 98, 2009, 19–28.
- ❖ Merson MH. The HIV-AIDS pandemic at 25 – the global response. *N Engl J Med*, 354(23), 2006, 2414–2417.
- ❖ Mohanraj VJ, Chen Y. Nanoparticles – A Review. *Tropical Journal of Pharmaceutical Research*, 51, 2006, 561-573.
- ❖ Molpeceres J, Aberturas MR, Guzman M. Biodegradable nanoparticles as a delivery system for cyclosporin: preparation and characterization. *J Microencapsulation*, 17, 2000, 599-614.
- ❖ Mosqueira VCF, Legrand P, Gulik A, Bourdon O, Gref R, Labarre D, Barratt G. Relationship between complement activation, cellular uptake and surface physicochemical aspects of novel PEG-modified nanocapsules. *Biomaterials*. 22, 2001, 2967-2979.
- ❖ Muller RH, Grau MJ. Increase in dissolution velocity and solubility of poorly water soluble drugs as nanosuspensions. *Proceeding of World Meeting APGI APV*; 2, 1998, 623-624.

- ❖ Muller RH, Jacobs C, Kayser O. Nanosuspension as particulate drug formulations in therapy rationale for development and what we can expect for the future. *Adv Drug Del Rev.* 47, 2001, 3-19.
- ❖ Muller RH, Jacobs C. Buparvaquone mucoadhesive nanosuspension: preparation, optimisation and long-term stability. *Int J Pharm.* 237, 2002, 151-161.
- ❖ Muller RH, Peters K. Nanosuspension for formulation of poorly soluble drugs I: Preparation by size reduction technique. *Int J Pharm.* 160, 1998, 229-237.
- ❖ Muller RH. Particle size analysis of latex suspensions and microemulsions by photon correlation spectroscopy. *J Pharm Sci.* 73, 1984, 915-918.
- ❖ Negi JS, Chattopadhyay P, Sharma AK, Ram V. Development of solid lipid nanoparticles (SLNs) of lopinavir using hot self nano-emulsification (SNE) technique. *Eur J Pharm Sci*, 48 (1-2), 2012, 231-9.
- ❖ Neves JD, Amiji M, Fernanda Bahia M, Sarmiento B. Nanotechnology-based systems for the treatment and prevention of HIV/AIDS. *Advanced Drug Delivery Reviews*, 62, 2010, 458-477.
- ❖ Nizri G, Magdassi S, Schimdt J, Cohen Y, Talmon Y. Microstructural characterization of micro- and nanoparticles formed by polymer-surfactant interaction. *Langmuir* 20, 2004, 4380-4438.
- ❖ Nowacek A, Gendelman HE. Nanoart, neuroAIDS and CNS drug delivery. *Nanomed*, 4 (5), 2009, 557-574.
- ❖ Patronidou C, Karakosta P, Kotti K, Kammona O, Karageorgiou V, Kiparissides C. PLGA nanocarriers for systemic and lymphatic oral delivery of proteins and peptides. *Abstracts/J Control Release*, 132, 2008, e1-e18.
- ❖ Pecora R. Dynamic light scattering measurements of nanometre particles in liquids. *J Nanopart Res*, 2, 2000, 123-131.
- ❖ Plapied L, N. Duhem, A. des Rieux, V. Preat, Fate of polymeric nanocarriers for oral drug delivery, *Curr. Opin. Colloid Interface*, 16, 2011, 228-237.
- ❖ PLGA, Purac biomaterials, The Netherlands.
- ❖ Ravi MN, Bakowsky U, Lehr CM. Preparation and characterization of cationic PLGA nanospheres as DNA carriers. *Biomaterials*, 25, 2004, 1771-1777.
- ❖ Reddy LH, Ferreira H, Dubernet C, Mouelhi SL, Desmaele D, Rousseau B, Couvreur P. Squalenoyl nanomedicine of gemcitabine is more potent after oral

- administration in leukemia-bearing rats: study of mechanisms. *Anticancer Drugs*, 19(10), 2008, 999-1006.
- ❖ Richman DD. HIV chemotherapy. *Nature*, 410(6831), 2001, 995–1001.
 - ❖ Rubas W, Cromwell ME, Shahrokh Z, Villagran J, Nguyen TN, Wellton M, NguyenTH, Mrsny RJ. Flux measurements across Caco-2 monolayers may predict transport in human large intestinal tissue, *J Pharm Sci*, 85, 1996, 165–169.
 - ❖ Russell-Jones GJ, The potential use of receptor-mediated endocytosis for oral drug delivery, *Adv Drug Deliv Rev*, 20, 1996, 83–97.
 - ❖ Salama NN, Eddington ND, Fasano A. Tight junction modulation and its relationship to drug delivery. *Adv Drug Deliv Rev*, 58, 2006, 15–28.
 - ❖ Senanayake TH, Warren G, Wei X, Vinogradov SV. Application of activated nucleoside analogs for the treatment of drug-resistant tumors by oral delivery of nanogel-drug conjugates. *Journal of Controlled Release*, 167, 2013, 200-209.
 - ❖ Shakweh M., Ponchel G., Fattal E. Particle uptake by Peyer's patches: a pathway for drug and vaccine delivery. *Expert. Opinion. Drug Delivery*. 1, 2004, 141–163.
 - ❖ Shakweh M., Besnard M., Nicolas V., Fattal E. Poly (lactide-co-glycolide) particles of different physicochemical properties and their uptake by Peyer's patches in mice. *Eur. J. Pharm. Biopharm*, 61, 2005, 1–13.
 - ❖ Schrager LK, D'Souza MP, Cellular and anatomical reservoirs of HIV-1 in patients receiving potent antiretroviral combination therapy. *JAMA*, 280, 1998, 67–71.
 - ❖ Smith J. Wood E, Dornish M. Effect of chitosan on epithelial cell tight junctions. *Pharm. Res*. 21, 2004, 43–49.
 - ❖ Song C X et al. Formulation and characterization of biodegradable nanoparticles for intravascular local drug delivery. *J Control Release*, 43, 1997, 197–212.
 - ❖ Soppimath, K. S., T. M. Aminabhavi, et al. Biodegradable polymeric nanoparticles as drug delivery devices. *J Control Release*, 70(1-2), 2001, 1-20.
 - ❖ Trickler WJ, Khurana J, Nagvekar AA, Dash AK. Chitosan and glyceryl monooleate nanostructures containing gemcitabine: potential delivery system for pancreatic cancer treatment. *AAPS PharmSciTech*, 11, 2010, 392-401.
 - ❖ Ubrich N. Preparation and Characterization of Propranolol hydrochloride nanoparticles: A comparative study. *Journal of Controlled Release*, 78, 2004, 269-273.

- ❖ USP 30, NF27. United States Pharmacopoeial Commission, Rockville, NY, 2007, 2214-15.
- ❖ Vivekananda B, Majeti N, Venkata Ravi K. Polymeric Nanoparticles for Oral Drug Delivery In Nanoparticle Technology for Drug Delivery, Taylor & Francis, 231-262, 2007.
- ❖ Vandana M, Sahoo SK, Long circulation and cytotoxicity of PEGylated gemcitabine and its potential for the treatment of pancreatic cancer, *Biomaterials*, 31, 2010, 9340-9356.
- ❖ Vandervoort J, Ludwig A. Biocompatible stabilizers in the preparation of PLGA nanoparticles: A factorial design study. *Int. J Pharm*, 238, 2002, 77-92.
- ❖ Vila A, Sanchez A, Tobio M, Calvo P, Alonso MJ. Design of biodegradable particles for protein delivery. *J Control Release*, 78, 2002, 15-24.
- ❖ Vyas TK, Shah L, Amiji MM. Nanoparticulate drug carriers for delivery of HIV/AIDS therapy to viral reservoir sites. *Expert Opin Drug Deliv* ,3(5), 2006, 613-628
- ❖ Walensky RP, Paltiel AD, Losina E, et al. The survival benefits of AIDS treatment in the United States. *J Infect Dis*, 194(1), 2006, 11-19.
- ❖ Wang B, Siahaan T, Soltero R.A. Drug delivery principles and applications. 2005, 15-41.
- ❖ Yun Y, Cho Y W, Park K, Nanoparticles for oral delivery: Targeted nanoparticles with peptidic ligands for oral delivery, *Adv Drug Deliv Reviews*, 2012.
- ❖ Zhang Z, Tan S, Feng SS, Vitamin E TPGS as a molecular biomaterial for drug delivery, *Biomaterials* 33, 2012, 4889-4906.

CHAPTER 3

ANALYTICAL METHODS

3.1 Materials

Gemcitabine HCl was obtained as gift sample from Ranbaxy laboratories, Gurgaon, India. Lopinavir was obtained as gift sample from Aurobindo Pharma, Hyderabad, India. Brij 35 and monobasic sodium phosphate were purchased from Sigma Aldrich, Germany. Monobasic potassium phosphate, sodium phosphate and HCl were obtained from SD finechem ltd, Mumbai, India. Acetonitrile, Water and Methanol were of HPLC grade and purchased from Merck Chemicals, India. All the other solvents and reagents used were of analytical grade and filtered through a 0.2 μ m Ultipor ® Nylon 66 membrane filter (Pall Life Sciences, USA) prior to use.

3.2 Estimation of Gemcitabine HCl by UV spectroscopy

3.2.1 Calibration Plot in Distilled Water

UV spectrophotometric analysis was performed as per method reported by Arias et al 2010. Standard stock solution was prepared by dissolving 10mg of Gemcitabine HCl in 100 ml of distilled water. Suitable aliquots of the stock solution were pipetted out into 10 ml volumetric flasks and the volume was made upto 10 ml with distilled water to give final concentrations ranging from 5-35 μ g/ml. The solutions were mixed using vortex mixer and their absorbances measured at λ_{max} 269 nm using distilled water as blank on Shimadzu 1700 UV-Visible Spectrophotometer and calibration curve was plotted. The above procedure was repeated three times. Standard concentrations (5.0, 15.0 and 30.0 μ g/ml) were prepared and subjected to estimate accuracy and precision.

3.2.2 Analytical Method Validation

The method was validated for accuracy, precision and linearity.

3.2.2.1 Linearity

The linearity of an analytical method is its ability within a definite range to obtain results directly proportional to the concentrations (quantities) of the analyte in the sample (Hubert et al; 2003). Linearity of a light absorption determination should be examined to ensure that Beer's law operates over the range of interest. For evaluation of the linearity of the UV method of Gemcitabine HCl, the standard solutions were prepared at 5, 10, 15, 20, 25 and 30 μ g/ml concentrations (n = 3) and absorbance

difference ($dA/d\lambda$) were taken at 269 nm. The mean absorbance difference was plotted against concentration to get a calibration curve. Least square regression method was used to determine the regression coefficient, r^2 and the equation for the best fitting line. The method can be said to be linear for estimation of Gemcitabine HCl if R^2 is near to 1.

3.2.2.2 Accuracy

Accuracy refers to the closeness of an individual observation or mean of the observations to true value (Bolton; 1990). The accuracy is expressed as % bias or % relative error (difference from added concentration) and it takes into account the total error, i.e. systematic and random errors, related to the test result (Hubert et al; 2003). The “true” value is the result which would be observed in absence of error. Accuracy of the assay is defined as the percentage of the agreement between the measured value and the true value as follows (Merodia et al; 2000). The accuracy was calculated by using following formula:

$$\text{Accuracy} = (\text{True value} - \text{Measured value}/\text{True value}) * 100 \quad \text{.....3.1}$$

3.2.2.3 Precision

It refers to the extent of variability of a group of measurements observed under similar conditions. Precision provides an indication of random errors and is generally subdivided into two cases: repeatability and reproducibility, which were determined by calculating RSD (Relative standard deviation) or CV (Coefficient of variation) of inter-day and intra-day determinations. One of the common ways of expressing the variability, which takes into account its relative magnitude, is the ratio of the standard deviation (SD) to the mean, SD/Mean . This ratio, often expressed as a percentage, is called the *Coefficient of Variation* abbreviated as CV or RSD, the *relative standard deviation*. In biological data, the CV is often between 20 -50%. The relatively large CV observed in biological experiments is due mostly to “biological variation”, the lack of reproducibility in living material (Bolton; 1990).

3.2.3 Results and Discussion

Gemcitabine HCl in distilled water showed a characteristic spectrum when scanned in the ultraviolet range between 200 and 600 nm. The scan showed absorption maximum at 269 nm and this wavelength was chosen as the analytical wavelength. Beer's law was obeyed between 5 and 35 $\mu\text{g/ml}$ (Table 3.1). Regression analysis was performed on the experimental data. Regression equation for standard curve was $y = 0.0297x + 0.0113$ (Fig. 3.1). Correlation coefficient was found to be 0.9997 signifying that a linear relationship existed between absorbance and concentration of the drug. The UV spectrum for Gemcitabine HCl is shown in Fig. 3.2. Parameters indicating linearity for the developed UV spectrometric method of analysis for Gemcitabine HCl are shown in Table 3.2.

Table 3.1 Calibration data for Gemcitabine HCl in distilled water by UV spectroscopy

Sr. No	Concentration ($\mu\text{g/ml}$)	Mean Absorbance \pm SD
1	5	0.158 \pm 0.032
2	10	0.312 \pm 0.012
3	15	0.463 \pm 0.023
4	20	0.597 \pm 0.031
5	25	0.746 \pm 0.053
6	30	0.906 \pm 0.088
7	35	1.053 \pm 0.084

*Average of 3 determinations

Table 3.2 Parameters for estimation of Gemcitabine HCl in distilled water by UV spectroscopy

Parameters	Results
λ_{max}	269 nm
Linearity range	5-35 $\mu\text{g/ml}$
Regression equation	$y = 0.0297x + 0.0113$
Correlation coefficient	0.9997

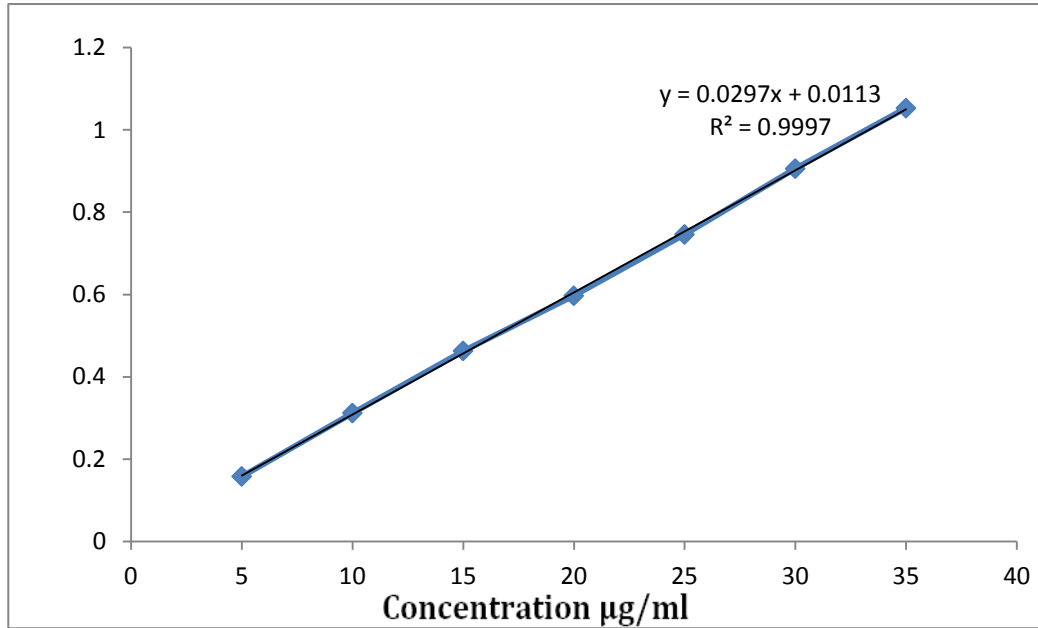


Fig. 3.1 Standard plot of Gemcitabine HCl in distilled water by UV spectroscopy

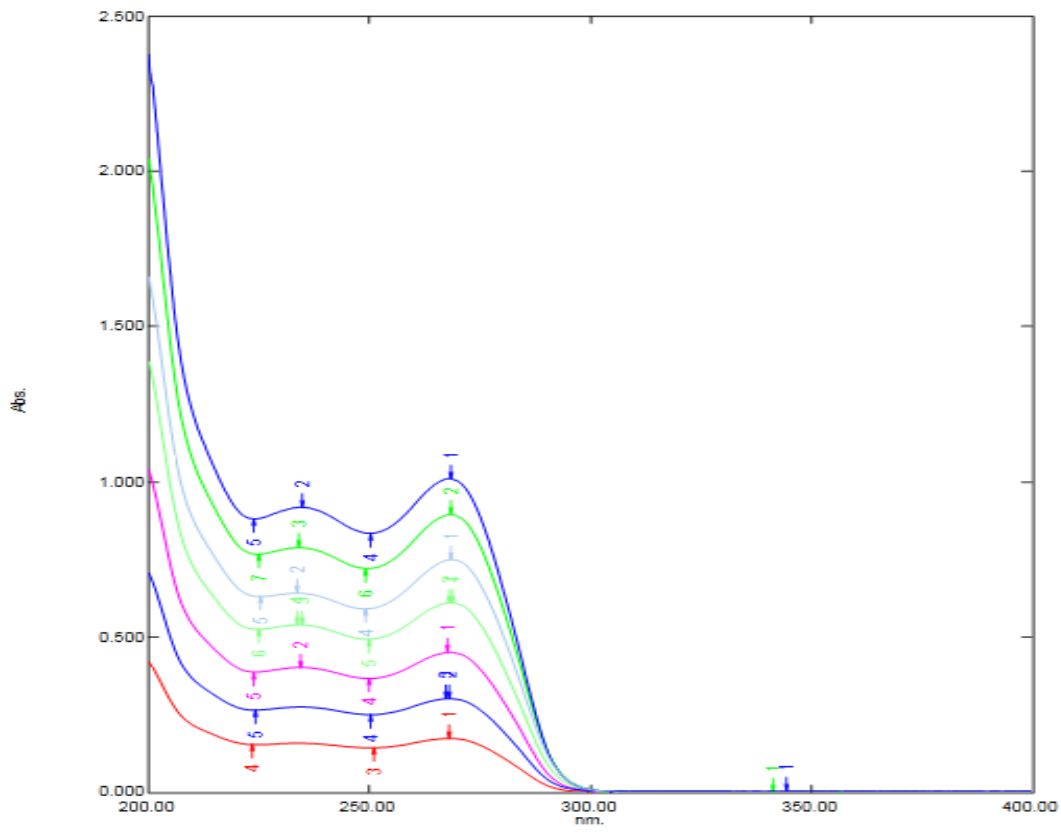


Fig. 3.2 UV spectrum of Gemcitabine HCl in distilled water

Table 3.3 shows Precision and accuracy for the Gemcitabine HCl assay by UV spectroscopy. The low % CV in Table 3.3 values indicated precision of the method. No

significant difference between the amount of drug added (actual) and observed concentration was noticed indicating accuracy of the method.

Table 3.3 Precision and accuracy for estimation Gemcitabine HCl in distilled water by UV spectroscopy

Standard Concentration ($\mu\text{g/ml}$)		Precision (%) ^a	Accuracy (%) ^b
Actual	Observed		
5	5.04 \pm 0.008	0.159	100.8
15	15.02 \pm 0.029	0.193	100.1
30	30.04 \pm 0.015	0.499	100.1

^a Expressed as relative standard deviation, RSD

$$\text{RSD} = (\text{standard deviation}/\text{mean concentration}) \times 100$$

^b Expressed as (mean observed concentration/actual concentration) \times 100

3.3 Estimation of Gemcitabine HCl by HPLC

Estimation of Gemcitabine HCl by HPLC was carried out as per reported method in United States Pharmacopoeia (USP 30 NF25). This method involves liquid-liquid extraction. The mobile phase consisted of mixture of buffer and methanol (97:3). The buffer was 13.8gm monobasic sodium phosphate and 2.5 ml of phosphoric acid in 1000 ml of deionised water (Final pH of solution was between 2.5-2.6). After preparation, the mobile phase was degassed and filtered through 0.45 μ nylon filter. Shimadzu isocratic HPLC with a UV-visible detector was used for HPLC analysis. The separation was done on analytical column C8 (250 X 4.6 mm), packed with reverse phase material 5 μm (Thermo, Hypersil) and connected to 2 cm pre column. The injection volume was 20 μl , the flow rate was 1.2 ml/min, run time was 10 min and detection wavelength was 269 nm. The required parameters were programmed using software.

3.3.1 The Calibration Plot of Gemcitabine HCl in Buffer: Methanol

Calibration plot of Gemcitabine HCl in buffer: methanol (97:3) was prepared in the concentration range of 10-50 µg/ml. The stock solution 1mg/ml was prepared by dissolving Gemcitabine HCl in buffer: methanol (97:3). Appropriate and accurate aliquots of the stock solutions were transferred to 10ml calibrated flasks and diluted up to the volume with buffer: methanol (97:3) in order to get a series of known final concentrations. Analytical method was validated for linearity, precision, and accuracy as described in section 3.2.

3.3.2 Results and Discussion

The retention time of Gemcitabine HCl was 6.2 min. The standard plot of Gemcitabine HCl in buffer: methanol is shown in Fig 3.3 and Table 3.4. HPLC chromatogram of Gemcitabine HCl is shown in Fig. 3.4 and 3.5. The parameters for calibration plot of Gemcitabine HCl by HPLC (Table 3.5) was fitted into a linear equation $y=25.644x+3.064$ with correlation coefficient of $R^2=0.9985$, which indicated the linearity of the plot. Precision and accuracy for the Gemcitabine HCl assay by HPLC are shown in Table 3.6.

Table 3.4 Calibration data for estimation of Gemcitabine HCl in buffer: methanol by HPLC

Sr. No.	Concentration (µg/ml)	Area under curve (mAU)
1	10	273.73±6.9
2	20	496.75±9.8
3	30	779.84±13.2
4	40	1014.37±19.3
5	50	1297.67±29.6

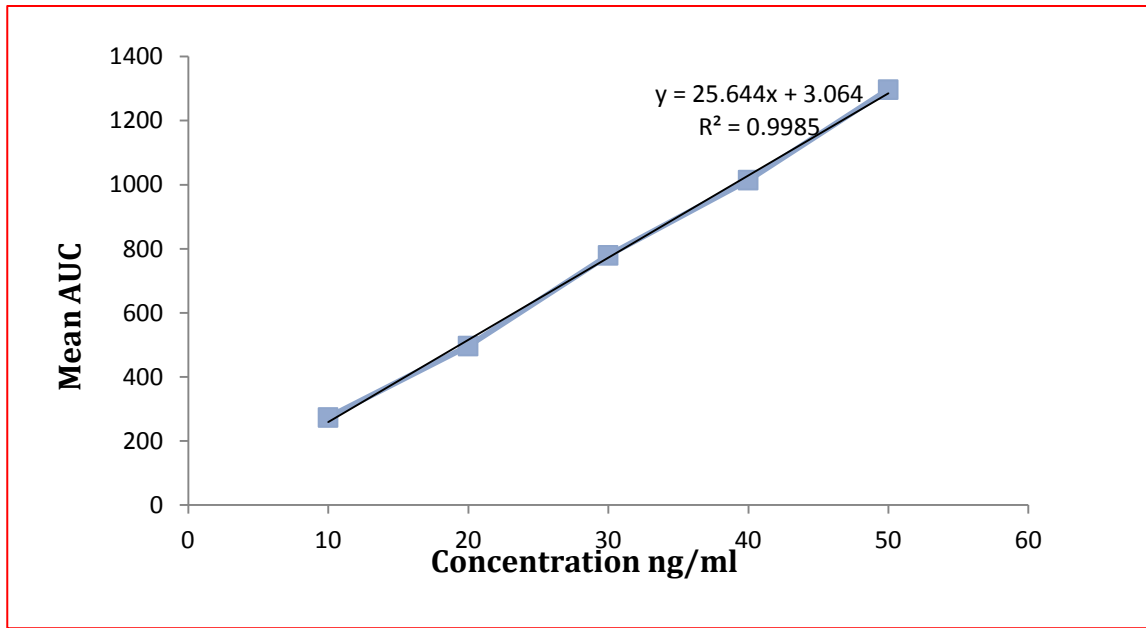


Fig. 3.3 Standard plot of Gemcitabine HCl in buffer: methanol (97:3) by HPLC

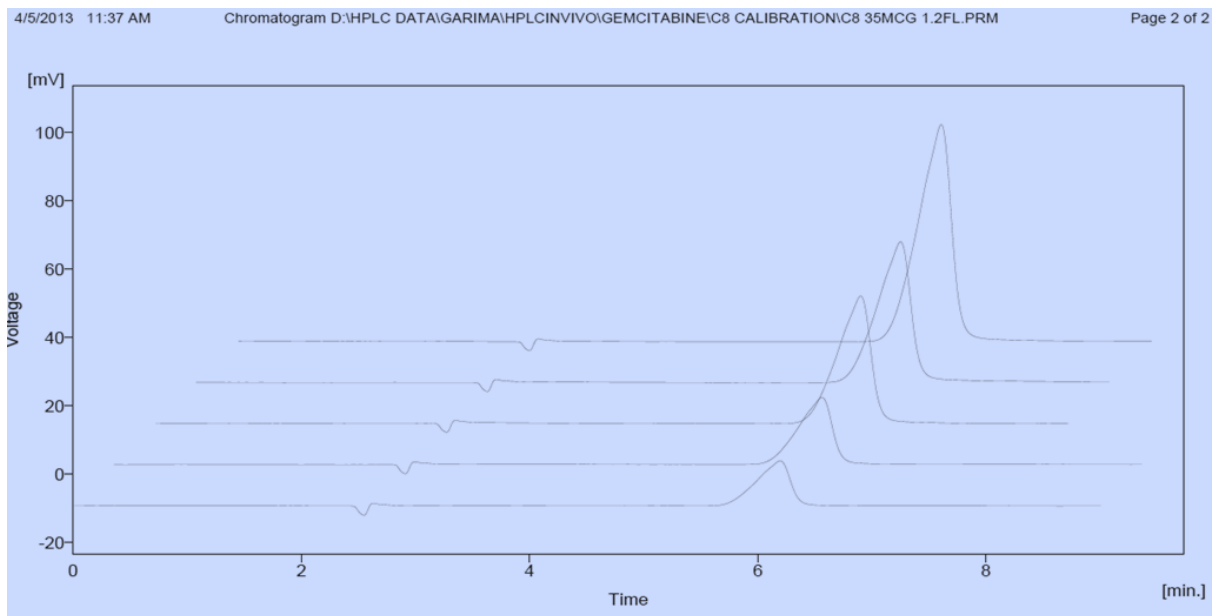


Fig. 3.4 Overlay graph of calibration curve of Gemcitabine HCl in buffer: methanol by HPLC

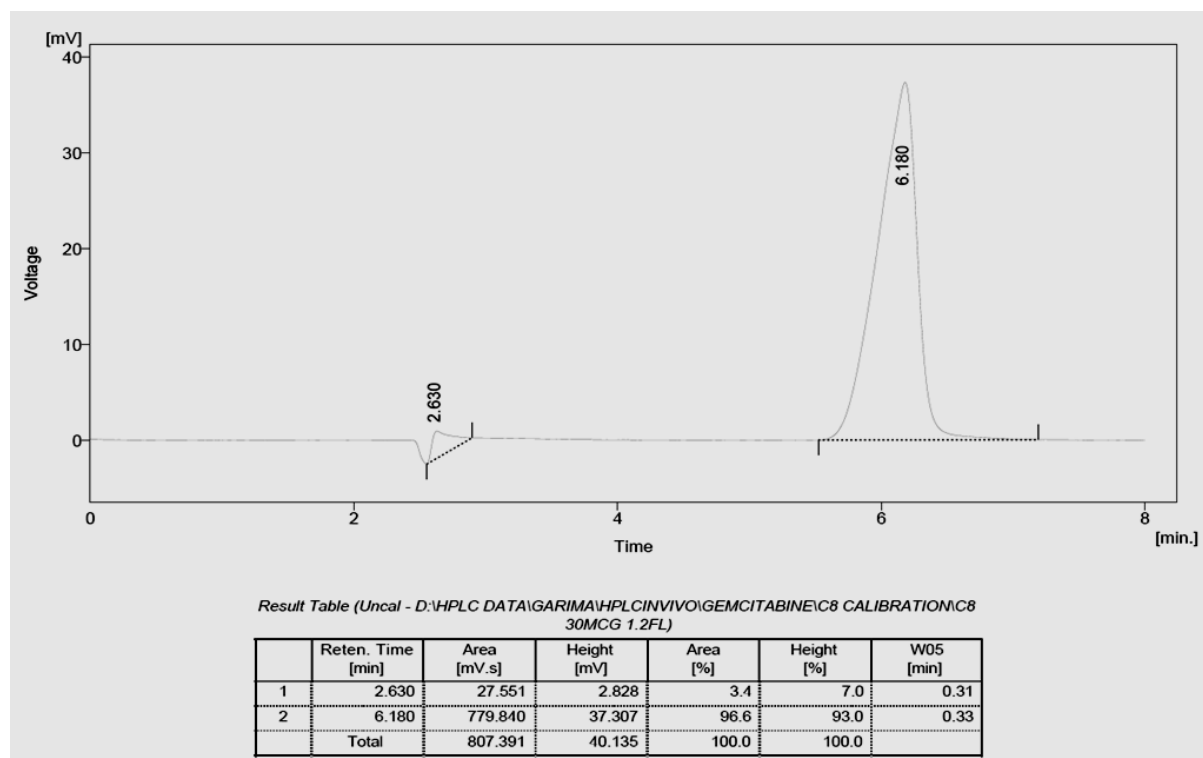


Fig 3.5 HPLC chromatogram of Gemcitabine HCl in buffer: methanol (retention time at 6.2 min)

Table 3.5 Parameters for estimation of Gemcitabine HCl in buffer: methanol by HPLC

Parameters	Results
λ_{max}	269 nm
Linearity range	10-50 $\mu\text{g/ml}$
Regression equation	$25.644x+3.064$
Correlation coefficient	0.9985
Retention time	6.2 min

Table 3.6 Precision and accuracy for Gemcitabine HCl in buffer: methanol by HPLC

Standard Concentration (µg/ml)		Precision (%) ^a	Accuracy (%) ^b
Actual	Observed		
10	9.98±0.081	0.81	99.8
30	30.87±0.092	0.298	102.9
50	49.86±0.05	0.1	99.7

a Expressed as relative standard deviation (RSD)

$$\text{RSD} = (\text{standard deviation}/\text{mean concentration}) \times 100$$

b Expressed as (mean observed concentration/actual concentration) × 100

3.4 HPLC Method for Estimation of Gemcitabine HCl in Plasma

3.4.1 Calibration Plot of Gemcitabine HCl in Plasma

Human Plasma was obtained from Suraktam Blood Bank, Vadodara, India. Calibration plot of Gemcitabine HCl in plasma was prepared in concentration in the range (400 - 4000 ng/ml). The blank plasma samples were spiked with stock solution prepared in distilled water (1mg/ml) to get concentration in above range. The protein precipitation was carried out by addition of acetonitrile. For 0.2 ml of plasma sample, 200 µl of acetonitrile was used. The separation of precipitate from organic phase was achieved by centrifugation (4000 rpm X 10min). The obtained organic phase (acetonitrile solution) was evaporated to dryness and used for analysis after reconstitution with mobile phase. The mobile phase consisted of 97 volumes of buffer (13.8 gm of monobasic sodium phosphate in 1000 ml distilled water, pH adjusted to 2.4-2.6 with orthophosphoric acid) and 3 volumes of methanol. Calibration curves were drawn by plotting peak area of curve vs. drug concentration. Program parameters were: Flow rate-1.2 ml/min, Detection wavelength- 269 nm, Run time- 10 min. The column was equilibrated by passing at least 150-200 ml of mobile phase. 20µl of sample was loaded using syringe through rheodyne injector.

Analytical method was validated for linearity, precision, and accuracy as described in section 3.2. The recovery studies were performed to know the extraction efficiency. Aqueous and plasma samples of known concentration were used. The aqueous sample of known concentration was prepared in same way as that of plasma sample except addition of plasma. The recovery in case of plasma sample compared to aqueous sample was recorded.

3.4.2 Results and Discussion

The retention time for Gemcitabine HCl was found to be 5.6min. The standard plot for Gemcitabine HCl is shown in Fig. 3.6 and Table 3.7. The HPLC chromatogram of Gemcitabine HCl in plasma is shown in Fig 3.7. The data for calibration plot of Gemcitabine HCl in plasma by HPLC was fitted into a linear equation $y=0.0706x-12.908$ with correlation coefficient of $R^2=0.9979$, which indicated the linearity of the plot (Table 3.8). Precision of the method was assessed by analyzing the plasma samples spiked with Gemcitabine HCl at different concentrations (200, 2000 and 4000ng/ml). Three replicate of each concentration were analyzed and results are given in Table 3.9. To evaluate precision, the mean values and the % RSD values were calculated for each concentration. The % RSD values for precision are presented in Table. The low % CV values indicate precision of the method.

Table 3.7 Calibration data of Gemcitabine HCl in plasma by HPLC

Sr. No.	Concentration (ng/ml)	Area under curve (mAU)
1	400	20.56±3.8
2	800	48.58±4.6
3	1200	66.49±8.7
4	1600	99.76±6.3
5	2000	123.45±7.2
6	2400	154.53±5.6
7	3200	213.56±8.8
8	4000	273.45±11.5

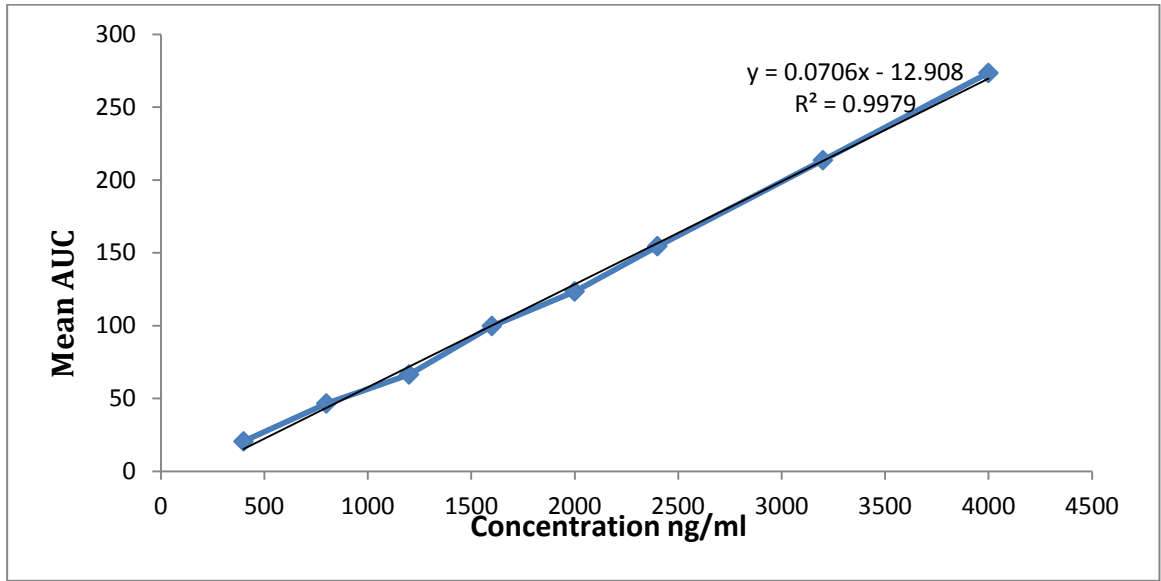


Fig. 3.6 Standard plot of Gemcitabine HCl in plasma by HPLC

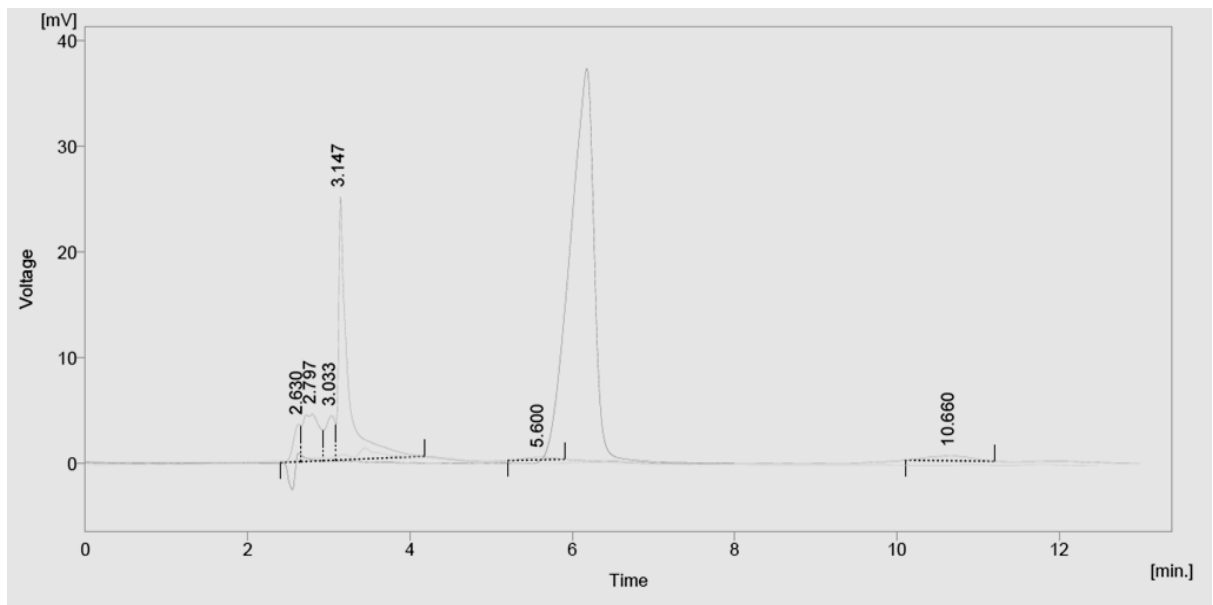


Fig. 3.7 HPLC chromatogram of Gemcitabine HCl in plasma (retention time at 5.6 min)

Table 3.8 Parameters for estimation of Gemcitabine HCl in plasma by HPLC

Parameters	Results
λ_{max}	269 nm
Linearity range	400-4000 ng/ml
Regression equation	$y=0.0706x-12.908$
Correlation coefficient	0.9979
Retention time	5.6 min

Table 3.9 Precision and accuracy for estimation of Gemcitabine HCl in plasma by HPLC

Standard Concentration (ng/ml)		Precision (%) ^a	Accuracy (%) ^b
Actual	Observed		
400	396.0±7.2	3.75	96.0
2000	1986.4±26.2	1.326	98.8
4000	3894.5±22.5	0.568	99.1

a Expressed as relative standard deviation (RSD)

$$\text{RSD} = (\text{standard deviation}/\text{mean concentration}) \times 100$$

b Expressed as (mean observed concentration/actual concentration) × 100

3.5 Estimation of Lopinavir by Derivative UV Spectroscopy

Stock solution

Standard stock solution (100 µg/ml) was prepared by dissolving 10 mg of Lopinavir in 100 ml of acetonitrile.

3.5.1 Calibration Plot in Acetonitrile

A derivative UV spectrophotometric method for estimation of Lopinavir in Acetonitrile was reported by Thakkar and Patel (2010). The analysis was performed by first scanning solution of 10 µg/ml in the ultraviolet range between 200 and 400 nm. As Lopinavir has absorption maxima at 210 nm, which is the region of absorption of various solvents and excipients, the zero order spectrum was converted into second derivative spectrum using UV probe software (scaling factor-10, $\Delta\lambda=2$). The wavelength, at which there was an absorption maxima of lopinavir, was selected as analytical wavelength. Suitable aliquots of the stock solution of Lopinavir were pipetted out into 10 ml volumetric flasks and the volume was made upto 10 ml with acetonitrile to give final concentrations ranging from 5-30 µg/ml. The absorbance of the solutions were measured and second derivative spectrum was recorded for each solution using acetonitrile as blank on Shimadzu 1601 UV-Visible Spectrophotometer and calibration curve was plotted. The above procedure was repeated three times. Standard concentrations (5.0, 10.0 and 20.0 µg/ml) were subjected to estimation of accuracy and precision.

3.5.2 Results and Discussion

3.5.2.1 Calibration Plot in Acetonitrile

Second derivative of Lopinavir in acetonitrile showed absorption maxima at 220 nm and this wavelength was chosen as the analytical wavelength. Beer's law was obeyed between 5 and 30 µg/ml (Table 3.10). The second derivative of Lopinavir UV spectrum is shown in Fig 3.8. Regression equation for standard curve was $y = 0.0338x + 0.0766$ (Fig. 3.9). Correlation coefficient for developed method was found to be 0.9993 signifying that a linear relationship existed between absorbance and concentration of the drug. Parameters indicating linearity for the used UV spectrometric method of analysis for lopinavir are shown in Table 3.11. Table 3.12 shows precision and

accuracy for the Lopinavir assay by UV spectroscopy. The low % CV values indicate precision of the method. No significant difference between the amount of drug added (actual) and observed concentration was noticed indicating accuracy of the method (Guidance for industry; 2001, Boulanger et al; 2003). The interference studies with formulation excipients studies were carried out and no difference in absorbance was observed at 220 nm.

Table 3.10 Calibration data for Lopinavir in acetonitrile by UV spectroscopy

Sr. No	Concentration ($\mu\text{g/ml}$)	Mean Absorbance \pm SD
1	5	0.234 \pm 0.021
2	10	0.423 \pm 0.004
3	15	0.586 \pm 0.011
4	20	0.762 \pm 0.052
5	25	0.919 \pm 0.049
6	30	1.084 \pm 0.034

*Average of 3 determinations

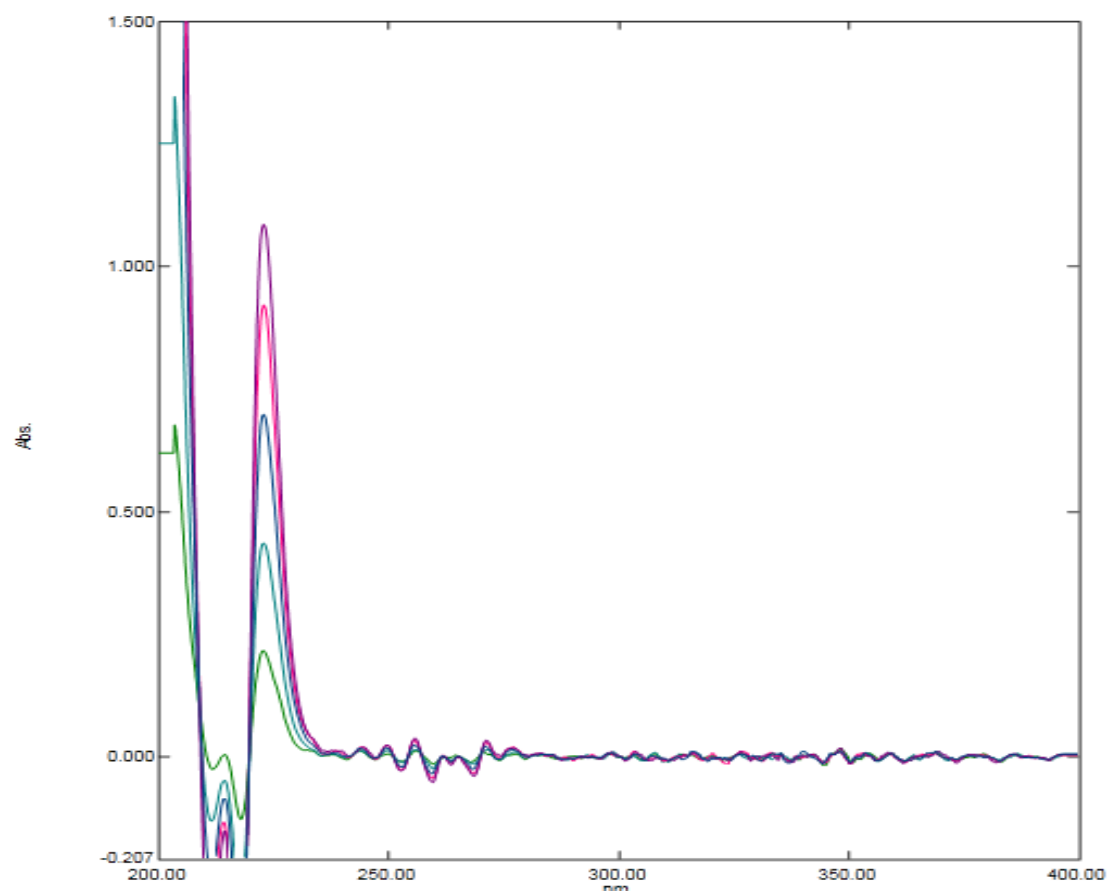


Fig. 3.8 Second derivative UV spectra of Lopinavir at concentration 5-30 $\mu\text{g/ml}$

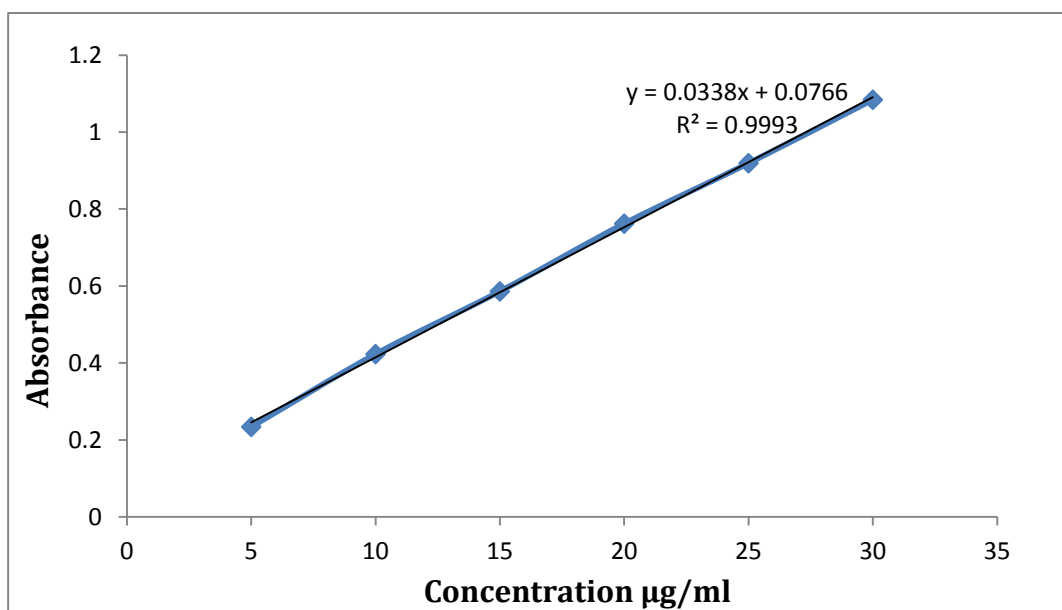


Fig. 3.9 Standard plot of Lopinavir in acetonitrile by UV spectroscopy

Table 3.11 Parameters for estimation of Lopinavir in acetonitrile by UV spectroscopy

Parameters	Results
λ_{\max}	220 nm
Linearity range	5-30 µg/ml
Regression equation	$y=0.0338x+0.0766$
Correlation coefficient	0.9993

Table 3.12 Precision and accuracy for estimation of Lopinavir in acetonitrile by UV spectroscopy

Standard Concentration (µg/ml)		Precision ^a (%)	Accuracy ^b (%)
Actual	Observed		
5	5.02±0.035	0.6972	100.4
10	10.08±0.015	0.1488	100.8
20	19.98±0.065	0.325	99.9

^a Expressed as relative standard deviation, RSD

RSD = (standard deviation/mean concentration) × 100

^b Expressed as (mean observed concentration/actual concentration) × 100

3.6 High Performance Liquid Chromatography (HPLC) Method for Estimation of Lopinavir

Estimation of Lopinavir by HPLC was carried out as per reported method with some modification (Indian Pharmacopoeia; 2007, Alex et al; 2011). This method involves liquid-liquid extraction using mixture of buffer and acetonitrile (60:40). The buffer was 0.025 M potassium dihydrogen phosphate (pH 4.9), the pH being adjusted with orthophosphoric acid. After preparation, the mobile phase was degassed and filtered through 0.45 μ inorganic filter. Shimadzu isocratic HPLC with a UV-visible detector was used for HPLC analysis. The separation was done on analytical column C18 (250 X 4.6 mm), packed with reverse phase material 5 μ m (Thermo, Hypersil) and connected to 2 cm pre column. The mobile phase consisted of 55 volumes of acetonitrile and methanol in the volume ratio 80:20 and 45 volumes of 0.02M potassium dihydrogen phosphate solution with pH adjusted to 3 using orthophosphoric acid. The injection volume was 20 μ l, the flow rate was 1 ml/min, run time was 10 min and detection wavelength was 210 nm. The required parameters were programmed using software.

3.6.1 Calibration Plot of Lopinavir in (Acetonitrile: Buffer)

Calibration plot of Lopinavir in acetonitrile: buffer was prepared in the concentration range of 5-25 μ g/ml. The stock solution (1mg/ml) was prepared by dissolving Lopinavir in acetonitrile: buffer (60:40). The buffer was 0.025 M potassium dihydrogen phosphate (pH 4.9), the pH being adjusted with orthophosphoric acid. Appropriate and accurate aliquots of the stock solutions were transferred to 10ml calibrated volumetric flasks and diluted up to the volume with acetonitrile: buffer (60:40) in order to get a series of known final concentrations. Analytical method was validated for linearity, precision, and accuracy as described in section 3.2.

3.6.2 Results and Discussion

The retention time of Lopinavir was 9.2 min. The HPLC chromatogram is shown in Fig 3.10. The calibration data and standard plot of Lopinavir in acetonitrile: buffer is shown in Fig 3.12 and Table 3.13. The regression equation for standard curve was $Y = 42.614x + 67.621$. Correlation coefficient for developed method was found to be 0.9985 signifying that a linear relationship existed between absorbance and concentration of the drug. Parameters indicating linearity for the used UV spectrometric method of

analysis for lopinavir are shown in Table 3.14. The accuracy and precision are shown in Table 3.15.

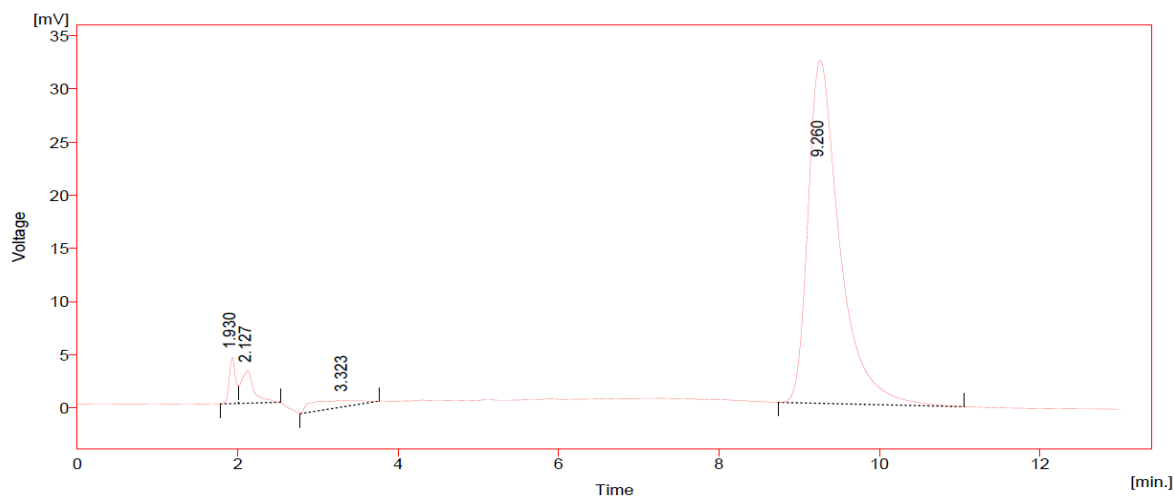


Fig. 3.10 Chromatogram of Lopinavir 25 mcg/ml in acetonitrile: buffer

Table 3.13 Calibration data of Lopinavir in acetonitrile: buffer (60:40) by HPLC

Sr. No.	Concentration ($\mu\text{g/ml}$)	Area under curve (mAU)
1	5	279.391 \pm 2.289
2	10	484.689 \pm 6.224
3	15	728.453 \pm 3.116
4	20	909.27 \pm 7.376
5	25	1132.56 \pm 4.215

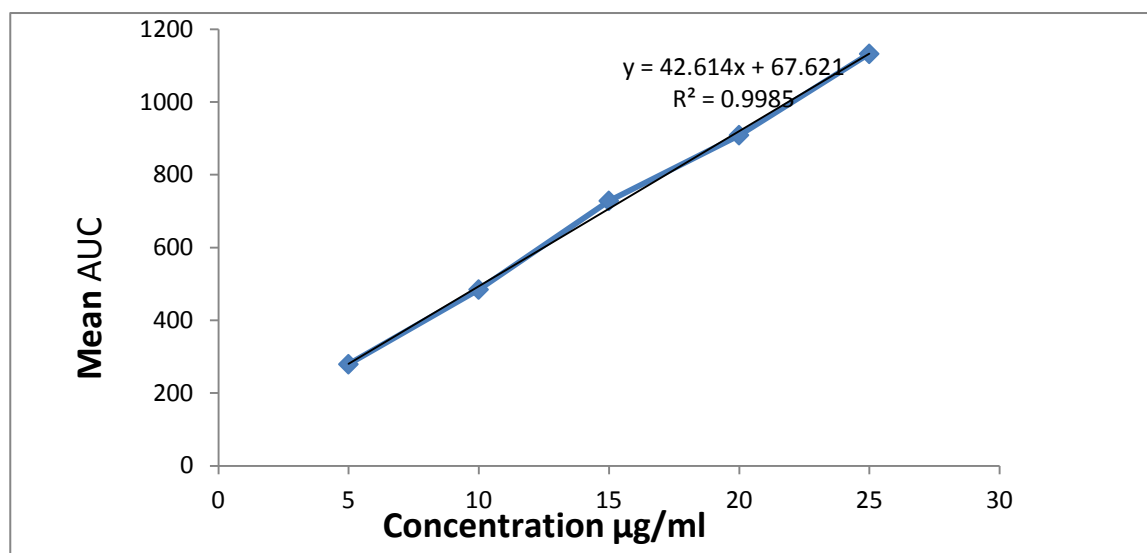


Fig. 3.11 Standard plot of Lopinavir in acetonitrile: buffer by HPLC

Table 3.14 Parameters for estimation of Lopinavir in acetonitrile: buffer by HPLC

Parameters	Results
λ_{max}	210 nm
Linearity range	5-25 µg/ml
Regression equation	$42.614x + 67.621$
Correlation coefficient	0.9985
Retention time	9.2 min

Table 3.15 Precision and accuracy for estimation of Lopinavir in acetonitrile: buffer by HPLC

Standard Concentration (µg/ml)		Precision (%) ^a	Accuracy (%) ^b
Actual	Observed		
5	5.08±0.081	1.59	101.6
15	15.34±0.021	0.137	102.2
25	24.95±0.05	0.210	99.8

3.7 Calibration plot of Lopinavir in plasma by HPLC

Human plasma was obtained from Suraktam Blood Bank, Vadodara, India. Calibration plot of Lopinavir in plasma was prepared in concentration in the range (200 -4000 ng/ml). The blank plasma samples were spiked with stock solution of lopinavir (1mg/ml) prepared in acetonitrile to get concentration in above range. Protein precipitation was carried out by addition of acetonitrile. For 0.2 ml of plasma sample, 200 μ l of acetonitrile was used. The separation of precipitate from organic phase was achieved by centrifugation (4000 rpm X 10min). The obtained organic phase (acetonitrile solution) was evaporated to dryness and used for analysis after reconstitution with mobile phase. The mobile phase consisted of 55 volumes of acetonitrile and methanol in the volume ratio 80:20 and 45 volumes of 0.02M potassium dihydrogen phosphate solution with pH adjusted to 3 using orthophosphoric acid. Calibration curves were drawn by plotting peak area of curve vs. drug concentration. Program parameters were: Flow rate-1.0 ml/min, Detection wavelength- 210 nm, Run time- 10 min. The column was equilibrated by passing at least 150-200 ml of mobile phase. 20 μ l of sample was loaded using syringe through rheodyne injector.

3.7.1 Validation

Analytical method was validated for linearity, precision, and accuracy as described in section 3.2. The recovery studies were performed to know the extraction efficiency of lopinavir in plasma. The aqueous sample of known concentration was prepared in same way as that of plasma sample except addition of plasma. The recovery in case of plasma sample compared to aqueous sample was recorded.

3.7.2 Results and Discussion

The HPLC chromatogram of Lopinavir in plasma is shown in Fig 3.12. The retention time for Lopinavir was found to be 8.337 min. The standard plot for Lopinavir is shown in Fig. 3.13 and Table 3.16. The data for calibration plot of Lopinavir in plasma by HPLC was fitted into a linear equation $y=0.169x+93.078$ with correlation coefficient of $R^2=0.9962$, which indicated the linearity of the plot (Table 3.17). Precision of the method was assessed by analyzing the plasma samples spiked with Lopinavir at different concentrations (200, 2000 and 4000ng/ml). Three replicate of each

concentration were analyzed and results are given in Table 3.18. To evaluate precision, the mean values and the % RSD values were calculated for each concentration.. The low % CV values indicate precision of the method. No significant difference between the amounts of drug added (actual) and observed concentration at all the concentration levels tested was noticed indicating accuracy of the method (Boulanger et al; 2003, Guidance for industry; 2001).

Table 3.16 Calibration data for estimation of Lopinavir in plasma by HPLC

Sr. No.	Concentration (ng/ml)	Area under curve (mAU)
1	200	76.453±6.24
2	400	175.477±9.21
3	800	214.36±8.65
4	1200	299.78±6.42
5	1600	348.76±14.85
6	2000	444.29±23.68
7	3200	620.21±31.23
8	4000	779.34±39.83

*Average of 3 determinations.

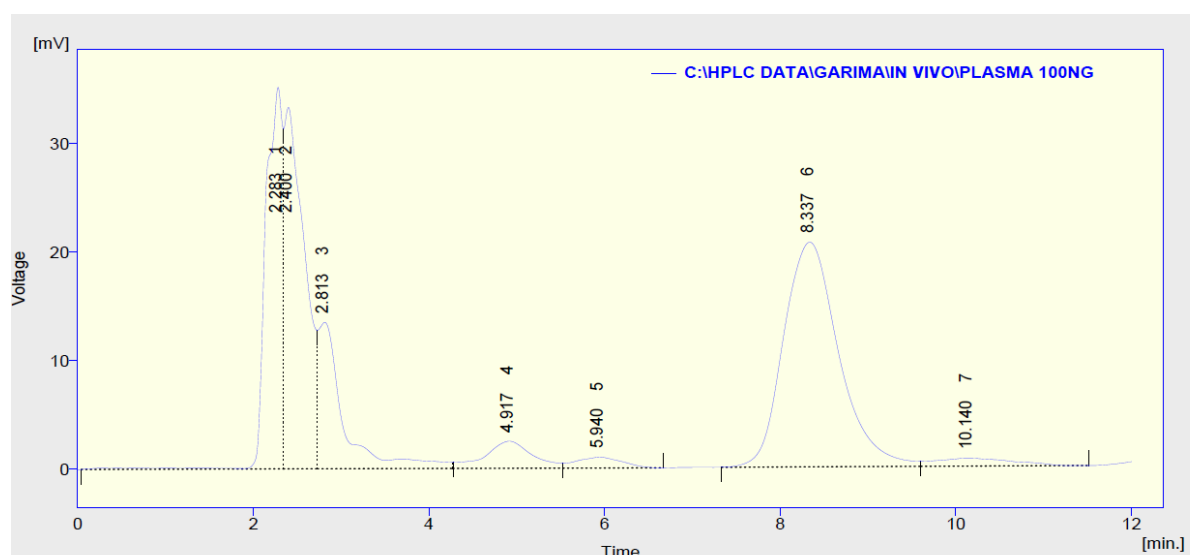


Fig. 3.12 HPLC chromatogram of Lopinavir in plasma (retention time at 8.337 min)

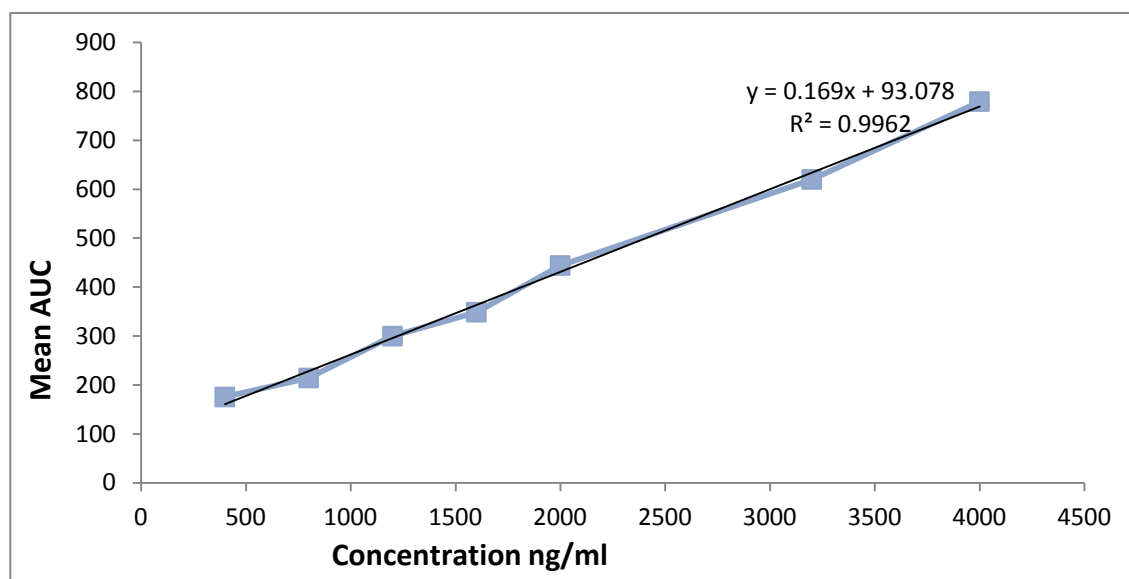


Fig. 3.13 Standard plot of Lopinavir in plasma by HPLC

Table 3.17 Parameters for estimation of Lopinavir in plasma by HPLC

Parameters	Results
λ_{max}	210 nm
Linearity range	200-4000 ng/ml
Regression equation	$y=0.169x+93.078$
Correlation coefficient	0.9962
Retention time	8.3 min

Table 3.18 Precision and accuracy for estimation of Lopinavir in plasma by HPLC

Standard Concentration (ng/ml)		Precision (%) ^a	Accuracy (%) ^b
Actual	Observed		
200	192.0±7.2	3.75	96.0
2000	1976.4±26.2	1.326	98.8
4000	3964.5±22.5	0.568	99.1

a Expressed as relative standard deviation (RSD)

$RSD = (\text{standard deviation}/\text{mean concentration}) \times 100$

b Expressed as $(\text{mean observed concentration}/\text{actual concentration}) \times 100$

3.7.3 Absolute Recovery:

The absolute recovery of Lopinavir at three concentration levels was determined by comparing the peak areas measured after analysis of spiked plasma samples (containing FU= 200, 500 and 2000 ng/ml) with those found after direct injection into the chromatographic system of non-biological samples at the same concentration levels. As shown in Table 3.19, the analyte recoveries were close to 100% and the extraction efficiency satisfactorily ranged from 96.8% to 98.8% for plasma samples.

Table 3.19 Extraction efficiency of Lopinavir at various concentrations in plasma

Concentration (ng/ml)	Extraction efficiency (\pm SD)
200	98.44 \pm 1.2
2000	96.8 \pm 1.8
4000	98.8 \pm 1.4

3.8 References

- ❖ Thakkar HP and Patel KH. A first derivative spectroscopic method for determination of Lopinavir in Tablets. *Chronicles of young scientists*, 1(3), 2010, 22-25.
- ❖ Indian Pharmacopoeia. Indian Pharmacopoeial Commission, Ghaziabad, 2, 2007, 697-700.
- ❖ Hubert PH, Chiap P, Crommen J, Boulanger B, Chapuzet E, Mercier N, Bervoas MS, Chevalier P, Grandjean D, Lagorce P, Lallier M, Laparra MC, Laurentie M, Nivet JC. Validation of the quantitative analytical procedures. Harmonization of the steps. *STP Pharma practice*, 13, 2003, 101-138.
- ❖ Boulanger B, Dewe W, Chiap P, Crommen J, Hubert PH. An analysis of the SFSTP guide on validation of bioanalytical methods: progress and limitations. *J Pharm Biomed Anal*, 32, 2003, 753-765.
- ❖ Bolton S, Swarbrick J. Basic definitions and concepts In: *Pharmaceutical statistics: Practical and clinical applications*. 3rd Ed., Marcel Dekker, New York, 1990, pp 24.
- ❖ Guidance for industry: Bioanalytical Method Validation, U.S. Department of Health and Human Services, Food and Drug Administration, Center for Drug Evaluation and Research (CDER), Center for Biologics Evaluation and Research (CBER), May 2001.
- ❖ Merodia M, Mirshahi T, Mirshahi M. Development of a sensitive method for the determination of ganciclovir by reversed phase high-performance liquid chromatography. *J Chromatogr*, 870, 2000, 159-167
- ❖ USP 30 NF 25. United States Pharmacopoeial Commission, Rockville, 2007, 2214-15.
- ❖ Alex AM, Chacko AJ Jose S, Souto EB. Lopinavir loaded solid lipid nanoparticles (SLN) for intestinal lymphatic targeting. *Eur J Pharm Sci*, 42, 2011, 11-18.

CHAPTER 4

EXPERIMENTAL GEMCITABINE HCl LOADED

NANOPARTICLES

4.1 Introduction

Gemcitabine HCl, an anticancer agent, is currently in clinical use for the treatment of several types of cancer. Gemcitabine is a difluoro analogue of deoxycytidine. Unfortunately, the drug is rapidly metabolised leading to a short plasma half-life and its cytostatic action is strongly exposure-time dependent. It is rapidly and extensively deaminated by cytidine deaminase in blood, liver, kidney and other tissues (Derakhshandeh and Fathi; 2012). In order to achieve the required concentration over sufficient periods of time, repeated application of relatively high doses is required (Vandana and Sahoo; 2010). This, in turn, leads to dose-limiting systemic toxicity. The plasma half life after intravenous infusion is 8- 17 min in human plasma. Therefore, it is required in high doses. Furthermore, Gemcitabine is a highly hydrophilic molecule with log P value 1.4 (Trickler et al; 2010). Till now, there is no oral formulation of Gemcitabine HCl in the market. It is available in the market in the freeze-dried form of an aqueous solution of the HCl salt known as Gemzar. After reconstitution Gemzar is used for intravenous administration as an infusion only (EliLilly; 1997).

Nanoparticles have been extensively studied by researchers in recent years for peroral drug delivery, for systemic effect following uptake from enteron, or to act locally in the gastrointestinal tract. Nanoparticulate delivery systems due to colloidal properties have the potential to improve drug stability, increase the duration of the therapeutic effect, minimise the drug degradation and metabolism as well as cellular efflux (Li et al; 2008, Sarmiento et al;2007).

Poly (D,L-lactide-co-glycolide), is a polymer of choice for developing an array of micro and nanoparticulate drug delivery systems as it has excellent biocompatibility and predictable biodegradability (Jain; 2000). Researchers have been extensively working for oral delivery of anticancer formulations through nanoparticulate systems.

Optimization of any pharmaceutical process begins with the objectives to find out and evaluate independent variables that affect formulation response, determine them and establish their best response values. However, considering the cost of the drugs and polymers, it is desirable to optimize the formulation development with minimum batches and maximum desired characteristics. Optimization by changing one-variable-at-a-time is a complex method to evaluate the effects of different variables on an

experimental outcome. This approach assesses one variable at a time instead of all simultaneously. The method is time-consuming, expensive and often leads to misinterpretation of results when interactions between different components are present. While developing formulations, various formulations as well as process variables related to effectiveness, safety and usefulness should be simultaneously optimized. Quality by design (QBD) is based on the improvement of the quality of formulation at designing level, planned and predefined quality of a formulation (Yu; 2008). While developing formulations, various formulations as well as process variables related to effectiveness, safety and usefulness should be simultaneously optimized. Studies based on factorial designs allow all the factors to be varied simultaneously, thus enabling evaluation of the effects of each variable at each level and showing interrelationship among them. The number of experiments required for these studies is dependent on the number of independent variables selected. Polynomial non-linear regression analysis are widely used for establishing approximate mathematical models in which the variables are screened by stepwise selection method according to statistical significance (Miller; 1984, Wagner and Shimshak; 2007) and final model is used to predict the relationship between different variables and their levels. But such predictions are often limited to low levels, resulting in poor estimation of optimum formulation (Levison et al; 1994, Shirakura et al; 1991). Therefore, it is important to understand the complexity of pharmaceutical formulations by using established statistical tools such as multiple regression analysis (MRA), full factorial design etc. Response surface methodology (RSM) accurately evaluates the impact of the independent variables on the dependent variables by varying all the important factors simultaneously in a systematic manner. RSM is a statistical technique which can address the present scenario and can be used to establish relationships between several independent variables and one or more dependent variables (Myer and Montgomery; 2002, Ray et al; 2009). RSM optimizes multiple variables by systematic variation of all variables in a well-designed experiment with a minimum number of experiments. The RSM optimization process involves the following steps: (1) performing statistically designed experiments; (2) estimating the coefficients of a mathematical model using regression analysis technique; and (3) predicting the response and checking the adequacy of the model. Among the available statistical design methods, a full factorial

design (FFD) involves a large number of experiments for accurately predicting the response. The number of formulations required for such studies is dependent on the number of independent variables selected after preliminary experiments. The dependent response is measured for each trial and then either simple linear equation (eq 4.1), or interactive equation (eq 4.2) or quadratic model (eq 4.3) is fitted by carrying out MRA and F-statistic to identify statistically significant terms.

$$Y = b_0 + b_1X_1 + b_2X_2 + b_3X_3 \tag{4.1}$$

$$Y = b_0 + b_1X_1 + b_2X_2 + b_3X_3 + b_{12}X_1X_2 + b_{13}X_1X_3 + b_{23}X_2X_3 + b_{123}X_1X_2X_3 \tag{4.2}$$

$$Y = b_0 + b_1X_1 + b_2X_2 + b_3X_3 + b_{12}X_1X_2 + b_{13}X_1X_3 + b_{23}X_2X_3 + b_1^2X_{11} + b_2^2X_{22} + b_3^2X_{33} + b_{123}X_1X_2X_3 \tag{4.3}$$

where, Y is estimated response; b_0 is constant; b_1, b_2, b_3 are linear coefficients; b_{12}, b_{23}, b_{13} are interaction coefficients; and b_1^2, b_2^2, b_3^2 are quadratic coefficients.

Based on the results obtained in preliminary experiments, variables which were found to be influencing majorly to dependent variables were selected to find the optimized condition required for lower PS and higher EE using MRA. In developing the regression equation, the test factors were coded according to the eq 4.4.

$$x_i = (X_i - X_i^X) / \Delta X_i \tag{4.4}$$

Where, x_i is the coded value of the i^{th} independent variable, X_i is the natural value of the i^{th} independent variable, X_i^X is the natural value of the i^{th} independent variable at the centre point and ΔX_i is the step change value.

Equation for quadratic model (eq 4.3) can be summarized as,

$$Y = b_0 + \sum_i b_i X_i + \sum_{i,j} b_{ij} X_i X_j + \sum_{ii} b_{ii} X_i^2 \tag{4.5}$$

Where, Y is the measured response, b_0 is the intercept term, b_i, b_{ij} and b_{ii} are, respectively the measures of the variables $X_i, X_i X_j$ and X_i^2 . The variable $X_i X_j$ represents the first order interactions between X_i and X_j ($i < j$). A full model (FM) was established after putting the values of regression coefficients in eq 4.5.

4.2 Materials

Gemcitabine HCl was obtained as a gift sample from Ranbaxy pharmaceuticals, Gurgaon, India. Poly (lactide -co-glycolide) PLGA (50:50) (inherent viscosity 0.2dl/g) was gift sample from Purac Biomaterials, The Netherlands. Pluronic F 68 was obtained as gift sample from BASF, Germany.

4.3 Equipments:

1. High speed magnetic stirrer (Remi, MS500, Remi equipments, Mumbai, India)
2. Probe sonicator (LABSONIC[®]M, Sartorius Ltd, Mumbai, India)
3. Digital pH meter (Lab India, Ltd, Mumbai, India)
4. High speed Centrifuge (Sigma 3K30, Germany)
5. Particle size Analyzer (Zeta sizer Nano series, Malvern Instruments, UK)
6. UV-VIS Spectrophotometer (Shimadzu, Japan)
7. Lyophilizer (Heto, Drywinner, Denmark)
8. Differential Scanning Calorimeter. (Shimadzu, Japan)
9. Transmission Electron Microscope (Philips, Tecnai 20, Holland)
10. Fourier Transform Infra red spectrophotometer (FTIR, Bruker, Germany)

4.4 Formulation of Gemcitabine HCl Loaded Nanoparticles by Multiple Emulsification Solvent Evaporation Method

Gemcitabine HCl loaded PLGA nanoparticles (NPs) were formulated by multiple emulsification solvent evaporation method (Kalaria et al., 2009). Gemcitabine HCl (10 mg) was dissolved in water (0.5 ml of acidified water pH 3) to form aqueous phase which was then added to a solution of 50 mg PLGA in 2.5 ml ethyl acetate to give a w/o emulsion which was sonicated for 60 s at 20 W and added dropwise under stirring to aqueous solution (5 ml) containing 0.75% Pluronic F68 to form the multiple (w/o/w) emulsion. The multiple emulsion was again sonicated for 60 s to reduce the particle size and continuously stirred on magnetic stirrer for solvent evaporation and precipitation of the polymer resulting into formation of NPs. The NPs suspension was centrifuged at 25,000 g for 30 min at 4 °C (3K30, Sigma Centrifuge; Osterode, Germany), supernatant was separated by alienation and the nanoparticle suspension was collected.

4.5 Preliminary Optimization of Parameters:

In preliminary optimization, the possible parameters influencing the formation of nanoparticles, size of nanoparticles and entrapment efficiency were identified and optimized. The parameters studied were: type of organic solvent, surfactant, volume of internal aqueous phase and pH of internal aqueous phase.

4.5.1 Type of Organic Solvent

Three different solvents, acetonitrile, dichloromethane and ethyl acetate were tried and particle size, PDI and entrapment efficiency were determined.

4.5.2 Type of Surfactant

Three different types of surfactants, Pluronic F68 (Poloxamer 188), Pluronic 127 (Poloxamer 407) and Poly vinyl alcohol (PVA) were taken and particle size, PDI and entrapment efficiency were determined.

4.5.3 Volume of Internal Aqueous Phase

Internal aqueous phase at different volumes (0.5 ml, 1.0 ml, 1.5 ml) were tried to formulate different batches of nanoparticles. Particle size, PDI and entrapment efficiency were determined.

4.5.4 pH of Internal Aqueous Phase

pH of internal aqueous phase was varied from pH 7 (distilled water) to pH 4, pH 3 and pH 2. pH was adjusted with 0.1 N HCl. Different batches were prepared and particle size, PDI and entrapment efficiency were determined.

4.6 Optimization by Factorial Design

Based on the preliminary experiments, Polymer concentration in organic phase (X_1), surfactant concentration (X_2) and sonication time for multiple emulsion (X_3) were selected as independent variables and particle size (PS) and entrapment efficiency (EE) were selected as dependent variables. A 3^3 randomized full factorial design was used (Joshi et al; 2010). In this design, three factors were evaluated, each at 3 levels, and experimental trials were performed at all 27 possible combinations with two replicates. Replicate experimental runs were carried out in complete randomized manner.

Table 4.1 Factorial design parameters and experimental conditions

Factors	Levels used, Actual (coded)		
	Low (-1)	Medium(0)	High (+1)
X ₁ -Polymer concentration in organic phase (%w/v)	1%	2%	3%
X ₂ -Concentration of surfactant; Pluronic F68 (%w/v)	0.50%	0.75%	1.0%
X ₃ - Sonication time	30 S	60 S	90 S

Table 4.2 Formulation of Gemcitabine HCl loaded nanoparticles by coded values

Batch	X1	X2	X3
F1	-1	-1	-1
F2	-1	-1	0
F3	-1	-1	1
F4	-1	0	-1
F5	-1	0	0
F6	-1	0	1
F7	-1	1	-1
F8	-1	1	0
F9	-1	1	1
F10	0	-1	-1
F11	0	-1	0
F12	0	-1	1
F13	0	0	-1
F14	0	0	0
F15	0	0	1
F16	0	1	-1
F17	0	1	0
F18	0	1	1
F19	1	-1	-1
F20	1	-1	0
F21	1	-1	1
F22	1	0	-1
F23	1	0	0
F24	1	0	1
F25	1	1	-1
F26	1	1	0
F27	1	1	1

A multilinear stepwise regression analysis was performed using Microsoft Excel software. The full models were used to plot two dimension contour plots for both PS and %EE. All the statistical operations were carried out by design expert (8.0.7.1, stat-ease, Inc. Minneapolis, USA). Table 4.1 and Table 4.2 summarize experimental runs studied, their factor combinations, and the translation of the coded levels to the experimental units employed during the study.

Optimization Data Analysis

Various RSM (Response Surface Methodology) computations for the current optimization study were performed employing Design Expert® software (version 8.0.7.1, Stat-Ease Inc, Minneapolis, USA). Polynomial models including interaction and quadratic terms were generated for the response variable using multiple regression analysis (MLRA) approach. The general form of MLRA model is represented as equation 4.6.

$$Y = b_0 + b_1X_1 + b_2X_2 + b_3X_3 + b_{12}X_1X_2 + b_{13}X_1X_3 + b_{23}X_2X_3 + b_1^2X_{11} + b_2^2X_{22} + b_3^2X_{33} + b_{123}X_1X_2X_3 \quad (4.6)$$

Where b_0 is the intercept representing the arithmetic average of all quantitative outcomes of 27 runs; b_{ij} are the coefficients computed from the observed experimental values of Y ; and X_1 , X_2 and X_3 are the coded levels of the independent variable(s). The terms X_1X_2 and X_i^2 ($i=1$ to 3) represents the interaction and quadratic terms, respectively. The main effects (X_1 , X_2 and X_3) represent the average result of changing one factor at a time from its low to high value. The interaction terms ($X_1X_2X_3$) show how the response changes when three factors are simultaneously changed. The polynomial terms (X_1^2 , X_2^2 and X_3^2) are included to investigate nonlinearity. The polynomial equation was used to draw conclusions after considering the magnitude of coefficients and the mathematical sign it carries, i.e., positive or negative. A positive sign signifies a synergistic effect, whereas a negative sign stands for an antagonistic effect.

The effects of different levels of independent variables on the response parameters were predicted from the respective response surface plots. A FM equation was established after putting the values of regression coefficients of EE and PS in equation 3.

The predicted values were calculated by using the mathematical model based on the coefficients of the model and the predicted values along with their observed values were recorded along with percentage of error obtained when predicted value and observed values were compared. Statistical validity of the polynomials was established on the basis of ANOVA provision in the Design Expert @software. Level of significance was considered at $P < 0.05$. F-Statistic was applied on the results of analysis of variance (ANOVA) of full model and reduced model to check whether the non-significant terms can be omitted or not from the FM (Bolton and Bon; 1997). The best fitting mathematical model was selected based on the comparisons of several statistical parameters including the coefficient of variation (CV), the multiple correlation coefficient (R^2), adjusted multiple correlation coefficient (adjusted R^2). For simultaneous optimization of PS and EE, desirability function (multi-response optimization technique) was applied and total desirability was calculated using Design Expert software (version 8.0.3). A check point analysis was performed to confirm the utility of the multiple regression analysis and established contour plots in the preparation of Gemcitabine HCl loaded PLGA NPs. Results of desirability criteria, check point analysis and normalized error were considered to select the formulation with lowest PS and highest EE.

Contour Plots

Contour plots are diagrammatic representation of the values of the responses that help in explaining the relationship between independent and dependent variables. Two dimensional contour plots were established between X_1 and X_2 at different levels (-1, 0, 1) of X_3 for PS and EE.

Response Surface Plots

To understand the main and the interaction effects of two variables, response surface plots were used as a function of two factors at a time maintaining all other factors at fixed levels (Box and wilson; 1951, Mak et al; 1995). These plots were obtained by calculating the values taken by one factor where the second varies (from -1 to 1 for instance) with constraint of a given Y value. The yield values for different levels of variables can also be predicted from the respective response surface plots.

Check Point Analysis

A check point analysis was performed to confirm the utility of the established contour plots and reduced polynomial equation in the preparation of NPs. Values of independent variables (X_1 and X_2) were taken from three check points on contour plots plotted at fixed levels of -1, 0 and 1 of X_3 and the values of PS (Y_1) and EE (Y_2) were calculated by substituting the values in the reduced polynomial equation. Gemcitabine HCl loaded NPs were prepared experimentally by taking the amounts of the independent variables (X_1 and X_2). Each batch was prepared three times and mean values were determined. Difference in the predicted and mean values of experimentally obtained EE and PS was compared by using student's 't' test.

Desirability Criteria

For simultaneous optimization of PS and EE, desirability function (multi-response optimization technique) was applied and total desirability was calculated using Design Expert software (version 8.0.3). The desirability lies between 0 and 1 and it represents the closeness of a response to its ideal value (eq 4.7). The total desirability is defined as a geometric mean of the individual desirability for PS and EE (Derringer and Suich; 1980).

$$D = (d_{PS} \times d_{EE})^{1/2} \quad (4.7)$$

Where, D is the total desirability, d_{EE} and d_{PS} are individual desirability for EE and PS. If both the quality characteristics reach their ideal values, the individual desirability is 1 for both. Consequently, the total desirability is also 1. Our optimization criteria included PS of less than 200 nm and maximum EE.

Normalized Error Determination

The quantitative relationship established by MRA was confirmed by evaluating experimentally prepared Gemcitabine HCl loaded NPs. PS and EE predicted from the MRA were compared with those generated from prepared batches of check point analysis using normalized error (NE). The equation of NE (eq 4.8) is expressed as follows:

$$NE = [\Sigma\{(Pre - Obs)/Obs\}^2]^{1/2} \quad (4.8)$$

where, Pre and Obs represents predicted and observed response, respectively.

4.7 Lyophilization of Gemcitabine HCl Loaded Nanoparticles and Optimization of Cryoprotectant

The optimized nanoparticle formulation was lyophilized using lyophilizer (Drywinner Hetodryer). Different cryoprotectants (Trehalose dehydrate, Mannitol and Sucrose) at different ratio (1:1w/w, 1:2w/w, 1:3w/w) were tried to select the cryoprotectant which showed minimum increment in particle size. Nanoparticulate suspension (2 ml) was dispensed in 10 ml semi-stoppered vials with rubber closures and frozen for 24 h at -80 °C. Thereafter, the vials are lyophilized (Heto Drywinner, Allerod, Denmark) using different cryoprotectants like trehalose, sucrose and mannitol in different concentrations. Finally, glass vials were sealed under anhydrous conditions and stored until being re-hydrated. Lyophilized NPs were re-dispersed in exactly the same volume of distilled water as before lyophilization. NP suspension was subjected to particle size measurement as described earlier. Ratio of final particle size (Kashi et al;2012) and initial particle size (S_i) was calculated to finalize the suitable cryoprotectant based upon lowest S_f/S_i ratio.

4.8 Characterization of Optimized Gemcitabine HCl Loaded Nanoparticles

4.8.1 Particle Size

The size analysis and polydispersity index of the NPs were determined using a Malvern Zetasizer Nano ZS (Malvern Instrument, Worcestershire, UK). Each sample was diluted ten times with filtered distilled water to avoid multi-scattering phenomena and placed in disposable sizing cuvette. Polydispersity index was noted to determine the narrowness of the particle size distribution. The size analysis was performed in triplicate and the results were expressed as mean size \pm SD.

4.8.2 Entrapment Efficiency and Drug Loading

EE and drug loading in the NPs was determined after separating the NPs from the aqueous supernatant (containing non-entrapped Gemcitabine HCl) by centrifugation at 25000 rpm for 30 min (3K 30, Sigma Laboratory Centrifuge, Osterode, Germany). The supernatant was diluted with appropriate amount of distilled water and analyzed for the amount of unentrapped drug by HPLC after filtration through 0.22 μ and appropriate dilution with mobile phase. Acetonitrile was added to the pellet to dissolve

the polymer and centrifuged. The supernatant was removed and the drug pellet was analyzed for the entrapped drug content.

EE was estimated by calculating amount of drug entrapped in NPs with respect to total drug added during preparation of formulation.

The EE was calculated according to following formula:

$$EE (\%) = (TD-FD/TD) \times 100$$

Where, TD is total amount of drug added and FD is amount of drug in supernatant

Drug loading was calculated as follows,

$$\text{Percentage drug loading} = A/B \times 100$$

Where A is the drug content in the NPs and B is the weight of NPs.

4.8.3 Zeta Potential

Zeta potential distribution was also measured using a Zetasizer (Nano ZS, Malvern instrument, Worcestershire, UK). Each sample was suitably diluted 10 times with filtered distilled water and placed in a disposable zeta cell. Zeta limits ranged from -200 to +200 mV. The electrophoretic mobility ($\mu\text{m}/\text{sec}$) was converted to zeta potential by in-built software using Helmholtz-Smoluchowski equation. Average of 3 measurements of each sample was used to derive average zeta potential.

4.8.4 Transmission Electron Microscope Studies

A sample of NPs (0.5 mg/ml) was suspended in water and bath sonicated for 30 s. 2 μl of this suspension was placed over a copper TEM grid (150 mesh), negatively stained with 2 μl uranyl acetate (1%) for 10 min and allowed to dry. The NPs were visualized at 80 kV under TEM (Philip Tecnai 20, USA) and images were captured using Gatan Digital Micrograph software.

4.8.5 Differential Scanning Calorimetric (DSC) Studies

All the samples were dried in desiccators for 24 h before thermal analysis. DSC studies of pure drug, PLGA, physical mixture of drug: polymer (1:1) and drug loaded NPs were performed in order to characterize the physical state of drug in the NPs. Thermograms were obtained using DSC model 41 (Shimadzu, Japan). Dry nitrogen gas was used as the purge gas through the DSC cell at a flow rate of 40 ml/min. Samples (4 - 8 mg) were sealed in standard aluminum pans with lids and heated at a rate of 10 $^{\circ}\text{C}/\text{min}$ from 20 to 300 $^{\circ}\text{C}$.

4.8.6 Fourier Transform Infrared (FTIR) Spectroscopy

FT-IR spectroscopy was employed to detect the possibilities of interactions between Lopinavir and various excipients used in the formulation. The IR spectra of pure drug, PLGA, physical mixture (of PLGA and Gemcitabine HCl in 1:1 ratio) and Gemcitabine HCl loaded PLGA NPs were recorded on Fourier Transform Infrared spectrophotometer (Bruker optics, Germany).

4.8.7 Stability Studies

The stability of Gemcitabine HCl loaded NPs in terms of drug content and particle size distribution was monitored for 3 months at 2-8 °C and RT (25-30 °C). Periodically, samples were withdrawn and the particle size as well as drug content was determined.

4.9 Results and Discussion

4.9.1 Preliminary Optimization

4.9.1.1 Type of Organic Solvent

Suitable organic solvent was selected on the basis of particle size, PDI and entrapment. Acetonitrile being miscible with water; partitioned and diffused into water, therefore multiple emulsion was not formed and hence nanoparticles could not form. An immiscible solvent was desirable. Therefore, dichloromethane was tried but coarse emulsion was formed and particle size did not reduce below 200nm. Ethyl acetate resulted in smaller particle size and better emulsification. Also, it has low toxicity (class 2) than dichloromethane (Class 4). Hence, ethyl acetate was selected as organic phase (Table 4.3).

Table 4.3 Effect of type of solvent on particle size, PDI and EE of Gemcitabine HCl loaded NPs

Solvent	PS \pm SD (nm)	PDI	EE (%)
Acetonitrile	No emulsification		
Dichloromethane	340 \pm 6.235	0.339 \pm .002	9.2 \pm 3.16
Ethyl acetate	226.3 \pm 2.213	0.224 \pm .004	16.6 \pm 2.31

4.9.1.2 Type of Surfactant

Three different surfactants were tried for gemcitabine HCl loaded PLGA nanoparticles. Polyvinyl alcohol resulted in higher viscosity solution leading to larger particles. Pluronic F 127 also resulted into higher particle size, may be due to higher molecular weight as compared to Pluronic F68, which resulted in smaller particle size, with less PDI. Also, the entrapment efficiency was higher for Pluronic F 68, may be due to smaller size and better stabilization of globules in emulsion preventing the escape of drug to outer aqueous phase (Table 4.4).

Table 4.4 Effect of type of surfactant on particle size, PDI and EE of Gemcitabine HCl loaded NPs

Surfactant	PS \pm SD (nm)	PDI	EE (%)
Polyvinyl alcohol	380 \pm 3.25	0.396 \pm .004	12.3 \pm 2.13
Pluronic F127	290.6 \pm 3.423	0.275 \pm .003	16.9 \pm 2.56
Pluronic F68	236.3 \pm 2.142	0.132 \pm .006	21.6 \pm 1.42

4.9.1.3 Volume of Internal Aqueous Phase

Volume of internal aqueous phase was varied to optimize the influence on particle size and entrapment. Higher internal volumes were resulted into larger emulsion globule size leading to larger particle sizes with less entrapment (Table 4.5). Due to higher inner volume of aqueous phase, chances of escaping and mingling of the hydrophilic drug to outer aqueous compartment were higher which leads to less entrapment (Peltonen et al., 2004). As the drug was highly hydrophilic, volume of 0.5 ml was optimized as it was sufficient to dissolve.

Table 4.5 Effect of volume of internal aqueous phase on particle size, PDI and EE of Gemcitabine HCl loaded NPs

Volume of internal aq phase	PS \pm SD (nm)	PDI	EE (%)
1.5 ml	336.9 \pm 3.65	0.216 \pm .0026	11.2 \pm 1.63
1.0 ml	288.6 \pm 2.23	0.227 \pm .0032	16.9 \pm 1.36
0.5 ml	213.6 \pm 2.142	0.198 \pm .0024	19.8 \pm 1.42

4.9.1.4 pH of Internal Aqueous Phase

Initially, distilled water and pH4 was used as internal aqueous phase, but entrapment efficiencies were very less. Gemcitabine HCl has pKa value of 3.58 and its solubility is more in acidic medium (38 mg/ml) as compared to solubility in distilled water (16.8 mg/ml) (Meneau and Ollivon; 2009). Therefore, when the drug was dissolved in acidified water (pH 3), the entrapment efficiency was doubled (Table 4.6). Acidified water (pH 4) was also tried but there was not much improvement in entrapment, as the solubility is higher below pKa. Further, when pH was reduced to 2, the entrapment efficiency was less. Hydrophilic drugs have lower affinity for organic phase and have tendency to move to the outer aqueous phase (Peltonen et al; 2004). The higher entrapment efficiency of highly hydrophilic drug can be attributed to the prevention of leak out of drug in outer aqueous phase as the drug was more soluble in the internal aqueous phase than the middle organic phase and the outer aqueous medium (Hans and Lowman; 2002).

Table 4.6 Effect of pH of internal aqueous phase on particle size, PDI and EE of Gemcitabine HCl loaded NPs

pH of Internal aqueous phase	PS \pm SD (nm)	PDI	EE (%)
pH 7 distilled water	246.3 \pm 2.142	0.193 \pm .0035	18.6 \pm 2.36
pH4 acidified water	223.9 \pm 1.47	0.213 \pm .0043	22.2 \pm 3.56
pH 3 acidified water	216.4 \pm 2.842	0.186 \pm .0018	36.4 \pm 3.41
pH2 acidified water	224.6 \pm 3.132	0.171 \pm .0047	28.3 \pm 2.15

4.9.2 Optimization by Factorial Design

From the preliminary optimization studies the polymer concentration in organic phase (X_1), surfactant concentration; Pluronic F68 (X_2), and sonication time of multiple emulsion (X_3) were selected as independent variables and particle size (PS) and entrapment efficiency (EE) as responses. The coded and actual values of formulation parameters are shown in Table 4.1. Total 27 batches of formulations were developed using 3^3 factorial design varying the three independent variables (Table 4.7). The

quality of formulation can be improved by optimizing the formulation systematically. A multilinear stepwise regression analysis was performed using Microsoft Excel software. The response was measured for each experiment and then either simple linear equation (4.1), or interactive equation (4.2) or quadratic (4.3) model was fitted by carrying out multiple regression analysis and F-statistic to identify statistically significant terms in the equation. The PS and EE obtained at various levels of three independent variables (X_1 , X_2 and X_3) were subjected to multiple regression to yield second order polynomial equations (eq 4.9 and 4.10, full model). The main effects of X_1 , X_2 and X_3 represent the average result of changing one variable at a time from its low to high value. The interactions (X_1X_2 , X_1X_3 , X_2X_3 and $X_1X_2X_3$) show how the PS and EE changes when two or more variables were simultaneously changed. The PS and EE of total 27 batches showed a wide variation from 140.23 ± 2.356 to 229.7 ± 1.768 nm and 8.4 ± 2.241 to $58.6 \pm 2.894\%$, respectively (Table 4.7)

Table 4.7 Full factorial design layout of Gemcitabine HCl loaded NPs showing the effect of independent variables X₁ (Polymer concentration), X₂ (Surfactant concentration) and X₃ (sonication time) on responses PS and EE

Sr. No.	X ₁	X ₂	X ₃	Y ₁ * (PS, nm)	Y ₂ * (EE, %)
1	-1	-1	-1	166.4±4.369	13.4± 1.29
2	-1	-1	0	152.4±2.136	34.23±2.01
3	-1	-1	1	140.23±2.753	22.23±1.83
4	-1	0	-1	171.5±1.253	18.2±0.963
5	-1	0	0	158.9±4.843	38.4±3.143
6	-1	0	1	148.6±5.346	26.4±2.147
7	-1	1	-1	176.3±3.382	8.4±2.753
8	-1	1	0	161.7±3.467	21.23±1.842
9	-1	1	1	153.5±316	17.85±1.943
10	0	-1	-1	181.3±1.259	29.34±0.975
11	0	-1	0	163.9±2.751	44.3±0.483
12	0	-1	1	144.3±1.372	31.46±1.379
13	0	0	-1	200.4±4.852	36.7±2.823
14	0	0	0	166.4±2.423	55.2±2.583
15	0	0	1	154.6±3.573	32.56±1.764
16	0	1	-1	210.6±1.381	10.6±0.678
17	0	1	0	173.8±2.058	34±1.483
18	0	1	1	158.9±1.076	23.6±2.148
19	1	-1	-1	184.6±3.821	34.8±2.394
20	1	-1	0	179.4±1.765	48.2±1.695
21	1	-1	1	168.3±3.014	42.6±1.682
22	1	0	-1	222.6±2.076	41.9±1.384
23	1	0	0	216.7±1.564	58.6±1.483
24	1	0	1	200.6±1.728	51.6±2.042
25	1	1	-1	229.7±3.385	34.6±1.523
26	1	1	0	188.3±3.103	43.46±1.458
27	1	1	1	180.1±4.210	26.8±0.482

*values are represented as mean ± s.d.

$$Y_{PS} = 176.29 + 18.93X_1 + 8.44X_2 - 16.65X_3 + 5.07X_1^2 - 9.27X_2^2 + 3.86X_3^2 + 2.78X_1X_2 - 2.73X_1X_3 - 3.71X_2X_3 - 4.58X_1X_2X_3 \quad (4.9)$$

$$Y_{EE} = 49.45 + 10.12X_1 - 4.44X_2 + 2.37X_3 - 0.70X_1^2 - 11.00X_2^2 - 14.01X_3^2 + 0.13X_1X_2 - 2.17X_1X_3 - 0.34X_2X_3 - 2.03X_1X_2X_3 \quad (4.10)$$

The significance of each coefficient of eq 4.9 and 4.10 were determined by student's 't' test and p-value, which are listed in Table 4.8. The larger the magnitude of the 't' value and the smaller the p-value, the more significant is the corresponding coefficient (Adinarayana and Ellaiah; 2002). Higher values of coefficients of X_1 , X_2 and X_3 for both PS and EE confirmed them as main contributing factors. Second order main effect of X_2 was significant for both PS and EE and X_3 was significant for EE. Small values of the coefficients of the terms, X_1^2 , X_1X_2 , X_2X_3 , X_1X_3 , and $X_1X_2X_3$ in eq 4.9 and X_1^2 , X_3^2 , X_1X_2 , X_2X_3 , X_1X_3 , and $X_1X_2X_3$ in eq 4.10 for PS and EE respectively implied that all these terms were least contributing factors and not significant ($p > 0.05$) in the preparation of the Gemcitabine HCl loaded PLGA NPs (Table 4.8).

Hence, least contributing factors were neglected from the full model and reduced polynomial equations (4.11 and 4.12) for PS and EE were generated

$$Y_{PS} = 182.26 + 18.93X_1 + 8.45X_2 - 16.35X_3 - 9.27X_2^2 \quad (4.11)$$

$$Y_{EE} = 49.29 + 10.12X_1 - 4.44X_2 + 2.62X_3 - 11X_2^2 - 14.01X_3^2 \quad (4.12)$$

For Particle size, positive sign of coefficient of X_1 and X_2 shows that PS increased with increase in polymer concentration and surfactant concentration, whereas negative sign of X_3 showed a decrease in particle size with increase in sonication time. Entrapment efficiency increased with increase in polymer concentration and surfactant concentration whereas decreased with increase in sonication time. As polymer concentration increased, particle size as well as entrapment efficiency was increased due to increase in viscosity leading to coarse emulsion with bigger globule sizes and more available polymer to entrap the drug. Surfactant concentration showed an increase in particle size at higher concentration due to coating of surfactant on surface of PLGA. Entrapment efficiency increased with increase in surfactant concentration due to better stabilisation of droplets upto optimum concentration but higher quantity of

surfactant increased the solubility of drug in outer phase, leading to decrease in entrapment. Sonication time reduced particle size because high energy waves leads to rapid dispersion of polymeric organic phase into aqueous phase resulting into smaller globule size of emulsion which is responsible for final particle size of nanoparticle. But, entrapment efficiency was also reduced with sonication time, may be high energy released into system lead to leaching of drug (Rubiana; 2005). Therefore, sonication time of 60s was optimized. When the values of three independent variables were compared, highest values of coefficients were found for X_1 for both the responses. Hence, polymer concentration was considered as major contributing variable for PS and EE of Gemcitabine HCl loaded NPs.

Table 4.8 Model coefficients estimated by multiple regression analysis for PS and EE of Gemcitabine HCl loaded NPs

Factor	PS			EE		
	Coefficients	t Stat	p-value	Coefficients	t Stat	p-value
Intercept	176.2941	37.76041	4.54E-17*	49.75926	24.73344	3.54E-14*
X_1	18.93167	8.759741	1.68E-07*	10.12333	10.8702	8.5E-09*
X_2	8.448333	3.90907	0.00125*	-4.44556	-4.77353	0.000207*
X_3	-16.652	-7.61886	1.04E-06*	2.378636	2.525586	0.022485*
X_1^2	5.079444	1.356932	0.193639	-0.70111	-0.43465	0.669621
X_2^2	-9.27056	-2.47655	0.024816*	-11.0011	-6.82009	4.12E-06*
X_3^2	3.862778	1.031909	0.317462	-14.0111	-8.68612	1.88E-07*
X_1X_2	2.7775	1.049327	0.30962	0.136667	0.11982	0.906117
X_1X_3	-2.73341	-0.93216	0.365107	-2.17227	-1.71914	0.104871
X_2X_3	-3.71917	-1.40508	0.179114	-0.34167	-0.29955	0.768376
$X_1X_2X_3$	-4.58375	-1.41394	0.176541	-2.0275	-1.45139	0.165997

* Significant at $p < 0.05$

The results of ANOVA of the second order polynomial equation of PS and EE are given in Table 4.9 and 4.10 respectively. Since the calculated F value was less than the tabulated F value for PDE and for PS (Bolton; 2004). It was concluded that the neglected terms did not significantly contribute in the prediction of PS and EE. Hence, F-Statistic of the results of ANOVA of full and reduced model justified the omission of non-significant terms of eq 9 and 10. The goodness of fit of the model was checked by determination coefficient R^2 . Higher values of determination coefficients explains that above 86% variations were explained by model. A higher value of correlation coefficient (R) signifies excellent correlation between the independent variables.

Table 4.9 Analysis of Variance (ANOVA) of full and reduced models for PS of Gemcitabine HCl loaded NPs

		df	SS	MS	F	R	R^2	Adjusted R^2
Regression	FM	10	13806.6	1380.66	16.42173	0.954578	0.911218	0.85573
	RM	4	13062.57	3265.641	34.38776	0.9285	0.862113	0.837043
Residual	FM	16	1345.203	84.07516				
	RM	22	2089.235	94.96522				

$$SSE2 - SSE1 = 2089.235 - 1345.203 = 744.032$$

$$\text{No. of parameters omitted} = 6$$

$$\text{MS of error (full model)} = 84.075$$

$$\begin{aligned} \text{F calculated} &= (SSE2 - SSE1 / \text{No. of parameters omitted}) / \text{MS of error (FM)} \\ &= (744.032 / 6) / 84.075 \\ &= 1.47 \end{aligned}$$

$$\text{F tabulated} = 2.74$$

Table 4.10 Analysis of Variance (ANOVA) of full and reduced models for EE of Gemcitabine HCl loaded NPs

		df	SS	MS	F	R	R ²	Adjusted R ²
Regression	FM	10	4311.58	431.158	27.61798	0.9722	0.9452	0.9112
	RM	5	4227.98	845.5961	53.26457	0.9627	0.9269	0.9095
Residual	FM	16	249.7839	15.61149				
	RM	21	333.3833	15.8754				

$$SSE2 - SSE1 = 333.38 - 249.78 = 83.59$$

$$\text{No. of parameters omitted} = 5$$

$$\text{MS of error (full model)} = 15.61$$

$$\begin{aligned} \text{F calculated} &= (SSE2 - SSE1 / \text{No. of parameters omitted}) / \text{MS of error (FM)} \\ &= (83.59 / 5) / 15.61 \\ &= 1.07 \end{aligned}$$

$$\text{F tabulated} = 2.85$$

Contour plots and response surface plots

Contour plots and Response surface plots for PS are shown in Fig 4.1 and 4.2 and contour and response surface plots for EE are shown in Fig. 4.3 and 4.4 respectively. The contour plots for particle size shows that at +1 level of sonication time (X_3), the PS increase linearly when the values of both independent variables (X_1, X_2) simultaneously increased. At fixed level of surfactant concentration, polymer concentration had major effect on PS. At +1 level of surfactant concentration, particle size less than 145 nm could be obtained at +0.5 level of sonication time and -0.5 level of PLGA concentration. At +1 level of PLGA concentration, lower particle size range could be achieved at higher level of sonication (+0.6) and lower level of surfactant concentration (-0.5).

For EE, at +1 level of sonication time, higher entrapment was achieved between -1 to +0.4 level of surfactant and 0.8 level of PLGA. Entrapment increased with increase in polymer concentration while decreased with surfactant concentration. Interaction effects of sonication time and surfactant concentration not have major effect on EE, whereas EE is linearly increased with polymer concentration. At 0 level of sonication

time, 0 level of surfactant concentration and +1 level of PLGA concentration, maximum EE was obtained. Overall, maximum entrapment (greater than 50 %) and particle size less than 160 nm could be achieved at 0.4 level of PLGA, 0.5 level of sonication time and -0.5 level of surfactant concentration.

Response surface plot of PLGA concentration and surfactant concentration showed a linear relationship with the particle size as PS increased with simultaneous increase in both variables. Response plot of sonication time versus PLGA concentration shows that both variables nullified the effect of each other on PS, as with increase in sonication time the PS decreased while with increase in PLGA concentration the PS increased.

For EE, response plots show nonlinear relationship with surfactant concentration and sonication time. The EE first increased and then decreased. Simultaneous increase in sonication time and PLGA concentration showed increase in EE, as PLGA has major effect on EE.

Desirability Criteria

From the results, the optimum levels of independent variables were screened by multiple regression analysis. Since PS and EE were taken into consideration simultaneously, the batch with smallest particle size of 120 nm exhibited EE near to 20 % (at $X_1 = -1$, $X_2 = -0.5$ to -1.0 , $X_3 = 1.0$) while that with highest EE of 60% produced particle size greater than 200 nm (at $X_1 = 1$, $X_2 = +0.5$ to -0.5 , $X_3 = -0.4$ to $+0.5$). Hence, desirability criteria obtained by Design Expert software (version 8.0.3) was used to find out optimized formulation parameters. Our criteria included maximum PDE and particle size not more than 200 nm. The optimum formulation offered by the software based on desirability was found at 0.0, -0.52, and 0.25 levels of X_1 , X_2 and X_3 respectively. The calculated desirability factor for offered formulations was 0.985, which was near to 1 and indicates suitability of the designed factorial model. The results of dependent variables from the software were found to be 56.39% for PDE and 166.68 nm for PS at these levels which is as per our desired criteria. The drug loading for optimized formulation was found to be $10.39 \pm 2.131\%$.

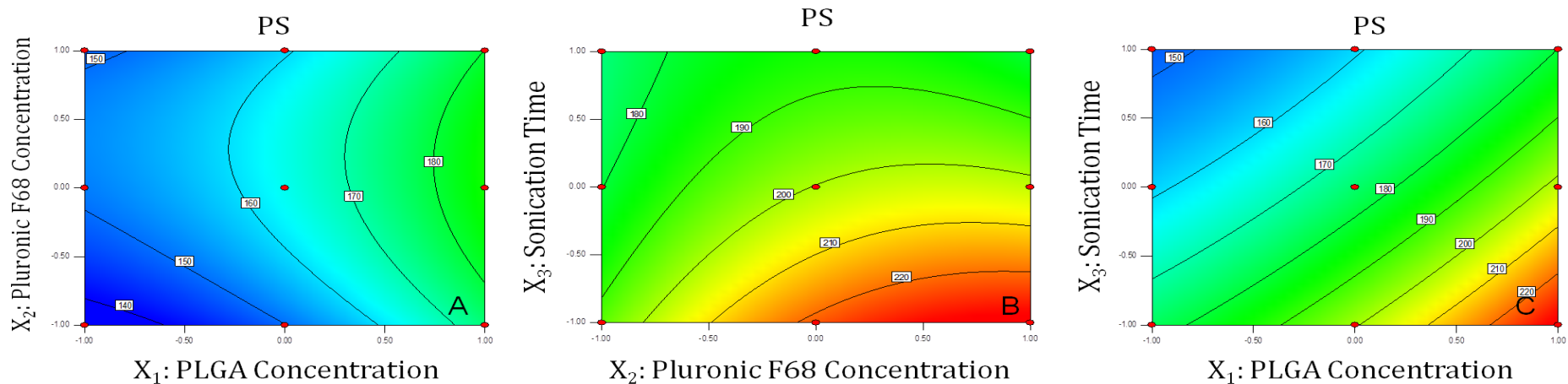


Fig. 4.1 Contour plots showing effect of (a) X_1 versus X_2 (at +1 level of X_3), (b) X_2 versus X_3 (at +1 level of X_1), (c) X_1 versus X_3 (at +1 level of X_2) on PS of Gemcitabine HCl loaded NPs

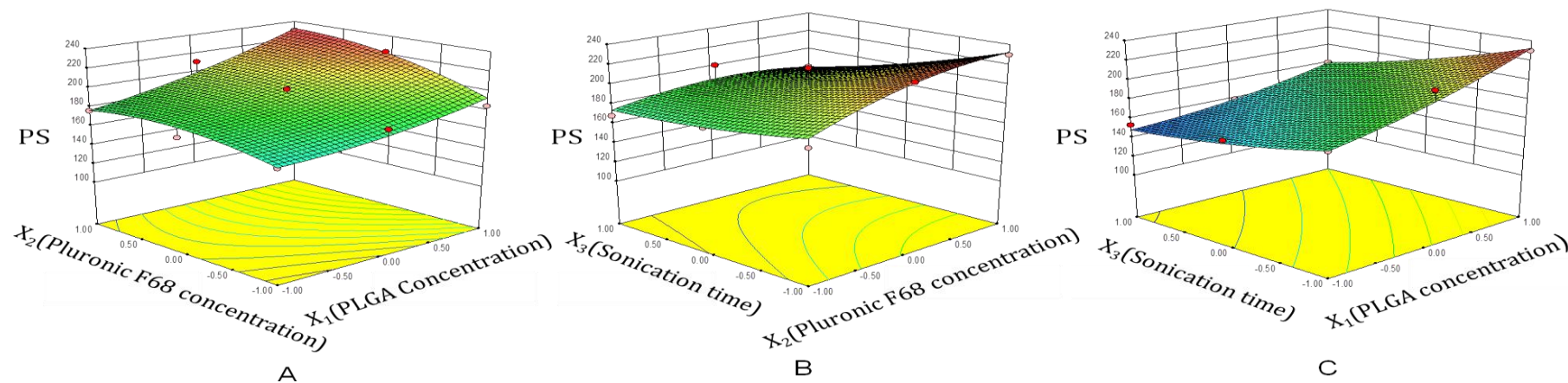


Fig. 4.2 Response surface plots showing effect of (a) X_1 versus X_2 (at +1 level of X_3), (b) X_2 versus X_3 (at +1 level of X_1), (c) X_1 versus X_3 (at +1 level of X_2) on PS of Gemcitabine HCl loaded NPs

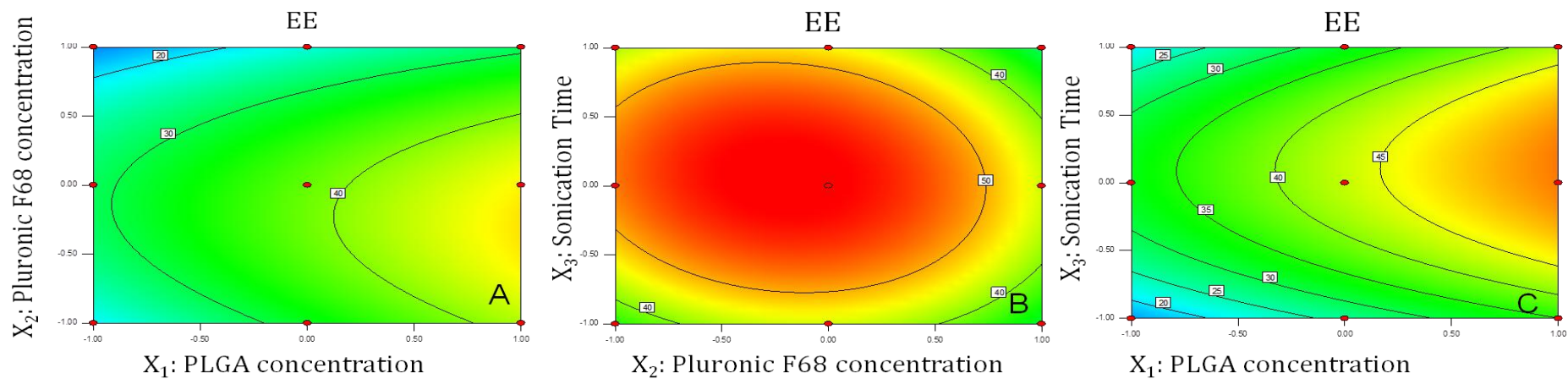


Fig. 4.3 Contour plots showing effect of (a) X_1 versus X_2 (at +1 level of X_3), (b) X_2 versus X_3 (at +1 level of X_1), (c) X_1 versus X_3 (at +1 level of X_2) on EE of Gemcitabine HCl loaded NPs

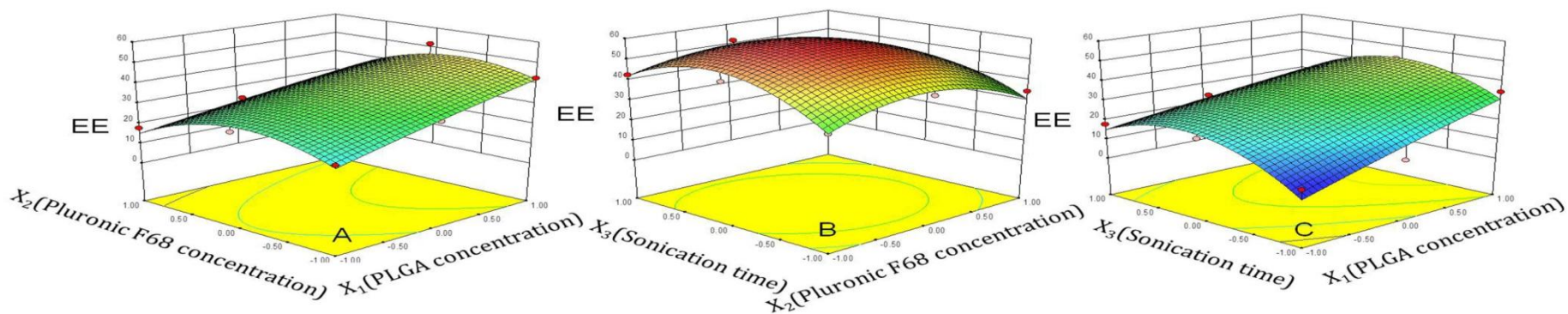


Fig. 4.4 Response plots showing effect of (a) X_1 versus X_2 (at +1 level of X_3), (b) X_2 versus X_3 (at +1 level of X_1), (c) X_1 versus X_3 (at +1 level of X_2) on EE of Gemcitabine HCl loaded NPs

Check point analysis

Three check points were selected as shown in the Table 4.11. When both experimentally obtained and theoretically computed PS and EE values were compared using student's 't' test, the difference was found to be non significant ($p > 0.05$) in both cases. The normalized error ($NE = [\sum\{(Pre - Obs)/Obs\}^2]^{1/2}$) between the observed and predicted values was found to be minimum. This confirms the utility of contour plots and established polynomial equation for both PS and EE in the preparation of Gemcitabine HCl loaded PLGA NPs.

Table 4.11 Check point analysis, t test analysis and normalized error determination for Gemcitabine HCl loaded NPs

Checkpoint batches with their predicted and measured values of PS and EE							
Batch No.	X ₁	X ₂	X ₃	PS		EE	
				Observed	Predicted	Observed	Predicted
1	-1 (1%)	0.5 (62.5mg)	0.5 (75S)	158.63	157.08	34.76	32.01
2	0 (2%)	-0.5(37.5mg)	-0.5(45S)	180.96	183.9	43.18	43.95
3	1 (3%)	-0.5(37.5mg)	+0.5 (75S)	188.14	186.49	55.96	56.68
t _{calculated}				0.959545		0.752995	
t _{tabulated}				2.9199		2.9199	
Normalized Error				0.02088		0.08211	

4.9.3 Optimization of Cryoprotectant for Lyophilization of Gemcitabine HCl Loaded Nanoparticles

Freeze drying causes increase in PS of NPs after lyophilization due to aggregation of particles during the process (Abdelwahed et al; 2006). If these aggregates are not separated during re-dispersion, it may cause instability to the system. The optimized Nanoparticle formulation was lyophilized using lyophilizer (Heto Drywinner, Vaccubrand, Denmark). Different cryoprotectants (Trehalose dehydrate, Mannitol and Sucrose) were used at different ratios to find out optimum concentration of cryoprotectant which showed minimum increment in particle size. The initial particle size of the formulation was 166.68 ± 1.09 nm. The results are shown in Table 4. 12. It

was observed that sucrose showed minimum particle size at 1:1 ratios indicating its suitability in maintaining particle size of Gemcitabine HCl loaded nanoparticles after lyophilization. Thus, this formulation was considered for further studies.

Table 4.12 Optimization of cryoprotectant concentration for Gemcitabine HCl loaded NPs

Cryoprotectant	Particle size after lyophilization (nm)	PDI
Trehalose dehydrate (1:1)	287.4 ± 12.8	0.377
Trehalose dehydrate (1:2)	396.7 ± 21.6	0.219
Trehalose dehydrate (1:3)	389.65±11.3	0.329
Sucrose (1:1)	196.8± 14.2	0.198
Sucrose (1:2)	248.6 ± 42.8	0.151
Sucrose (1:3)	496.3 ± 76.2	0.256
Mannitol (1:1)	637.5 ± 22.8	0.858
Mannitol (1:2)	478.23± 14.3	0.481
Mannitol (1:3)	637.2 ± 12.2	0.452

4.9.4 Characterization of Gemcitabine HCl Loaded Nanoparticles

The zeta potential of optimized batch was found to be -20.6 ± 2.321 mV. Negative value of zeta might be due to negative charge of PLGA. The high negative zeta potential will prevent aggregation and increase stability. Moreover, negatively charged particles will be uptaken by the Peyer's patches and then translocated to the systemic circulation (Florence; 2004).

TEM images of nanoparticles revealed discrete round structures without aggregation. Nanoparticles were seen as reservoir systems, having walled structures (Fig. 4.5). The diameters of NPs were in the range of 100-200nm; below 200nm, similar to particle size results obtained by Malvern Zetasizer. The particle size distribution of optimized batch is shown in Fig. 4.6 with mean particle diameter of 166.4 nm and PDI 0.078.

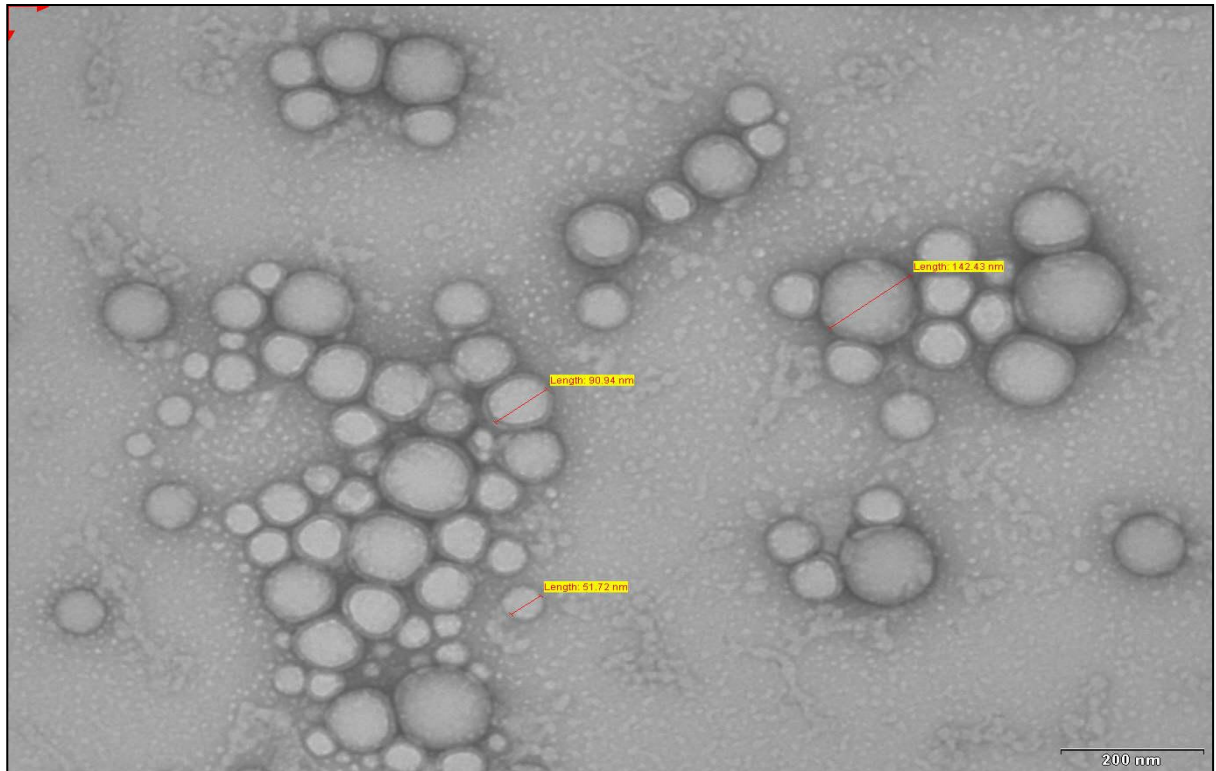


Fig. 4.5 TEM image of Gemcitabine HCl loaded NPs

	Diam. (nm)	% Intensity	Width (nm)
Z-Average (d.nm): 166.4	Peak 1: 177.9	100.0	44.80
PdI: 0.078	Peak 2: 0.000	0.0	0.000
Intercept: 0.955	Peak 3: 0.000	0.0	0.000
Result quality : Good			

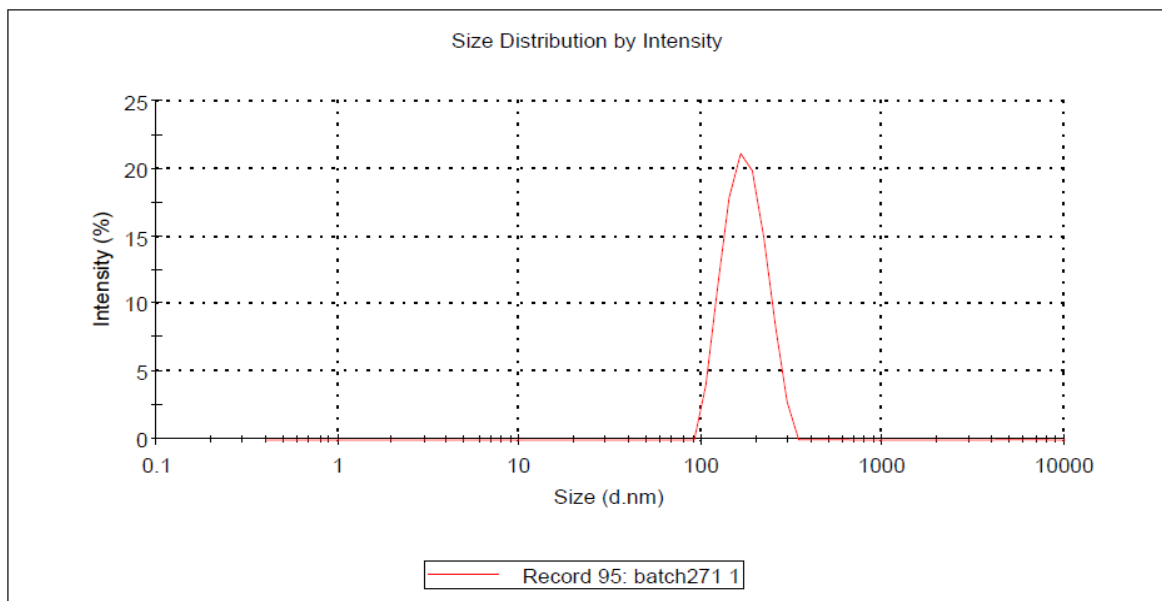


Fig. 4.6 Particle size distribution of optimized Gemcitabine HCl loaded NPs by Malvern Zetasizer

DSC thermograms of Gemcitabine HCl, PLGA, physical mixture (Gemcitabine HCl and PLGA) and Gemcitabine HCl loaded NPs are shown in Fig. 4.7. Pure Gemcitabine HCl showed an endothermic peak at 277.49 °C showing the crystalline structure of drug, while PLGA showed endothermic peak at 51.06 °C corresponding to its glass transition temperature (Montgomery; 2004). Physical mixture of drug and PLGA showed endothermic peaks of PLGA and drug respectively at 51.06°C and 277.49°C indicating the compatibility between them. There was no peak of Gemcitabine in the thermogram of NPs indicating the amorphization of drug in the polymer matrix but peak of PLGA was present at 51.06°C.

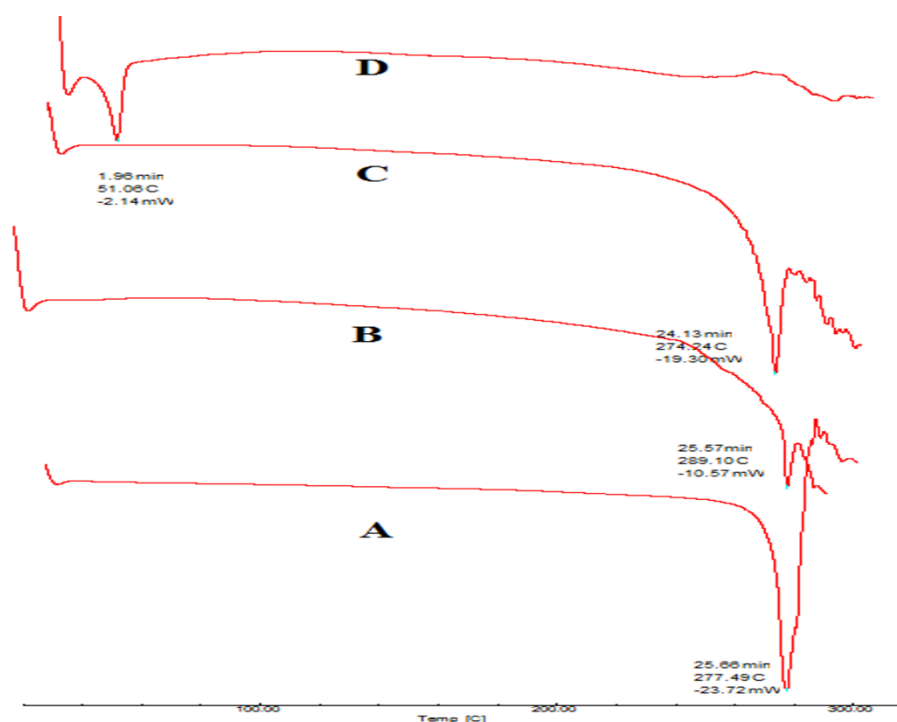


Fig. 4.7 DSC thermogram of Gemcitabine HCl (A), PLGA (B), Physical mixture (C) and Gemcitabine HCl loaded NPs (D)

FTIR spectra of pure drug, PLGA, physical mixture and drug loaded NPs are shown in Fig. 4.8. The PLGA spectrum showed characteristic peaks at 3519.60 cm^{-1} and 1749.87 cm^{-1} indicative of O-H stretching and C=O stretching (due to alpha-substitution) respectively. FTIR spectra of native gemcitabine shows characteristic peaks of amine bands at 1680 cm^{-1} and characteristic peak of ureido group at 1721 cm^{-1} with 3393 cm^{-1} for stretching vibration of (NH_2) (Vandana and Sahoo; 2010). The spectrum of physical mixture (C) showed characteristic peaks of both drug (3393 cm^{-1} and 1680 cm^{-1}) and the polymer (3511.18 cm^{-1} and 1757.40 cm^{-1}), indicating their compatibility. The

intensity of both the peaks N-H of pure drug at 1680 cm^{-1} and stretching vibration of NH_2 at 3393 cm^{-1} were found to be weak in the spectra of Gemcitabine HCl loaded PLGA NPs. The peak of PLGA at 3511.18 cm^{-1} was present with a slight shift to 3497 cm^{-1} , while characteristic peak for ureido group of Gemcitabine HCl 1721.25 cm^{-1} was absent, indicating that the drug was almost completely incorporated in the PLGA NPs.

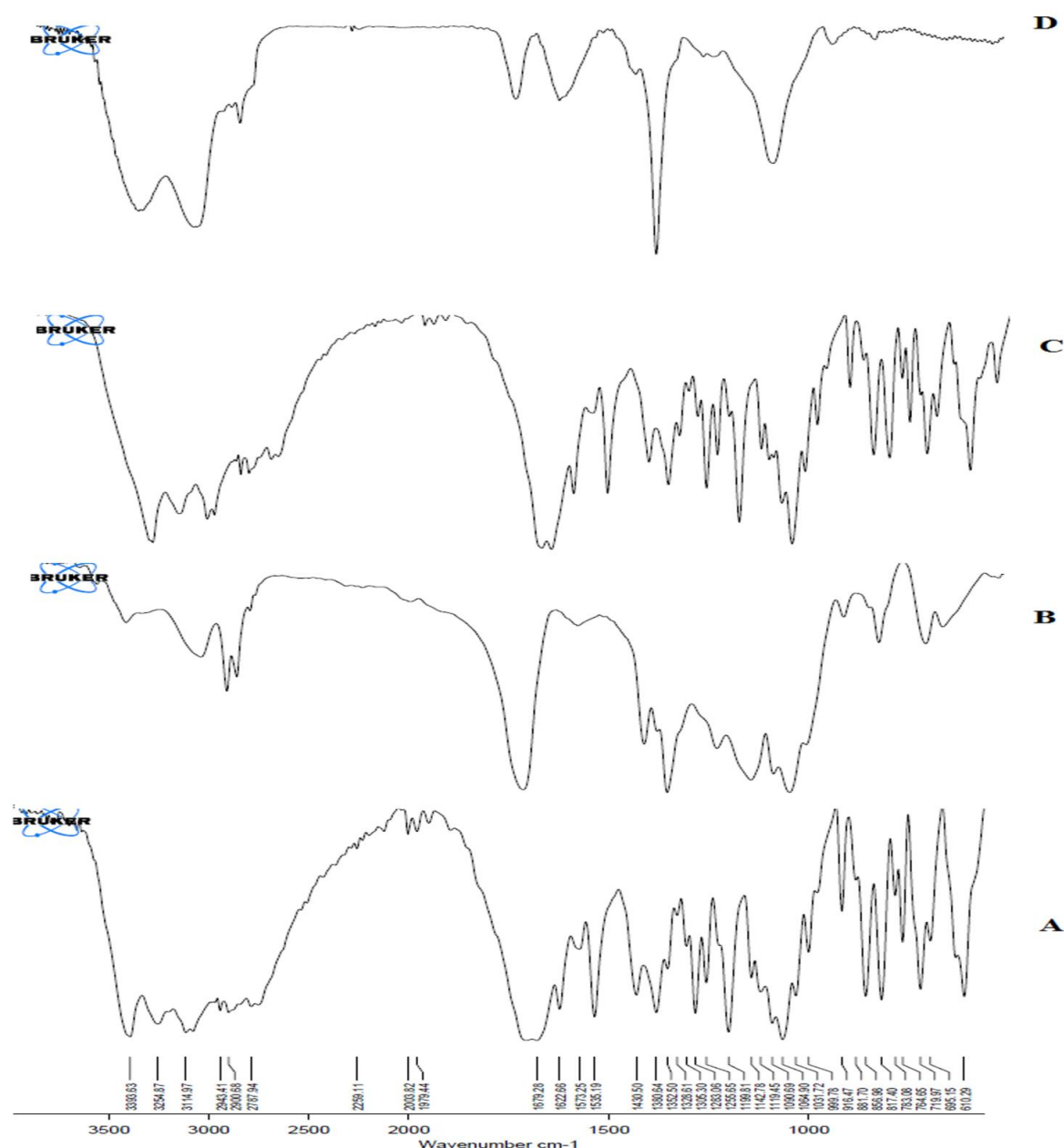


Fig. 4.8 FTIR spectra of Gemcitabine HCl (A), PLGA (B), Physical mixture (C), Gemcitabine HCl loaded NPs (D)

Stability studies

The stability of Gemcitabine HCl loaded NPs in terms of drug content and particle size distribution was monitored for 3 months at 2-8 °C and RT (25-30 °C). The NPs showed physical stability for the period of 3 months at 2-8°C. The particle size and drug content of the NPs at different time interval is given in Table 4.13. The drug content at room temperature was found to decrease after 3 months; also the particle size was increased above 200 nm, which was not desirable. Hence, RT was not suitable for storage of NPs. It was found that no significant difference was observed in the particle size and drug content of NPs after 3 months at refrigerated conditions indicating its suitability for storage at 2 -8°C.

Table 4.13: Stability of Gemcitabine HCl loaded NPs at RT and (2-8°C)

Sr. No	Time	Drug content (%) (2-8 °C)	Drug content (%) (RT)	Particle size (nm) (2-8 °C)	Particle size (nm) (RT)
1	Initial	99.8±1.1	99.8±1.4	166.56±12.6	166.4±12.6
2	1 month	99.6±1.3	94.5±1.0	164.67±10.2	188.3±12.5
3	2 months	99.6±1.0	79.4±1.5	168.53±15.3	214.6±11.2
4	3 months	98.9±1.6	68.8±1.3	169.76±13.9	236.9±10.9

4.10 References

- ❖ Abdelwahed W, Degobert G, Stainmesse S, and Fessi H. Freeze-drying of nanoparticles: formulation, process and storage considerations. *Adv Drug Deliv Rev*, 58, 2006,1688-1713.
- ❖ Adinarayana K and Ellaiah P. Response surface optimization of the critical medium components for the production of alkaline protease by a newly isolated *Bacillus* sp. *J Pharm Pharm Sci*, 5, 2002, 272-278.
- ❖ Bolton SBC. (2004). *Pharmaceutical Statistics: Practical and Clinical Applications*, 4th edn (USA: Marcel Dekker).
- ❖ Box GEP, Wilson KB. (1951). On the experimental attainment of optimum conditions. *J Roy Stat Soc*, 13,1951, 1-45.
- ❖ Derakhshandeh K and Fathi S. Role of chitosan nanoparticles in the oral absorption of Gemcitabine. *International Journal of Pharmaceutics*, 437, 2012, 172-177.
- ❖ Derringer G and Suich R. Simultaneous optimization of several response variables. *Journal of Quality Technology*, 12, 1980, 214-219.
- ❖ EliLilly (1997). *Summary of Product Characteristics: Gemcitabine*, UK Prescribing Information. Eli Lilly. In, (Eli Lilly, Co.).
- ❖ Hans ML and Lowman AM. Biodegradable nanoparticles for drug delivery and targeting. *Current Opinion in Solid State and Materials Science*, 6, 2002, 319-327.
- ❖ Jain RA. The manufacturing techniques of various drug loaded biodegradable poly(lactide-co-glycolide) (PLGA) devices. *Biomaterials*, 21, 2000, 2475-2490.
- ❖ Kalaria DR, Sharma G, Beniwal V, and Ravi Kumar MNV. Design of biodegradable nanoparticles for oral delivery of doxorubicin: in vivo pharmacokinetics and toxicity studies in rats. *Pharm Res*, 26, 2009, 492-501.
- ❖ Kashi TS, Eskandarion S, Esfandyari-Manesh M, Marashi SM, Samadi N, Fatemi SM, Atyabi F, Eshraghi S, and Dinarvand R. Improved drug loading and antibacterial activity of minocycline-loaded PLGA nanoparticles prepared by solid/oil/water ion pairing method. *Int J Nanomedicine*, 7, 2012, 221-234.
- ❖ Levison KK, Takayama K, Isowa K, Okabe K, and Nagai T. Formulation optimization of indomethacin gels containing a combination of three kinds of

- cyclic monoterpenes as percutaneous penetration enhancers. *J Pharm Sci*, 83, 1994, 1367-1372.
- ❖ Li X, Xu Y, Chen G, Wei P, and Ping Q. PLGA nanoparticles for the oral delivery of 5-Fluorouracil using high pressure homogenization-emulsification as the preparation method and *in vitro/in vivo* studies. *Drug Dev Ind Pharm*, 34, 2008, 107-115.
 - ❖ Mak KWY, Yap MGS, and Teo WK. Formulation and optimization of two culture media for the production of tumour necrosis factor- β in *Escherichia coli*. *Journal of Chemical Technology and Biotechnology*, 62, 1995, 289-294.
 - ❖ Meneau BPCBF and Ollivon PCM . Interaction of an anticancer drug, gemcitabine, with phospholipid bilayers. *Acta Biomater J Therm Anal Calorim*, 98, 2009, 19–28.
 - ❖ Miller AJ. Selection of subsets of regression variables. *J R Stat Soc Ser A*, 147, 1984, 389-425.
 - ❖ Montgomery DC (2004). *Introduction to factorial designs.*, (New York: John Wiley and Sons).
 - ❖ Peltonen L, Aitta J, Hyvonen S, Karjalainen M, and Hirvonen J. Improved entrapment efficiency of hydrophilic drug substance during nanoprecipitation of poly(l)lactide nanoparticles. *AAPS PharmSciTech*, 5, 2004, E16.
 - ❖ Myer RH and Montgomery DC (2002). *Response Surface Methodology: Process and product optimization using designed experiment*, second edn (New York: John Wiley and Sons).
 - ❖ Ray S, Lalman JA and Biswas, N. Using the Box-Benken technique to statistically model phenol photocatalytic degradation by titanium dioxide nanoparticles. *Chem Eng J*, 150, 2009, 15-24.
 - ❖ Rubiana M. Mainardes RCE. PLGA nanoparticles containing praziquantel: effect of formulation variables on size distribution. *International Journal of Pharmaceutics*, 290, 2005, 137-144.
 - ❖ Sarmento B, Ribeiro A, Veiga F, Ferreira D and Neufeld R (2007). Oral bioavailability of insulin contained in polysaccharide nanoparticles. *Biomacromolecules*, 8, 2007, 3054-3060.

- ❖ Shirakura O, Yamada M, Hashimoto M, Ishimaru S, Takayama K, and Nagai T. (1991). Particle-Size Design Using Computer Optimization Technique. *Drug Dev Ind Pharm*, 17,1991, 471-483.
- ❖ Trickler WJ, Khurana J, Nagvekar AA, and Dash AK. Chitosan and glyceryl monooleate nanostructures containing gemcitabine: potential delivery system for pancreatic cancer treatment. *AAPS PharmSciTech*, 11, 2010, 392-401.
- ❖ Vandana M and Sahoo SK. Long circulation and cytotoxicity of PEGylated gemcitabine and its potential for the treatment of pancreatic cancer. *Biomaterials*, 31, 2010,9340-9356.
- ❖ Wagner JM, and Shimshak DG. Stepwise selection of variables in data envelopment analysis: Procedures and managerial perspectives. *Eur J Oper Res*, 180, 2007, 57-67.
- ❖ Yu, LX. Pharmaceutical quality by design: product and process development, understanding, and control. *Pharm Res*, 25, 2008, 781-791.

CHAPTER 5

EXPERIMENTAL LOPINAVIR LOADED

NANOPARTICLES

5.1 Introduction

Lopinavir is a potent protease inhibitor used as a leading component in combined chemotherapy commonly referred as Highly Active Anti-Retroviral Therapy (HAART). Lopinavir has poor oral bioavailability due to poor drug solubility characteristics as well as extensive first pass metabolism, primarily mediated by cytochrome P450 and P-glycoprotein efflux which limits intestinal uptake. Lopinavir is always co-administered with ritonavir, as ritonavir inhibits the cytochrome P450 enzyme, responsible for extensive first pass metabolism (Prot et al; 2006).

Colloidal drug carriers like nanoparticles can target anti-retrovirals to the intestinal lymphatic tissue with high viral load. Targeting means delivering of drug directly to a specific site, without accumulation at undesirable tissues, which is not possible with free drug. The advantage associated with nanosystems is that the absorption, biodistribution and elimination of drug in the body is dependent on the inherent properties of nanosystems like size, surface properties and charge, not dependent on the properties of drug as the drug is entrapped inside the system. Further, nanoparticles have the ability to circumvent the p glycoprotein efflux which is present on the membranes of HIV reservoir cells as well as intestinal epithelial cells. This in turn, increases the absorption as well as target the antiretroviral drug to HIV reservoir sites.

A pharmaceutical formulation like nanoparticles is composed of several formulation factors and process variables. Several responses relating to the effectiveness, usefulness, stability, as well as safety must be optimized simultaneously. Most of the time, the relationship between formulation and process variables, and the aforementioned performance characteristics of the controlled release drug delivery systems is not well understood due to the complexity of the controlled release formulations. Therefore, quantitative prediction of the performance of a formulation from the basic physicochemical properties of the drug and independent and dependent variables is often difficult.

Statistical approach such as response surface methodology (RSM) based on polynomial regression has been used in the development and formulation of different types of controlled release drug delivery systems. The response surface method (RSM) has widely been used for selecting acceptable pharmaceutical formulations. The RSM includes (1) statistical factorial experimental designs, (2) modelling between causal

factors and response variables, and (3) multi-objective optimization for seeking the best formulation under a set of pragmatic constraints. Compared with a normal analysis based on one-factor-at-a-time experiments, we can greatly reduce the number of experiments for the preparation of model formulations.

In a classical way, multiple regression analysis has been applied on the basis of a quadratic polynomial equation. Finally, multi-objective optimization algorithms are applied for predicting the best formulation

5.2 Materials

Lopinavir was obtained as a gift sample from Aurobindo Pharmaceuticals, Hyderabad, India. Poly (lactide -co-glycolide) PLGA (50:50) (inherent viscosity 0.2dl/g) was gift sample from Purac Biomaterials, The Netherlands. Pluronic F 68 was obtained as gift sample from BASF, Germany. Brij 35 was purchased from Sigma Aldrich, USA.

5.3 Equipments

1. High speed magnetic stirrer (Remi, MS500, Remi equipments, Mumbai, India)
2. High speed Centrifuge (Sigma 3K30, Germany)
3. Particle size Analyzer (Zeta sizer Nano series, Malvern Instruments, UK)
4. UV-VIS Spectrophotometer (Shimadzu, Japan)
5. High Performance liquid chromatography (HPLC Shimadzu, Japan)
6. Lyophilizer (Heto, Vaccubrand, Denmark)
7. Differential Scanning Calorimeter. (Mettler Toledo DSC 822e, Japan)
8. Transmission Electron Microscope (Philips, Tecnai 20, Holland)
9. Fourier Transform Infra red spectrophotometer (FTIR, Bruker, Germany)

5.4 Formulation of Lopinavir Loaded Nanoparticles

Lopinavir loaded PLGA nanoparticles (NPs) were prepared using solvent diffusion (nanoprecipitation) method (Fessi et al; 1989). The optimized formulation was prepared by dissolving PLGA (25 mg) and drug (15 mg) in 2.5 ml of acetone. The organic phase was added at the rate of 0.5 ml/min into 5 ml of aqueous phase containing 0.25% w/v Pluronic F68 with continuous stirring on magnetic stirrer at room temperature. Stirring was continued until the complete evaporation of organic solvent. The NPs suspension was centrifuged at 25,000 g for 30 min at 4 °C (3K30, Sigma Centrifuge, Osterode, Germany), supernatant was alienated and nanoparticles were collected.

5.5 Preliminary Optimization of Parameters

In preliminary optimization, the possible parameters influencing the formation of nanoparticles, size of nanoparticles and entrapment efficiency were identified and optimized. The parameters studied were type of organic solvent and type of surfactant. Constant parameters for optimization of Lopinavir loaded PLGA NPs are given in Table 5.1.

Table 5.1 Constant parameters for optimization of Lopinavir loaded NPs

Parameters	Observation
Rate of addition of organic phase	0.5 ml/min.
Stirring speed	900 rpm
Needle size	26 ½ Gauge
Stirring time	5 hrs
Organic: Aqueous Phase	1:2

5.5.1 Type of Organic Solvent

Two different solvents, acetone and acetonitrile were used and particle size, PDI and entrapment efficiency were determined.

5.5.2 Type of Surfactant

Three different types of surfactants, Pluronic F68 (Poloxamer 188), Pluronic 127 (Poloxamer 407) and Poly vinyl alcohol (PVA) were taken and particle size and PDI were determined.

5.6 Optimization by Factorial Design

Based on the preliminary experiments, drug concentration in organic phase (X_1), Polymer concentration in organic phase (X_2) and Surfactant concentration (X_3) were selected as independent variables and particle size (PS) and entrapment efficiency (EE) were selected as dependent variables. A 3^3 randomized full factorial design was used in the study (Joshi et al; 2010). In this design, three factors were evaluated, each at 3 levels, and experimental trials were performed at all 27 possible combinations with two replicates. The replicate experimental runs were carried out in complete randomized manner. A multilinear stepwise regression analysis was performed using Microsoft

Excel software. The full models were used to plot two dimension contour plots for both PS and EE. All the statistical operations were carried out by Design Expert (8.0.7.1, Stat-ease, Inc. Minneapolis, USA). Table 5.2 and Table 5.3 summarize experimental runs studied, their factor combinations, and the translation of the coded levels to the experimental units employed during the study.

Table 5.2 Factorial design parameters and experimental conditions

Factors	Levels used, Actual (coded)		
	Low (-1)	Medium(0)	High (+1)
X ₁ -Drug Concentration in organic phase(%w/v)	0.2%	0.3%	0.4%
X ₂ -Polymer concentration in organic phase (%w/v)	1%	2%	3%
X ₃ - Surfactant concentration	0.50%	0.75%	1.0%

Table 5.3 Formulation of Lopinavir loaded NPs utilizing coded values

Batch	X1	X2	X3
F1	-1	-1	-1
F2	-1	-1	0
F3	-1	-1	1
F4	-1	0	-1
F5	-1	0	0
F6	-1	0	1
F7	-1	1	-1
F8	-1	1	0
F9	-1	1	1
F10	0	-1	-1
F11	0	-1	0
F12	0	-1	1
F13	0	0	-1
F14	0	0	0
F15	0	0	1
F16	0	1	-1
F17	0	1	0
F18	0	1	1
F19	1	-1	-1
F20	1	-1	0
F21	1	-1	1
F22	1	0	-1
F23	1	0	0
F24	1	0	1
F25	1	1	-1
F26	1	1	0
F27	1	1	1

5.7 Optimization Data Analysis

Various RSM (Response Surface Methodology) computations for the current optimization study were performed employing Design Expert® software (version 8.0.7.1, Stat-Ease Inc, Minneapolis, USA). Polynomial models including interaction and quadratic terms were generated for the response variable using multiple regression analysis (MLRA) approach. The general form of MLRA model is represented as equation 5.1.

$$Y = b_0 + b_1X_1 + b_2X_2 + b_3X_3 + b_{12}X_1X_2 + b_{13}X_1X_3 + b_{23}X_2X_3 + b_1^2X_1^2 + b_2^2X_2^2 + b_3^2X_3^2 + b_{123}X_1X_2X_3 \quad (5.1)$$

Where b_0 is the intercept representing the arithmetic average of all quantitative outcomes of 27 runs; b_{ij} are the coefficients computed from the observed experimental values of Y ; and X_1 , X_2 and X_3 are the coded levels of the independent variable(s). The terms X_1X_2 and X_i^2 ($i=1$ to 3) represents the interaction and quadratic terms, respectively. The main effects (X_1 , X_2 and X_3) represent the average result of changing one factor at a time from its low to high value. The interaction terms ($X_1X_2X_3$) show how the response changes when three factors are simultaneously changed. The polynomial terms (X_1^2 , X_2^2 and X_3^2) are included to investigate nonlinearity. The polynomial equation was used to draw conclusions after considering the magnitude of coefficients and the mathematical sign it carries, i.e., positive or negative. A positive sign signifies a synergistic effect, whereas a negative sign stands for an antagonistic effect.

The effects of different levels of independent variables on the response parameters were predicted from the respective response surface plots. A FM equation was established after putting the values of regression coefficients of EE and PS in equation 3. The predicted values were calculated by using the mathematical model based on the coefficients of the model and the predicted values along with their observed values were recorded along with percentage of error obtained when predicted value and observed values were compared. Statistical validity of the polynomials was established on the basis of ANOVA provision in the Design Expert ®software. Level of significance was considered at $P < 0.05$. F-Statistic was applied on the results of analysis of variance (ANOVA) of full model and reduced model to check whether the non-significant terms

can be omitted or not from the FM (Bolton and Bon; 1997). The best fitting mathematical model was selected based on the comparisons of several statistical parameters including the coefficient of variation (CV), the multiple correlation coefficient (R^2), adjusted multiple correlation coefficient (adjusted R^2). For simultaneous optimization of EE and PS, desirability function (multi-response optimization technique) was applied and total desirability was calculated using Design Expert software (version 8.0.3). A check point analysis was performed to confirm the utility of the multiple regression analysis and established contour plots in the preparation of Lopinavir loaded PLGA NPs. Results of desirability criteria, check point analysis and normalized error were considered to select the formulation with lowest PS and highest EE.

Contour Plots

Contour plots are diagrammatic representation of the values of the responses that help in explaining the relationship between independent and dependent variables. Two dimensional contour plots were established between X_1 and X_2 at different levels (-1, 0, 1) of X_3 for PS and EE.

Response Surface Plots

To understand the main and the interaction effects of two variables, response surface plots were used as a function of two factors at a time maintaining all other factors at fixed levels (Box, 1951; Mak et al., 1995). These plots were obtained by calculating the values taken by one factor where the second varies (from -1 to 1 for instance) with constraint of a given Y value. The yield values for different levels of variables can also be predicted from the respective response surface plots.

Check Point Analysis

A check point analysis was performed to confirm the utility of the established contour plots and reduced polynomial equation in the preparation of NPs. Values of independent variables (X_1 and X_2) were taken from three check points on contour plots plotted at fixed levels of -1, 0 and 1 of X_3 and the values of EE (Y_1) and PS (Y_2) were calculated by substituting the values in the reduced polynomial equation. Lopinavir loaded NPs were prepared experimentally by taking the amounts of the independent variables (X_1 and X_2). Each batch was prepared three times and mean values were determined. Difference in the predicted and mean values of experimentally obtained EE and PS was compared by using student's 't' test.

Desirability Criteria

For simultaneous optimization of EE and PS, desirability function (multi-response optimization technique) was applied and total desirability was calculated using Design Expert software (version 8.0.3). The desirability lies between 0 and 1 and it represents the closeness of a response to its ideal value (eq 5.2). The total desirability is defined as a geometric mean of the individual desirability for PS and EE (Derringer and Suich; 1980).

$$D = (d_{PS} \times d_{EE})^{1/2} \quad (5.2)$$

Where, D is the total desirability, d_{PS} and d_{EE} are individual desirability for PS and EE. If both the quality characteristics reach their ideal values, the individual desirability is 1 for both. Consequently, the total desirability is also 1. Our optimization criteria included PS of less than 200 nm and maximum EE.

Normalized Error Determination

The quantitative relationship established by MRA was confirmed by evaluating experimentally prepared Lopinavir loaded NPs. EE and PS predicted from the MRA were compared with those generated from prepared batches of check point analysis using normalized error (NE). The equation of NE (eq 5.3) is expressed as follows:

$$NE = [\sum\{(Pre - Obs)/Obs\}^2]^{1/2} \quad (5.3)$$

Where, Pre and Obs represents predicted and observed response, respectively.

5.8 Lyophilization of Lopinavir Loaded Nanoparticles and Optimization of Cryoprotectant

The optimized nanoparticle formulation was lyophilized using lyophilizer (Drywinner Hetodryer). Different cryoprotectants (Trehalose dehydrate, Mannitol and Sucrose) at different ratio (1:1w/w, 1:2w/w, 1:3w/w) were tried to select the cryoprotectant which showed minimum increment in particle size. Nanoparticulate suspension (2 ml) was dispensed in 10 ml semi-stoppered vials with rubber closures and frozen for 24 h at -80 °C. Thereafter, the vials are lyophilized (Heto Drywinner, Allerod, Denmark) using different cryoprotectants like trehalose, sucrose and mannitol in different concentrations. Finally, glass vials were sealed under anhydrous conditions and stored until being re-hydrated. Lyophilized NPs were re-dispersed in exactly the same volume of distilled water as before lyophilization. NP suspension was subjected to particle size

measurement as described earlier. Ratio of final particle size (Kashi et al;2012) and initial particle size (S_i) was calculated to finalize the suitable cryoprotectant based upon lowest S_f/S_i ratio.

5.9 Characterization of Optimized Lopinavir Loaded Nanoparticles

5.9.1 Particle Size

The size analysis and polydispersity index of the NPs were determined using a Malvern Zetasizer Nano ZS (Malvern Instrument, Worcestershire, UK). Each sample was diluted ten times with filtered distilled water to avoid multi-scattering phenomena and placed in disposable sizing cuvette. Polydispersity index was noted to determine the narrowness of the particle size distribution. The size analysis was performed in triplicate and the results were expressed as mean size \pm SD.

5.9.2 Entrapment Efficiency and Drug Loading

The drug content in the NPs was determined by dissolving 10 mg of lyophilized NPs in 10 ml of acetonitrile and analyzed by HPLC after filtration through 0.22 μ and appropriate dilution with mobile phase. Drug loading was calculated as follows,

$$\text{Percentage drug loading} = A/B \times 100$$

Where A is the drug content in the NPs and B is the weight of NPs.

EE was estimated by calculating amount of drug entrapped in NPs with respect to total drug added during preparation of formulation.

The PDE was calculated according to following formula:

$$\text{EE (\%)} = (\text{ED}/\text{TD}) \times 100$$

where, TD is total amount of drug added and ED is entrapped drug (drug content in NPs)

5.9.3 Zeta Potential

Zeta potential distribution was also measured using a Zetasizer (Nano ZS, Malvern instrument, Worcestershire, UK). Each sample was suitably diluted 10 times with filtered distilled water and placed in a disposable zeta cell. Zeta limits ranged from -200 to +200 mV. The electrophoretic mobility ($\mu\text{m}/\text{sec}$) was converted to zeta potential by in-built software using Helmholtz-Smoluchowski equation. Average of 3 measurements of each sample was used to derive average zeta potential.

5.9.4 Transmission Electron Microscope Studies

A sample of NPs (0.5 mg/ml) was suspended in water and bath sonicated for 30 s. 2 μl of this suspension was placed over a formvar coated copper TEM grid (150 mesh) and

negatively stained with 2 μ l uranyl acetate (1%) for 10 min, allowed to dry and the images were visualized at 80 kV under TEM (Philip Tecnai 20, USA) and captured using Gatan Digital Micrograph software.

5.9.5 Differential Scanning Calorimetric (DSC) Studies

All the samples were dried in desiccators for 24 h before thermal analysis. DSC studies on pure drug, PLGA, physical mixtures of drug: polymer (1:1) and drug loaded NPs were performed in order to characterize the physical state of drug in the NPs. Thermograms were obtained using DSC model 2910 (Shimadzu, Japan). Dry nitrogen gas was used as the purge gas through the DSC cell at a flow rate of 40 ml/min. Samples (4 - 8 mg) were sealed in standard aluminium pans with lids and heated at a rate of 10 $^{\circ}$ C /min from 20 to 300 $^{\circ}$ C.

5.9.6 Fourier Transform Infrared (FTIR) Spectroscopy

FT-IR spectroscopy was employed to detect the possibilities of interactions between Lopinavir and various excipients used in the formulation. The IR spectra of pure drug, PLGA, physical mixture (of PLGA and Lopinavir in 1:1 ratio) and Lopinavir loaded PLGA NPs were recorded on Fourier Transform Infrared spectrophotometer (Bruker optics, Germany).

5.9.7 Stability Studies

The stability Lopinavir loaded NPs were studied at 2-8 $^{\circ}$ C and room temperature for 3 months. Periodically, samples were withdrawn and the particle size as well as drug content was determined.

5.10 Results and Discussion

5.10.1 Preliminary Optimization

5.10.1.1 Type of Solvent

Initially, two different water miscible solvents were tried for nanoprecipitation and particle size, PDI and entrapment efficiency were determined. Acetone produced smaller particle sizes and higher entrapment due to faster diffusion into aqueous phase and faster evaporation than acetonitrile (Table 5.4). Hence, acetone was optimized for further studies.

Table 5.4 Effect of type of solvent on particle size, PDI and EE of Lopinavir loaded NPs

Solvent	PS \pmSD (nm)	PDI	EE (%)
Acetone	168.9 \pm 1.564	0.193 \pm .003	73.2 \pm 3.56
Acetonitrile	213.4 \pm 2.147	0.172 \pm .004	42.3 \pm 2.13

5.10.1.2 Type of Surfactant

Three different surfactants were initially used for formulation development namely Pluronic F-68, Pluronic F-127 and Poly vinyl alcohol (PVA). From these, better one was selected based on resultant particle size and entrapment. Results are presented in Table 5.5. When Pluronic F-68 was used, smallest particle size and higher entrapment was observed as compared to Pluronic F-127 and PVA due to better stabilization of droplets. So Pluronic F-68 was used as stabilizer for further development of formulation.

Table 5.5 Effect of type of surfactant on particle size, PDI and EE of Lopinavir loaded NPs

Surfactant	Z-avg size(nm)	PDI	EE (%)
Pluronic F-68	148.4 nm\pm0.95	0.147\pm0.002	82.3\pm4.23
Pluronic F-127	178.95nm \pm 5.05	0.101 \pm 0.04	56.23 \pm 3.43
PVA	163.85nm \pm 6.35	0.13 \pm 0.03	42.1 \pm 2.63

5.10.2 Optimization by Factorial Design

From the preliminary optimization studies, the drug concentration in organic phase (X_1), Polymer concentration (X_2), and surfactant concentration (X_3) were selected as independent variables whereas particle size and entrapment efficiency as responses. The coded and actual values of formulation parameters are shown in Table 5.2. Total 27 batches of formulations were developed using 3^3 factorial design varying the three independent variables (Table 5.6).

Table 5.6 Full factorial design layout of Lopinavir loaded NPs showing the effect of independent variables X₁ (Drug concentration), X₂ (Polymer concentration) and X₃ (surfactant concentration) on responses PS (Particle size) and EE (entrapment efficiency)

Sr. No.	X ₁	X ₂	X ₃	Y ₁ * (EE, %)	Y ₂ * (PS, nm)
1	-1	-1	-1	36.56±2.21	126.62±4.16
2	-1	-1	0	29.43±1.05	131.33±6.13
3	-1	-1	1	21.03±2.28	140.83±1.41
4	-1	0	-1	50.92±1.86	127.33±2.68
5	-1	0	0	48.71±2.34	136.36±4.53
6	-1	0	1	38.23±2.43	139.73±2.68
7	-1	1	-1	51.13±1.49	159.73±3.72
8	-1	1	0	57.33±1.19	163.56±3.91
9	-1	1	1	40.32±0.71	176.91±1.69
10	0	-1	-1	61.66±2.56	144.13±2.13
11	0	-1	0	55.47±1.34	148.03±1.98
12	0	-1	1	47.47±1.04	152.63±6.23
13	0	0	-1	83.37±1.42	155.63±4.61
14	0	0	0	73.26±1.35	159.63±3.73
15	0	0	1	63.16±2.17	165.23±7.26
16	0	1	-1	91.41±2.43	162.64±2.34
17	0	1	0	84.65±2.57	169.72±3.87
18	0	1	1	77.51±1.93	173.83±4.23
19	1	-1	-1	93.03±1.27	142.16±2.13
20	1	-1	0	91.48±1.86	163.36±2.43
21	1	-1	1	87.66±1.76	175.53±3.57
22	1	0	-1	95.7±2.43	214.86±3.89
23	1	0	0	91.48±1.67	231.33±2.59
24	1	0	1	75.36±2.38	233.66±1.73
25	1	1	-1	93.86±1.26	207.43±2.75
26	1	1	0	85.13±2.76	237.13±1.37
27	1	1	1	71.16±1.43	236.16±3.26

*values are represented as mean ± s.d.

The PS and EE obtained at various levels of three independent variables (X_1 , X_2 and X_3) were subjected to multiple regressions to yield second order polynomial equations (eq 5.4 and 5.5, full model). The main effects of X_1 , X_2 and X_3 represent the average result of changing one variable at a time from its low to high value. The interactions (X_1X_2 , X_1X_3 , X_2X_3 and $X_1X_2X_3$) show how the PS and EE changes when two or more variables were simultaneously changed. The PS and EE of total 27 batches showed a wide variation from 126.6 ± 4.16 to 237.1 ± 1.37 nm and 21.03 ± 2.28 to 95.7 ± 2.43 %, respectively (Table 5.6)

$$Y_{PS} = 164.99 + 29.95X_1 + 20.13X_2 + 8.94X_3 + 15.64X_1^2 - 6.41X_2^2 - 2.55X_3^2 + 8.18X_1X_2 + 3.62X_1X_3 + 0.088X_2X_3 - 0.95X_1X_2X_3 \quad \text{----- (5.4)}$$

$$Y_{EE} = 75.25 + 22.85X_1 + 7.15X_2 - 7.59X_3 - 6.53X_1^2 - 3.53X_2^2 - 3.03X_3^2 - 6.98X_1X_2 - 0.40X_1X_3 - 1.02X_2X_3 - 2.75X_1X_2X_3 \quad \text{----- (5.5)}$$

The significance of each coefficient of eq 5.4 and 5.5 were determined by student's 't' test and p-value. The larger the magnitude of the 't' value and the smaller the p-value, the more significant is the corresponding coefficient (Adinarayana and Ellaiiah; 2002). Higher values of coefficients of X_1 , X_2 and X_3 for both PS and EE confirmed them as main contributing factors. Second order main effect of X_1 was significant for both PS and EE and interaction effect of X_1X_2 was significant for EE. Small values of the coefficients of the terms X_2^2 , X_3^2 , X_1X_2 , X_2X_3 , X_1X_3 , and $X_1X_2X_3$ in eq 5.4 for PS and X_2^2 , X_3^2 , X_2X_3 , X_1X_3 , and $X_1X_2X_3$ in eq 5.5 for EE respectively implied that all these terms were least contributing factors and not significant ($p > 0.05$) in the preparation of the Lopinavir loaded PLGA NPs (Table 5.7, 5.8).

Hence, least contributing factor were neglected from the full model and Reduced polynomial equations (5.6 and 5.7), for PS and EE were generated

$$Y_{PS} = 159.01 + 29.95X_1 + 20.13X_2 + 8.54X_3 + 15.611X_1^2 \quad (5.6)$$

$$Y_{EE} = 70.88 + 22.85X_1 + 7.15X_2 - 7.55X_3 - 6.53X_1^2 - 6.98X_1X_2 \quad (5.7)$$

Table 5.7 Model coefficients estimated by multiple regression analysis for PS of Lopinavir loaded NPs

Factor	Coefficients	t Stat	P-value
Intercept	164.9974	21.46391	3.21E-13
X1	29.955	8.417914	2.85E-07
X2	20.13889	5.659403	3.55E-05
X3	8.946932	2.486162	0.024342
X12	15.64278	2.537981	0.021929
X22	-6.41556	-1.0409	0.313396
X32	-2.55556	-0.41463	0.683919
X1X2	8.186667	1.878437	0.078668
X1X3	3.622386	0.750263	0.463987
X2X3	0.088333	0.020268	0.98408
X1X2X3	-0.95125	-0.17821	0.860793

Table 5.8 Model coefficients estimated by multiple regression analysis for EE for Lopinavir loaded NPs

Factor	Coefficients	t Stat	P-value
Intercept	75.25963	22.58931	1.45E-13
X1	22.85889	14.82174	9.14E-11
X2	7.15	4.636073	0.000275
X3	-7.59807	-4.87155	0.00017
X12	-6.53556	-2.44662	0.02635
X22	-3.53222	-1.3223	0.204659
X32	-3.03222	-1.13513	0.273041
X1X2	-6.98167	-3.69622	0.001958
X1X3	-0.40261	-0.19241	0.849846
X2X3	-1.0275	-0.54398	0.593957
X1X2X3	-2.75625	-1.19144	0.250856

For entrapment efficiency (EE), positive sign of coefficient of X_1 and X_2 shows that entrapment increased with increase in drug concentration and polymer concentration due to more availability of drug to get entrapped and more polymer quantity to entrap the drug. Negative sign of X_3 showed a decrease in entrapment with increase in surfactant concentration, as higher surfactant concentration will solubilise drug in outer aqueous phase.

For Particle size, coefficients of all the variables have positive sign meaning that all the variables had synergistic effect on particle size. Particle size increased with increase in polymer concentration due to higher viscosity of solution and more entrapment of drug inside the particles leading to bigger sized particles. Increase in particle size with surfactant concentration could be attributed to coating of surfactant on surface of PLGA. When the values of three independent variables were compared, highest values of coefficients were found for X_1 for both the responses. Hence, drug concentration was considered as major contributing variable for EE and Drug concentration and polymer concentration both were major contributing variables for EE of Lopinavir loaded NPs.

The results of ANOVA of the second order polynomial equation of PS and EE are given in Table 5.9 and 5.10 respectively. Since the calculated F value was less than the tabulated F value for PDE and for PS (Bolton; 2004). It was concluded that the neglected terms did not significantly contribute in the prediction of PDE and PS. Hence, F-Statistic of the results of ANOVA of full and reduced model justified the omission of non-significant terms of eq 5.4 and 5.5. The goodness of fit of the model was checked by determination coefficient R^2 . Higher values of determination coefficients explains that above 86% variations were explained by model. A higher value of correlation coefficient (R) signifies excellent correlation between the independent variables.

Table 5.9 Analysis of Variance (ANOVA) of full and reduced models for PS of Lopinavir loaded NPs

		df	SS	MS	F	R	R2	Adj R2
Regression	FM	10	27460.13	2746.013	12.0476	0.939555	0.882763	0.80949
	RM	4	26234.1	6558.525	29.61008	0.918341	0.84335	0.814868
Residual	FM	16	3646.886	227.9304				
	RM	22	4872.919	221.4963				

$$SSE2 - SSE1 = 4872.919 - 3646.886 =$$

Numbers of parameters omitted = 6

MS of error full model = 227.93

F calculated = $(SSE2 - SSE1 / \text{No. of parameters omitted}) / \text{MS of error (FM)}$

F Tabulated = 2.74

Table 5.10 Analysis of Variance (ANOVA) of full and reduced models for EE of Lopinavir loaded NPs

		df	SS	MS	F	R	R2	Adj R2
Regression	FM	10	12398.93	1239.893	28.96011	0.97347	0.947644	0.914922
	RM	5	12193.88	2438.776	57.53921	0.965387	0.931972	0.915775
Residual	FM	16	685.0213	42.81383				
	RM	21	890.0765	42.38459				

$$SSE2 - SSE1 = 890.07 - 685.02 =$$

Numbers of parameters omitted = 5

MS of error full model = 42.81

F calculated = $(SSE2 - SSE1 / \text{No. of parameters omitted}) / \text{MS of error (FM)}$

F Tabulated = 2.85

Contour and Response Surface Plots

For PS, at fix level (-1) of X_1 , at all levels of X_2 and X_3 , particle size of less than 160 nm could be achieved. At fix level of X_2 , plot between X_1 and X_3 explains that X_1 has major influence on particle size, but particle size of 140 nm could be achieved at less than 0.5 level of X_1 , at all levels of X_3 . At -1 level of X_3 , lower particle size could be achieved at lower levels of both the factors, as both factors causes major influence on increase in particle size (Fig. 5.1).

Response surface plot at -1 level of X_1 shows that interaction effect of both the factors X_2 and X_3 causes least influence on increase in particle size. There is a linear relationship between the factors. At -1 level of X_2 , particle size shows a non linear relationship, X_1 having major influence on increase in particle size. X_3 causes only slight increase in particle size. At -1 level of X_3 , Factor X_1 and X_2 has non linear relationship on particle size. Major increase in particle size occurs as the both factors have synergistic effect on increase in particle size (Fig. 5.2).

For EE, at fix level (-1) of X_1 , Contour graph between X_2 and X_3 explains that PLGA concentration has major influence on entrapment, but Pluronic F 68 concentration negate the effect of PLGA concentration, even at highest level of PLGA and lowest level of surfactant, EE of 50 % could achieved. At Fix level of X_2 , Contour plot between X_1 and X_3 shows that Drug concentration overpowers the effect of surfactant concentration, Higher entrapments (greater than 80%) could be achieved at 0.5 to 1 level of X_1 , at all levels of X_3 . At Fix level of X_3 , Contour plot between X_1 and X_2 shows the synergistic effect of X_1 and X_2 leading to increase in entrapment at all levels. Highest entrapment above 90% could be achieved at 1.0 level of X_1 and lowest -1 level of X_2 (Fig. 5.3).

Response surface plot between X_1 and X_2 , at fix level of X_3 shows synergistic effect of both factors on increase in entrapment. While plot between X_1 and X_3 shows pulling effect of X_1 , overpowering the effect of X_3 , leading to higher entrapment.

While plot between X_2 and X_3 shows the antagonistic effects of each other at fix level of X_1 (Fig. 5.4).

Thus, higher entrapment could be achieved even at less PLGA concentration by increasing the concentration of Lopinavir, at optimum concentration of surfactant.

In all, Contour and response plots could explain the relationship of all the factors, in all possible combinations on both the responses.

Optimized Formulation

From the results, the optimum levels of independent variables were screened by multiple regression analysis. Our desirability criteria were maximum entrapment with minimum particle size (less than 200 nm). Since PS and EE were taken into consideration simultaneously, the batch with smallest particle size of 126.6 ± 4.16 nm exhibited EE near to 22 % (at $X_1 = -1$, $X_2 = -1.0$, $X_3 = -1.0$) while that with highest EE of 95.7 ± 2.43 % produced particle size greater than 200 nm (at $X_1 = 1$, $X_2 = 0.0$, $X_3 = -1$). Hence, the optimum formulation with **EE $93.03 \pm 1.27\%$ and particle size 142.16 ± 2.13 nm** found at 1.0, -1, and -1 levels of X_1 , X_2 and X_3 respectively was selected. The above formulation was selected based on our desirability criteria and also we wanted a formulation with good entrapment at lowest concentration of polymer. The drug loading for optimized formulation was found to be $25.11 \pm 3.141\%$.

Check Point Analysis

Three check points were selected as shown in the Table 5.11. When both experimentally obtained and theoretically computed PS and EE values were compared using student's 't' test, the difference was found to be non significant ($p > 0.05$) in both cases. The normalized error ($NE = [\sum\{(Pre - Obs)/Obs\}^2]^{1/2}$) between the observed and predicted values was found to be minimum. This confirms the utility of contour plots and established polynomial equation for both PS and EE in the preparation of Lopinavir loaded PLGA NPs.

Table 5.11 Check point analysis, t test analysis and normalized error determination for Lopinavir loaded NPs

Checkpoint batches with their predicted and measured values of PS and EE							
Batch No.	X_1	X_2	X_3	PS (nm)		EE (%)	
				Observed	Predicted	Observed	Predicted
1	-1(0.2%)	0.0 (2%)	0.5(62.5mg)	152.63	148.94	44.86	45.72
2	0(0.4%)	0.0 (2%)	0.5(62.5 mg)	167.96	163.23	66.86	67.10
3	1 (0.6%)	-1(1%)	0.0 (50 mg)	189.24	184.4	88.43	87.03
$t_{\text{calculated}}$				0.0068		0.8956	
$t_{\text{tabulated}}$				2.9199		2.9199	
Normalized Error				0.04507		0.0251	

5.10.3 Optimization of Cryoprotectant for Lyophilization of Lopinavir Loaded Nanoparticles

The optimized Nanoparticle formulation was lyophilized using lyophilizer (Heto Drywinner, Vaccubrand, Denmark). Different cryoprotectants (Trehalose dehydrate, Mannitol and Sucrose) were used at different ratios to find out optimum concentration of cryoprotectant which showed minimum increment in particle size. The initial particle size of the formulation was 142.16 ± 2.13 nm. The results are shown in Table 5.12. It was observed that sucrose showed minimum particle size at 1:1 ratios indicating its suitability in maintaining particle size of Lopinavir loaded nanoparticles after lyophilization. Thus, this formulation was considered for further studies.

Table 5.12 Optimization of cryoprotectant for Lopinavir loaded NPs

Cryoprotectant	Particle size after lyophilization (nm)	PDI
Trehalose dehydrate (1:1)	294.4 ± 12.8	0.343
Trehalose dehydrate (1:2)	396.7 ± 21.6	0.299
Trehalose dehydrate (1:3)	425.65 ± 11.3	0.329
Sucrose (1:1)	184.9 ± 14.2	0.198
Sucrose (1:2)	259.6 ± 54.8	0.222
Sucrose (1:3)	296.3 ± 76.2	0.256
Mannitol (1:1)	827.5 ± 22.8	0.654
Mannitol (1:2)	628.23 ± 14.3	0.781
Mannitol (1:3)	437.2 ± 12.2	0.452

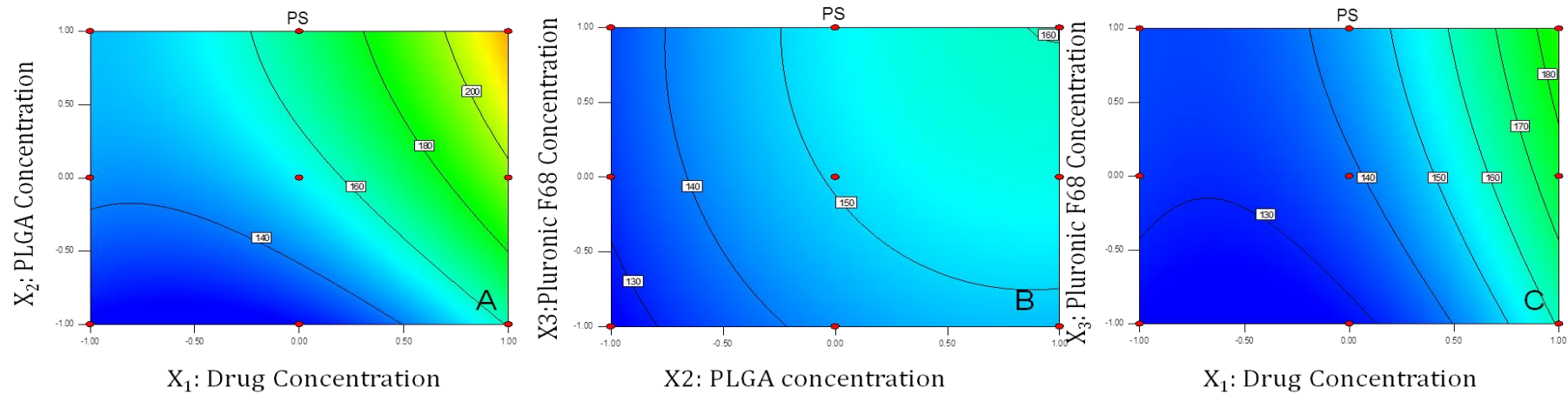


Fig. 5.1 Contour plot showing the effect of (a) X_1 versus X_2 (at -1 level of X_3), (b) X_2 versus X_3 (at -1 level of X_1), (c) X_1 versus X_3 (at -1 level of X_2) on PS of Lopinavir loaded NPs

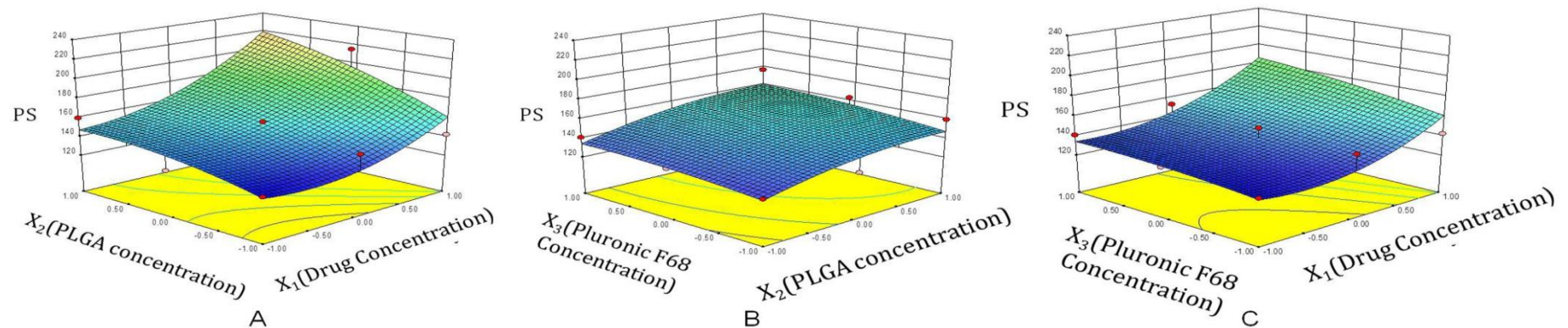


Fig. 5.2 Response plot showing the effect of showing effect of (a) X_1 versus X_2 (at -1 level of X_3), (b) X_2 versus X_3 (at -1 level of X_1), (c) X_1 versus X_3 (at -1 level of X_2) on PS of Lopinavir loaded NPs

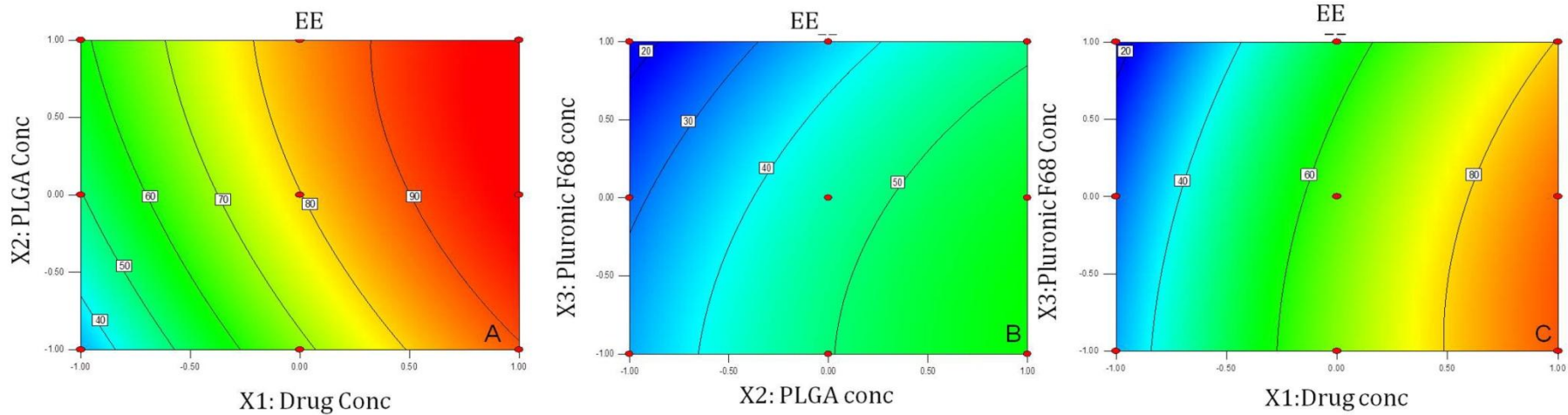


Fig. 5.3 Contour plot showing the effect of showing effect of (a) X_1 versus X_2 (at -1 level of X_3), (b) X_2 versus X_3 (at -1 level of X_1), (c) X_1 versus X_3 (at -1 level of X_2) on EE of Lopinavir loaded NPs

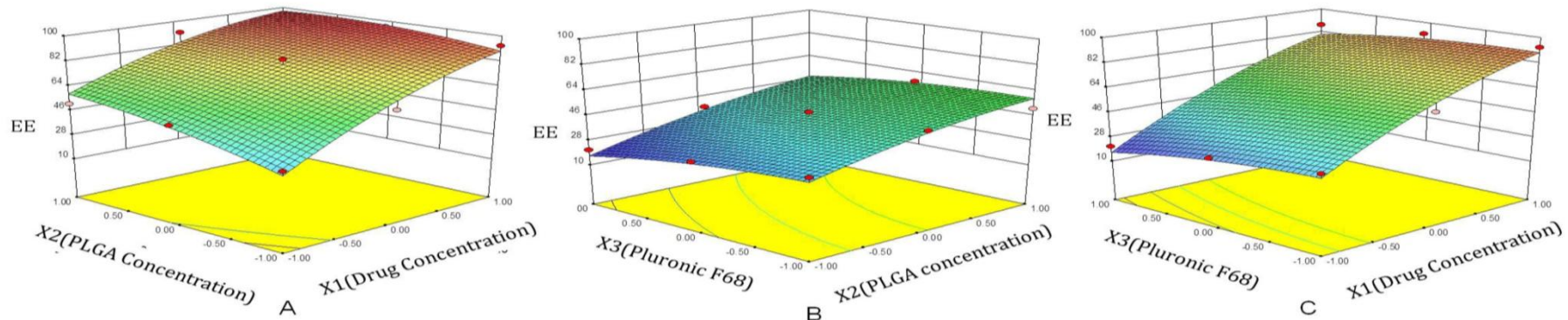


Fig. 5.4 Response plot showing the effect of showing effect of (a) X_1 versus X_2 (at -1 level of X_3), (b) X_2 versus X_3 (at -1 level of X_1), (c) X_1 versus X_3 (at -1 level of X_2) on EE of Lopinavir loaded NPs

5.10.4 Characterization of Optimized Lopinavir Loaded Nanoparticles

The zeta potential of optimized batch was found to be -27.2 ± 2.423 mV. Negative value of zeta was due to negative charge of PLGA. The high negative zeta potential will prevent aggregation and increase stability. Moreover, negatively charged particles will be uptaken by the Peyer's patches and then translocated to the systemic circulation (Florence, 2004). TEM images (Fig. 5.5) of nanoparticles revealed discrete round structures without aggregation. Nanoparticles were seen as matrix structures with particle sizes below 200 nm, similar to particle size distribution graph obtained with Malvern Zetasizer (Fig. 5.6).

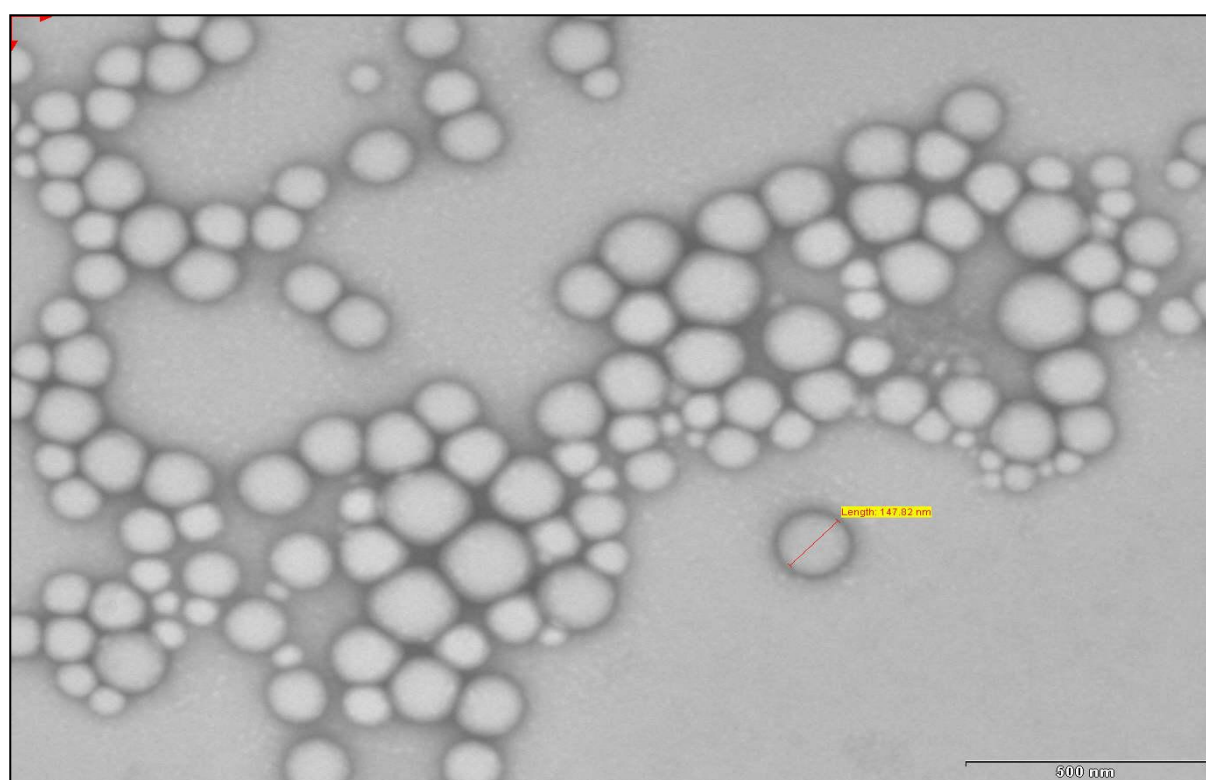


Fig. 5.5 TEM images of Lopinavir loaded Nanoparticles

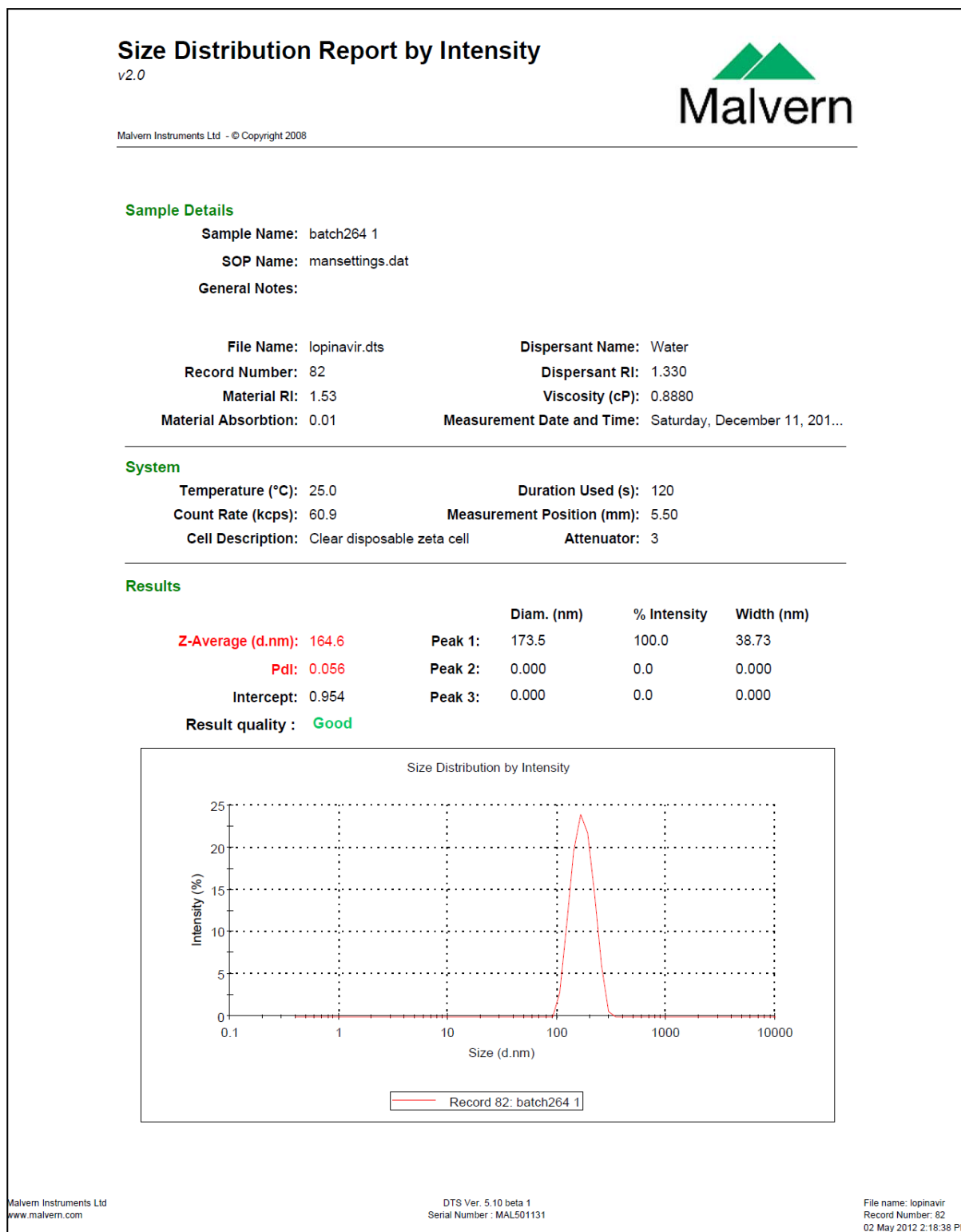


Fig. 5.6 Particle size distribution of Lopinavir loaded NPs by Malvern Zetasizer

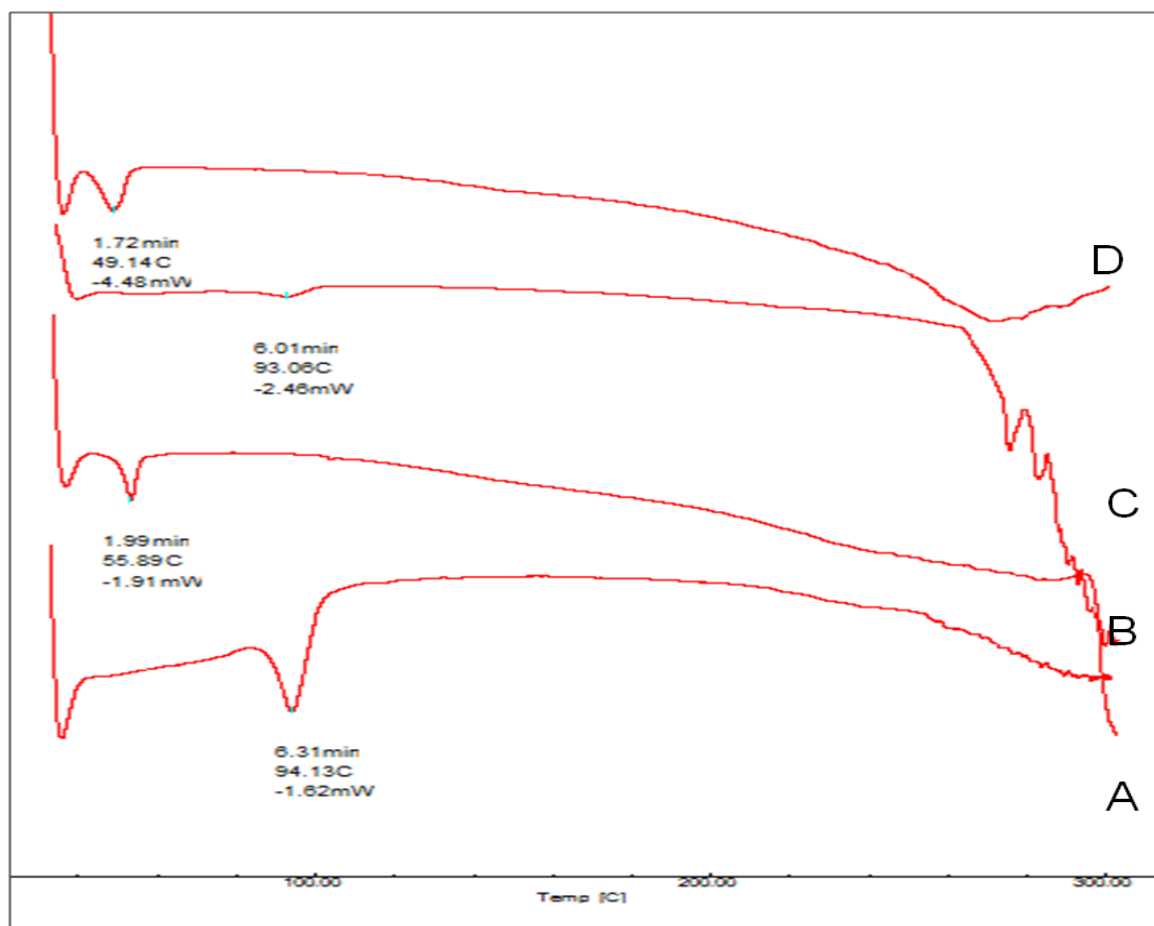


Fig. 5.7 DSC thermograms of Lopinavir (A), PLGA (B), Physical mixture of Lopinavir/PLGA (C) and Lopinavir loaded PLGA NPs

DSC thermograms of Lopinavir, PLGA, physical mixture (Lopinavir and PLGA) and Lopinavir loaded NPs are shown in Fig. 5.7. Pure Lopinavir showed an endothermic peak at 94.13 °C showing the crystalline structure of drug, while PLGA showed endothermic peak at 51.06 °C corresponding to its glass transition temperature (Montgomery; 2004). Physical mixture of drug and PLGA showed endothermic peaks of PLGA and drug respectively at 51.06°C and 94.13°C indicating the compatibility between them. There was no peak of Lopinavir in the thermogram of NPs indicating the amorphization of drug in the polymer matrix.

FTIR spectra of pure drug, PLGA, physical mixture and drug loaded NPs are shown in Fig. 5.8. The PLGA spectrum showed characteristic peaks at 3509.60 cm^{-1} , at 3128 cm^{-1} and 1749.87 cm^{-1} indicative of O-H stretching, C-H stretch and C=O stretching (due to alpha-substitution) respectively (Eason; 2007). The Lopinavir spectrum shows peaks at

1659 cm^{-1} , 3376 cm^{-1} . Physical mixture of Lopinavir and PLGA has retained the distinct peaks of Lopinavir (3376 cm^{-1} and N-H 1659 cm^{-1}) as well as PLGA (3509 cm^{-1} , 3128 cm^{-1}). Lopinavir loaded NPs showed absence of peak at 3376 cm^{-1} corresponding to Lopinavir but peak corresponding to PLGA was present confirming the encapsulation of drug in PLGA matrix.

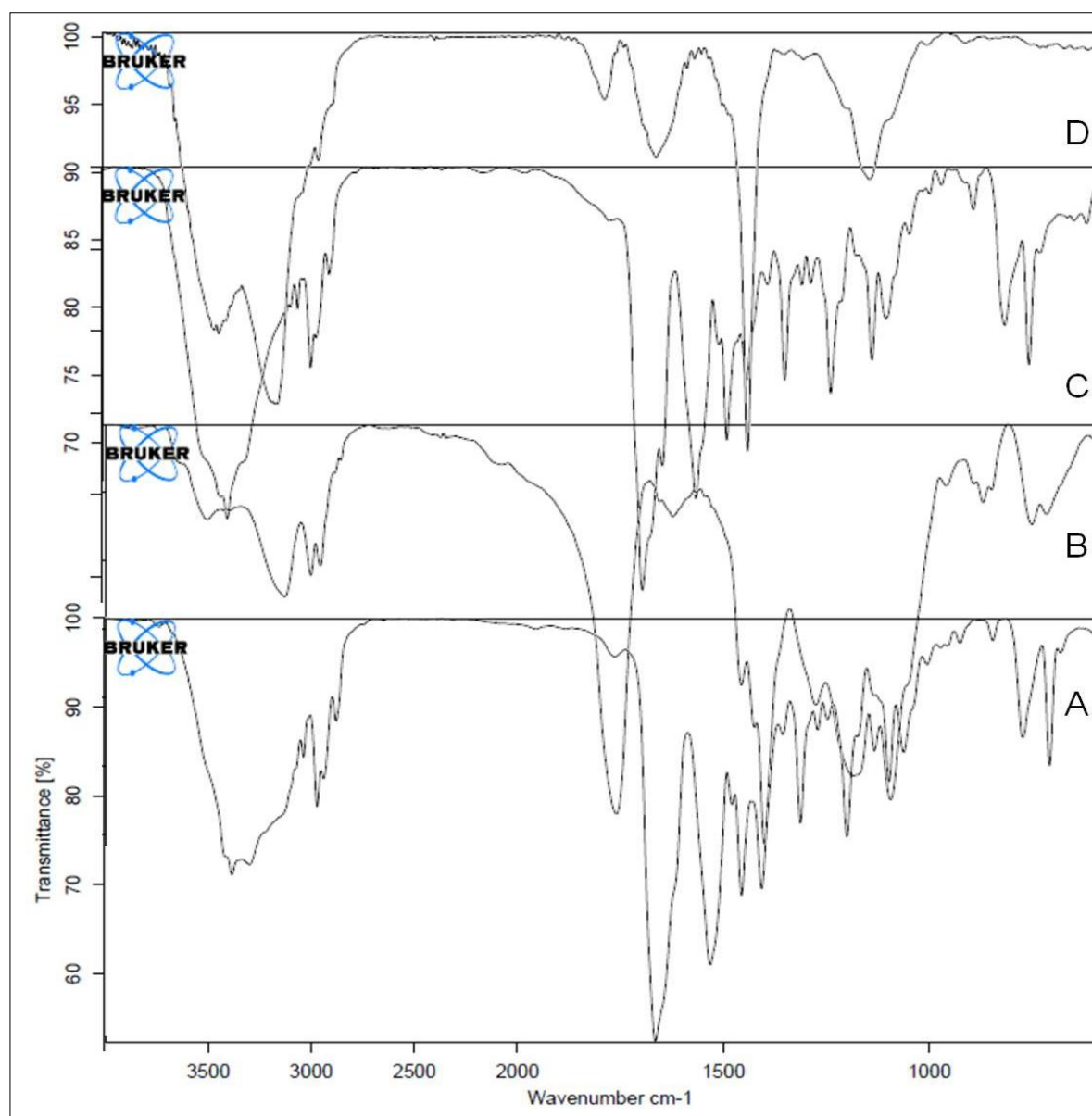


Fig. 5.8 FTIR spectra of Lopinavir (A), PLGA (B), Physical mixture of Lopinavir and PLGA (C) and Lopinavir loaded PLGA NPs (D)

Stability Studies

The stability of Lopinavir loaded NPs in terms of drug content and particle size distribution was monitored for 3 months at 2-8 °C and RT (25-30 °C). The NPs showed physical stability for a period of 3 months at refrigerated conditions. The particle size and drug content of the NPs at different time interval is given in Table 5.13. At RT, Particle size was increased and drug content was found to be decreased. It was found that no significant difference was observed in the particle size and drug content of NPs after 3 months at refrigerated conditions indicating its suitability for storage at 2 -8°C.

Table 5.13 Stability of Lopinavir loaded NPs at RT and (2-8°C)

Sr. No	Time	Drug content (%) (2-8 °C)	Drug content (%) (RT)	Particle size (nm) (2-8 °C)	Particle size (nm) (RT)
1	Initial	99.8±1.1	99.8±1.4	142.14±12.6	142.14±8.3
2	1 month	99.6±1.3	96.5±2.4	142.67±10.2	168.3±13.5
3	2 months	99.6±1.0	89.4±2.5	144.16±15.3	190.6±14.2
4	3 months	98.9±1.6	78.8±3.4	146.6±13.9	204.1±8.9

5.11 References

- ❖ Adinarayana K and Ellaiah P. Response surface optimization of the critical medium components for the production of alkaline protease by a newly isolated *Bacillus* sp. *J Pharm Pharm Sci*, 5, 2002, 272-278.
- ❖ Bolton S and Bon C. (1997). *Pharmaceutical statistics: practical and clinical applications*, third edn (New York: Marcel Dekker Inc).
- ❖ Bolton SBC. (2004). *Pharmaceutical Statistics: Practical and Clinical Applications*, 4th edn (USA: Marcel Dekker).
- ❖ Box GEP, Wilson KB. On the experimental attainment of optimum conditions. *J Roy Stat Soc*, 13, 1951,1-45.
- ❖ Derringer G and Suich R. Simultaneous optimization of several response variables. *Journal of Quality Technology* 12, 1980, 214-219.
- ❖ Eason, R. (2007). *Pulsed Laser Deposition of Thin Films: Applications-Led Growth of Functional ...* (New Jersey: Wiley publishers).
- ❖ Fessi H, Puisieux F, Devissaguet JP, Ammoury N, and Benita S. Nanocapsule formation by interfacial polymer deposition following solvent displacement. *International Journal of Pharmaceutics* 55,1989, R1-R4.
- ❖ Joshi SA, Chavhan SS, Sawant KK. Rivastigmine-loaded PLGA and PBCA nanoparticles: Preparation, optimization, characterization, in vitro and pharmacodynamic studies. *Eur J Pharm Biopharm.* 76, 2010, 189–199.
- ❖ Kashi TS, Eskandarion S, Esfandyari-Manesh M, Marashi SM, Samadi N, Fatemi SM, Atyabi F, Eshraghi S, and Dinarvand R. Improved drug loading and antibacterial activity of minocycline-loaded PLGA nanoparticles prepared by solid/oil/water ion pairing method. *Int J Nanomedicine*, 7, 2012, 221-234.
- ❖ Mak K W Y, Yap M G S and Teo W K. Formulation and optimization of two culture media for the production of tumour necrosis factor- β in *Escherichia coli*. *Journal of Chemical Technology and Biotechnology* 62, 1995, 289-294.
- ❖ Montgomery, D. C. (2004). *Introduction to factorial designs.*, (New York: John Wiley and Sons).
- ❖ Prot M, Heripret L, Cardot-Leccia N, Perrin C, Aouadi M, Lavrut T, Garraffo R., Long-term treatment with lopinavir-ritonavir induces a reduction in peripheral adipose depots in mice. *Antimicrob Agents Chemother*, 50, 2006, 3998–4004.

CHAPTER 6

IN-VITRO AND EX-VIVO RELEASE STUDIES

6.1 *In vitro* Release Studies

In vitro release studies are quality control tool to assess batch to batch product release performance. The *in vitro* release test also used to approve minor changes in formulation. Because of the labour and expense involved with assessing *in vivo* drug release, *in vitro* drug release studies at 37°C (physiological temperature) have gained increasing importance. *In vitro* drug release test may be used as an alternative for *in vivo* bioequivalence tests in order to minimize unnecessary tests with humans (Donato et al; 2008).

An *in vitro* release profile reveals fundamental information on the structure (e.g., porosity) and behaviour of the formulation on a molecular level, possible interactions between drug and polymer, and their influence on the rate and mechanism of drug release and model release data (Costa and Sousa Lobo; 2001, D'Souza and DeLuca; 2006). Such information facilitates a scientific and predictive approach to the design and development of sustained delivery systems with desirable properties.

6.2 *Ex vivo* Diffusion Studies

Compared to *in vivo* absorption studies, *in vitro* studies using tissue segments can be used to study the permeability of the compounds. As it is relatively easier, more rapid and, in the case of segmental absorption studies, avoids complicated surgery and maintenance of surgically prepared animals; it has the potential to reduce animal usage since a number of variables can be examined in each experiment. Also, it Provides insights into mechanism (e.g., carrier-mediated vs. passive), routes (e.g., transcellular vs. paracellular), and segmental differences (e.g., small vs. large intestine) involved in transepithelial transport. These studies are analytically simpler because compounds are being analyzed in an aqueous buffer solution as opposed to whole blood or plasma (Ronald et al; 1996).

6.3 Kinetics of Drug Release

In order to examine the release mechanism of drug from the prepared nanoparticles, the results of the *in vitro* release study was examined according to following equations as described by Costa and Sousa Lobo (2001).

A) ZERO ORDER RELEASE

$$Q = K_0t$$

Where, Q = amount of drug release at time t

K_0 = Zero order release constant

t = time

Regression value of plot of amount of drug release versus time t gives the idea of release mechanism. R^2 value nearer to 1 indicating zero order release (Costa et al; 2001 and (Kikkinides et al; 1998)

B) FIRST ORDER RELEASE EQUATION

$$\ln(100-Q) = \ln Q_0 - K_1t$$

Where, Q = amount of drug release at time t

K_1 = First order release constant

The regression coefficient (R^2) value obtained from the log % ARR (Amount Remaining to Release) versus time, nearer to 1 indicates first order release. (Costa et al; 2001)

The dosage forms containing water soluble drugs in porous matrices follow this model (Mulye and Turco; 1995).

C) HIGUCHI SQUARE ROOT OF TIME EQUATION:

$$Q = K_h t^{1/2}$$

Where, Q = Amount of drug release at time t

K_h = Higuchi square root of time release constant

The regression co-efficient of percentage drug release versus square root of time nearer to one indicates anomalous release (Higuchi; 1961, Higuchi; 1963). This relation can be used to describe the drug dissolution from several types of modified release pharmaceutical dosage forms, as in the case of some transdermal systems (Costa et al; 1996) and matrix tablets with water soluble drugs.

D. KORSMEYER-PEPPAS EQUATION

$$\text{Log } (M_t/M_\infty) = \text{Log } K + n \text{ Log } t$$

Where, M_∞ = total drug release after infinite time.

M_t/M_∞ = fractional drug release at time t .

K = kinetic constant incorporating structural and geometrical characteristic of the drug/polymer system (devices).

n = diffusion exponents that characterizes the mechanism of drug release

t = time

Graph of log % drug release versus log time was plotted, n value was obtained and release kinetic was determined using following specifications. This type of drug release is controlled by combination of polymer swelling, erosion and diffusion through the hydrated matrix (Diffusion and chain relaxation).

- The value of $n < 0.5$ or $n = 0.5$ indicating fickian diffusion
- The value of n between 0.5 to 1 ($0.5 < n < 1$) indicating non-fickian release
- The value of $n = 1$, indicating the Zero order release or case 2 transport
- The value of $n > 1$, indicating the Super case 2 transport

This model is generally used to analyze the release of pharmaceutical polymeric dosage forms, when the release mechanism is not well known or when more than one type of release phenomena could be involved (Korsmeyer et al;1983, Peppas;1985).

E) HIXON-CROWELL CUBE ROOT MODEL

$$\text{Kinetic equation: } 3\sqrt[3]{Q_0} - 3\sqrt[3]{Q_t} = K_H C \cdot t$$

$$\text{Plot: } 3\sqrt[3]{Q_0} - 3\sqrt[3]{Q_t} \text{ vs. } t$$

Where, Q_0 = initial concentration of drug present

Q_t = amount of drug release at time t

K_H is the kinetic constant for distribution from constantly changing surface area observed in slow dissolving tablets (Receding geometry) (Hixon and Crowell; 1931, Niebergall et al; 1963).

6.4 Gemcitabine HCl loaded NPs

6.4.1 *In vitro* release studies through dialysis membrane

In vitro release of Gemcitabine HCl from PLGA NPs was evaluated by the dialysis bag diffusion technique reported by Yang et al (1999). Dialysis membrane (LA-401, molecular weight cut off: 12000 Dalton; Himedia, India), 150µm in thickness was used as an artificial membrane for preliminary *in vitro* studies because of simplicity, homogeneity and uniformity. The membrane was activated by washing it in running tap water for 3-4 h, followed by treatment with 0.3%w/v of sodium sulphide solution at 80 C for 1 min. Then, it is washed with hot water at 60° C for 2 min followed by acidification with 0.2% sulphuric acid for 2-3 min. Finally it was rinsed with hot water at 60° C for 2-3 min.

The diffusion medium consisted of pH-7.4 Phosphate buffer. The diffusion membrane was soaked in PBS of pH-7.4 over night. The nanoparticulate dispersion equivalent to 5 mg of Gemcitabine HCl was placed in the dialysis bag, which was sealed at both ends. The dialysis bag was immersed in 25 ml of the receptor phase, which was stirred at 100 rpm and maintained at $37 \pm 2^\circ\text{C}$. The receptor compartment was covered to prevent the evaporation of release medium. Samples were withdrawn at regular time intervals (0, 2, 4, 6, 12, 24, 48, 72, 96, 120 h), and the same volume was replaced by fresh release medium. The acceptor phase was changed every day to maintain sink condition. The samples were analyzed by HPLC (Shimadzu, Kyoto, Japan) at 269 nm as per method reported earlier for EE determination. All the experiments were performed in triplicate, and the average values were taken. The Kinetic analysis of the release data was done by fitting to different exponential equations such as zero order, first order, Higuchi, and Peppas- Korsmeyer to characterize the release.

6.4.2 *Ex vivo* diffusion studies through stomach and intestinal segment

Ex vivo studies using stomach and intestinal segment was performed to study the permeability and absorption of formulation. All animal experiments were approved by Committee for the Purpose of Control and Supervision of Experiments on Animals (CPCSEA), Ministry of Social Justice and Empowerment, Government of India, New Delhi, India. Male wistar rats (250-300g) were sacrificed by euthanasia. Stomach and a

part of intestine were isolated and washed with HBSS. The isolated organs were washed and cleansed with their respective solutions. 2ml of the nanoparticulate suspension (4mg/ml) was filled into the stomach which was tied at both the ends. The tissue was placed in an organ bath with continuous aeration at 37°C. The receptor compartment (organ tube) was filled with 30 ml of 0.1N HCl. At predetermined intervals of time (15, 30, 60, 90 and 120 min), aliquots were withdrawn from the receptor compartment. Fresh buffer was used to replenish the receptor compartment. The samples were analysed by HPLC at 269nm. The percent diffusion of drug was calculated and plotted graphically. After 2h, to mimic the *in vivo* gastric emptying, the solution from the stomach was transferred to the intestine which was then tied at both ends. The receptor compartment was replaced with PBS pH 6.8 and the tissue was mounted in the organ tube. At predetermined time intervals (30, 60, 120, 180, 240 min), aliquots were withdrawn from the receptor compartment. Fresh buffer was used to replenish the receptor compartment. The percent diffusion of drug was calculated and plotted graphically. The similar study was also performed using plain drug solution. The diffusion studies across the tissues were performed in triplicate. (Modi et al; 2013)

6.5 Lopinavir loaded NPs

6.5.1 *In vitro* drug release studies

In vitro release of Lopinavir from PLGA Nanoparticles was evaluated by the dialysis bag diffusion technique. The diffusion medium consists of pH 6.8 phosphate buffer containing Brij 35 (0.785 gm in 50 ml) (Indian Pharmacopoeia; 2007). The nanoparticulate dispersion equivalent to 1 mg of Lopinavir was placed in the dialysis bag, which was sealed at both ends. The dialysis bag was immersed in 70 ml of the receptor compartment, which was stirred at 50 rpm and maintained at $37 \pm 2^\circ\text{C}$. The receptor compartment was covered to prevent the evaporation of release medium. Samples were withdrawn at regular time intervals (0, 1, 2, 4, 6, 12, 24, 30, 48, 60, 72, 96 and 120 h), and the same volume was replaced by fresh release medium. The acceptor phase was changed everyday to maintain sink condition. The samples were analyzed by HPLC using C18 column (250 X 4.0 mm, 5 μ) at 210 nm using Acetonitrile: water (60:40) as mobile phase. Similar procedure was followed for Plain drug suspension.

6.5.2 *Ex vivo* drug release studies

Ex vivo drug release studies were performed on stomach and intestine segments. All animal experiments were approved by Committee for the Purpose of Control and Supervision of Experiments on Animals (CPCSEA), Ministry of Social Justice and Empowerment, Government of India, New Delhi, India. Male wistar rats (250-300g) were sacrificed by euthanatia. Stomach and a part of intestine were isolated. The isolated organs were washed and cleansed with their respective solutions. The study was conducted for 6h to simulate gastric emptying time. 2ml of the nanoparticulate suspension was filled into the stomach which was tied at both the ends. The tissue was placed in an organ bath with continuous aeration at 37°C. The receptor compartment (organ tube) was filled with 30 ml of 0.1N HCl containing Brij 35. At predetermined intervals (15, 30, 60, 90 and 120 min.) of time, aliquots were withdrawn from the receptor compartment. Fresh buffer was used to replenish the receptor compartment. The 10 microlitre of sample was injected and analyzed by HPLC (Shimadzu, Japan) using C18 column (250 X 4.0 mm, 5 μ) at 210 nm using Acetonitrile : Buffer (KH₂PO₄) (60:40) as mobile phase. The percent diffusion of drug was calculated against time and plotted graphically. After 2h, to mimic the in vivo gastric emptying, the solution from the stomach was transferred to the intestine which was then tied at both ends [4]. The receptor compartment was replaced with PBS pH 6.8 containing Brij 35 and the tissue was mounted on the organ tube. At predetermined intervals (30, 60, 120, 180, 240, 300 and 360 min.) of time, aliquots were withdrawn from the receptor compartment. Fresh buffer was used to replenish the receptor compartment. The samples were analyzed by HPLC using C18 column (250 X 4.0 mm, 5 μ) at 210 nm using Acetonitrile:Buffer (KH₂PO₄) (60:40) as mobile phase. The percent diffusion of drug was calculated and plotted graphically. The study was also performed using plain drug suspension following the above mentioned procedure(Alex et al; 2011).

6.6 Results and discussion

6.6.1 *In vitro* drug release studies of Gemcitabine HCl loaded NPs

In vitro drug release studies from plain drug solution and Gemcitabine HCl loaded NPs is shown in Fig. 6.1. The plain drug solution released more than 40 % drug in 1h and within 4h nearly 100% of drug was released. Whereas, from drug loaded NPs 25.96±3.254 % of drug was released in 4h, followed by 56.89±4.259% in 24h and 98.2±2.371% of drug released at the end of 120h (Table 6.1). The data obtained from *in vitro* drug release studies were fitted to different kinetic equations; r^2 values calculated are given in Table 6.3. The data from *in vitro* drug release studies followed Korsmeyer–Peppas model and fickian diffusion. The regression coefficient of the plot of $\log M_t/M_\infty$ versus $\log t$ for NPs was found to be 0.995 with value of release exponent (n) as 0.37 which was less than 0.5 (Peppas; 1985)

Table 6.1 *In vitro* drug release data for plain drug solution and Gemcitabine HCl loaded NPs by using dialysis technique

Time (h)	Plain drug solution % Drug release ± SD	Nanoparticles % Drug release ± SD
0	0	0
1	42.9±3.860	16.32±2.471
2	59.8±2.450	21.5±3.145
4	76.48±1.789	25.96±3.254
6	96.4±4.786	32.76±2.415
8		38.53±1.863
12		42.63±2.469
24		56.89±4.212
48		69.79±3.456
72		76.48±4.360
96		89.45±3.321
120		98.23±2.371

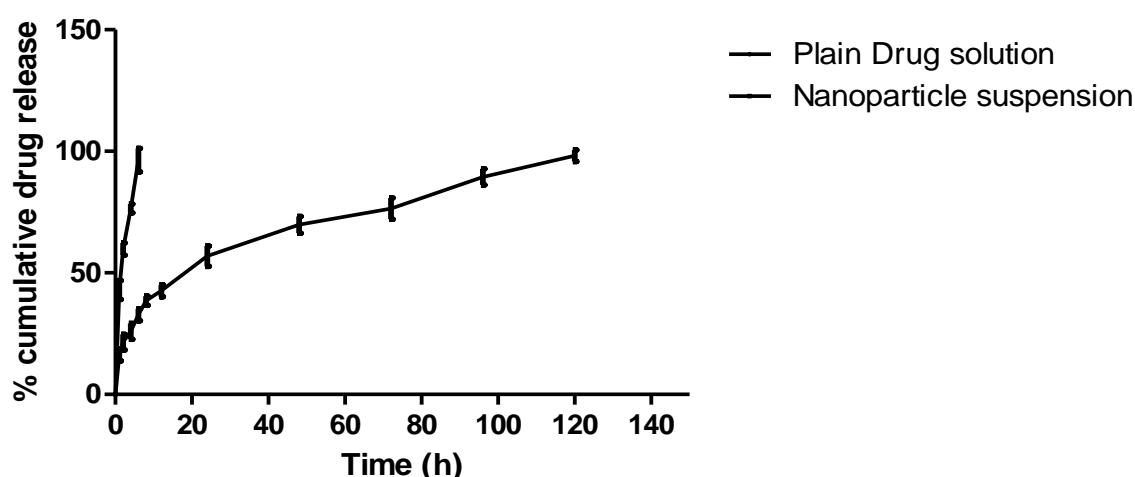


Fig. 6.1 *In vitro* release profile of Gemcitabine HCl loaded NPs and plain drug solution in PBS 7.4 through dialysis membrane

6.6.2 *Ex vivo* drug release studies of Gemcitabine HCl loaded NPs

The *ex vivo* drug release from plain drug solution showed (Table 6.2, Fig. 6.2) that nearly complete drug was released in the stomach, whereas from NPs only 10% of drug was released in the stomach and most of the drug was released in the intestinal segment. This indicates that the NPs will be reaching to the Peyer’s patches. At the end of 6h study nearly 40 % of drug was released. Because of entrapment of drug inside NPs, release from NPs was sustained. The drug release from NPs in stomach and intestine followed Korsmeyer-Peppas model and fickian diffusion (0.985 and n=0.486) (Table 6.3).

Table 6.2 *Ex vivo* drug release data for plain drug solution and Gemcitabine HCl loaded NPs in rat stomach and intestine segment

Time (h)	Plain drug solution % Drug release ± SD	Nanoparticle suspension % Drug release ± SD
0.0	0.00	0.00
0.5	32.45±2.54	8.56±1.963
1.0	56.89±3.25	12.46±3.123
2.0	90.56±2.86	18.69±2.543
3.0		22.36±2.348
4.0		28.63±2.786
5.0		34.83±3.412
6.0		41.86±1.967

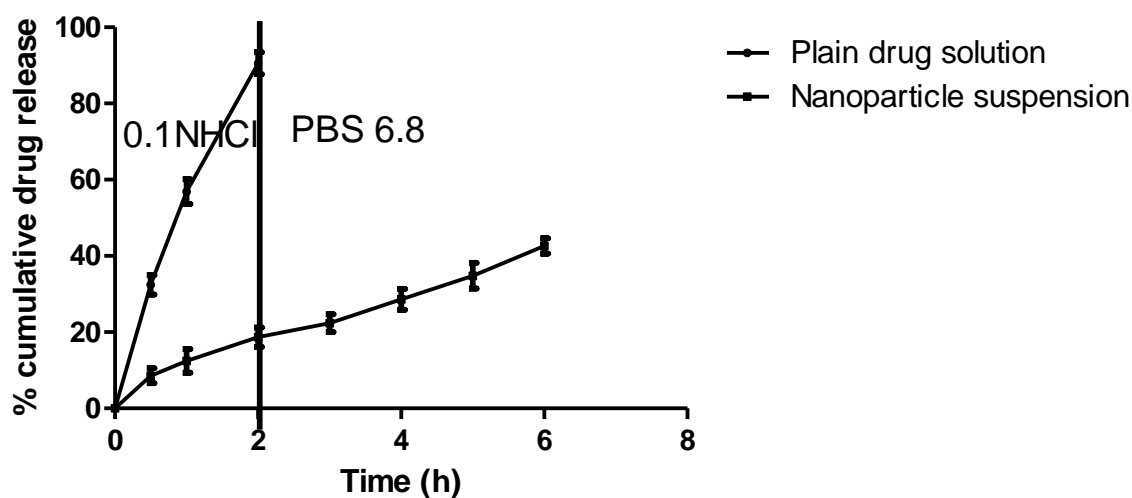


Fig. 6.2 *Ex vivo* drug release studies of Gemcitabine HCl loaded PLGA NPs and plain drug solution in rat stomach (at 0.1 N HCl for 2h) and intestine (PBS 6.8 for 4h).

Table 6.3 Release kinetics of Gemcitabine HCl loaded NPs

Formulation	<i>R</i> ² values			
	Zero order	First order	Higuchi Model	Korsmeyer-Peppas model
Gemcitabine HCl nanoparticles				
<i>In vitro</i> kinetics	0.8686	0.9198	0.9788	0.9954
<i>Ex vivo</i> kinetics	0.9796	0.983	0.9622	0.9914

6.6.3 *In vitro* drug release studies for Lopinavir loaded NPs

In vitro drug release studies for Lopinavir loaded NPs and plain drug suspension are shown in Table 6.4 and Fig. 6.3. Plain drug suspension released nearly 50 % drug in initial 3 hour, where as drug release from NPs was near to 10 % in initial 3 hour reaching to 50 % in 24 h and near to 100 % in 120 hours. The drug release was sustained from the NPs due to entrapment of drug inside the polymer matrix due to nanoprecipitation. Data of drug release from plain drug suspension and Lopinavir loaded NPs were fitted to various kinetic models to assess the mechanism of drug

release. Drug release from Lopinavir loaded PLGA NPs followed the Korsmeyer peppas model and non fickian diffusion with r2 value of .9969 and n =0.647 (Table 6.6).

Table 6.4 *In vitro* drug release profile of Lopinavir loaded NPs and plain drug suspension in PBS 7.4 by dialysis technique

Time (h)	Plain drug suspension % Drug release \pm SD	Nanoparticle suspension % Drug release \pm SD
0.	0.000	0.00
1.	15.13 \pm 1.997	5.21 \pm 2.096
2.	26.43 \pm 1.698	7.34 \pm 1.032
3.	48.83 \pm 2.352	8.56 \pm 2.127
4.	68.56 \pm 3.698	15.23 \pm 1.752
6.	78.06 \pm 1.736	24.75 \pm 2.056
8.	90.29 \pm 2.141	27.69 \pm 2.568
12.	97.23 \pm 2.687	34.86 \pm 2.048
24.		50.43 \pm 3.588
36.		62.35 \pm 2.021
48.		73.65 \pm 3.567
60.		81.78 \pm 2.986
72.		86.96 \pm 3.184
96.		93.24 \pm 3.124
120.		98.52 \pm 2.980

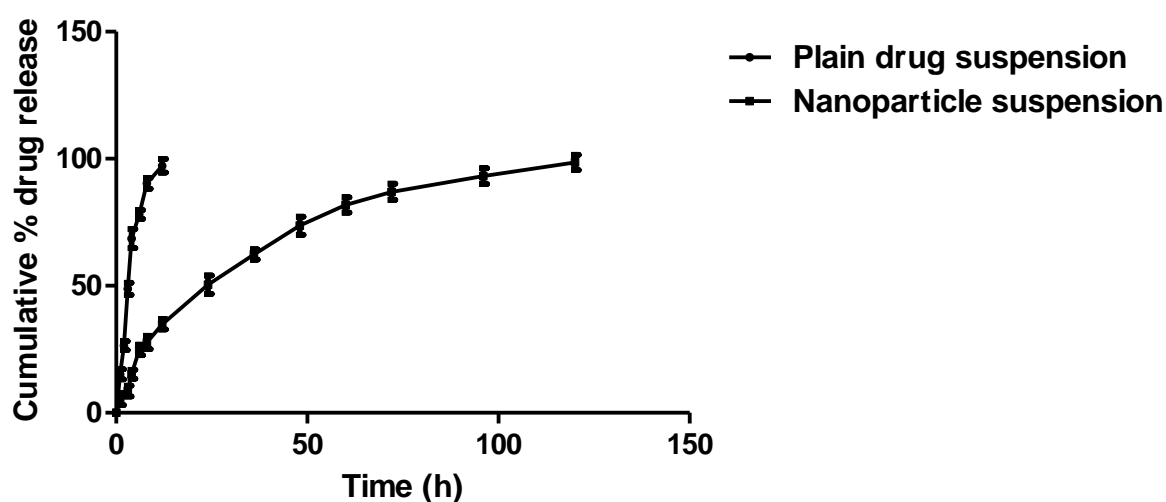


Fig. 6.3 *In vitro* drug release profile of Lopinavir loaded NPs and plain drug solution in PBS 7.4 by dialysis technique

6.6.4 Ex vivo drug release studies for Lopinavir loaded NPs

The *ex vivo* drug release studies from plain drug solution and Lopinavir loaded nanoparticulate formulation was studied in rat stomach and intestine for eight hours to simulate gastric emptying. Initially, the drug release was checked in stomach segment for 2 hours. From plain drug solution, more than 60% of drug was released in stomach, whereas drug release from NPs was slow and sustained; nearly 13% of drug was released in stomach in initial hours (Table 6.5, Fig. 6.4). Only small fraction of drug was released before the NPs could reach to the Peyer's patches in intestine, indicating the protection of drug inside NPs in stomach and availability of more drug at M cells. Low aqueous solubility of drug entrapped in polymeric system was the reason for slow release. When data of drug release from NPs were fitted to various kinetic equations, the drug release from NPs was found to be diffusion controlled as it follows Korsmeyer peppas model with r^2 value of 0.9652 and mechanism of drug release was non fickian diffusion ($n=0.879$) (Table 6.6).

Table 6.5 Ex vivo drug release studies of Lopinavir loaded NPs in rat stomach (0.1N HCl for 2 h) and intestinal segment (PBS 6.8 for 6h)

Time (h)	Plain drug solution % Drug release \pm SD	Nanoparticle suspension % Drug release \pm SD
0.00	0.000	0.00
0.25	16.930 \pm 2.265	3.51 \pm 2.698
0.50	36.930 \pm 3.200	4.73 \pm 1.956
1.00	49.750 \pm 2.563	7.45 \pm 2.753
1.50	59.860 \pm 4.623	9.97 \pm 3.456
2.00	71.560 \pm 3.412	12.56 \pm 2.063
2.50	78.940 \pm 2.573	18.56 \pm 3.563
3.00	86.940 \pm 2.212	24.63 \pm 3.214
4.00	91.630 \pm 3.430	36.12 \pm 2.269
5.00		45.86 \pm 1.897
6.00		48.63 \pm 2.321
7.00		49.56 \pm 2.256
8.00		51.45 \pm 2.053

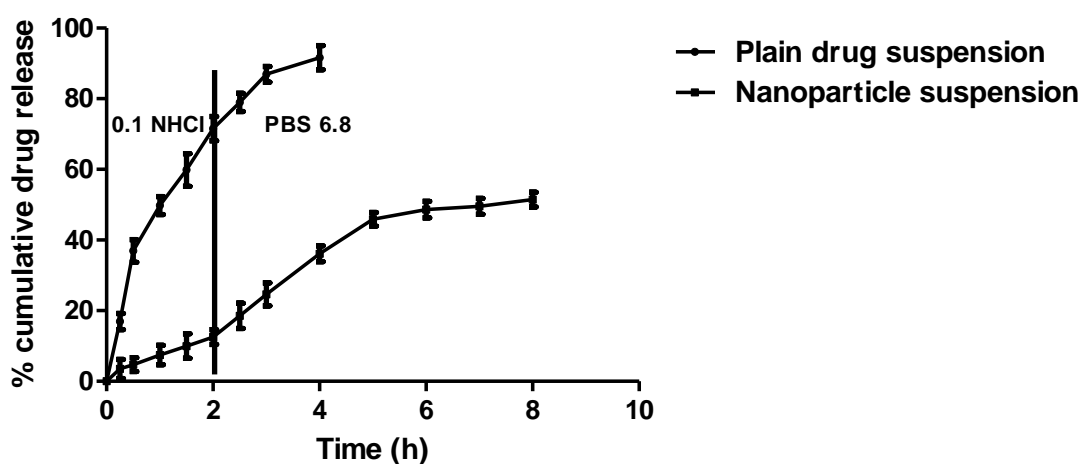


Fig. 6.4 Ex vivo drug release studies of Lopinavir loaded NPs in rat stomach (0.1N HCl for 2 h) and intestinal segment (PBS 6.8 for 6h)

Table 6.6 Release Kinetics of Lopinavir loaded PLGA NPs

Formulation	<i>R</i> ² values			
	Zero order	First order	Higuchi Model	Korsmeyer-Peppas model
Lopinavir Nanoparticles				
<i>In vitro</i>	0.8761	0.9781	0.982	0.9969
<i>Ex vivo</i>	0.9521	0.9629	0.9197	0.9652

6.7 References

- ❖ Alex A, Paul W, Chacko AJ and Sharma CP. Enhanced delivery of lopinavir to the CNS using Compritol-based solid lipid nanoparticles. *Ther Deliv*, 2, 2011, 25-35.
- ❖ Costa P and Sousa Lobo JM. Modeling and comparison of dissolution profiles. *Eur J Pharm Sci*, 13, 2001, 123-133.
- ❖ D'Souza SS and DeLuca PP. Methods to assess in vitro drug release from injectable polymeric particulate systems. *Pharm Res*, 23, 2006, 460-474.
- ❖ Donato EM, Martins LA, Froehlich PE and Bergold AM. Development and validation of dissolution test for lopinavir, a poorly water-soluble drug, in soft gel capsules, based on in vivo data. *J Pharm Biomed Anal*, 47, 2008, 547-552.
- ❖ Higuchi T. Rate of release of medicaments from ointment bases containing drugs in suspension. *J Pharm Sci*, 50, 1961, 874-875.
- ❖ Higuchi T. Mechanism of sustained-action medication. Theoretical analysis of rate of release of solid drugs dispersed in solid matrices. *J Pharm Sci*, 52, 1963, 1145-1149.
- ❖ Hixson AW, Crowell JH. Dependence of reaction velocity upon surface and agitation. *Ind Eng Chem*, 23, 1931, 923-931.
- ❖ Indian Pharmacopoeia. Indian Pharmacopoeial Commission; Ghaziabad, INDIA, 2, 2007, 697-700.
- ❖ Kikkinides ES, Charalambopoulou GC, Stubos AK, Kanellopoulos NK, Varelas CG, and Steiner CA. A two-phase model for controlled drug release from biphasic polymer hydrogels. *J Control Release*, 51, 1998, 313-325.
- ❖ Korsmeyer RW, Gurny R, Doelker E, Buri P, and Peppas NA. Mechanisms of potassium chloride release from compressed, hydrophilic, polymeric matrices: effect of entrapped air. *J Pharm Sci*, 72, 1983, 1189-1191.
- ❖ Modi J, Joshi G, Sawant KK. Chitosan based mucoadhesive nanoparticles of ketoconazole for bioavailability enhancement: formulation, optimization, in vitro and ex vivo evaluation. *Drug Dev Ind Pharm*, 39, 2013, 540-547.
- ❖ Mulye NV, Turco SJ. A simple model based on first order kinetics to explain release of highly water soluble drugs from porous dicalcium phosphate dihydrate matrices. *Drug Dev Ind Pharm*, 21, 1995, 943-953.

- ❖ Niebergall P, Milosovich G, Goyan JE. Dissolution rate studies. II. Dissolution of particles under conditions of rapid agitation. *J Pharm Sci*, 52, 1963, 236–241.
- ❖ Peppas NA. Analysis of Fickian and non-Fickian drug release from polymers. *Pharm Acta Helv*, 60, 1985,110-111.
- ❖ Ronald TB, Philip LS, Wilson G. Models for Assessing Drug Absorption and Metabolism, Methods for Evaluating Intestinal Permeability and Metabolism in vitro, *Pharmaceutical Biotechnology*, 8, 1996, 13-34.
- ❖ Yang SC, Lu LF, Cai Y, Zhu JB, Liang BW, and Yang CZ. Body distribution in mice of intravenously injected camptothecin solid lipid nanoparticles and targeting effect on brain. *J Control Release*, 59,1999, 299-307.

CHAPTER 7

CELL LINE STUDIES

7.1 Cell Line Studies

At early stages of development, cell cultures are usually preferred to whole animal studies. Prediction of *in vivo* absorption based on *in vitro* methodology may help reduce the volume of necessary clinical investigations. Cell monolayers have been widely employed for studying the cellular uptake and cytotoxicity of delivery systems. They present many advantages, including easy to culture and studies can be performed within a controlled environment. In many cases a significant correlation between the studies performed on *in vitro* cell monolayers and *in vivo* human studies has been observed. Hence, *in vitro* studies can be used as predictive tools for estimating the fate and activity of the delivery system in the actual human body (Tavelin et al; 2003). Cell culture techniques predominantly employing Caco-2 cell lines have been established in the last decade as a screening and study tool of intestinal absorption. Easy handling, reproducible experimental conditions, and a lack of inter individual variability led to establishment of cell culture models in many labs. For bio analytical purposes, tissue forming cell lines, such as the human epithelial cell line, Caco-2, can be employed at the single cell level or grown to confluent and polarized monolayers after differentiation. Full differentiation is a time-dependent process which also might affect the expression of receptor proteins, activity of brush border enzymes, the expression of certain integrins, or on ultra structural morphology, like the formation of microvilli at the apical cell membrane. Consequently, assays confirming complete differentiation are inevitable requirements.

7.2 Intestinal Transport and Uptake Studies Using Cell Lines

Intestinal absorption is required for a sufficiently high bioavailability of drugs administered by the peroral route. Intestinal absorption is rather complex process, which, despite recent advances, is fundamentally still poorly understood. Therefore, experimental verification of drug absorption remains a must in current industrial drug development practice. One of most frequently used and best established cell lines for the determination of drug permeability across intestinal membranes is the human colon adenocarcinoma cell line Caco-2, grown on semi-permeable filter supports. Caco-2 cells spontaneously differentiate into enterocyte-like cells and in spite of their colonic origin, a number of active transport mechanisms normally found in the absorptive enterocytes of the small intestine are present in this cell line. The use of the Caco-2 cell model

permits the investigation of simultaneous absorption routes at the same time (e.g. passive diffusion, active efflux, and metabolism).

The aim of this study was to evaluate the qualitative and quantitative cellular uptake, transport/ permeability of Gemcitabine HCl loaded NPs and Lopinavir loaded NPs in Caco 2 cell lines, intestinal barrier model. Tolerability and safety of Gemcitabine HCl loaded NPs and Lopinavir loaded NPs were assessed by cytotoxicity studies on Caco2 cells.

In vitro cytotoxicity studies were also performed on K562 leukemic cancer cell lines to assess the inhibition of tumour growth, for Gemcitabine HCl loaded NPs and plain drug solution

7.3 Materials

Gemcitabine HCl was obtained as a gift sample from Ranbaxy Pharmaceuticals Ltd, Gurgaon, India. Lopinavir was obtained as gift sample from Aurobindo Pharmaceutical Ltd, Hyderabad. Lucifer yellow was purchased from Sigma Aldrich, USA. Caco-2 cells and K562 cells were obtained from NCCS, Pune, INDIA. Dulbecco's eagle medium (DMEM), penicillin-streptomycin solution, Trypsin-EDTA solution, Fetal bovine serum (FBS) and Hank's balanced salt solution (HBSS) were purchased from Himedia, Mumbai, India. RPMI 1640 medium was purchased from Life Technologies Pvt Ltd., New Delhi, India. 12-well Transwell inserts were purchased from Nunc, Denmark. 6, 24 and 96 well plates were purchased from Costar, Corning, USA. Rhodamine B was purchased from Himedia, Mumbai. 6 Coumarin and MTT dye were purchased from Sigma Aldrich, Germany.

7.4 Methods

7.4.1 Cell Culture

Caco-2 cells (NCCS, Pune) of passages between 33 and 40 were used as *in vitro* gastrointestinal barrier for oral chemotherapy. Caco-2 cells were cultured in 25cm² tissue culture flasks. Dulbecco's MEM medium with 1.5mM L-glutamine, supplemented with 20% FBS, 1mM sodium pyruvate, 1.5 g/L of sodium bicarbonate and 1% penicillin-streptomycin solution was used as culture medium. Cells were cultured as a monolayer at 37°C in a humidified atmosphere containing 5% CO₂ and medium was replenished every alternate day (Zhou et al., 2005) .

K562 cells were used as model of *in vitro* anti proliferative studies on cancer cells. The cells were cultured in RPMI1640 supplemented with 2 mM L-glutamine, 10% fetal bovine serum and 1% penicillin-streptomycin solution in a humidified atmosphere of 5% CO₂. In all experiments, exponentially growing cells were used (Luo et al., 2010).

7.4.2 Method of Preparation for Rhodamine B Loaded PLGA NPs and 6-Coumarin Loaded PLGA NPs

Rhodamine B was used as hydrophilic model dye. PLGA NPs loaded with Rhodamine B were formulated by multiple emulsification/ solvent evaporation method reported for Gemcitabine HCl, by replacing half of drug with Rhodamine B.

6- Coumarin was used as hydrophobic model dye. 6-Coumarin loaded PLGA NPs were formulated by nanoprecipitation method adopted for Lopinavir, by replacing half of drug with 6-Coumarin.

7.4.3 Qualitative Uptake of Nanoparticles in Caco-2 cells by Confocal Microscopy

Caco-2 Cells were seeded on rounded cover slips in 6 well plates (Costar; IL, USA) for 24 h. On reaching 80 % confluence, the culture medium was replaced with HBSS. After 30 min of incubation at 37 °C, cell monolayers were washed three times with HBSS for 5 min at 37 °C. The cells were incubated with 100µl of 100µg/ml of Rhodamine B solution, 6-Coumarin solution, Rhodamine B loaded PLGA nanoparticles and 6-Coumarin loaded PLGA nanoparticles. To investigate time dependent uptake, cells were incubated with NPs and plain dye solution for 30 min, 60 min and 90 min. Then, cell monolayers were fixed with 70% ethanol solution for 20 min and rinsed with 1× HBSS. After rinsing, the nuclei were counterstained with DAPI for 3 min and rinsed again with 1× HBSS, mounted in glycerol and localization of Dye loaded NPs in cells was observed using Carl Zeiss confocal laser microscope (LSM 710) at (Rhodamine B: λ_{ex} 540 λ_{em} 625nm Red fluorescence; 6-Coumarin: λ_{ex} 430 λ_{em} 485 nm Green fluorescence) and DAPI: λ_{ex} 350 λ_{em} 470 (Blue fluorescence)). The images were analysed by Zen imaging software (Cartiera et al., 2009).

7.4.4 Quantitative uptake studies of 6-Coumarin loaded Nanoparticles in Caco-2 cells

Quantitative cellular uptake by flow cytometry

1×10^5 Caco-2 cells were seeded on 6-well plate and allowed to attach and grow. After 24 h, cells were incubated with 1 ml of medium containing 100 $\mu\text{g/ml}$ 6-Coumarin, 6-Coumarin loaded PLGA NPs for 1h, 2h and 4h. Cells treated with only medium were used as respective controls. At the end of the incubation period, the cell monolayer was washed three times with cold $1 \times$ PBS to eliminate excess of dye or NPs, which were not taken up by the cells and then trypsinized. Cells were collected by centrifugation at 400 g (Eppendorf centrifuge, USA) and analyzed in FACS (FACS Canto-II, BD Biosciences, San Jose, CA, USA) using software provided with the instrument (BD FACS Diva 6.1.3 software, BD Biosciences, San Jose, CA, USA) for total amount of NPs uptake by 10,000 cells.

7.4.5 Cytotoxicity studies (MTT assay)

Fresh MTT reagent was prepared. MTT reagent is available as a yellow colored powder. One hundred twenty five mg of this powder was accurately weighed and dissolved in 20 ml of deionized water. The solution was transferred in a 25 ml volumetric flask and the volume was made up to 25 ml using deionised water.

The *in vitro* cytotoxicity of Gemcitabine HCl loaded NPs, Lopinavir loaded NPs, plain Gemcitabine HCl solution and plain Lopinavir suspension was evaluated for Caco-2 cells and K562 cells using the MTT assay. The cells were cultured in 96-well plates at a seeding density of 1.0×10^4 cells/well for 48 h. Gemcitabine HCl was diluted with DMEM culture medium to different concentrations. Experiments were initiated by replacing the culture medium in each well with 150 μl of sample solutions (0.1, 1, 10, 100, 200 $\mu\text{g/ml}$) at 37 °C in the CO₂ incubator. After 4, 24 and 48 h of incubation, the medium was removed and 150 μl of MTT reagent (1 mg/ml) in the serum-free medium was added to each well. The plates were then incubated at 37 °C for another 4 h. At the end of the incubation period, the medium was removed and the intracellular formazan was solubilised with 150 μl DMSO and quantified by reading the absorbance at 590nm on a micro-plate multi-detection instrument, SpectraMax M2 with Soft Max® Pro (Molecular Devices Corporation Sunnyvale, CA, USA). The medium treated cells were used as

controls. Percentage of cell viability was calculated based on the absorbance measured relative to the absorbance of cells exposed to the negative control.

7.4.6 Transport/permeability across human intestinal epithelial cells (Caco-2 Cells)

Caco-2 cells at passage 39–45 cultured in Transwell® inserts (12565009, Nunc, Denmark) (0.4µ pore diameter, 1.13cm² area) were used for transport experiments after 21 days post seeding. Prior to the experiment, the inserts were washed twice and equilibrated for 30min with pre-warmed transport medium, Hank's balanced salt solution (HBSS), containing 25mM of HEPES, pH 7.4. As Gemcitabine HCl is hydrophilic, plain drug solution (200 µg /ml) was prepared in transport buffer. For Lopinavir, DMSO (1%) in transport buffer was used as co solvent. The integrity of the monolayers was checked by monitoring the permeability of the paracellular leakage marker, Lucifer yellow across the monolayers. The cell monolayers were considered tight enough for the transport experiments when the apparent permeability coefficient (*P_{app}*) for Lucifer yellow was less than 0.5×10⁻⁶cm/s. All transport studies were conducted at 37°C. The transport buffer containing 150 µl test compounds was added on the apical (0.5 ml) side while the basolateral side of the inserts contained 1.5 ml volume of transport buffer. After the incubation of 30, 60, 120, 180min and 240 min, aliquot of 100 µl was withdrawn from the receiver chambers and was immediately replenished with an equal volume of pre-warmed HBSS. The concentrations of the test compounds in the transport medium were immediately analyzed by a HPLC method as described earlier (Ina Hubatsch, 2007). The apical-to-basolateral permeability coefficient (*P_{app}* in cm/s) was calculated according to following equation:

$$P_{app} = \frac{dQ/dt}{A \cdot C_0 \cdot 60}$$

where *dQ/dt*—the amount of nanogel/drug in basolateral compartment as a function of time (mg/min), *A* — the monolayer area (cm²), *C₀* — the initial concentration of NPs/drug in apical compartment (mg/mL) (Senanayake et al., 2013) 2013). Here, initial drug concentration was 0.2 mg/ml, Area was 1.13cm².

7.5 Results and discussion

7.5.1 Qualitative cell uptake studies by confocal microscopy

Rhodamine B loaded NPs

The monolayers of Caco-2 cell lines were chosen as the model of intestinal barrier to assess the capability of hydrophilic drug molecule loaded NPs to transport. Caco2 cells unlike other cells grows in monolayers, show a cylindrical polarized morphology with microvilli on apical side. Caco 2 cells on differentiation express several morphological and biochemical characteristics of small intestinal enterocytes also has tight junctions between adjacent cells and express many small intestine enzymes and transporters (Kaustubh Kulkarni, 2011). For this, hydrophilic dye; Rhodamine B was chosen to play the role of drug. The nuclei were stained with DAPI. The micrograph images of nanoparticles confirmed the internalization of NPs in the Caco-2 cells. The NPs were observed as red fluorescence spots in the perinuclear regions (Fig. 7.1, 7.3, 7.5). The uptake of NPs in Caco-2 cells was time dependent, as reported by other researchers (Trapani et al., 2009). While the plain dye solution could not be internalized much, due to hydrophilic nature of the dye as evident from the Fig. 7.2, 7.4, 7.6. Although it was seen near boundary, but it had little uptake compared to NPs. The uptake efficiency of a hydrophilic drug can be significantly improved by encapsulating the drug in nanocarriers, as colloidal and surface properties of nanoparticles are different from native drug. Gemcitabine HCl is hydrophilic drug, hydrophilic drugs generally needs membrane transporters for entering the cells, while NPs could be taken by endocytosis(Arias et al., 2009). *In vitro* studies using cell monolayers suggest that PLGA nanoparticles are efficient drug carriers and can significantly enhance and sustain the cellular delivery of water soluble drugs.

6-Coumarin loaded NPs

The confocal micrograph images of 6 Coumarin solution and 6-Coumarin loaded NPs are shown in Fig. 7.7 to 7.12. 6-Coumarin was chosen as hydrophobic model dye. The micrograph images clearly show the enhanced uptake of NPs in Caco2 cells in comparison to plain dye solution, which explains enhanced endocytosis and absorption through the M cells of Peyer's patches of intestine, as hypothesized. Also, it could explain the bypass of p-glycoprotein pump efflux, which is a hindrance for absorption and cell uptake of most anticancer as well as anti HIV drugs.

7.5.2 Quantitative cell uptake studies of 6-Coumarin loaded NPs

Relative extent of uptake of 6-Coumarin loaded PLGA NPs in comparison to plain dye solution was analysed by FACS analysis. The shift of peak for florescent intensity clearly shows a significantly higher uptake and internalization for PLGA NPs (Fig. 7.13, 7.14).

The fluorescence intensity increased gradually with the incubation time and so also the uptake of NPs indicating time dependent uptake of NPs. Enhanced therapeutic activity for the drug can be correlated by enhanced uptake of carrier system in Caco 2 cells leading to greater absorption through oral GALT. Mean fluorescence intensity for Coumarin loaded NPs was significantly higher than the plain dye solution at all time points. Time dependent uptake studies for 4h were done to simulate intestinal emptying time. As the incubation time was increased from 1h to 4h, the mean fluorescence intensity was significantly increased. Mean fluorescence intensity (MFI) for NPs was doubled from 1h to 4h. Coumarin loaded NPs has 2.1 fold higher MFI at 1h, which increased to 3.6 fold to 6.4 fold higher MFI than plain dye solution at the end of 4h. This clearly showed a significantly higher uptake as compared to plain dye solution. Also, uptake was time dependent, as intensity was increased with time.

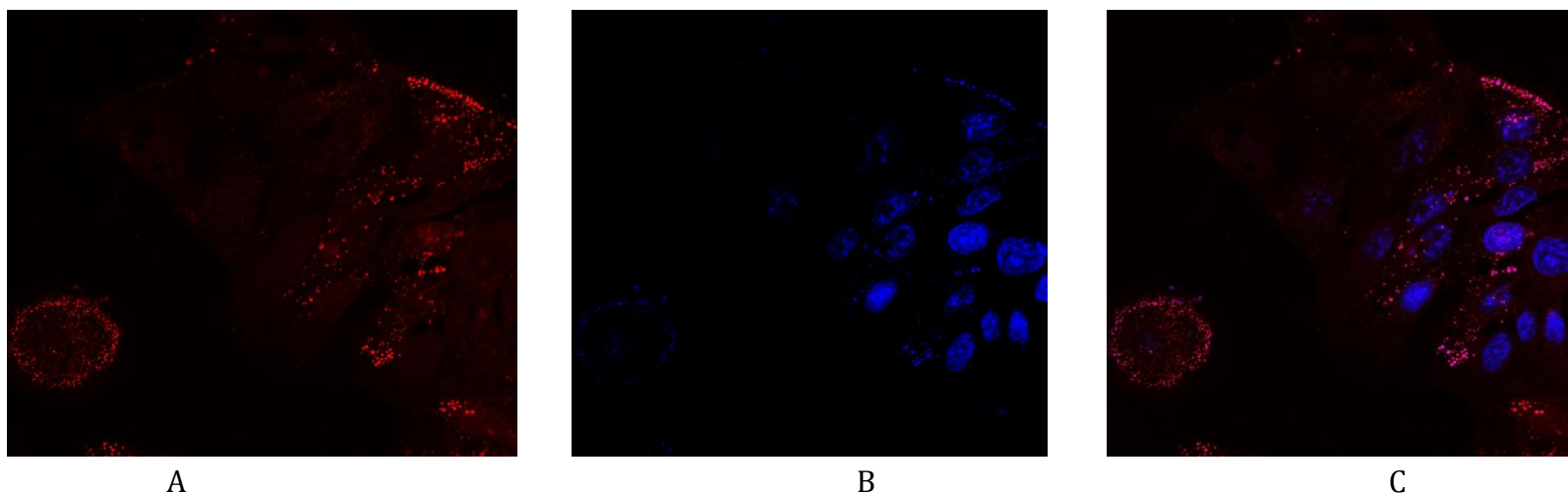


Fig. 7.1 Rhodamine B loaded NPs at 30 min in Caco-2 cells (A) NPs (B) DAPI stained nuclei (C) Overlapped image showing internalization of NPs in cells

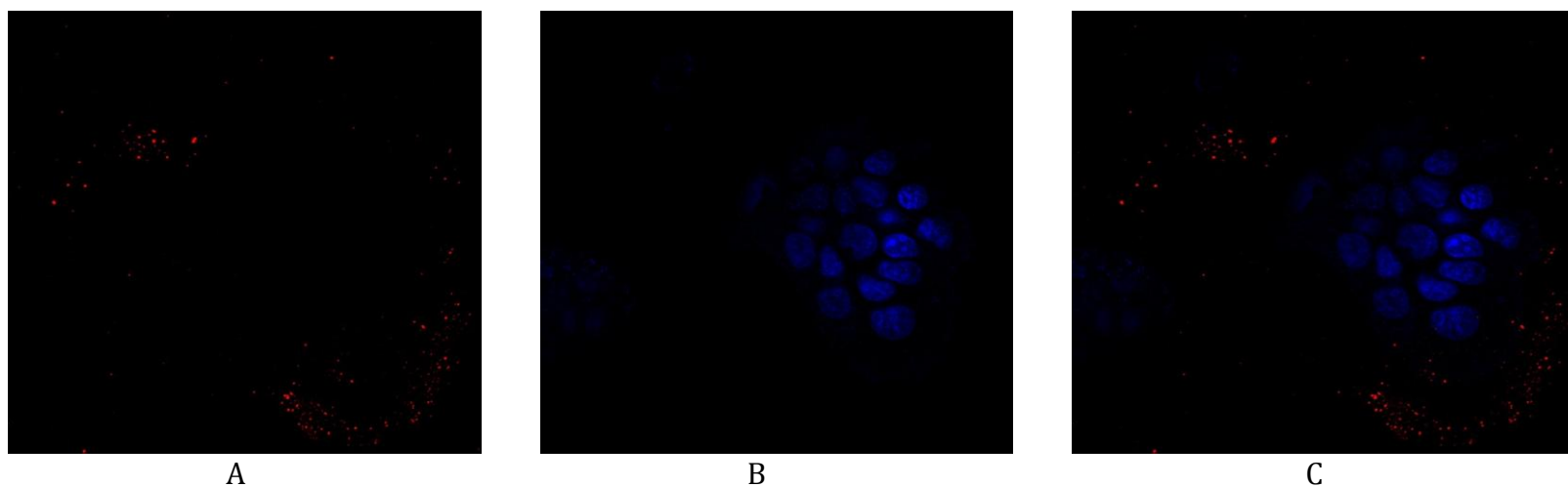


Fig. 7.2 Rhodamine B solution at 30 min in Caco-2 cells (A) Dye solution (B) DAPI Stained nuclei (C) Overlapped image showing no internalization

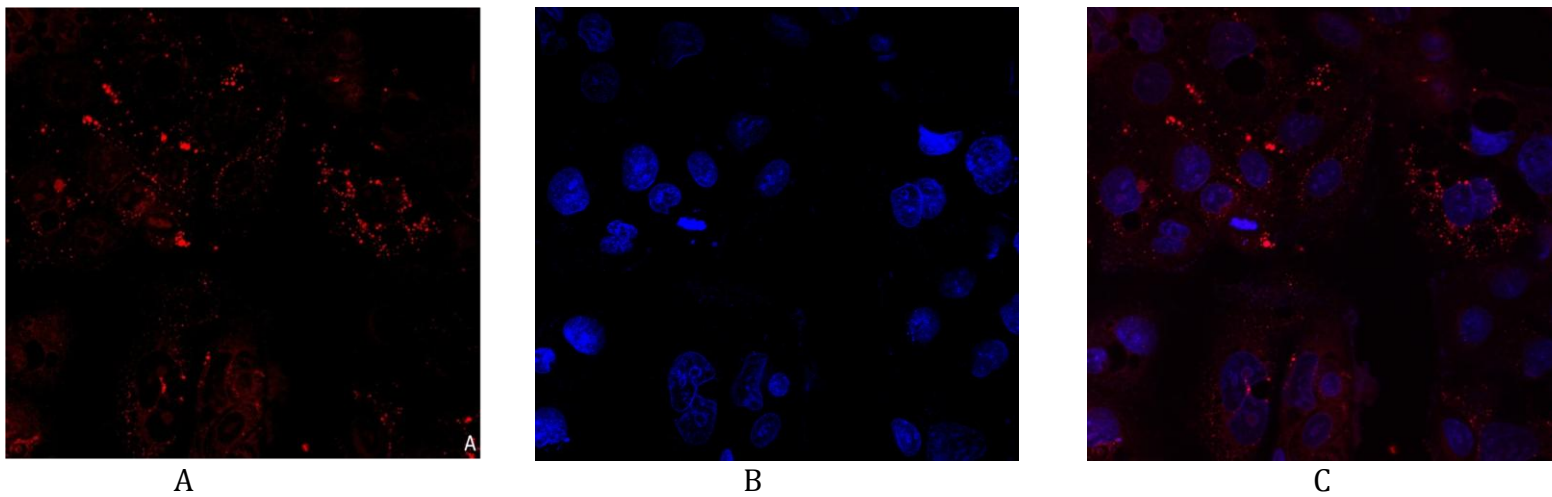


Fig. 7.3 Rhodamine B loaded NPs at 60 min in Caco-2 cells; (A) NPs (B) DAPI stained nuclei (C) Overlapped image showing internalization of NPs in cells

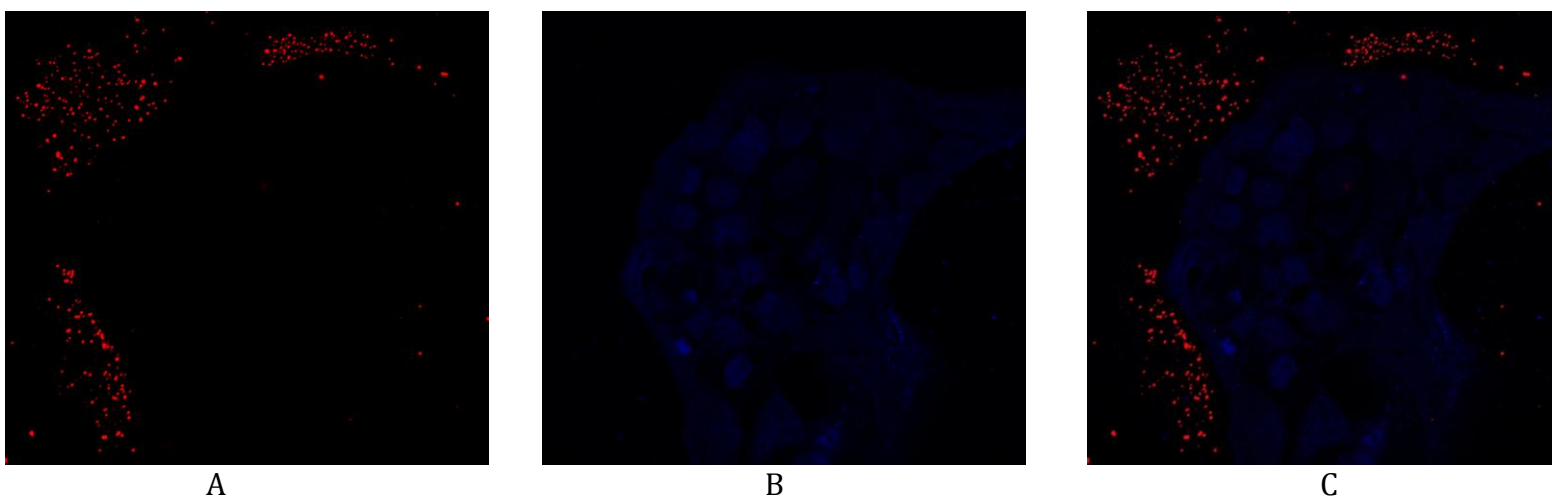


Fig. 7.4 Rhodamine B solution at 60 min in Caco-2 cells (A) Dye solution (B) DAPI Stained nucleus (C) Overlapped image showing no internalization

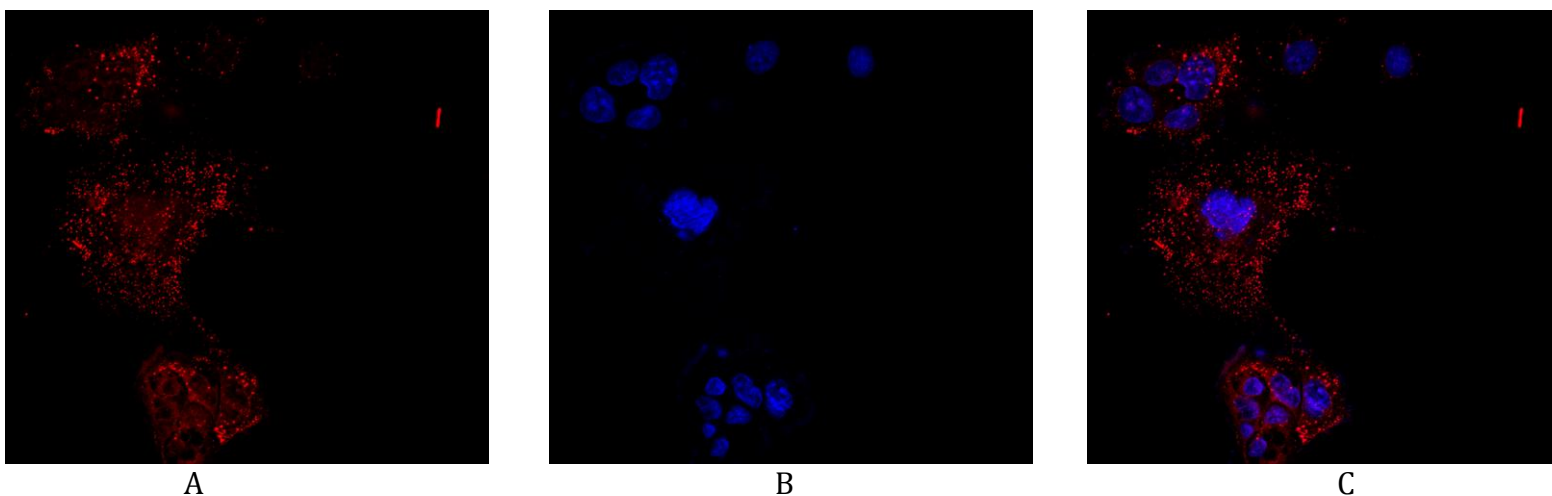


Fig. 7.5 Rhodamine B loaded NPs at 90 min in Caco-2 cells; (A) NPs (B) DAPI stained Nuclei (C) Overlapped image showing internalization of NPs in cells

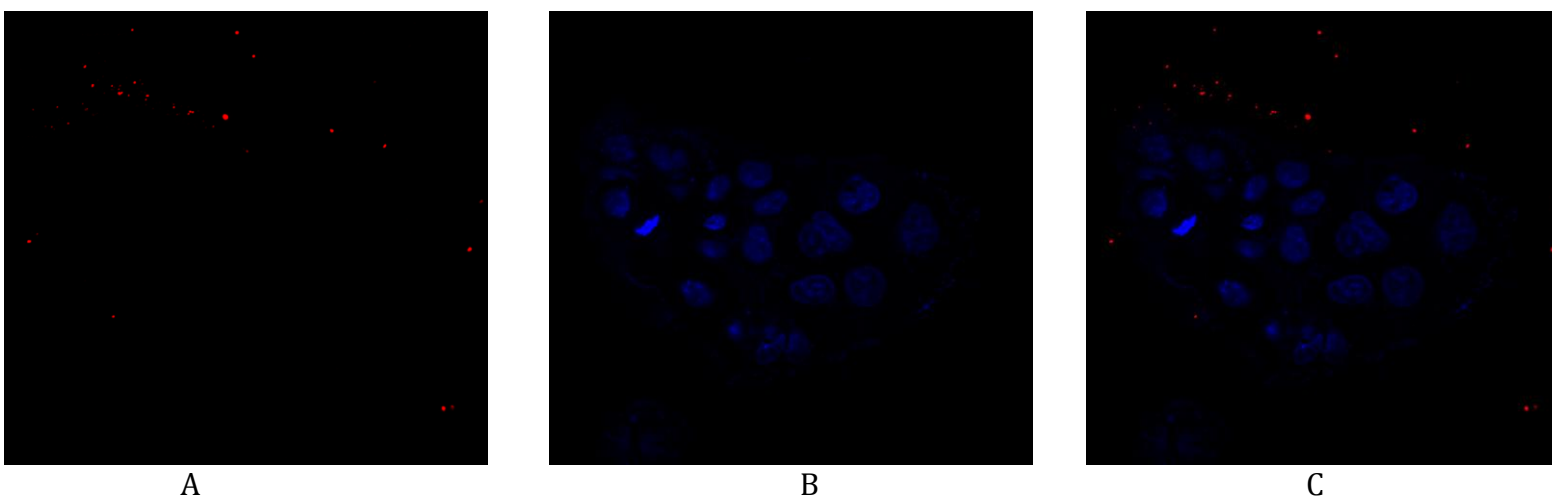


Fig. 7.6 Rhodamine B solution at 90 min in Caco-2 cells; (A) Dye solution (B) DAPI Stained nucleus (C) Overlapped image showing no internalization

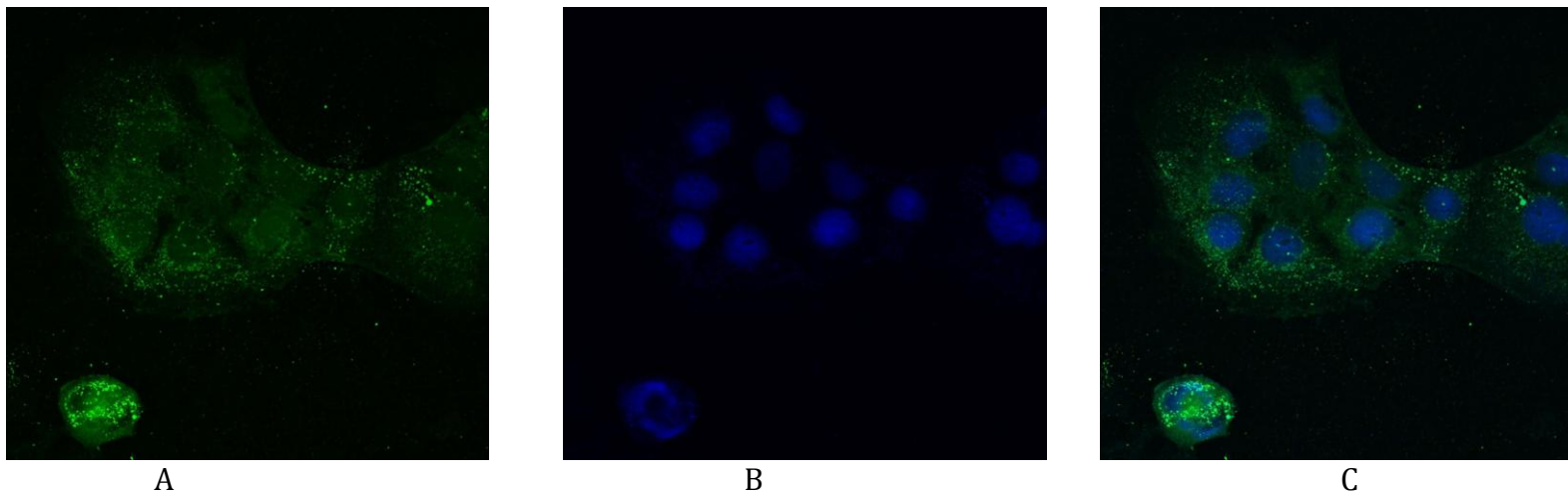


Fig. 7.7 6-Coumarin loaded NPs at 30 min in Caco-2 cells; (A) NPs (B) DAPI stained nuclei (C) Overlapped image showing internalization of NPs in cells

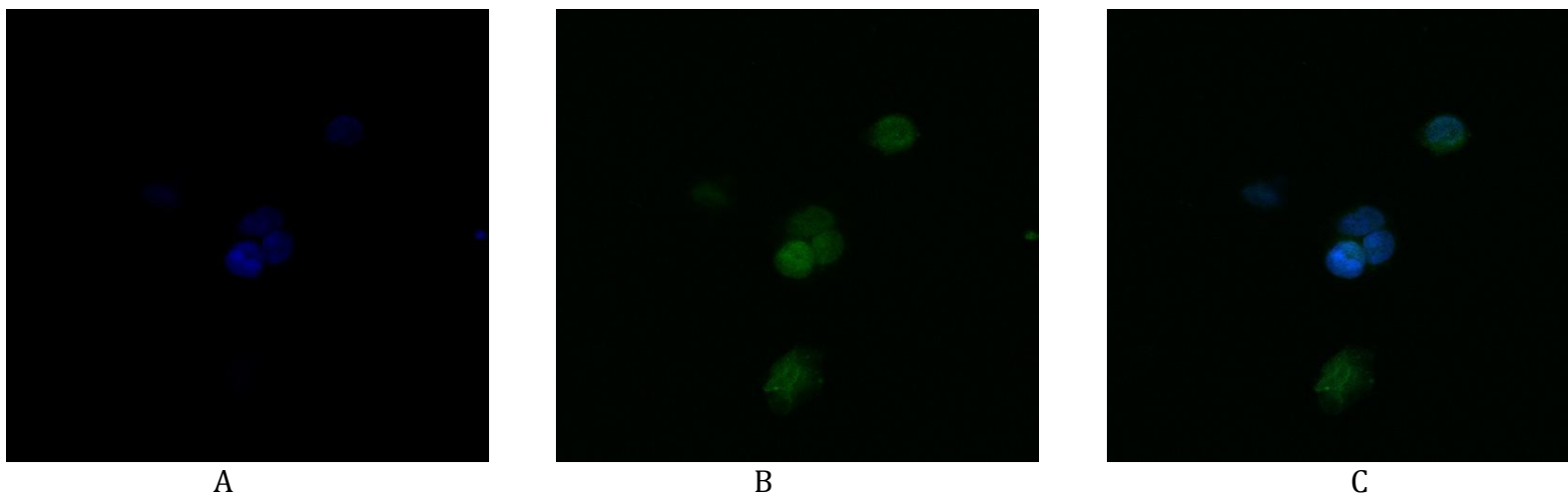
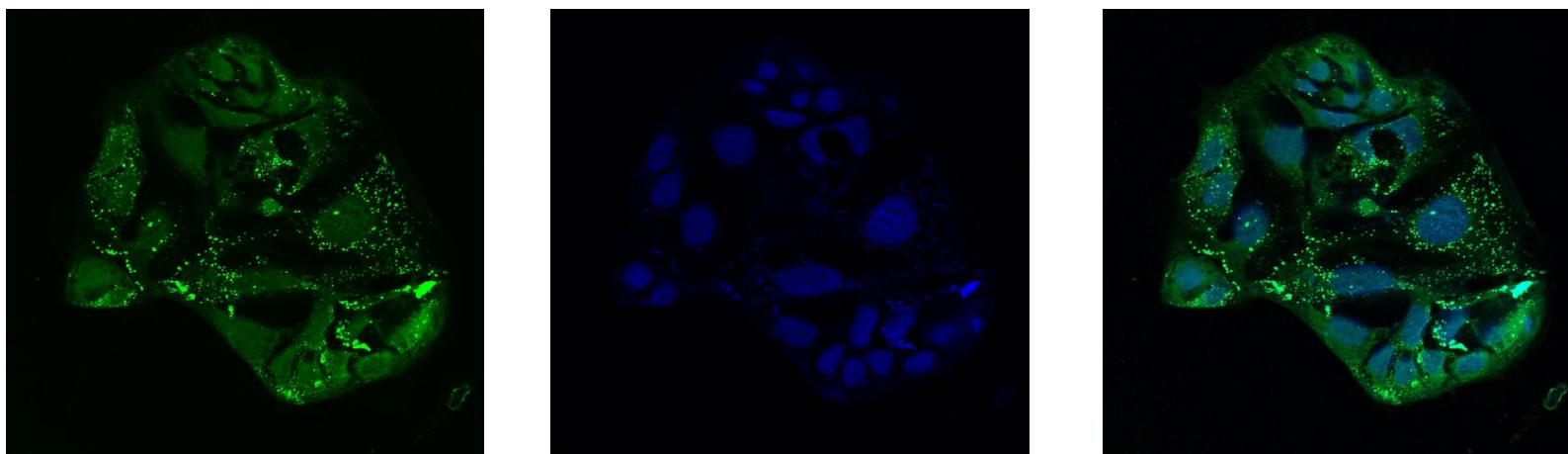


Fig. 7.8 6-Coumarin solution at 30 min in Caco-2 cells; (A) Dye solution (B) DAPI stained nuclei (C) Overlapped image showing less fluorescence in cells

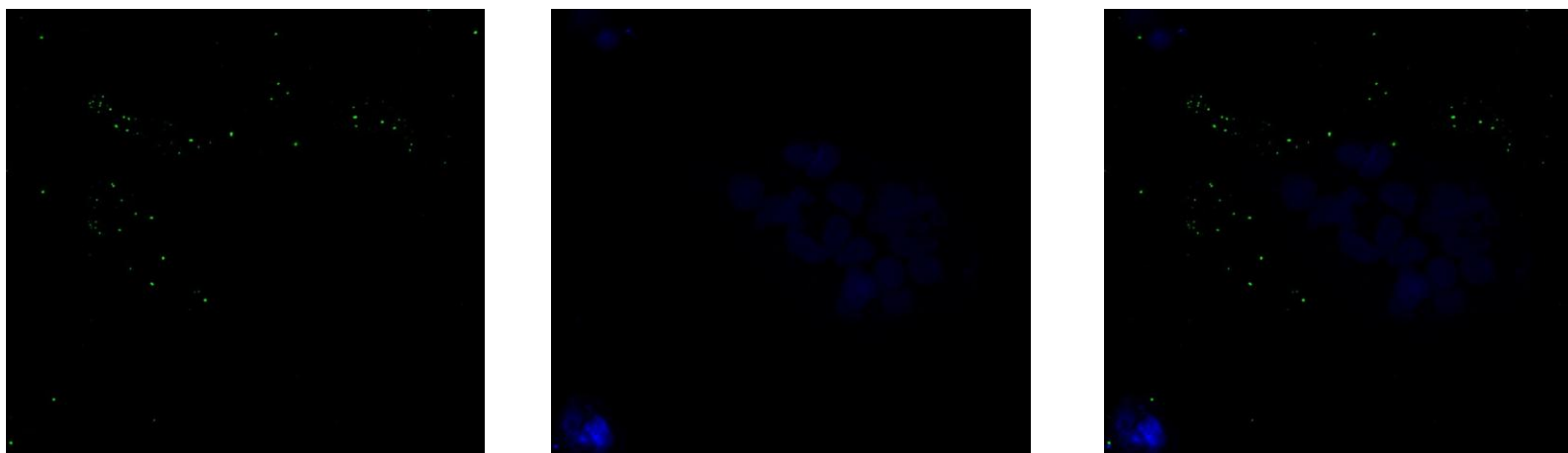


A

B

C

Fig. 7.9 6-Coumarin loaded NPs at 60 min in Caco-2 cells; (A) NPs (B) DAPI stained nuclei (C) Overlapped image showing internalization of NPs in cells



A

B

C

Fig. 7.10 6-Coumarin solution at 60 min in Caco-2 cells; (A) Dye solution (B) DAPI stained nuclei (C) Overlapped image showing less fluorescence in cells

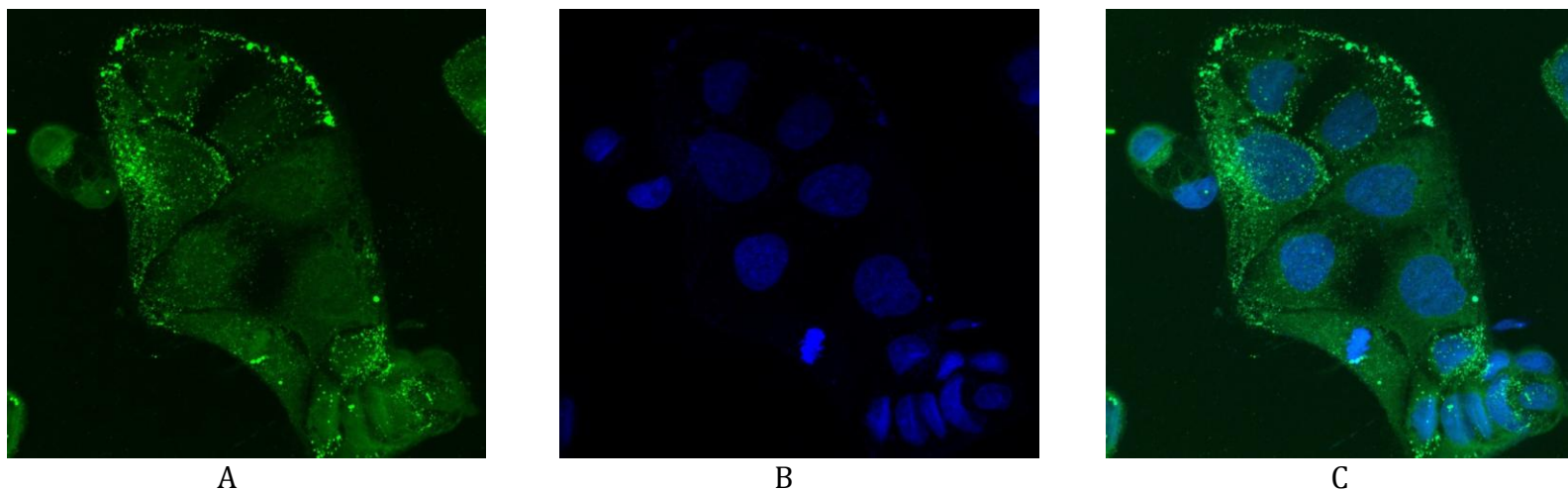


Fig. 7.11 6-Coumarin loaded NPs at 90 min in Caco-2 cells; (A) NPs (B) DAPI stained nuclei (C) Overlapped image showing internalization of NPs in cells

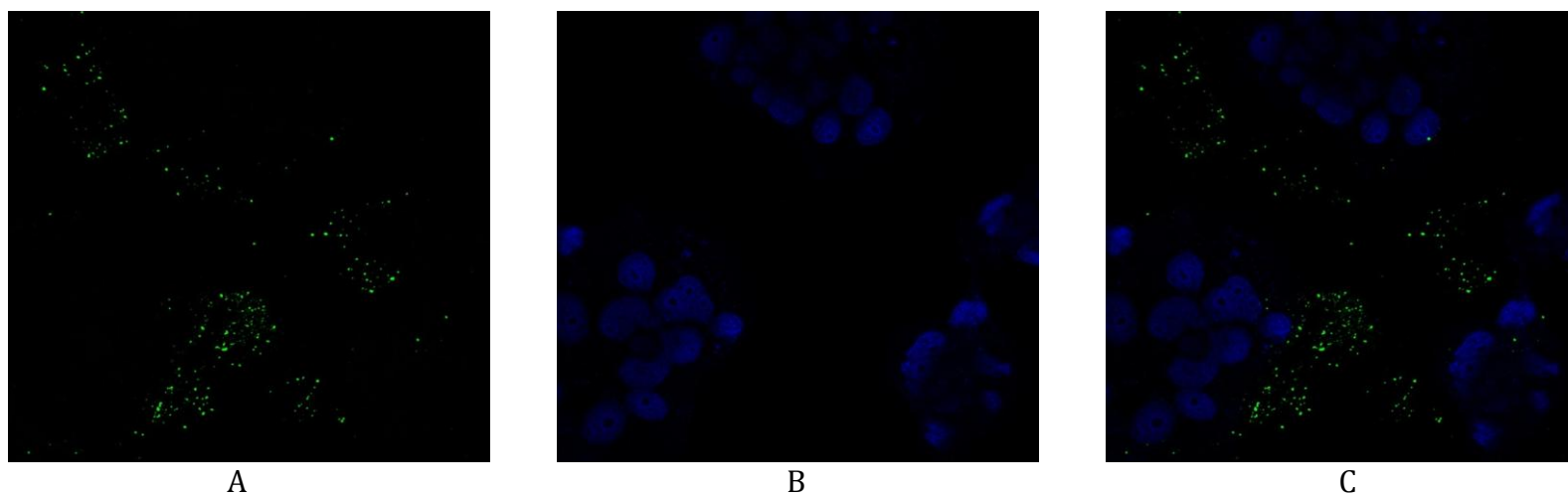


Fig. 7.12 6-Coumarin solution at 90 min in Caco-2 cells; (A) Dye solution (B) DAPI stained nuclei (C) Overlapped image showing less fluorescence in cells

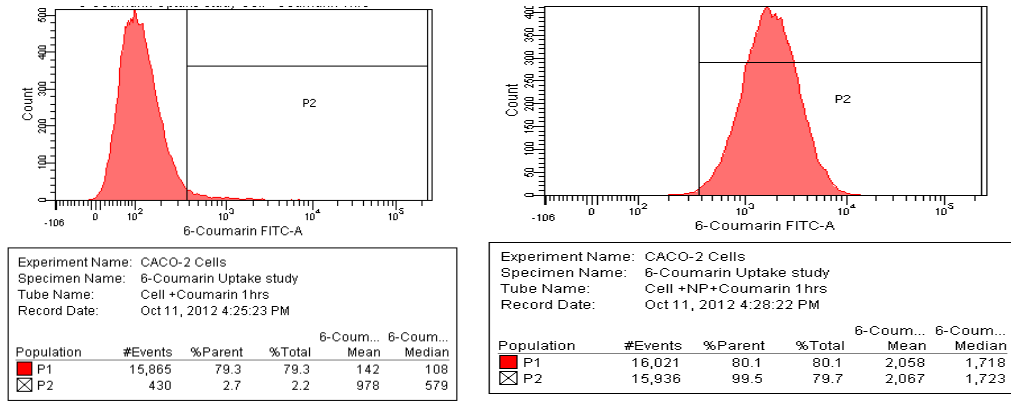


Fig. 7.13(a) Quantitative cellular uptake of 6-Coumarin solution and 6-Coumarin loaded NPs at 1h.

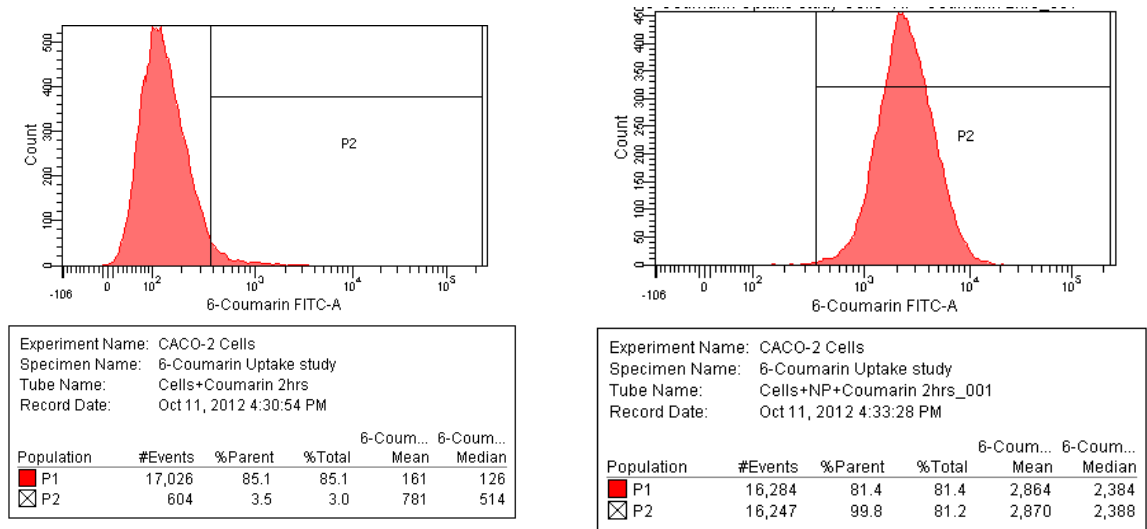


Fig. 7.13(b) Quantitative cell uptake of 6-Coumarin and 6-Coumarin loaded NPs at 2h

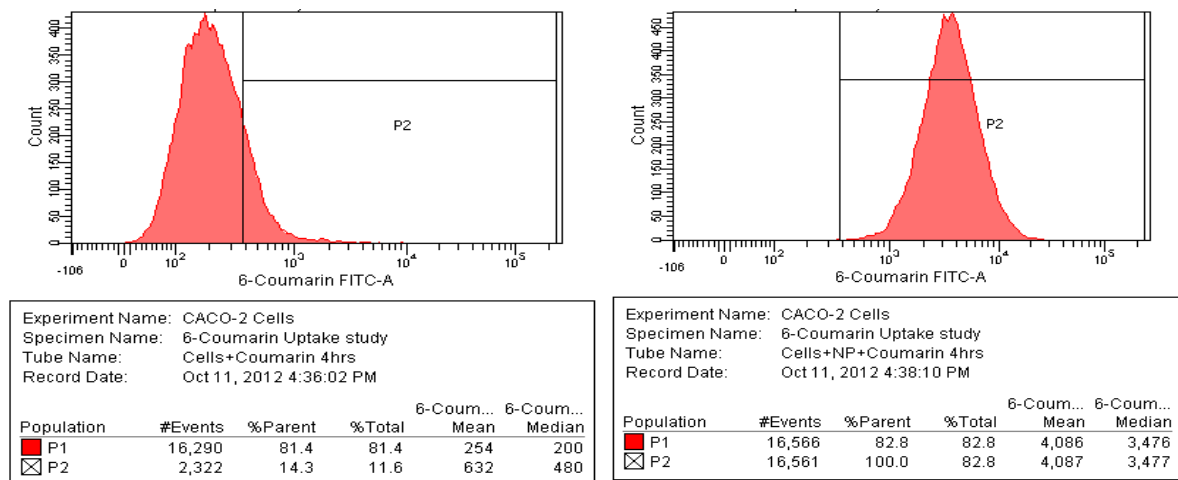
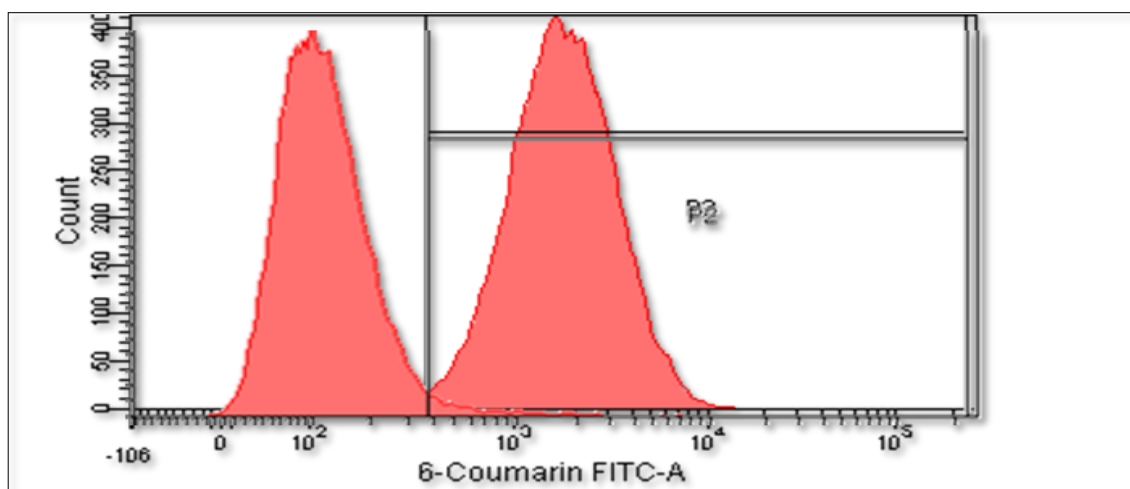
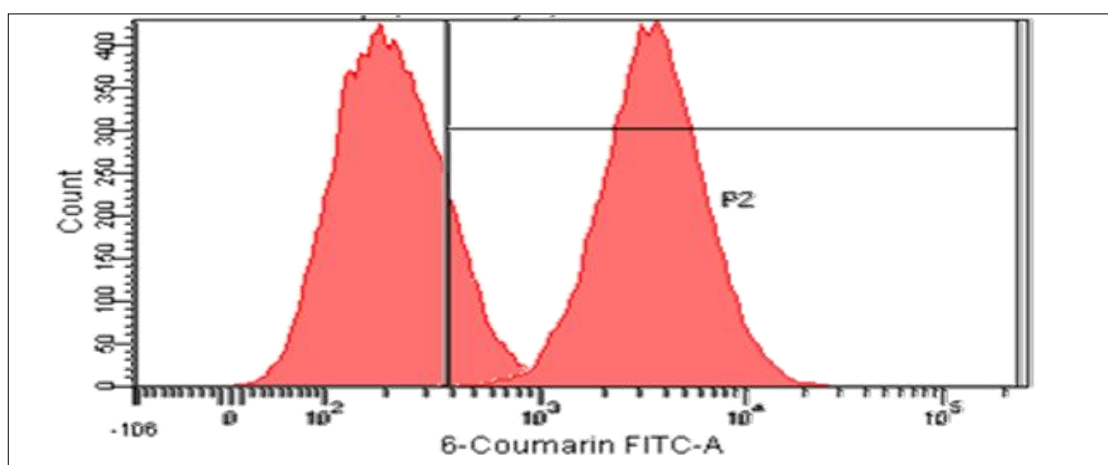


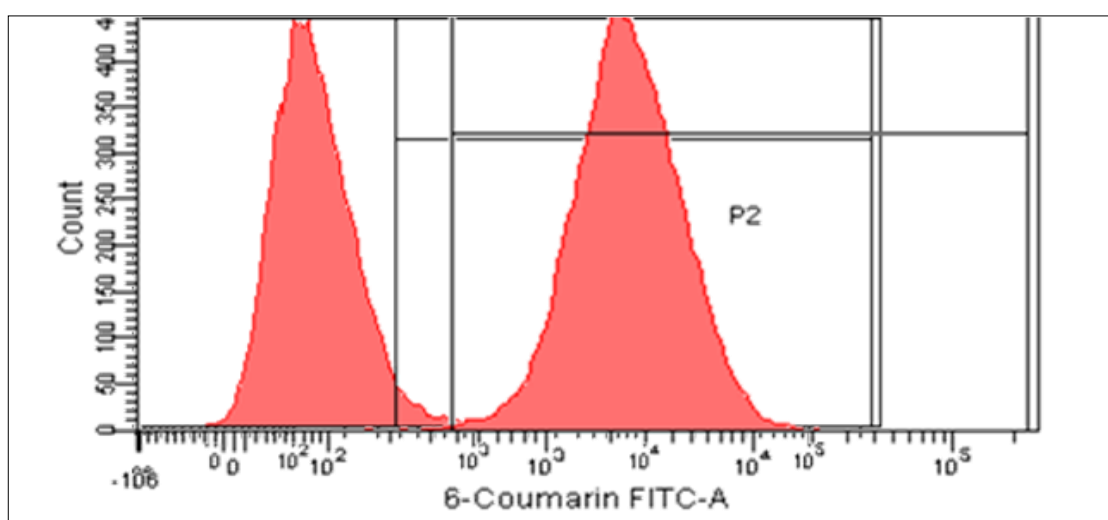
Fig. 7.13(c) Quantitative cell uptake of 6-Coumarin and 6-Coumarin loaded NPs at 4h.



A



B



C

Fig 7.14 Overlay graph of mean fluorescent intensity of 6-Coumarin loaded NPs showing a shift in intensity in comparison to plain dye solution at 1h (A), 2h (B) and 4h(C)

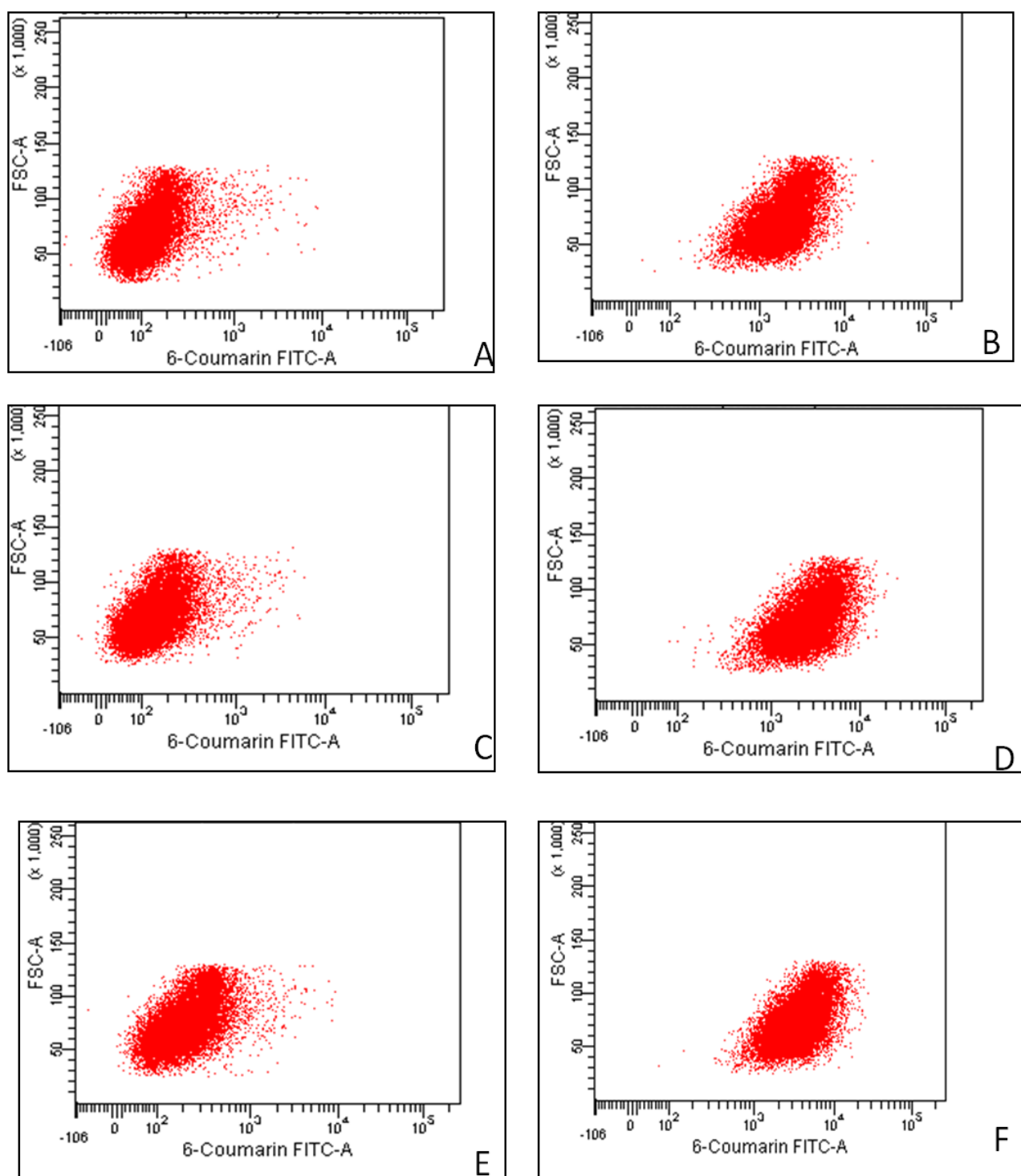


Fig. 7.15 Mean fluorescent intensity graphs showing the 6-Coumarin and 6-Coumarin loaded NPs uptake in Caco 2 cells at 1h (A, B), 2h (C,D) and 4h (E,F)

7.5.3 Cytotoxicity studies

Gemcitabine HCl loaded NPs and plain Gemcitabine HCl solution

Cytotoxicity studies of the formulations were done to assess the Mitochondrial activity of the cell by the 3-(4, 5-dimethylthiazol-2-yl)-2,5- diphenyl-2H-tetrazolium bromide (MTT) assay. MTT assays were done to assess the antiproliferative effect for anticancer formulations as well as to assess the safety/ tolerability of other formulations on viability of cells.

Cytotoxicity studies for anticancer drug Gemcitabine HCl in Caco-2 cells and K562 cells were assessed by mitochondrial activity (MTT assay). It is a quantitative colorimetric method, based on the reduction of a yellow tetrazolium salt to insoluble purple formazan crystals by the mitochondrial dehydrogenases of viable cells (Mosmann, 1983). As Caco-2 cell lines were used as *in vitro* absorption barrier, we wanted to check the toxicity/ safety of formulation on absorption barrier. At initial 6h, Gemcitabine HCl loaded NPs had negligible cytotoxicity on the Caco-2 cells as compared to the plain drug solution at all concentrations, which could be attributed to the protective effect of PLGA entrapment and slow release of drug. Thus, the concentration upto 200 mcg/ml was used for permeation studies which were performed for 6h (Table 7.1, Fig. 7.16). Also at 24 h, the PLGA NPS were found to have less cytotoxicity to plain drug solution (Fig. 7.17). Therefore, The anticancer drug loaded in PLGA NPS would cause less toxicity in the intestine cells as compared to native drug which may lead to gastrointestinal toxicities as reported by Veltkamp et al (Veltkamp et al., 2008). The expression pattern for Caco-2 cells closely resembles the gene expression profile of transporters within the normal colon, suggesting that this cell line may serve as an *in vitro* model of colonic drug adsorption. Caco-2 has molecular "fingerprint" of distinctly different from tumor samples, indicating that the Caco-2 model would unlikely predict accurate drug absorption for colon cancer sites (Calcagno et al., 2006).

However, for K562 cell lines, Gemcitabine HCl loaded NPs showed higher anti-proliferative effect than plain drug solution at all concentrations and at all time points (Table 7.2). Cytotoxicity curve and IC₅₀ value were determined for Gemcitabine HCl, Gemcitabine HCl loaded NPs. The IC₅₀ value for Gemcitabine HCl loaded NPs and Plain gemcitabine HCl solution are given in Table 7.3. The Gemcitabine HCl loaded NPs were found to be 2.4 fold, 3.4 fold and 8.59 fold more cytotoxic on K 562 cancer cells after 6, 24h and 48h incubation respectively, which could be attributed by higher uptake via

endocytosis and more internalization of PLGA NPs with time duration due to more lipophilicity as compared to plain drug solution (Fig. 7.18 to 7.20).

Table 7.1 *In vitro* cytotoxicity studies of Gemcitabine HCl loaded NPs in Caco2 cells

Conc ($\mu\text{g/ml}$)	% viability of cells at 6h		% viability of cells at 24h	
	PDS	NPs	PDS	NPs
0.1	100.01 \pm 3.569	100 \pm 3.78	97.63 \pm 2.435	99.46 \pm 2.541
1	96.56 \pm 2.36	98.563 \pm 1.942	89.32 \pm 2.235	96.35 \pm 2.342
10	89.97 \pm 1.638	96.76 \pm 2.56	83.53 \pm 3.245	92.43 \pm 2.362
100	84.69 \pm 1.472	95.93 \pm 1.435	81.41 \pm 3.324	90.13 \pm 1.631
200	81.23 \pm 1.654	93.78 \pm 2.85	80.43 \pm 2.15	88.68 \pm 2.382

Table 7.2 *In vitro* cytotoxicity studies of Gemcitabine HCl loaded NPs in K562 cells

Conc ($\mu\text{g/ml}$)	% cell viability at 6h		% cell viability at 24h		% cell viability at 48h	
	PDS	NPs	PDS	NPs	PDS	NPs
0.1	98.63 \pm 1.346	94.36 \pm 4.35	96.13 \pm 3.12	82.63 \pm 2.36	91.43 \pm 3.44	78.64 \pm 2.87
1	90.31 \pm 2.423	75.69 \pm 6.42	89.71 \pm 2.47	70.94 \pm 2.46	79.82 \pm 3.62	66.72 \pm 5.23
10	79.24 \pm 2.13	54.36 \pm 4.23	78.53 \pm 5.42	51.23 \pm 3.53	71.49 \pm 2.96	44.56 \pm 3.47
100	68.23 \pm 1.82	44.63 \pm 2.42	62.45 \pm 2.37	39.74 \pm 1.96	54.98 \pm 5.23	26.43 \pm 2.43
200	61.73 \pm 1.84	38.45 \pm 3.41	58.26 \pm 4.21	26.41 \pm 3.86	48.67 \pm 4.25	11.45 \pm 3.76

Table 7.3 IC₅₀ values of plain drug solution and Gemcitabine HCl loaded NPs in Caco -2 cells and K562 cells

Condition	IC ₅₀ values	
	Gemcitabine HCl	Gemcitabine HCl loaded NPs
Caco 2 (6 h)	8.628	10.50
Caco 2 (24h)	8.694	9.472
K562(6 h)	8.648	3.580
K562 (24 h)	12.91	3.798
K562 (48 h)	13.29	1.547

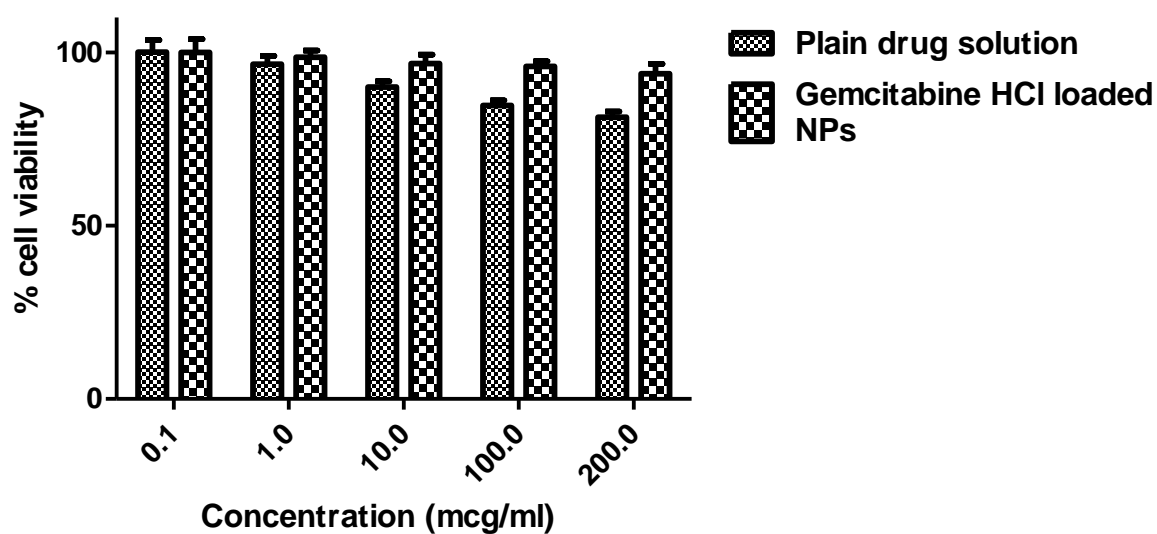


Fig. 7.16 *In vitro* Cytotoxicity of Gemcitabine HCl loaded NPs and plain drug solution on Caco 2 cells at 6h.

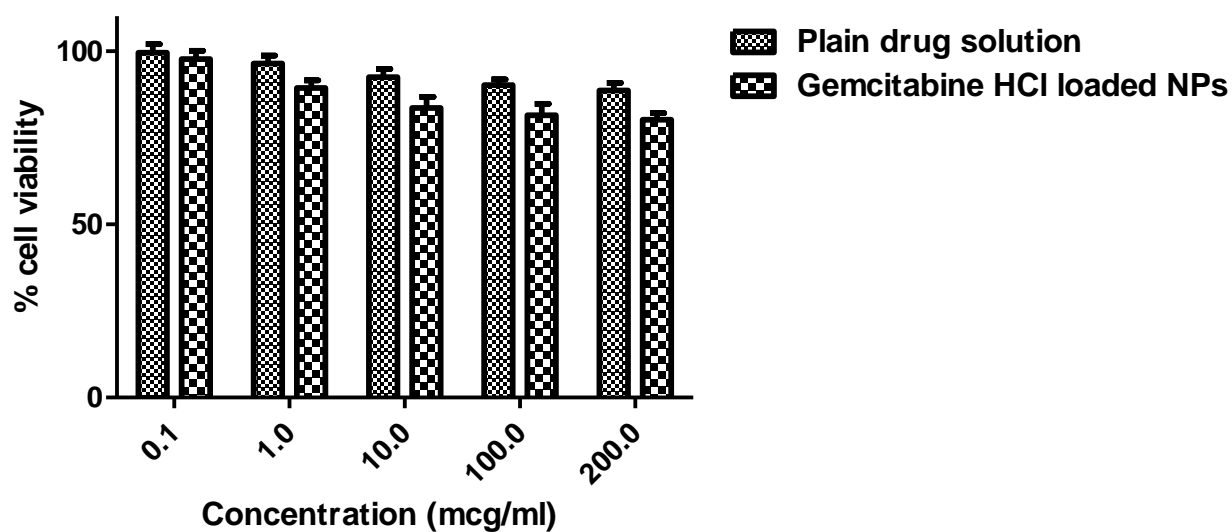


Fig. 7.17 *In vitro* Cytotoxicity of Gemcitabine HCl loaded NPs and plain drug solution on Caco 2 cells at 24h.

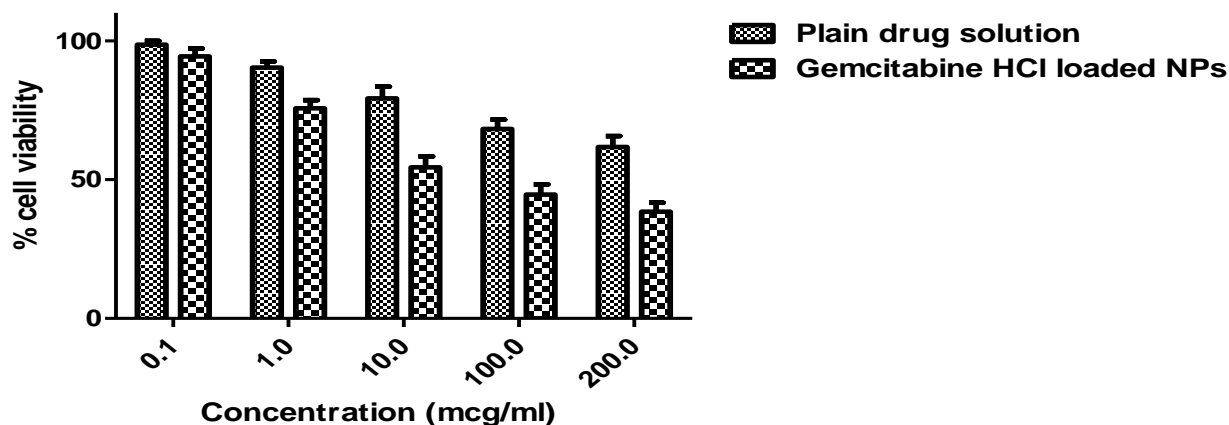


Fig. 7.18 *In vitro* Cytotoxicity of Gemcitabine HCl loaded NPs and plain drug solution on K562 cells at 6h

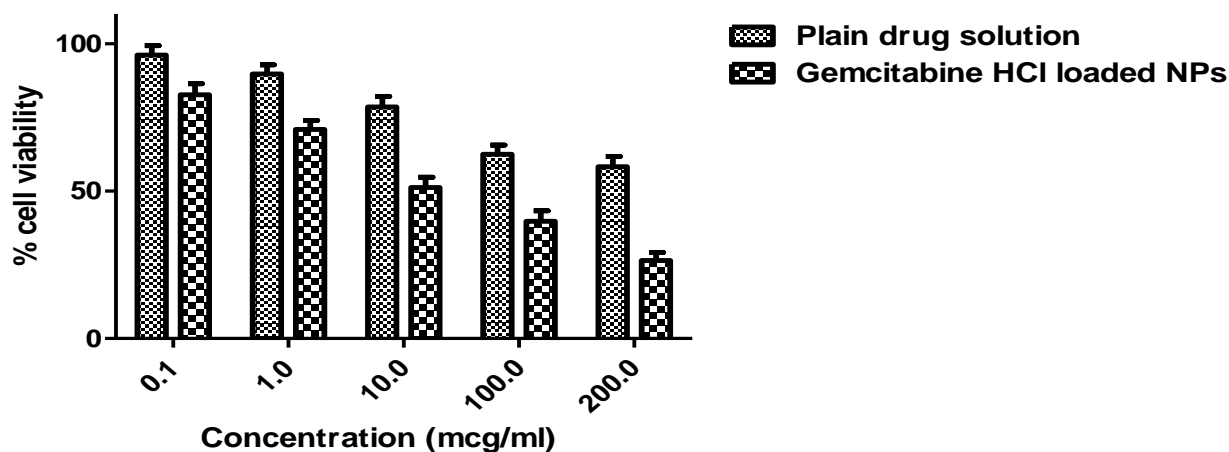


Fig. 7.19 *In vitro* Cytotoxicity of Gemcitabine HCl loaded NPs and plain drug solution on K562 cells at 24h

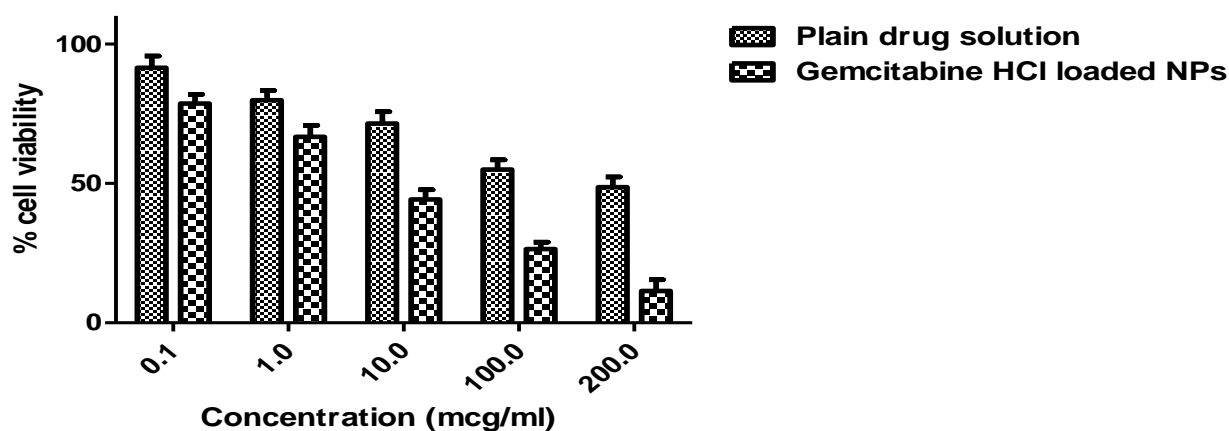


Fig. 7.20 *In vitro* Cytotoxicity of Gemcitabine HCl loaded NPs and plain drug solution on K562 cells at 48h

Lopinavir loaded NPs and Lopinavir suspension

Tolerability of Lopinavir loaded NPs as well as Lopinavir was assessed in Caco 2 cells by MTT assay to check the safety of NPs (Silva et al., 2011). As Caco 2 cells were used as absorption model, biocompatibility and tolerability of NPs on Caco 2 cells was desirable. IC 50 values for Lopinavir loaded NPs were more than the plain drug suspension. At initial 6h upto concentration of 100mcg/ml, the Lopinavir loaded NPs did not exhibited cytotoxicity. Hence, for permeability studies concentration upto 200 mcg/ml was used (Agarwal et al., 2008). Lopinavir loaded in NPs was much less cytotoxic than the plain drug suspension (Table 7.4). This proves the biocompatibility of PLGA nanoparticles and explains that composition of nanocarrier did not contribute to toxicity in Caco 2 cells (Semete et al., 2010). Lopinavir found to have no cytotoxicity effects on Caco 2 cells at 6h and 24h (Fig. 7.21, 7.22). As viability of cell was more than 80 % at all concentrations concluded to lack of cytotoxicity due to formulation of PLGA nanoparticles. These results are in line with research findings of some other nanocarriers on Caco 2 cells (Silva et al., 2012) and similar to research findings of some other researchers on MT4 cells (Molla et al., 2002).

Lopinavir is always given in combination with ritonavir, contribution of ritonavir to in vivo antiviral action is negligible (Molla et al., 2002), it enhances only Lopinavir bioavailability.

Table 7.4 *In vitro* cytotoxicity of Lopinavir loaded NPs and plain drug suspension on Caco 2 cells

Conc ($\mu\text{g} / \text{ml}$)	% viability of cells at 6h		% viability of cells at 24h	
	PDS	NPs	PDS	NPs
0.1	100.63	101.85	99.63	99.86
1	99.23	99.86	99.45	97.56
10	98.23	99.23	89.23	92.47
100	96.13	98.15	82.53	88.56
200	94.65	96.43	78.53	85.13

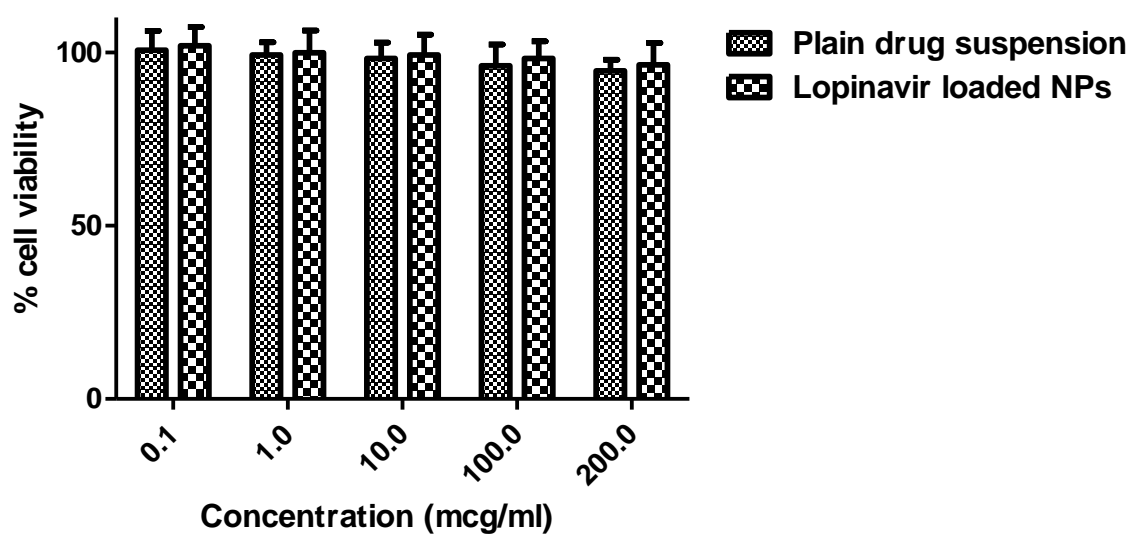


Fig. 7.21 *In vitro* Cytotoxicity of Lopinavir loaded NPs and plain drug suspension on Caco 2 cells at 6h

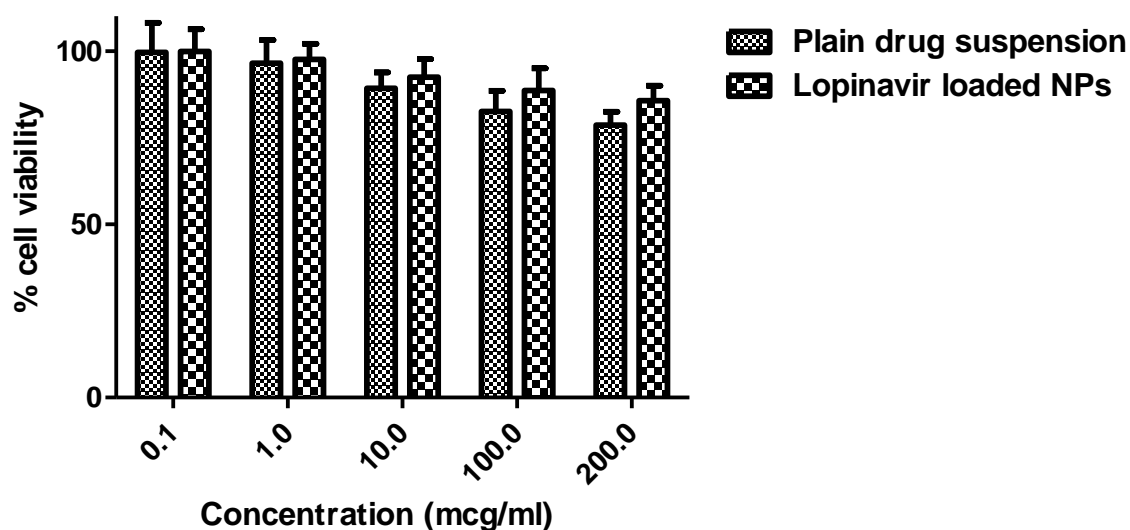


Fig. 7.22 *In vitro* Cytotoxicity of Lopinavir loaded NPs and plain drug suspension on Caco 2 cells at 24h

7.5.4 Transport / permeability studies in Caco-2 cells

Gemcitabine HCl loaded NPs and plain drug solution

Gastrointestinal permeability of Gemcitabine HCl loaded NPs was assessed *in vitro* by calculating permeability coefficients in Caco 2 cells model of gastrointestinal barrier. Human colon carcinoma cells forms confluent monolayers of tight junctions after

differentiation of 14-21 days which exhibit similar properties to intestinal epithelial cells. Transepithelial permeability of Gemcitabine HCl was measured at concentration lower than, 200 mcg/ml as no toxicity on Caco 2 cells was reported at this concentration. The permeability coefficient for Gemcitabine HCl solution was found to be 0.72×10^{-5} . The permeability coefficient for Gemcitabine HCl loaded NPs was found to be 4.6×10^{-5} which is 6.38 times more than the plain drug solution (Table 7.5). The higher permeability coefficient for nanoparticles corresponds to the lipophilicity of PLGA NPs in which the drug covered, whereas lower permeability coefficient for plain drug solution was because of high hydrophilicity of drug as well as poor permeation (log P 1.4). As the drug is substrate for p glycoprotein pump, the low permeability can also be attributed to that. The permeation coefficient values less than 1×10^{-5} values have poor permeability, whereas permeability coefficient between $1-10 \times 10^{-5}$ is for moderate to good permeability (Yee, 1997). These results are in line with our hypothesis that NPs would be capable of being absorbed through M cells of peyer's patches.

Table 7.5 Drug transfer across the Caco 2 cell lines for Gemcitabine loaded NPs and plain drug solution

Time	Plain drug solution		Gemcitabine HCl loaded NPs	
	mcg/ml	Drug transfer (mg)	mcg/ml	Drug transfer (mg)
30	1.00	0.0015	5.95	0.0089
60	2.4	0.0036	17.61	0.0264
120	8.24	0.0123	34.16	0.0512
180	15.17	0.0227	59.12	0.0886
240	18.95	0.0284	91.24	0.136
	dQ/dt=.0001		dQ/dt =.0006	

Lopinavir loaded NPs and plain Lopinavir suspension

The permeability coefficient of Lopinavir loaded NPs was found to be 8.84×10^{-5} whereas for Lopinavir solution across the Caco 2 cell was found to be 2.9×10^{-5} (Table 7.6). Lopinavir has a log P value of 4.67 (Drug Bank) and it is lipophilic drug, therefore it is permeable to Caco 2 cells, but Lopinavir loaded shown a 3.04 times increase in

permeability, which could be attributed to the higher uptake of NPs by endocytosis in Caco 2 cells. There is significant enhancement in permeability of Lopinavir by loading the drug in NPs.

Table 7.6 Drug transfer across the Caco 2 cell lines for Lopinavir loaded NPs and plain drug solution

Time	Plain drug solution		Lopinavir loaded NPs	
	mcg/ml	Drug transfer (mg)	mcg/ml	Drug transfer (mg)
30	10.56	0.0158	48.36	0.0725
60	22.46	0.0336	68.7	0.103
120	38.45	0.0576	136.12	0.204
180	46.86	0.0702	183.23	0.274
240	69.23	0.103	216.42	0.324
		dQ/dt=.0004		dQ/dt=.0012

7.6 References

- ❖ Agarwal, S., Boddu, S. H., Jain, R., Samanta, S., Pal, D., and Mitra, A. K. (2008). Peptide prodrugs: improved oral absorption of lopinavir, a HIV protease inhibitor. *Int J Pharm* 359, 7-14.
- ❖ Arias, J. L., Reddy, L. H., and Couvreur, P. (2009). Polymeric nanoparticulate system augmented the anticancer therapeutic efficacy of gemcitabine. *J Drug Target* 17, 586-598.
- ❖ Calcagno, A. M., Ludwig, J. A., Fostel, J. M., Gottesman, M. M., and Ambudkar, S. V. (2006). Comparison of drug transporter levels in normal colon, colon cancer, and Caco-2 cells: impact on drug disposition and discovery. *Mol Pharm* 3, 87-93.
- ❖ Cartiera, M. S., Johnson, K. M., Rajendran, V., Caplan, M. J., and Saltzman, W. M. (2009). The uptake and intracellular fate of PLGA nanoparticles in epithelial cells. *Biomaterials* 30, 2790-2798.
- ❖ Ina Hubatsch, E. G. E. R. P. A. (2007). Determination of drug permeability and prediction of drug absorption in Caco-2 monolayers. *Nature Protocols* 2.
- ❖ Kaustubh Kulkarni, M. H. (2011). Caco 2 cell culture models for oral drug absorption. In *Oral Bioavailability Basic principles, Advanced concepts and applications*, X.L. Ming HU, ed. (New Jersey: John Wiley and Sons).
- ❖ Luo, H., Li, J., and Chen, X. (2010). Antitumor effect of N-succinyl-chitosan nanoparticles on K562 cells. *Biomed Pharmacother* 64, 521-526.
- ❖ Molla, A., Mo, H., Vasavanonda, S., Han, L., Lin, C. T., Hsu, A., and Kempf, D. J. (2002). *In vitro* antiviral interaction of lopinavir with other protease inhibitors. *Antimicrob Agents Chemother* 46, 2249-2253.
- ❖ Mosmann, T. (1983). Rapid colorimetric assay for cellular growth and survival: application to proliferation and cytotoxicity assays. *J Immunol Methods* 65, 55-63.
- ❖ Semete, B., Booyesen, L., Lemmer, Y., Kalombo, L., Katata, L., Verschoor, J., and Swai, H. S. (2010). In vivo evaluation of the biodistribution and safety of PLGA nanoparticles as drug delivery systems. *Nanomedicine* 6, 662-671.
- ❖ Senanayake, T. H., Warren, G., Wei, X., and Vinogradov, S. V. (2013). Application of activated nucleoside analogs for the treatment of drug-resistant tumors by

- oral delivery of nanogel-drug conjugates. *Journal of Controlled Release* 167, 200-209.
- ❖ Silva, A. C., Gonzalez-Mira, E., Garcia, M. L., Egea, M. A., Fonseca, J., Silva, R., Santos, D., Souto, E. B., and Ferreira, D. (2011). Preparation, characterization and biocompatibility studies on risperidone-loaded solid lipid nanoparticles (SLN): high pressure homogenization versus ultrasound. *Colloids Surf B Biointerfaces* 86, 158-165.
 - ❖ Silva, A. C., Kumar, A., Wild, W., Ferreira, D., Santos, D., and Forbes, B. (2012). Long-term stability, biocompatibility and oral delivery potential of risperidone-loaded solid lipid nanoparticles. *International Journal of Pharmaceutics* 436, 798-805.
 - ❖ Trapani, A., Sitterberg, J., Bakowsky, U., and Kissel, T. (2009). The potential of glycol chitosan nanoparticles as carrier for low water soluble drugs. *International Journal of Pharmaceutics* 375, 97-106.
 - ❖ Veltkamp, S. A., Plum, D., van Tellingen, O., Beijnen, J. H., and Schellens, J. H. (2008). Extensive metabolism and hepatic accumulation of gemcitabine after multiple oral and intravenous administration in mice. *Drug Metab Dispos* 36, 1606-1615.
 - ❖ Yee, S. (1997). *In vitro* permeability across Caco-2 cells (colonic) can predict *in vivo* (small intestinal) absorption in man--fact or myth. *Pharm Res* 14, 763-766.
 - ❖ Zhou, S., Feng, X., Kestell, P., Paxton, J. W., Baguley, B. C., and Chan, E. (2005). Transport of the investigational anti-cancer drug 5,6-dimethylxanthenone-4-acetic acid and its acyl glucuronide by human intestinal Caco-2 cells. *European Journal of Pharmaceutical Sciences* 24, 513-524.

CHAPTER 8

IN-VIVO STUDIES

8.1 Introduction

Oral administration is regarded as the preferred route of drug administration, offering numerous advantages including, convenience, ease of compliance, availability to large population, and cost effectiveness. Thus, oral bioavailability plays an important role for successful therapy by this route. Oral bioavailability depends on number of factors like aqueous solubility, dissolution rate, drug permeability, presystemic metabolism, first pass metabolism and susceptibility to efflux mechanisms. Thus, only *in vitro* evaluation will not be able to predict exact role of nanoparticles in improving bioavailability. Hence, to find exact improvement in bioavailability, nanoparticles uptake studies after oral administration and pharmacokinetic studies must be performed. Bioavailability is one of the principal pharmacokinetic properties of drugs. It is one of the essential tools in pharmacokinetics, as bioavailability must be considered when calculating dosages for non-intravenous routes of administration. It is a subcategory of absorption and is the fraction of an administered dose of unchanged drug that reaches the systemic circulation. Relative bioavailability or bioequivalence is the most common measure for comparing the bioavailability of one formulation of the same drug to another. The mean responses such as C_{max} and AUC are compared to determine relative bioavailability. The AUC refers to the extent of bioavailability while C_{max} refers to the rate of bioavailability.

8.2 Animals

Male Wistar rats weighing 250 ± 20 g were used for oral bioavailability studies and for intestinal lymphatic transport studies. Animals were housed in propylene cages (38cm×23cm×10cm) under laboratory conditions of controlled environment of temperature 30 ± 2 °C and $60 \pm 5\%$ RH. Three rats per cage were fed ad libitum with animal feed allowing free access to drinking water. Animals were fasted overnight. All surgical and experimental procedures were reviewed and approved by the Animal Ethics Committee of Department of Pharmacy, M S University of Baroda, Vadodara, Gujarat, India. All animal experiments were approved by Committee for the Purpose of Control and Supervision of Experiments on Animals (CPCSEA), Ministry of Social Justice and Empowerment, Government of India, New Delhi, India.

8.3 *In Vivo* Nanoparticle uptake into Rat Intestinal Tissue after Oral Delivery by Confocal Laser Scanning Microscopy

8.3.1 Method

In vivo nanoparticle uptake studies in rat intestine after oral administration were performed to study the penetration and absorption of Gemcitabine HCl loaded nanoparticles and Lopinavir loaded nanoparticles. For this purpose, Rhodamine was used as hydrophilic and 6-Coumarin was used as hydrophobic model dye respectively.

The dye loaded nanoparticles were administered orally to the rats with the aid of a syringe and infant feeding tube. After 2h, the animals were sacrificed by euthanasia. Intestine was isolated and washed with HBSS. The isolated intestine tissue was fixed with 10% formalin for 4h at 4°C and then transferred to 30% sucrose in PBS solution for cryopreservation. Then, tissue was transferred to OCT compound for 1h at 4°C. Slices transverse to the intestinal surface, 10 µm in thickness, were cut from the ileum, included in the OCT Compound (Leica Microsystem srl, Milan, Italy), using a cryostat (Leica CM1510, Leica Microsystem srl, Milan, Italy) at -20°C. Each slice was placed on a microscope slide, and mounted in glycerol, covered by cover glass and visualized in confocal microscope (Carl Zeiss, LSM 710) at (Rhodamine B: λ_{ex} 540 λ_{em} 625nm Red fluorescence; 6-coumarin: λ_{ex} 430 λ_{em} 485 nm Green fluorescence). The images were analysed by Zen imaging software (Carl Zeiss, Jena, Germany) (Cartiera et al., 2009). Negative control image of transverse intestine section was taken without administration of fluorescent NPs.

8.3.2 Results and Discussion

Fig 8.1 (a) and (b) shows the confocal micrograph images of transverse section of rat ileal tissue after oral administration of Rhodamine loaded NPs. The images showed the penetration of NPs in the intestinal tissue of rat after oral administration, confirming the absorption of NPs showing red fluorescence at the villi in comparison to negative control intestinal tissue section slide (c). Fig 8.1 (d) and (e) shows the confocal micrograph image of rat ileal tissue after oral administration of 6-Coumarin loaded NPs. The images showed green fluorescence at the base of the villi region where the Peyer's patches are intense. This confirmed the penetration of NPs in the intestinal tissue after oral delivery.



Fig. 8.1(a) Transeverse section of intestine of rat after oral delivery of Rhodamine loaded Nanoparticles (at 10x)

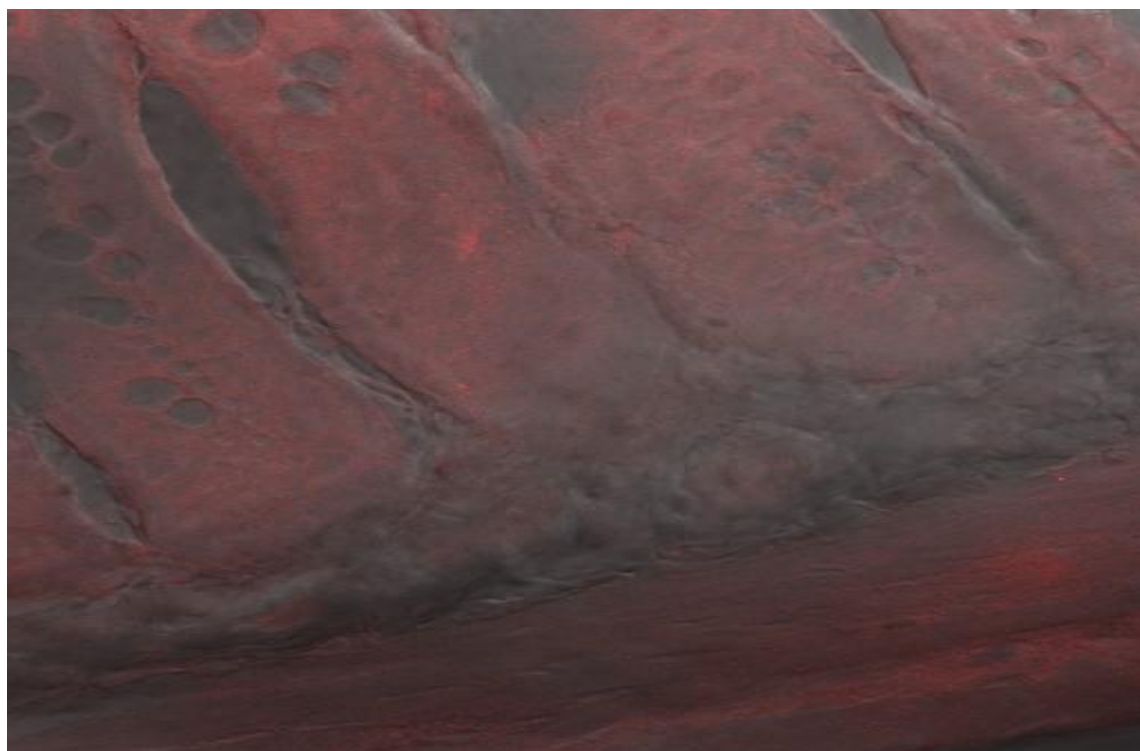


Fig. 8.1 (b) Transeverse section of intestine of rat after oral delivery of Rhodamine loaded Nanoparticles (at 63x)

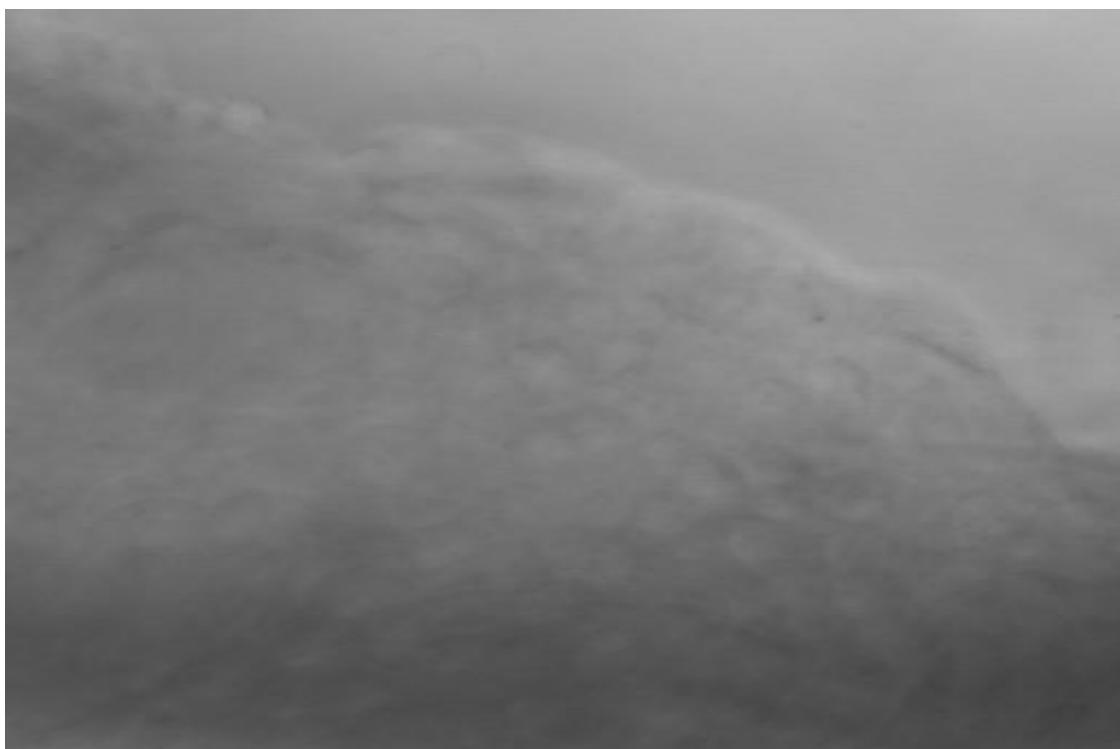


Fig. 8.1 (c) Negative control, transverse section of intestinal tissue without administration of fluorescent Nanoparticles (at 10x)

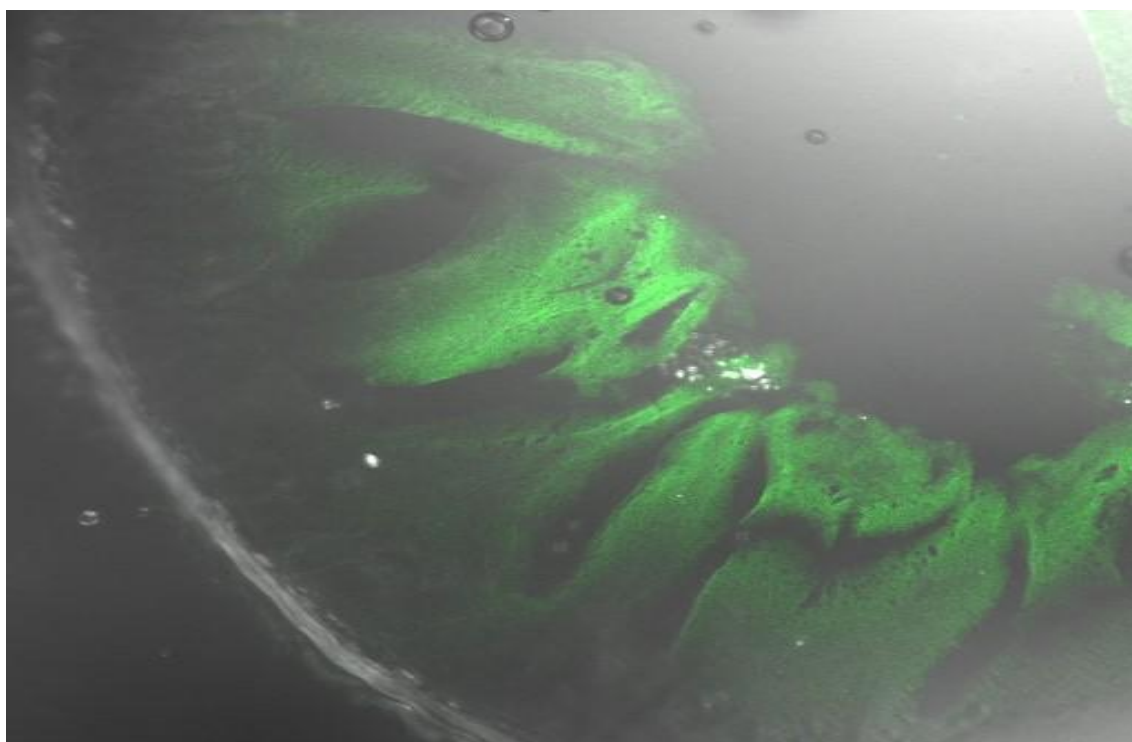


Fig. 8.1(d) Transverse section of intestine of rat after oral delivery of 6-Coumarin loaded Nanoparticles (at 10 x)

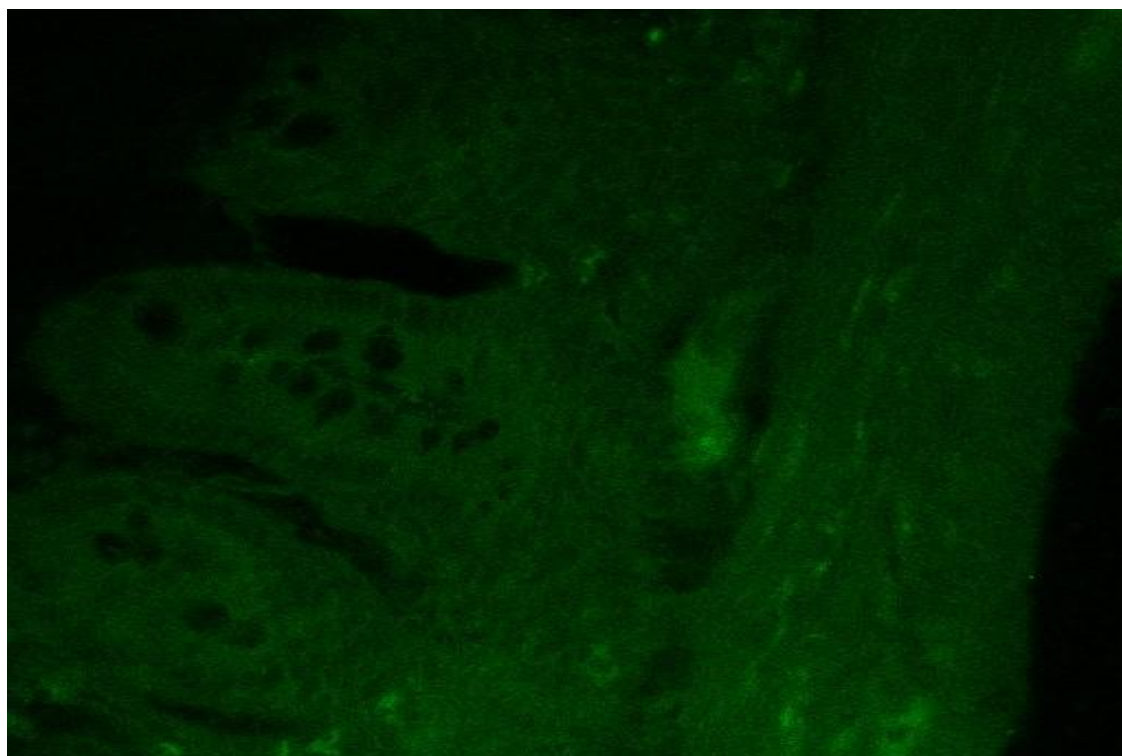


Fig. 8.1(e) Transverse section of intestine of rat after oral delivery of 6-Coumarin loaded Nanoparticles (at 63x)

8.4 *In Vivo* Pharmacokinetic Studies for Gemcitabine HCl Loaded Nanoparticles

8.4.1 Methods

Three groups of male Wistar rats with each group containing 5 animals were subjected to single oral dose bioavailability study. The 1st group was given distilled water, the 2nd group was given a solution of Gemcitabine HCl in distilled water, and the third group received Gemcitabine HCl loaded NPs. In 2nd and 3rd tested groups, Gemcitabine was administered at a dose of 10 mg/kg (Vandana and Sahoo, 2010). The formulations were administered orally with the aid of a syringe and infant feeding tube. Blood samples were drawn by retro-orbital venous plexus puncture with the aid of capillary tubes at 0.5, 2, 4, 8, 24, 48, 72h post oral dose. The samples were collected in heparinised Eppendorf tubes containing 10 μ M tetrahydrouridine to inhibit gemcitabine metabolism by cytidine deaminase and centrifuged at 3400 rpm for 15 min, and plasma was collected and stored at -20 °C until analysis. Gemcitabine HCl detection was performed at 269 nm, using X-Terra C8 analytical column. To this 200 μ l of acetonitrile was added and vortexed for 5min followed by centrifugation at 5000rpm

for 15 min. The organic phase was separated and evaporated under reduced pressure in a vacuum oven. The residue was dissolved in mobile phase solution (0.15 ml), vortexed for 1min followed by centrifugation at 13,000rpm for 5min. Then 20 μ l of supernatant solution was injected in to the HPLC column. Calibration curves for Gemcitabine HCl in plasma samples were drawn as reported in analytical methods.

8.4.2 Results and Discussion

The plasma drug concentration versus time profile for plain drug solution and gemcitabine HCl loaded NPs after oral delivery in rats (n=5) at drug concentration of 10 mg/kg (Vokurka, 2004) are shown in Fig. 8.2. Table 8.1 gives the plasma concentrations of plain drug and Gemcitabine HCl loaded NPs at different time points. The pharmacokinetic parameters including C_{max} (in ng/ml) and T_{max} – the maximum drug concentration encountered after the drug administration and the time at which C_{max} is reached, AUC_{0–inf} (ng h/ml) – the total area under the curve which represents the *in vivo* therapeutic effects, t_{1/2} (h) – the half-life of the drug in the plasma and relative bioavailability were analysed from kinetic software 5.0 version (Table 8.2). C_{max} for plain drug solution was only 489.43±60.06 ng/ml, due to very low bioavailability of Gemcitabine HCl by oral route as Gemcitabine (dFdC) is extensively deaminated by cytidine deaminase into 2, 2-difluorodeoxyuridine (dFdU), which has been reported to be present mainly in liver of humans and kidney of rats. In a clinical study conducted by Veltkamp et al, oral bioavailability of plain gemcitabine HCl was found to be very low due to extensive first pass effect, necessitating high doses at which serious gastrointestinal toxicities can occur (Veltkamp et al., 2008). C_{max} for PLGA nanoparticles was found to be 1586.23±122.5 ng/ml, which was significantly higher than the plain drug solution. A higher C_{max} for NPs could be achieved as drug loaded in PLGA NPs was capable to bypassing hepatic first pass metabolism and able to reach directly to systemic circulation by virtue of size and surface properties of the nanocarrier system. A peak plasma concentration nearer to IC₅₀ value; 1.5 mcg/ml was achieved, which would be sufficient for the cytotoxicity to tumour cells. T_{max} for NPs was found to be 4h while for plain drug solution, it was found to be 1 h. Delayed T_{max} would be justified by the fact that, after intestinal transit, major drug would be released at lymphatic site and then reach systemic circulation. Also, t_{1/2} was increased upto 18.99 h for NPs, which is 3 times higher as compared to plain drug solution; t_{1/2} of

6.42h. AUC_{last} for Gemcitabine HCl loaded NPs was found to be $54,444.7 \pm 3200$ ng.h/ml, which is significantly higher than AUC_{last} for plain drug solution; 2534.72 ± 686.5 ng.h/ml ($P < 0.05$, $P < 0.01$, $P < 0.001$ student's unpaired t test). Plasma concentration from plain drug solution were nearly undetectable after 4h and AUC_{last} was very less due to extensive metabolism to inactive metabolite, while NPs could achieve higher AUC due to slow and sustained release from NPs, which would delay the drug metabolism. Gemcitabine loaded PLGA NPs showed 21.47 fold increase in relative bioavailability (F) in comparison to plain drug solution after oral delivery. Improvement in bioavailability could be attributed to ability of nanoparticles to reach the oral lymphatic region after absorption through M cells of Peyer's patches and reaching to systemic circulation through mesenteric lymph duct. Although we have not compared the plasma profile of marketed intravenous formulation of Gemcitabine HCl but it is reported that, the half life of continuous long infusion for gemcitabine HCl (Gemzar) is 8-20 min and also the C_{max} for continuous infusion are in thousands of ng/ml which is undesirable and causes toxicity. Thus, the orally delivered PLGA nanoparticles of Gemcitabine HCl could deliver the drug to the M cells of Peyer's patches from where it directly reach to systemic circulation, thus protecting the drug from first pass metabolism as well as from gastrointestinal environment and avoiding the serious side effects associated with infusions. Also, Oral NPs for Gemcitabine HCl would be beneficial for lymphatic tumours, as higher concentration to tumour could be easy to achieve, which would be otherwise difficult to reach after iv injection, due to opsonization. However, we need to conduct elaborate toxicological studies and clinical studies.

Table 8.1 Plasma concentration time profile of Gemcitabine HCl loaded NPs and plain drug solution in male Wistar rats (n=5)

Time (h)	Gemcitabine HCl solution (ng/ml)	Gemcitabine HCl loaded NPs (ng/ml)
0.5	36.39 ± 15.63	26.39 ± 8.25
1.0	489.43 ± 60.06	143.82 ± 33.56
2.0	263.93 ± 72.53	289.23 ± 58.56
4.0	188.36 ± 65.50	1586.23 ± 122.5
24.0	23.36 ± 6.94	964.12 ± 148.53
48.0		423.12 ± 56.56
72.0		113.42 ± 46.75

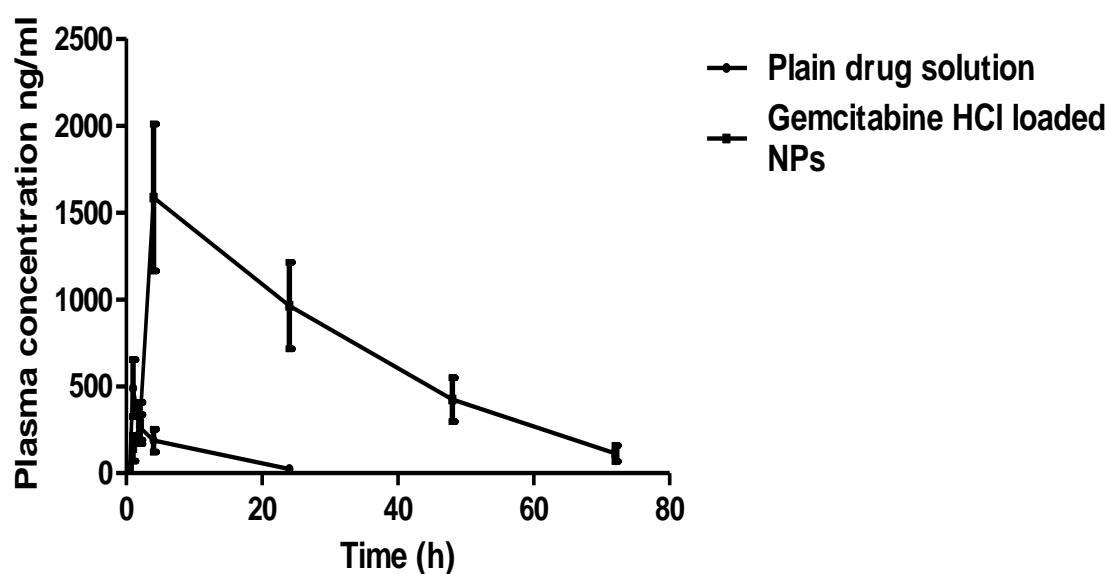


Fig. 8.2 Plasma concentration time profile of Gemcitabine HCl loaded NPs and plain drug solution in male Wistar rats (n=5) showing the bioavailability enhancement of Nanoparticles

Table 8.2 Pharmacokinetic parameters after oral administration of Gemcitabine HCl loaded NPs and Plain drug solution to male Wistar rats (n=5) for single dose oral bioavailability study

	C _{max} (ng/ml)	T _{max} (h)	AUC _{last} (ng.h/ml)	AUC _{total} (ng.h/ml)	MRT (h)	t _{1/2} (h)	F
Plain Drug solution	489.43±60.06	1	2534.72±686.5	2751.33±853.96	9.51	6.42	1
Gemcitabine loaded NPs	1586.23±122.5**	4	54,444±3200***	57552.3±2826***	30.8*	18.99*	21.47

* P< 0.05 ** P< 0.01 *** P<0.001

8.5 *In Vivo* Pharmacokinetic Studies for Lopinavir Loaded Nanoparticles

8.5.1 Methods

Three groups of male Wistar rats with each group containing 5 animals were subjected to single oral dose bioavailability study. The 1st group was given distilled water, the 2nd group was given a suspension of Lopinavir in 5% methylcellulose, and the third group received Lopinavir loaded NPs. In 2nd and 3rd tested groups, Lopinavir was administered at a dose of 10 mg/kg (Aji Alex et al., 2011). The formulations were administered orally with the aid of a syringe and infant feeding tube. Blood samples were drawn by retro-orbital venous plexus puncture with the aid of capillary tubes at 0.5, 2, 4, 8, 24, 48, 72, 96h post oral dose. The samples were collected in heparinised Eppendorf tubes and centrifuged at 3400 rpm for 15 min, and plasma was collected and stored at -20°C until analysis. To this, 200 μl of acetonitrile was added and vortexed for 5min followed by centrifugation at 5000rpm for 15 min. The organic phase was separated and evaporated under reduced pressure in a vacuum oven. The residue was dissolved in mobile phase solution (0.15 ml), vortexed for 1min followed by centrifugation at 13,000rpm for 5min. Then 20 μl of supernatant solution was injected in to the HPLC column. Lopinavir detection was performed at 210 nm, using X-Terra C18 analytical column. Calibration curves for Lopinavir in plasma samples were drawn as reported in analytical methods.

8.5.2 Results and discussion

The plasma concentration- time curve for Lopinavir after oral administration of the plain drug and Lopinavir Loaded PLGA NPs are given in Fig. 8.3. Table 8.3 gives the mean plasma concentration after oral administration at different time points. The pharmacokinetic parameters of all these formulations were determined by Kinetica software (Kinetica 5.0, Thermo Fisher Scientific). Non compartmental analysis for extra vascular administration was performed and the pharmacokinetic parameters obtained are given in Table 8.4. Statistical analysis of data was done by student's unpaired t test ($P < 0.05$, $P < 0.01$, $P < 0.001$).

After oral administration, Lopinavir loaded NPs exhibited higher plasma level concentration compared to plain drug solution. The AUC_{last} for NPs was found to be

22335.3± 2310 ng.h/ml, which was significantly higher than PD which showed AUC_{last} of 1596.5± 216.5 ng.h/ml. Significant improvement in C_{max} in case of NPs compared to plain drug solution was observed. The C_{max} for Lopinavir loaded nanoparticles was found to be 834.62± 86.8 ng/ml, where as for plain drug suspension, it was 143.42±22.43 ng/ml. This improvement in AUC and C_{max} could be explained by the combination of the following effects: firstly, the NPs were absorbed from M cells of intestine due to particle size less than 200nm. Secondly, a decrease in first pass metabolism by liver microsomal enzymes, as NPs directly reaches systemic circulation through GALT. When T_{max} of the NPs was compared with plain drug suspension, an increase in T_{max} was observed in case of NPs.

When t_{1/2} of the NPs was compared with plain drug suspension, it was observed that there was significant difference in t_{1/2} (17.93 h) as compared to PD (8.45 h). Similarly, when the mean residence time (MRT) of the formulations was compared with PD, there was increase in MRT observed which indicated that elimination was extended.

There was about 13.9 times increase in bioavailability (F) of Lopinavir loaded NPs and it could be attributed to capability of NPs to reach the systemic circulation, after absorption with M cells of payer's patches.

Recently, scientists are working on improving the bioavailability of Lopinavir, without co administration of Ritonavir. Ritonavir is always co-administered with Lopinavir to inhibit microsomal metabolism of Lopinavir. Alex et al formulated SLNs for oral delivery of Lopinavir and could achieve enhanced bioavailability of Lopinavir. Our findings are in line with those results. By formulating PLGA NPs, Lopinavir could bypass liver metabolism, therefore higher AUC was achieved as well as we could get increased MRT of drug in body. Moreover, Resistance to HIV occurs by high viral loads in the lymphatic tissues, which is a major site for storage and replication of virus (Von Briesen et al; 2000). Therefore, by delivering NPs directly to GALT, the drug was delivered to lymphatic viral reservoir sites. Hence, Lopinavir loaded PLGA NPs has tremendous potential for bioavailability enhancement and targeting the viral reservoir sites.

Table 8.3 Plasma concentration time profile of plain drug solution and Lopinavir loaded NPs in male Wistar rats (n=5)

Time (h)	Lopinavir solution (ng/ml)	Lopinavir loaded NPs (ng/ml)
0.5	19.52±8.32	11.17± 6.42
2.0	89.64± 18.72	56.47± 22.63
4.0	143.42± 22.43	336.89± 25.36
8.0	92.42± 26.21	834.62± 86.82
24.0	33.46± 11.30	442.75± 53.28
48.0		127.23± 31.24
72.0		78± 24.78
96.0		24.21±6.83

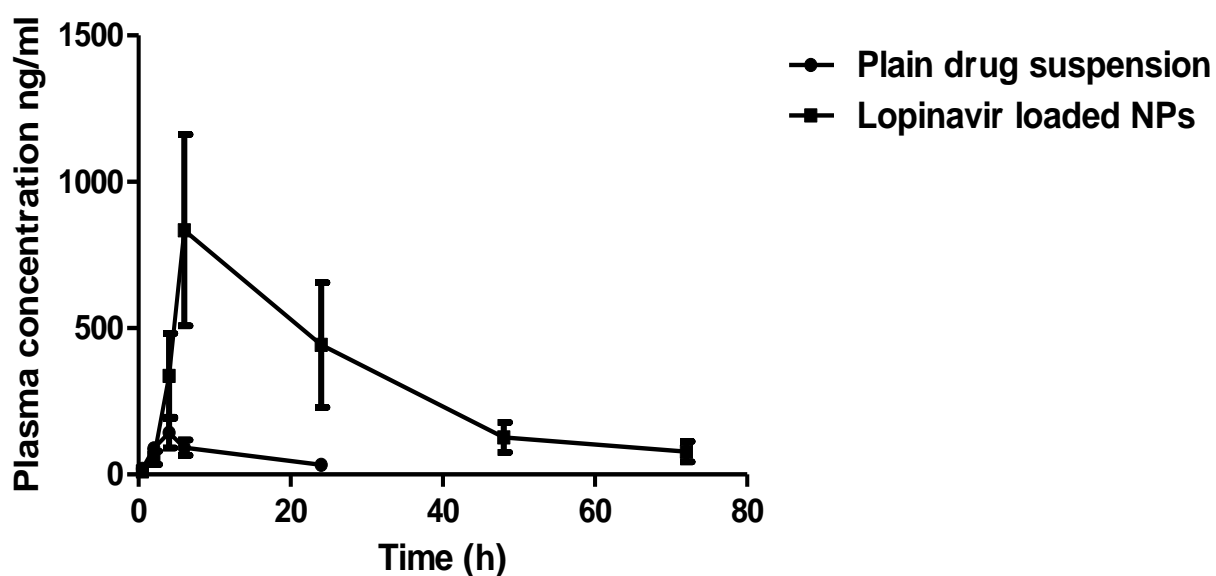


Fig. 8.3 Plasma concentration time profile of Lopinavir loaded NPs and plain drug suspension in male Wistar rats (n=5) showing the bioavailability enhancement of nanoparticles

Table 8.4 Pharmacokinetic parameters after oral administration of Lopinavir loaded NPs and Plain drug suspension to male Wistar rats (n=5) for single dose oral bioavailability study

	C_{max} (ng/ml)	T max (h)	AUC_{last} (ng.h/ml)	AUC_{total} (ng.h/ml)	MRT (h)	t_{1/2} (h)	F
Plain Drug solution	143.42±22.43	4	1596.5± 216.5	2101.08± 253.23	17.069	8.45	1
Lopinavir loaded NPs	834.62± 86.8**	6	22335.3± 2310***	22961± 2241***	29.491*	17.93*	13.9

* P< 0.05 ** P< 0.01 *** P<0.001

8.6 References

- ❖ Alex A, Chacko MR, Jose S, and Souto E B. Lopinavir loaded solid lipid nanoparticles (SLN) for intestinal lymphatic targeting. *Eur J Pharm Sci*, 42, 2011, 11-18.
- ❖ Vandana M, and Sahoo SK. Long circulation and cytotoxicity of PEGylated gemcitabine and its potential for the treatment of pancreatic cancer. *Biomaterials*, 31, 2010, 9340-9356.
- ❖ Veltkamp SA, Jansen RS, Callies S, Pluim D, Visseren-Grul CM, Rosing H, Kloeker-Rhoades S, Andre VA, Beijnen JH, Slapak CA and Schellens JH. Oral administration of gemcitabine in patients with refractory tumors: a clinical and pharmacologic study. *Clin Cancer Res*, 14, 2008, 3477-3486.
- ❖ Vokurka J. Effect of Gemcitabine on Vascular Endothelium in the Rat. . *Acta Vet Brno*, 73, 2004, 201-204.

CHAPTER 9

SUMMARY AND CONCLUSIONS

Summary and Conclusions

Oral delivery is the easiest and most convenient way for drug delivery. But, the challenges associated with oral route include exposure to extreme pH variations, hepatic first pass effect, intestinal motility, mucus barrier, P-glycoprotein efflux pump and impermeable epithelium. Most of drugs for treatment of cancer and AIDS suffer from abovementioned problems and cannot be given orally. Anticancer drugs are given by intravenous chemotherapy sessions which are very painful to patients. For AIDS, resistance to most of drugs is another barrier in efficient eradication of virus. Oral delivery of anticancer drugs and avoidance of resistance to antiretroviral drugs can be beneficial to patients. Oral chemotherapy can provide a long-time, continuous exposure of the cancer cells to the anticancer drugs of a relatively lower thus safer concentration.

Oral delivery of nanoparticles is extremely researched now days by scientists. Nanoparticle technology has the capability of improving the stability of drugs, minimizing the metabolic degradation and cellular efflux by virtue of colloidal surface properties. Nanoparticles given orally are efficiently taken up by M cells of Peyer's patches of intestine, thereby reaching GALT and systemic circulation directly.

Gemcitabine HCl, an anticancer agent, is currently in clinical use for the treatment of several types of cancer. Gemcitabine is a difluoro analogue of deoxycytidine. Unfortunately, the drug is rapidly metabolised with a short plasma half-life and its cytostatic action is strongly exposure-time dependent. It is rapidly and extensively deaminated by cytidine deaminase in blood, liver, kidney and other tissues. In order to achieve the required concentration over sufficient periods of time, repeated application of relatively high doses is required. This, in turn, leads to dose-limiting systemic toxicity. The plasma half life after intravenous infusion is 8- 17 min in human plasma. Therefore, it is required in high doses. Furthermore, Gemcitabine is highly hydrophilic molecule with log P value 1.4. Till now, there is no oral formulation of Gemcitabine HCl in the market.

Lopinavir is a potent protease inhibitor used as a leading component in combined chemotherapy commonly referred as Highly Active Anti-Retroviral Therapy (HAART). Lopinavir has poor oral bioavailability due to poor drug solubility characteristics as well as extensive first pass metabolism, primarily mediated by cytochrome P450 and P-

glycoprotein efflux which limits intestinal uptake. In marketed preparations, Lopinavir is always co-administered with ritonavir, as ritonavir inhibits the cytochrome P450 enzyme, responsible for extensive first pass metabolism.

The present investigation was aimed to develop PLGA based nanoparticles for Gemcitabine HCl and Lopinavir for bioavailability enhancement after oral delivery. For both the drugs chosen, action at lymphatic site is desirable. Gemcitabine HCl acts on lymphatic tumours and Lopinavir at lymphatic viral reservoirs to combat resistance. PLGA nanoparticles were formulated and optimized by factorial design. It was hypothesized that drug loaded NPs would be taken up intact by M Cells in GALT, thereby will reach the lymphatic circulation and then to systemic circulation. Therefore, the drug will first reach at site of action by bypassing the hepatic first pass metabolism and opsonization in blood. Also, nanoparticles due to smaller size less than 200 nm, directly delivered inside the cells bypassing the p-glycoprotein flux through the cell wall; which is another issue in oral delivery.

Gemcitabine HCl Loaded NPs

Gemcitabine HCl loaded nanoparticles were formulated by multiple emulsification and solvent evaporation method using sonication. As Gemcitabine HCl is highly hydrophilic drug, its entrapment inside nanoparticles was a challenge. The process and formulation parameters were optimized systematically. After preliminary experiments, pH of internal aqueous phase was identified as critical parameter. By optimizing pH of internal aqueous phase to 3, higher entrapment was able to be achieved. The important parameters such as PLGA concentration (X_1), surfactant concentration (X_2) and sonication time of secondary emulsion (X_3) were optimized by 3^3 factorial design using Particle size and entrapment efficiency as responses. Optimization by 3^3 factorial design confirmed that Polymer concentration was the major contributing factor for particle size and entrapment efficiency. Contour and response surface plots showed utility in explaining the effects of various formulation variables on responses. Full model and reduced model equations were generated and ANOVA explained the omission of non significant terms. The formulation was optimized by desirability criteria of maximum entrapment with minimum particle size less than 200 nm.

The optimized nanoparticles were evaluated for particle size, zeta potential, entrapment efficiency, drug loading, surface morphology, DSC, FTIR, *in vitro*, *ex vivo* drug release studies in rat stomach and intestine. Qualitative and quantitative uptake studies by confocal microscopy, transepithelial permeability studies in Caco 2 cells, cytotoxicity studies in Caco 2 cells as well as K562 leukemic cancer cell lines, *in vivo* single dose bioavailability studies in male Wistar rats and stability studies.

Gemcitabine HCl loaded NPs showed particle size of 166.68 ± 3.59 nm (PDI 0.136) and entrapment efficiency of $56.39 \pm 2.583\%$. Drug loading for optimized formulation was found to be $10.39 \pm 2.131\%$. Zeta potential was -20.6 ± 2.321 mV. Particle size below 200 nm, with entrapment efficiency greater than 50 % was achieved.

The TEM micrographs of nanoparticles showed discrete round structures below 200nm sizes. It confirmed that multiple emulsification solvent evaporation method was effective for formulating nanoparticles of hydrophilic drug using PLGA. DSC studies showed change in crystallinity of Gemcitabine HCl compared to plain drug. It confirmed amorphization of drug and entrapment inside nanoparticles. DSC scan of bulk Gemcitabine HCl sample showed a single sharp endothermic peak at 277.49 °C ascribed to the melting of the drug while PLGA showed endothermic peak at 51.06 °C corresponding to its glass transition temperature (Tg). But in NPs, disappearance of melting endothermic peak was observed which indicated substantial crystalline change and amorphization of drug in the polymer matrix.

FTIR spectra of native gemcitabine showed characteristic peaks of amine bands at 1680 cm^{-1} and characteristic peak of ureido group at 1721 cm^{-1} with 3393 cm^{-1} for stretching vibration of (NH_2). The spectrum PLGA showed peaks at (3511.18 cm^{-1} and 1757.40 cm^{-1}), the intensity of both the peaks N-H of pure drug at 1721.25 cm^{-1} and at 1680 cm^{-1} were found to be weak in the spectra of Gemcitabine HCl loaded PLGA NPs. The peak of PLGA at 3511.18 cm^{-1} was present with a slight shift to 3497 cm^{-1} , while peak for Gemcitabine HCl was absent, indicating that the drug was completely incorporated in the PLGA NPs. The Gemcitabine HCl loaded nanoparticles were found to be stable for the period of 3 months at $2-8$ °C conditions.

The drug release from nanoparticles was slow and sustained. The plain drug solution released more than 40 % drug in 1h and within 4h all of drug was released. Whereas

from drug loaded NPs, 25.96 ± 3.254 % of drug was released in initial 4h, followed by 56.89 ± 4.259 % in 24h and 98.2 ± 2.371 % of drug released at the end of 120h. The release followed Korsmeyer–Peppas model and fickian diffusion. The regression coefficient of the plot of $\log M_t/M_\infty$ versus $\log t$ for NPs was found to be 0.995 with value of release exponent (n) as 0.37 which was less than 0.5.

The *ex vivo* drug release from plain drug solution showed that nearly complete drug was released in the stomach, whereas from NPs, 10% of drug was released in the stomach in initial hours and most of the drug was released in the intestinal segment. At the end of 6h study, nearly 40 % of drug was released. Because of entrapment of drug inside NPs, release from NPs was sustained. The drug release from NPs in stomach and intestine followed Korsmeyer-Peppas model and fickian diffusion (0.985 and $n=0.486$).

The uptake studies in Caco 2 cell lines confirmed the internalization of nanoparticles in the Caco-2 cells. The NPs were observed as red fluorescence spots in the perinuclear regions. The uptake of NPs in Caco-2 cells was time dependent, increased with incubation time upto 2h. Whereas, the plain dye solution did not show the uptake due to hydrophilic nature of the dye. We could find that, the uptake efficiency of a hydrophilic drug can be improved by encapsulating the drug in nanocarriers, as colloidal and surface properties of nanoparticles are different from native drug. Further, transport studies were performed to assess the increased permeation through intestine barrier. The permeability coefficient for Gemcitabine HCl solution was found to be 0.72×10^{-5} . The permeability coefficient for Gemcitabine HCl loaded NPs was found to be 4.6×10^{-5} which is 6.38 times more than the plain drug solution. The higher permeability coefficient for nanoparticles corresponds to the lipophilicity of PLGA NPs in which the drug is entrapped, whereas lower permeability coefficient for plain drug solution was because of high hydrophilicity of drug as well as poor permeation ($\log P$ 1.4). As the drug is substrate for p glycoprotein pump, the low permeability can also be attributed to that. The uptake studies and transport studies revealed that permeability of Gemcitabine HCl after loading it in nanoparticles was greatly improved. It would lead to enhancement of absorption via The nanoparticle formulation was found to be safe on Caco 2 cells with lesser cytotoxicity as compared to free drug.

Cytotoxicity studies by MTT assay confirmed that Gemcitabine HCl loaded nanoparticles were found to be 2.4 fold, 3.4 fold and 8.59 fold more cytotoxic on K 562 cancer cells

after 6, 24h and 48h incubation respectively, which could be attributed by higher uptake via endocytosis and more internalization of PLGA NPs with time duration.

In vivo uptake studies by confocal microscopy in rat intestinal tissue after oral delivery of Rhodamine loaded NPs confirmed the penetration and absorption of NPs in intestinal tissue after oral administration.

In vivo single dose bioavailability studies results showed C_{max} for PLGA nanoparticles was found to be 1586.23 ± 122.5 ng/ml, which was significantly higher than the plain drug solution. A higher C_{max} for NPs could be achieved as drug loaded in PLGA NPs was capable to bypass hepatic first pass metabolism and able to reach directly to systemic circulation by virtue of size and surface properties of nanocarrier system. C_{max} for plain drug solution was only 489.43 ± 60.06 ng/ml, due to very low bioavailability of Gemcitabine HCl by oral route as Gemcitabine (dFdC) is extensively deaminated by cytidine deaminase into 2, 2-difluorodeoxyuridine (dFdU), which has been reported to be present mainly in liver of humans and kidney of rats. T_{max} for NPs was found to be (4h) while for plain drug solution was found to be 1 h. Delayed T_{max} would be justified by the fact that, after intestinal transit, major drug would be released at lymphatic site and then reach systemic circulation. Also, $T_{1/2}$ was increased upto 18.99 h for NPs, which is 3 times higher as compared to plain drug solution; $t_{1/2}$ of 6.42h. AUC_{last} for Gemcitabine HCl loaded NPs was found to be $54,444.7 \pm 3200$ ng.h/ml, which is significantly higher than AUC_{last} for Plain drug solution; 2534.72 ± 686.5 ng.h/ml ($P < 0.01$, student's unpaired t test). Plasma concentration from plain drug solution were undetectable after 4h and AUC_{last} was very less as due to extensive metabolism to inactive metabolite, while NPs could achieve higher AUC due to slow and sustained release from NPs, which would protect the drug from metabolism. Gemcitabine loaded PLGA NPs showed 21.47 fold increase in relative bioavailability in comparison to plain drug solution after oral delivery. Improvement in bioavailability could be attributed to ability of nanoparticles to reach the oral lymphatic region after absorption through M cells of Peyer's patches and reaching to systemic circulation through mesenteric lymph duct. Thus, PLGA nanoparticles could play important role in improving entrapment, uptake, permeability, C_{max} and $t_{1/2}$ Gemcitabine HCl which will ultimately lead to enhancement in its bioavailability. Oral chemotherapy would be possible in coming years for a drug like Gemcitabine HCl having hydrophilicity and

given by continuous IV infusion due to shorter half life in minutes, leading to too higher concentration and undesirable toxicity to tissues.

Lopinavir Loaded NPs

Lopinavir loaded nanoparticles were formulated by nanoprecipitation method using water miscible solvent acetone. The process and formulation parameters were optimized systematically. After preliminary experiments, the important parameters such as drug concentration (X_1), PLGA concentration (X_2) and surfactant concentration (X_3) were optimized by 3^3 factorial design using particle size and entrapment efficiency as responses. Optimization by 3^3 factorial design confirmed that increase in drug and polymer concentration lead to increase in entrapment and particle size. Contour and response surface plots showed utility in explaining the effects of various formulation variables on responses. Full model and reduced model equations were generated and ANOVA explained the omission of non significant terms. The formulation was optimized by desirability criteria of maximum entrapment with minimum particle size less than 200 nm.

The optimized nanoparticles were evaluated for particle size, zeta potential, entrapment efficiency, drug loading, surface morphology, DSC, FTIR, *in vitro* drug release, *ex vivo* drug release studies in rat stomach and intestine, qualitative cell uptake studies by confocal microscopys, transepithelial permeability studies in Caco 2 cells, cytotoxicity studies to confirm tolerability in Caco 2 cells, *in vivo* single dose bioavailability studies in male Wistar rats and stability studies.

Optimized formulation of Lopinavir loaded NPs had EE of $93.03 \pm 1.27\%$ and particle size of 142.16 ± 2.13 nm at +1, -1, and -1 levels of X_1 , X_2 and X_3 respectively. Drug loading for optimized formulation was found to be $25.11 \pm 3.141\%$. Zeta potential was -27.2 ± 2.423 mV. Thus, this confirmed that nanoprecipitation method was successful for formulating lipophilic drug loaded PLGA NPs.

The TEM micrographs of nanoparticles showed discrete round structures below 200nm sizes. DSC studies confirmed amorphization of drug and entrapment inside nanoparticles. Disappearance of melting endothermic peak was observed which indicated crystallinity change and amorphization of drug in the polymer matrix.

FTIR studies of Lopinavir loaded NPs showed absence of peak at 3376 cm^{-1} corresponding to Lopinavir but peak corresponding to PLGA was present, indicating the incorporation of drug inside the NPs. Lopinavir loaded nanoparticles was found to be stable for the period of 3 months at refrigerated conditions.

In vitro drug release data showed that plain drug suspension released nearly 50 % drug in 3h, whereas drug release from NPs was near to 10 % in 3 hour reaching to 50 % in 24 h and near to 100 % in 120 hours. The drug release was sustained from the NPs. Lopinavir loaded PLGA NPs followed the Korsmeyer peppas model and non fickian diffusion with r^2 value of .9969 and $n = 0.647$.

Ex vivo drug release studies in stomach and intestine showed that from plain drug suspension, more than 60% of drug was released in stomach, whereas drug release from NPs was slow and sustained; nearly 13% of drug was released in stomach in initial hours. Only small fraction of drug was released before the NPS could reach to the Peyer's patches in intestine, indicating the stability of NPs in stomach. Low aqueous solubility of drug entrapped in polymeric system was the reason for slow release. When data of drug release from NPs were fitted to various kinetic equations, the drug release from NPs was found to be diffusion controlled as it follows Korsmeyer peppas model with r^2 value of 0.9652 and mechanism of drug release was non fickian diffusion ($n=0.879$).

The uptake studies in Caco 2 cell lines confirmed the internalization of nanoparticles in the Caco-2 cells. The NPs were observed as green fluorescence spots in the perinuclear regions. The uptake of NPs in Caco-2 cells was time dependent, increased with incubation time. Plain dye solution showed limited uptake. The uptake efficiency of a lipophilic drug could also be enhanced by encapsulating the drug in nanocarriers, which are uptaken by endocytosis and bypass p-glycoprotein efflux. Further, transport studies were performed to assess the increased permeation through intestine barrier.

Quantitative uptake studies using FACS showed that mean fluorescent intensity of 6-Coumarin loaded nanoparticles in Caco 2 cells was doubled from 1h to 4h. 6-Coumarin loaded NPs had 2.1 fold higher MFI at 1h, which increased to 3.6 fold to 6.4 fold higher MFI than plain dye solution at the end of 4h.

The permeability coefficient of Lopinavir loaded NPs in Caco 2 cells was found to be 8.84×10^{-5} whereas for Lopinavir solution was found to be 2.9×10^{-5} . Lopinavir has a log P

value of 4.67 (Drug Bank) and it is lipophilic drug, therefore it is permeable to Caco 2 cells, but Lopinavir loaded NPs showed a 3.04 times increase in permeability, which could be attributed to the higher uptake of NPs by endocytosis in Caco 2 cells. There was significant enhancement in permeability of Lopinavir by loading the drug in NPs, as nanoparticles also bypass p-glycoprotein pump.

The uptake studies and transport studies revealed that permeability of Lopinavir after loading it in nanoparticles was greatly improved. It would lead to enhancement of absorption via The nanoparticle formulation was found to be safe on Caco 2 cells with lesser cytotoxicity as compared to free drug. Confocal microscopy of rat intestinal section after oral delivery 6-Coumarin loaded NPs confirmed penetration and uptake of NPs.

After oral administration, Lopinavir loaded NPs exhibited higher plasma level concentration compared to plain drug solution. The AUC_{last} for NPs was found to be 22335.3 ± 2310 ng.h/ml, which was significantly higher than PD which showed AUC_{last} of 1596.5 ± 216.5 ng.h/ml. Significant improvement in C_{max} in case of NPs compared to plain drug solution was observed. The C_{max} for Lopinavir loaded nanoparticles was found to be 834.62 ± 86.8 , where as for plain drug suspension, it was 143.42 ± 22.43 . The C_{max} for plain drug solution was very less due to extensive metabolism of Lopinavir by liver microsomal CYP3A4 as well as p glycoprotein efflux pump which secret it back in intestinal lumen. This improvement in AUC and C_{max} could be explained by the combination of the following effects: firstly, the drug molecules were absorbed from M cells of intestine due to particle size less than 200nm bypassing the efflux pump. Secondly, a decrease in first pass metabolism by liver microsomal enzymes, as NPs directly reaches systemic circulation through GALT. When T_{max} of the NPs was compared with plain drug suspension, an increase in T_{max} was observed in case of NPs. When $t_{1/2}$ of the NPs was compared with plain drug suspension, it was observed that there was significant difference in $t_{1/2}$ (17.93) as compared to PD (8.45). Similarly, when the mean residence time (MRT) of the formulations was compared with plain drug suspension, there was marked increase observed which indicated that elimination was extended for nanoparticles. There was about 13.9 times increase in bioavailability of Lopinavir loaded NPs

This work could be a contribution towards the enhancement of bioavailability of Gemcitabine HCl and Lopinavir which are used in treatment of cancer and AIDS respectively. By encapsulating the drug in PLGA nanoparticles, adopting different methods for formulation depending upon the solubility of drug, a significant enhancement in absorption, uptake and permeation through intestinal barrier could be achieved leading to enhanced bioavailability. Therefore, Gemcitabine HCl, an anticancer agent which is currently administered as continuous iv infusion could be used as an oral chemotherapeutic agent, benefitting the patients by avoiding complications of parenteral administration. Thus, the orally delivered PLGA nanoparticles of Gemcitabine HCl could deliver the drug to the M cells of Peyer's patches from where it directly reach to systemic circulation, thus protecting the drug from first pass metabolism as well as from gastrointestinal environment and avoiding the serious side effects associated with infusions. Also, Oral NPs for Gemcitabine HCl would be beneficial for lymphatic tumours, as higher concentration to tumour could be easy to achieve, which would be otherwise difficult to reach after iv injection, due to opsonization.

Also, Lopinavir which is always co administered with ritonavir for bioavailability enhancement, could be given alone as 13.9 times increase in bioavailability was achieved as compared to plain drug. Thus orally delivered NPs of Lopinavir has tremendous potential for improving the bioavailability of Lopinavir without co administration of Ritonavir and directly delivering the drug at lymphatic viral reservoir sites.

However, we need to conduct elaborate toxicological studies and preclinical studies and further investigations in human beings under clinical conditions before they can be commercially exploited.

PRESENTATIONS AND PUBLICATIONS

1. **Garima Joshi**, Krutika Sawant. Orally delivered polymeric nanoparticles of Gemcitabine HCl presented at **4th BioNanoMed 2013 at Danube University, Krems, Austria.**
2. **Garima Joshi**, Krutika Sawant. Orally delivered polymeric nanoparticles of Lopinavir: Development, statistical optimization, in vitro and ex vivo studies presented at **Nanotech 2012, 18- 21 June 2012, Santa Clara, California, USA.**
3. **Garima Joshi**, Krutika Sawant. Orally delivered polymeric nanoparticles of Lopinavir: Development, statistical optimization, in vitro and ex vivo studies. NSTI-Nanotech 2013, CRC Press, ISBN-978-1-4665-6276-9, Vol-3, 2012.
4. **Garima Joshi**, Abhinesh Kumar, Krutika Sawant. Orally delivered Polymeric Nanoparticles of Gemcitabine HCl for Bioavailability Enhancement: Optimization by Factorial Design, Characterization, Cell line studies and In vivo Pharmacokinetics. Manuscript under review in European Journal of Pharmaceutics and Biopharmaceutics, Elsevier, 2013.

Other Publications on Bioavailability enhancement:

1. Umang Shah, **Garima Joshi**, Krutika Sawant. Improvement in antihypertensive and antianginal effects of felodipine by enhanced absorption from PLGA nanoparticles optimized by factorial design. **Material science and Engineering C, Elsevier, 2013 (Impact factor 2.5)**
2. Sandip Chavhan, **Garima Joshi**, Kailash Petkar, Krutika Sawant. Enhanced hypolipidemic activity of simvastatin by particle size engineering, **Biochemical Engineering Journal, Elsevier 2013. (Impact factor 2.984)**
3. Krishna Thakar, **Garima Joshi**, and Krutika Sawant. Bioavailability enhancement of Baclofen by Gastroretentive Floating Formulation: Statistical Optimization, in vitro and in vivo Pharmacokinetic studies, **Drug Dev Industrial Pharmacy, 2012. DOI: 10.3109/03639045.2012.709249. (Impact factor 1.5)**
4. Jigar Modi, **Garima Joshi**, Krutika Sawant. Chitosan based mucoadhesive nanoparticles of Ketoconazole for bioavailability enhancement: formulation, optimization, *in vitro* and *ex vivo* evaluation. **Drug Dev Industrial pharmacy, 2012. DOI:10.3109/03639045.2012.666978, (Impact factor 1.5)**